Synthesis, Characterization and Evaluation of the Biological Activities of Copper (II), Zinc (II) and Nickel (II) Schiff Base Complexes of Quinoline Derivative Ligands

Dadi Dinku Telila

A Dissertation Submitted to the Department of Applied Chemistry, College of Applied Natural Sciences

Presented in Partial Fulfillment of the Requirement of the Degree of Doctor of Philosophy in Applied Chemistry (Bioinorganic Chemistry)

Office of Postgraduate Studies

Adama Science and Technology University

Adama, Ethiopia

November 2024

Synthesis, Characterization and Evaluation of the Biological Activities of Copper (II), Zinc (II) and Nickel (II) Schiff Base Complexes of Quinoline Derivative Ligands

By:

Dadi Dinku Telila

Main Advisor: Prof. Tegene Desalegn (PhD)

Co-Advisor: Prof. Taye Beyene (PhD)

A Dissertation Submitted to the Department of Applied Chemistry, College of Applied Natural Sciences

Presented in Partial Fulfillment of the Requirement of the Degree of Doctor of Philosophy in Applied Chemistry (Bioinorganic Chemistry)

Office of Postgraduate Studies

Adama Science and Technology University

DECLARATION

I declare that this dissertation titled “Synthesis, Characterization and Evaluation of the Biological Activities of Copper (II), Zinc (II) and Nickel (II) Schiff Base Complexes of Quinoline Derivative Ligands” is my own work and has not been submitted to any university for similar purpose. The references used in this dissertation are duly recognized by proper citations.

Dadi Dinku Telila		Jul 04, 2024
Name of student	Signature	Date

Recommendation of Advisors/ Supervisors

We, the supervisors of this research work, hereby certify that we have closely advised/supervised the student while writing this dissertation and read the draft dissertation titled "Synthesis, Characterization and Evaluation of the Biological Activities of Copper (II), Zinc (II) and Nickel (II) Schiff Base Complexes of Quinoline Derivative ligands" prepared under my guidance by Dadi Dinku. Therefore, we recommend the submission of the dissertation to the department for the final open defense.

Prof. Tegene Desalegn (PhD)		Jun 29, 2024
Major Advisor	Signature	Date
Prof. Taye B. Demissie	Taye Beyene	Jun 29, 2024
Co- Advisor	Signature	Date

Approval Sheet for the Dissertation

We hereby certify that the recommendation and suggestion given by the progress review committee are appropriately incorporated into the final PhD Dissertation titled "Synthesis, Characterization and Evaluation of the Biological Activities of Copper (II), Zinc (II) and Nickel (II) Schiff Base Complexes of Quinoline Derivative Ligands" by Dadi Dinku.

Prof. Tegene Desalegn (PhD)	_____	_____
Major Advisor	Signature	Date
Prof. Taye Beyene (PhD)	_____	_____
Co- Advisor	Signature	Date

We, the undersigned, the reviewers of the PhD Dissertation open defense by Dadi Dinku have read and evaluated the dissertation titled "Synthesis, Characterization and Evaluation of the Biological Activities of Copper (II), Zinc (II) and Nickel (II) Schiff Base Complexes of Quinoline Derivative Ligands" and examined the candidate during the open defense. This is, therefore, to certify that the dissertation had been accepted for partial fulfillment of the requirements of the degree of Doctor of Philosophy in **Bioinorganic Chemistry**.

Dr. Hizkeal Tsade Tefera (PhD)	_____	_____
Chairperson	Signature	Date
Dr. Akalu Tefera (PhD)	_____	_____
Internal Examiner	Signature	Date
Dr. Worku Dinku (PhD)	_____	_____
Internal Examiner	Signature	Date
Prof. Abi Tadesse (PhD)	_____	_____
External Examiner	Signature	Date
Dr. Balina Terfasa (Asso. Prof.)	_____	_____
External Examiner	Signature	Date

Final approval and acceptance of the dissertation is contingent upon submission of its final copy to the Office of Postgraduate Studies (OPGS) through the Department Graduate Council (DGC) and School Graduate Committee (SGC).

_____	_____	_____
Department Head	Signature	Date
_____	_____	_____
College Dean	Signature	Date
_____	_____	_____
Office of Postgraduate Studies, Dean	Signature	Date

ABBREVIATIONS AND ACRONYMS

^{1}H NMR	Proton Nuclear Magnetic Resonance
^{13}C NMR	Carbon Nuclear Magnetic Resonance
FT-IR	Fourier-Transform Infrared Spectroscopy
UV–Vis	Ultraviolet Visible spectroscopy
pXRD	powder X-ray Diffraction
TGA	Thermogravimetric analysis
DTA	Differential thermo analysis
DFT	Density functional theory
ONO	Oxygen-Nitrogen-Oxygen
λ max	Maximum wavelength
λ	Wavelength
μg/mL	Micro gram per milliliter
nm	Nanometer
mL	Milliliter
M.pt.	Melting point
°C	Degree Celsius
TLC	Thin Layer Chromatography
AAs	Amino Acids
DNA	Deoxyribonucleic acid
SBL_1	Schiff Base Ligand 1

SBL_2	Schiff Base Ligand 2
$ZnSBL_1$	Zinc Schiff base ligand complex 1
$CuSBL_1$	Copper Schiff base ligand complex 1
$NiSBL_1$	Nickel Schiff base ligand complex 1
$ZnSBL_2$	Zinc Schiff base ligand complex 2
$CuSBL_2$	Copper Schiff base ligand complex 2
$NiSBL_2$	Nickel Schiff base ligand complex 2

TABLE OF CONTENTS

Contents **Pages**

LIST OF FIGURES AND TABLES

List of Figures

List of Tables

LIST OF APPENDIXES

ACKNOWLEDGMENT

It is with immense pleasure that I extend my deepest sense of indebtedness and gratitude to my esteemed advisors, Prof. Tegene Desalegn (PhD) and Prof. Taye Beyene (PhD), for their invaluable guidance and unwavering commitment throughout my research work and dissertation writing process. Their critical feedback and insightful direction have been instrumental in shaping my academic pursuits. I express my sincere appreciation to Rajalakshmanan Eswaramoorthy (PhD) for his invaluable input and constructive ideas in refining my PhD dissertation. Special thanks are also due to Mr. Beyan Abdi for his collaborative efforts and methodological. I am indebted to Fekadu Muleta (PhD) for his proactive advice and support during the initial stages of my laboratory work, as well as for his material assistance and guidance. I also appreciate the insightful comments and guidance provided by Akalu Tefera (PhD) and Indris Yirbu (PhD) from the inception of the proposal to the current stage of the dissertation and I thank Worku Dinku (PhD) for his insightful comments on my current dissertation paper. Furthermore, I extend my gratitude to Bonga University and Adama Science and Technology University (ASTU) for providing me with the opportunity, material resources, and financial support to pursue my academic endeavors. The University of Botswana deserves acknowledgment for its instrument support in the characterization process. I am thankful to staff of the Department of Chemistry at Bonga and Adama Science and Technology University for their constructive ideas and unwavering support. My heartfelt gratitude extends to my colleagues, beloved brothers, and my entire family for their unwavering support in realizing my academic aspirations. Lastly yet importantly, I am deeply grateful to my wife and children for their patience and understanding, as they have shouldered the family responsibilities, enabling me to achieve my educational dreams.

ABSTRACT

The rise of drug-resistant bacterial infections has become a critical global health concern that demands immediate attention. Owing to their unique chemical structures and properties, transition metal complexes of Schiff base ligands offer innovative bioactivities and functionalities that make them valuable candidates for developing new drug candidates to counter the growing threat of multidrug-resistant pathogens. In this study, novel Schiff base ligands derived from a quinoline derivative and amino acids, and their Ni(II), Cu(II) and Zn(II) complexes were synthesized, characterized, and evaluated for their biological activities. Two Schiff base ligands, namely (E)-2-(((7-chloro-2-hydroxyquinolin-3-yl)methylene)amino)-3-phenylpropanoic acid (SBL1) and (E)-2-(((7-chloro-2-hydroxyquinolin-3-yl)methylene)amino)-3-methylbutanoic acid (SBL2), from 2,7-dichloroquinoline-3-carboaldehyde and Phenylalanine/Valine. Subsequently their metal (II) complexes NiSBL1, CuSBL1, ZnSBL1, NiSBL2, CuSBL2, and ZnSBL2 were synthesized and characterized using various spectroscopic techniques such as Uv-Vis, ^{1}H-NMR, ^{13}C-NMR, FT-IR, and pXRD. Analysis of the FT-IR spectra confirmed the tridentate nature of the Schiff base ligands (SBL1 and SBL2) with ONO active binding sites. The pXRD analysis indicated that CuSBL2 possessed amorphous nature and the rest two are crystalline in nature.

The antibacterial properties of these compounds were evaluated using the disc diffusion method. Notably, the CuSBL1 complex exhibited superior antibacterial activity against various strains compared to the other synthesized complexes, attributed to its small crystalline size of 29.7 nm as determined by pXRD results. Furthermore, SBL1 and SBL2 demonstrated antibacterial efficacy against *B. cereus, S. aureus, E. coli, S. typhi,* and *C. albicans*, with varying degrees of inhibition at a concentration of 100 µg/mL. ZnSBL1, NiSBL1, and CuSBL1 complexes also displayed antibacterial activities against these strains at the same concentration, with CuSBL1 showing the highest activity. Additionally, SBL2 and its metal complexes exhibited antibacterial effects against different strains at concentrations of 100 µg/mL and 200 µg/mL, with CuSBL2 demonstrating the strongest antibacterial activity compared to the other two NiSBL2 and ZnSBL2 complexes. Overall, this study highlights the potential of Schiff base compounds and their metal complexes as promising candidates for combating drug-resistant microbial infections, particularly CuSBL1 and CuSBL2 showing notable antibacterial efficacy warranting next level investigation.

Keywords: Schiff base ligand, Phenylanine, Valine, Tridentate, Metal complex, Antimicrobial and Molecular Docking

1. INTRODUCTION

1.1. Background

The chemistry of transition metal complexes has received considerable attention largely due to their diverse applications. Transition metal complexes are also important owing to their potential biological activities such as antibacterial, antifungal, antimalarial, and antitumor (Srivastava, 2021). Microbial infections are life-threatening diseases; they weaken the immune system and deteriorate most health conditions. The burden of infections due to antimicrobial resistance, especially in Africa and Asia, is alarming (Awolope *et al.,* 2023). According to the European Center for Disease Prevention and Control, about 33,000 people die annually from infections (Awolope *et al.*, 2023). Dealing with infectious diseases remains an important and challenging problem due to various factors like emerging infectious diseases and the increasing number of multidrug resistant microbial pathogens (Yamgar *et al.*, 2014). Over decades, Schiff base continue to attract attention of drug designer because of their distinctive chelating features. Schiff bases are known to possess antibacterial, antifungal, and other biological applications. Reports stress that the antibacterial activity of Schiff base ligands containing donor atoms can be enhanced significantly by coordination to metal ions (Al-redha *et al*., 2022).

Schiff base compounds and their metal complexes have been extensively investigated due to their wide range of applications (Zoubi, 2013). Increasing interest in Schiff base complexes has coincided with the advancement of bioinorganic chemistry; as a result, it has become evident that many of these substances could serve as useful templates for physiologically significant organisms (Deepika *et al.,* 2022). Due to their ease of synthesis, sensitivity to the central metal atom, unique features conferred by the imine group (-C = N-), and structural similarity to naturally occurring biological molecules, Schiff bases are gaining much popularity in the family of ligands. In inorganic chemistry, Schiff base ligand is considered important ligands due to their distinct characteristics of chelating. Strong chelate complexes can be prepared using Schiff bases with numerous donor atoms, such as the (-HC = N) group, which makes them particularly interesting (Cholan *et al.,* 2024).

The introduction of metal ions or metal ion binding components into a biological system for the treatment of diseases is one of the main branches in the field of bioinorganic chemistry (Hossain *et al.*, 2018). The chemistry of metal complexes with Schiff base ligands containing oxygen and nitrogen as donor atoms has recently gained increasing attention (Adeleke *et al.*, 2021). These ligands are known to coordinate to metal atom in different ways under different reaction conditions. Schiff bases are commonly synthesized by the condensation reaction of aromatic aldehydes or ketones with primary amines resulting in an azomethine moiety with at least one aryl group attached to the carbon or nitrogen atom. The interest in Schiff base ligands is primarily associated with ease of their synthesis, selectivity to the central metal ion, structural diversity, and their broad biological applications (Adeleke *et al.*, 2021; Teran *et al.*, 2019).

One of the major areas of research related to Schiff base metal complexes is the study of their biological activity to discover safe and effective therapeutic agents for the treatment of microbial infections and many other diseases. Several Schiff base metal complexes reported to possess diverse spectrum of biological and pharmaceutical activities. For instance, transition metal complexes of Schiff base ligands bearing "O" and "N" donor atoms are very important because of their biological properties such as antibacterial, antifungal, anti-inflammatory, analgesic, anticonvulsant, antitubercular, antioxidant, and anthelmintic, antimicrobial, anticancer and antidiabetic activities (Ommenya *et al.*, 2020; Teran *et al.*, 2019; Ibrahim, 2018). Several Schiff bases and their copper complexes have been developed and used as highly efficient metal-based modulators of multiple drug resistance. Additionally, Schiff base copper complexes have the ability to attach to DNA or damage it, increase the amount of reactive oxygen species (ROS) inside cells, activate the mitochondrial pathway, and trigger caspase-dependent apoptosis (Kun Hu *et al.*, 2018).

Quinoline, which is now one of the most important heterocyclic compounds, displaying a wide range of applications in pharmaceutical industries and organic synthesis, was first discovered by German chemist Friedlieb Ferdinand Runge in 1834, as a hygroscopic colorless liquid obtained by the distillation of coal tar (Dhayalan, 2022). Quinolines and their derivatives have been labeled as 'privileged scaffolds' owing to their prevalent existence in natural and synthetic molecules that exhibit notable applications in pharmacological, agrochemical, and electronic industries (Dhayalan, 2022). For instance, quinoline scaffolds are essential to the creation of anticancer

medications because of their superior performance through many modes of action (Kun Hu *et al.*, 2018).

It is well known that some metals, including copper, zinc, and silver, are toxic to microbes. On the other hand, micronutrients like zinc and copper are poisonous in high doses yet are required in small amounts for the proper operation of many human systems. Among the transition metals, Zinc is the second-most abundant trace metal in the human body and has the ability to promote the activities of over 300 enzymes, including those involved in the production of DNA and RNA (Aljahdali *et al.*, 2020). Data from the literature demonstrated the critical function that zinc plays in the synthesis and mineralization of bone (Veljovic *et al.*, 2012).

According to Stanić et al., (2010) the human body contains zinc. It is the most prevalent in the brain, second to iron. Several investigations have demonstrated the significance of Zn^{2+} ions in metalloenzymes and metal-based therapeutics. Their ability to inhibit germs is attributed to two different mechanisms: (i) direct interaction with microbial membranes that results in membrane instability and increased permeability; (ii) interaction with nucleic acids that prevents the respiratory system's enzymes from functioning (Muleta *et al.*, 2022).

The anti-inflammatory, antidiabetic, antioxidant, and antibacterial properties of Zn(II) complexes have also been shown in various studies (Damena *et al.*, 2022a). Promising antibacterial effects of Zn(II) complexes of quinoline derivative ligands were demonstrated in the in-vitro biological activity screening study carried out against four bacterial species, including *Escherichia coli*, *Pseudomonas aeruginosa* (Gram-negative), *Staphylococcus aureus*, and *Bacillus subtilis* (Gram-positive) (Abdel-rahman *et al.*, 2022; Damena *et al.*, 2022a).

Copper has received the most attention due to its importance for life. A biological system requires copper for many different compounds to work correctly. Many researchers have been interested in the coordination chemistry of copper because of its well-understood biological properties. Since copper is a known biologically active metal and drug complexing ion, there has been interest in using copper for medical purposes. A few Schiff-base-based copper (II) complexes have been effectively produced and employed as biological system models primarily as an antibacterial (Kumar *et al.*, 2016).

On the other hand, Cu(II) based complexes recently gained more focus in inorganic synthesis and investigations. For instance, Cu(II) indomethacin complexes are used as anti-inflammatory drugs in veterinary medicine (Tufa *et al.,* 2018). Several reports have shown copper complexes exhibit high potential for biomedical uses. The exceptional affinity for biological ligands and redox characteristics, make copper as an ideal choice among transition metals to drive biochemical reactions (Demircioğlu, 2021; Raczuk *et al.*, 2022).

Similar to copper and zinc, nickel has certain purposes in the biological system. Nickel is an element found in our DNA and RNA. It works with nucleic acids to accomplish a number of functions, including stabilizing the structure of RNA and activating enzymes that break down or use glucose. The production of red blood cells depends critically on nickel (Kumar *et al.,* 2016). Nickel is found in the body in highest concentrations in the nucleic acids, particularly RNA, and is thought to be somehow involved in protein structure or function (Kumar *et al.,* 2016). Previous research indicates that coordinated Nickel (II) complexes containing Schiff base ligand show antibacterial activity. According to Chandra and Tyagi (2008), there have been reports of compounds with dual antibacterial and antifungal properties found in the six coordinated Ni (II) complexes of Schiff base ligand (Kumar *et al.,* 2016). It is well recognized that complexation of metals with Schiff base ligand leads to enhanced ligand bioactivity and hence, to deter the growth of multidrug-resistant microbial infections and newly developing infectious diseases.

1.2. Statement of the problem

The search for new antimicrobial agents is an important line of research because of the resistance acquired by several pathogenic microorganisms, which cause damage to human health, exhibit multi-drug resistance due to inadequate and improper use of antibiotics. Thus, there is a huge demand for the discovery of new drugs to treat these infectious diseases caused by pathogens. The field of coordination chemistry, which deals with the study of metal complexes has achieved much attention resulting in the synthesis of new metal complexes for biological application (Hadjer *et al.,* 2018). The design and synthesis of metal complexes with a biologically active scaffold is an imperative and lively research area in bioinorganic chemistry. Metal chelation is one of the excellent routes to increase the lipophilic character of the organic moiety that may facilitate the absorption of the drug from the gastrointestinal tract. On coordination, drugs/ligands exhibited

significantly improved bioactivity profiles, while some inactive ligands may acquire pharmacological properties (Mohamed *et al.*, 2016).

In general, the presence of a lone pair of electrons of the nitrogen atoms' sp^2 hybridized orbital in the azomethine group is critical for their chemical and biological activities (Belay *et al.*, 2024). Schiff bases have been used in the preparation of many drugs and they possess a broad spectrum of biological activities such as antifungal, antibacterial, anti-inflammatory and anticancer activities (Sridhar *et al.*, 2017).

The rate at which multi drug-resistant (MDR) microbial diseases are emerging and escaping treatments is so rapid that the scientific community is finding it extremely difficult to stay up. Antibiotic-resistant diseases expected to kill 10 million people yearly by 2050, surpassing cancer in mortality rates, according to a 2019 WHO report. Research indicates that over 3 million people die each year from infections linked to bacteria (Muleta, 2023).

Antibiotics that can successfully treat bacterial infections with MDR are hard to come by because not many drugs with unique modes of action being developed despite this mounting danger. Therefore, there is a need to produce more potent antibacterial agents to overcome newly emerging infection and MDR microbial diseases and diseases linked with biofilms (Muleta, 2023).

To find viable and effective antibiotic medications with unique biological activity modes, extensive pharmaceutical research is required to develop cheap, less toxic and were efficacies antimicrobial agents. These days, a lot of interest is being paid to the chemistry of Schiff base ligand metal complexes because of their possible medical applications. The purpose of this study is developing novel Schiff base ligands by utilizing quinoline derivatives derived from natural products, as well as amino acids and their metal complexes, and assess their potential for bioactivity.

It observed from the review of literature that there is no research being conducted in this study title to develop new pseudo halide metal complexes and Schiff bases for biological activity. Thus, continuous research is desperately needed in order to come up with bioactive compounds which can be developed into new, cheap, less toxic and more efficacies antimicrobial drugs (agents) for combating newly emerging infecting and MDR microbial serotypes.

In the domain of metal-based pharmaceuticals, Schiff-based compounds and their metal complexes are remarkable (Y. Li *et al.*, 2020). Amino acid containing Schiff base ligands caught the attention of the researchers because they are good biological organic chelates that easily react

with aromatic carbonyl groups and ortho-hydroxy aldehydes to generate multidentate Schiff base transition metal complexes (Sumathi, 2022). Transition metals and their compounds play important roles in many biological processes in pharmaceutical and medical applications, as demonstrated by the discovery of cisplatin. Metal ion coordination compounds, including those made of chromium, cobalt, copper, manganese, molybdenum, palladium, ruthenium, tungsten, and zinc, have been utilized to treat a variety of disorders (Aljahdali *et al.,* 2020).

Formation of stable chelate complexes with transition metals which catalyze physiological processes (El-mossalamy *et al.,* 2024). In current research, work it was aimed to improve the activities of the resulting metal Schiff base complexes against the drug resistant microbes as the starting material quinoline derivative Schiff base ligand has biological activity by itself and the metals selected for this research work is essential metals for biological activities. In this context, with the aim of developing new antimicrobial Schiff base metal complex compounds, it was planned to synthesize, characterize a novel Schiff base derived from 2,7-dichloroquinoline-3-carboaldehyde with selected amino acids (Phenylaniline and Valine) and their transition metal (II), (copper, zinc and nickel) complexes and evaluate their antimicrobial activities against selected microbial strains.

1.3. Objectives

1.3.1. General Objective

The general objective of this study was to synthesize, characterize and evaluate the biological activities of Schiff base ligands and their Copper (II), Zinc (II) and Nickel (II) complexes.

1.3.2. Specific Objectives

The specific objectives of this research work were to:

- Synthesize Schiff base ligands from 2, 7-dichloroquinoline-3-carboaldeyde and amino acid (Phenylaniline and Valine).
- Characterize Schiff base ligands from 2, 7-dichloroquinoline-3-carboaldeyde and amino acid (Phenylaniline and Valine).
- Synthesize the Ni(II), Cu(II) and Zn(II) complexes with synthesized Schiff base ligand.
- Characterize the Ni(II), Cu(II) and Zn(II) complexes with synthesized Schiff base ligand.

- Evaluate the *in vitro* antibacterial activities of the Schiff base ligand and Ni(II), Cu(II) and Zn(II) complexes against two selected Gram-positive(+) and two Gram-negative(-) *bacterial strains* using disc diffusion method.
- Evaluate the *in vitro antifunga*l activities of the Schiff base ligand and Ni(II), Cu(II) and Zn(II) complexes against *Candida albicans* fungi species using disc diffusion method.
- Conduct the DFT and molecular docking analysis of the synthesized Schiff base ligand and Ni(II), Cu(II) and Zn(II) complexes.

1.4. Significance of the study

Transition metals and their complexes have evolved greatly due to their synthetic, biological potential, catalytic, unusual structural aspects, unique stereo and magneto chemistry. The ligands like 2-phenyl-2-(O-tolylamino) acetonitrile and quinolone, semicarbazones, benzothiazolines, dithiocarbamates, their Schiff bases and the corresponding metal complexes play vital roles in the progress of coordination and bioinorganic chemistry. The different modes of bonding of the ligands in the metal complexes and their derivatives produce appreciable change in their biological activity. Azomethine linkage and their metal complexes are gaining importance due to their unique structural and stereochemical aspects, and their uses as models in industrial, biological, analytical and antimicrobial systems (Habila *et al.*, 2020). The participation of metal ions in many of the bond forms and bond breaking enzymatic processes of biochemistry makes it clear that individual chemical bonds in organic molecules are sometimes strengthened and other times weakened, through coordination of the molecules with metal ions. Since the carbon-nitrogen double bonds in organic Schiff bases are susceptible to both hydrolytic cleavage and to coordination with metal ions, when coordination takes place between a metal ion and an organic ligand, the properties of both are changed in a variety of ways. Many unstable organic ligands are stabilized due to complexation and stabilized towards hydrolysis. For instance, it was showed that the hydrolysis of the Schiff base is much more rapid than that of its metal chelates (Ashraf *et al.*, 2020;Sayed *et al.*, 2020;Habila *et al.*, 2020;Wafaa *et al.*, 2018;Ejidike *et al.*,, 2015).

2. LITERATURE REVIEW

2.1. Chemistry of Schiff base ligands

Schiff bases named after Hugo Schiff, a German chemist, who discovered in 1864 (Belay *et al.*, 2024). Schiff bases are defined as chemical compounds (imines) having a hydrocarbyl group on the nitrogen atom $R_1R_2C = NR_3$ ($R_3 \neq H$) in accordance with the IUPAC recommendation (Fig. 2.1). The capacity of Schiff bases to form complexes with transition metal ions is determined by this shared characteristic (Raczuk *et al.,* 2022).

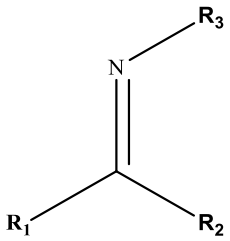

Figure 2.1. The specific structure fragment characteristic of Schiff bases, where R_1, R_2 and R_3 are alkyl or (more often) aryl groups. R_1 or/and R_2 may be hydrogen atoms.

Schiff base ligands are considered as privileged ligands as they simply synthesized by condensation of primary amines and carbonyl compounds, aldehydes, or ketones. The formation of carbon–nitrogen double bond plays important role in organic synthesis. Recent trends witness that the diverse structure of the Schiff base ligands contributed to constantly evolving researches involving these organic compounds Furthermore, it continues to be a possible field of study in the future with huge impact (Siham, 2023).

The enol (enol-imine) and keto (keto-amine) forms are the two potential tautomeric forms that Schiff bases generally exhibit. The H-atom moved from the hydroxyl O-atom to the imine N-atom during an intramolecular proton transfer mechanism, which causes this tautomerism. Schiff bases have been extensively researched because to their potential applications in pharmacology, industry, biology, and chemistry, among other fields. For biological activities like antibacterial, antioxidant, antiviral, antipyretic, anti-inflammatory, antifungal, and anticancer properties (Demircioğlu, 2021).

Schiff bases are azomethine-containing compounds that represent a great class of ligand and frequently employed in coordination chemistry. Because of their wide range of pharmacological qualities, Schiff bases have been identified as a prominent class of biologically active drug compounds that have attracted the interest of medicinal chemists. These substances have been synthesized by numerous researchers to combat a variety of illnesses with the least amount of toxicity and greatest impact. Schiff bases have been particularly useful as chelating ligands in coordination chemistry involving primary groups and transition metals (Hanan, 2020; Julius *et al.,* 2023; Patil *et al.*, 2021).

Schiff bases are often tridentate or bidentate ligands that can combine with transition metals to generate extremely stable complexes. Schiff base reactions are helpful in chemical synthesis for creating carbon-nitrogen bonds (Zoubi, 2013). Recent discoveries about the antibacterial, antifungal, and oxygen carrier qualities of Schiff bases and their metal complexes have led to an increase in their significance in contemporary coordination chemistry (Raman *et al.,* 2005).

Since the discovery of cisplatin, Schiff base transition-metal complexes have been employed in medical and pharmaceutical chemistry. Several Schiff base complexes containing chromium, cobalt, copper, manganese, molybdenum, palladium, ruthenium, tungsten, vanadium, and zinc have been reported for use in the treatment of various diseases due to their recognized antimicrobial and antioxidant, anticancer, antiproliferative, anti-inflammatory, DNA binding and cytotoxicity, and anti-diabetic properties (Yusuf *et al.*, 2021).

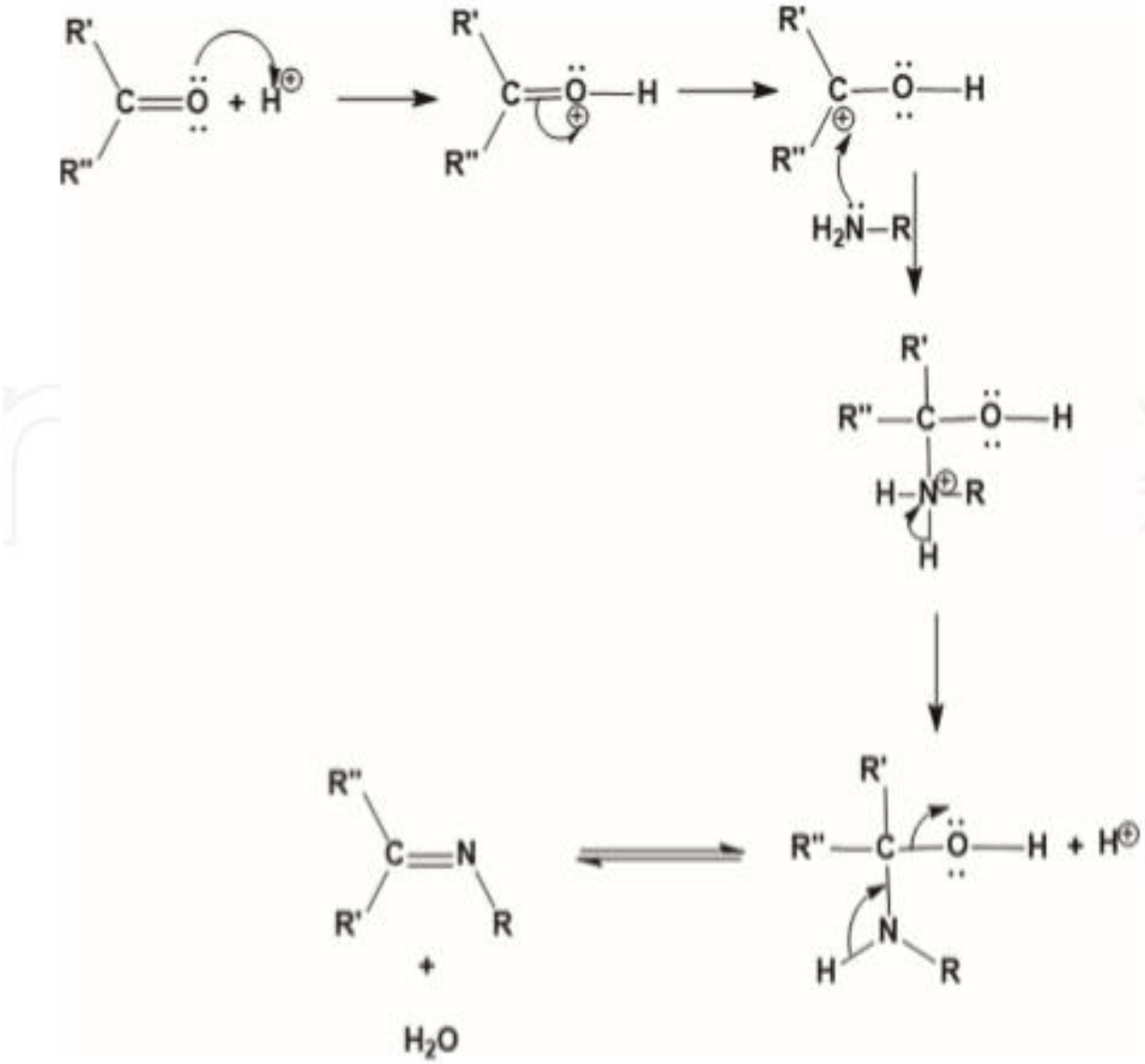

Scheme 2.2: Reaction mechanism of Schiff Base Synthesis

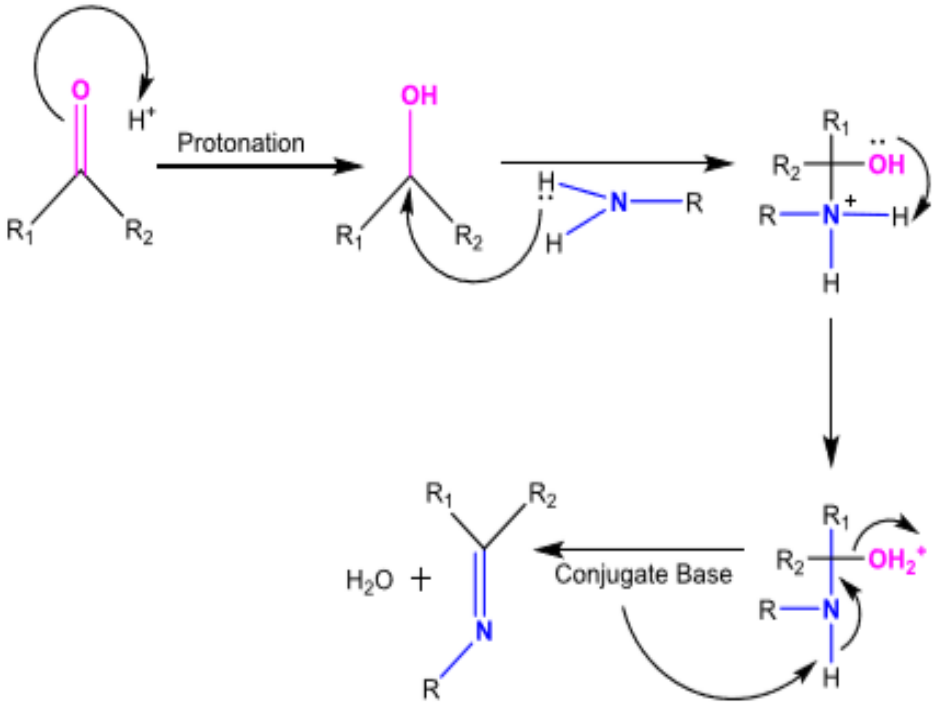

i. Acidic media

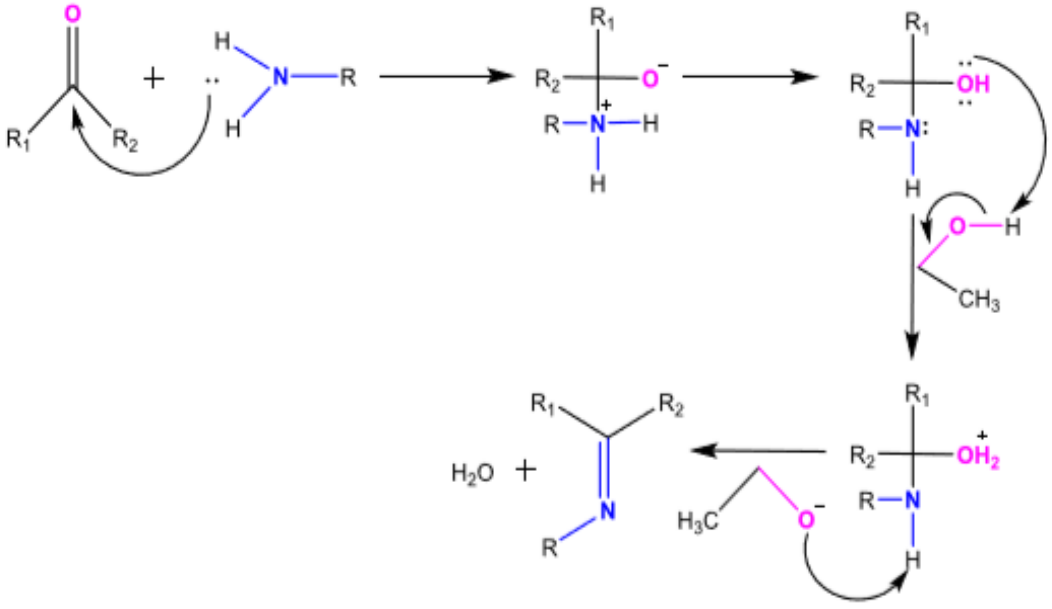

ii. Basic media

Scheme 2.3: Synthesis of Schiff base ligand i) under acidic media and ii) under basic media (Gautam *et al.*, 2023)

Schiff base derivatives have garnered interest from numerous researchers because of their broad variety of applications and potential for metal binding. These ligands had extensively studied in relation to their production, and they have been instrumental in the development of coordination chemistry. Salicylaldehyde and its derivatives provide hydroxyl groups in Schiff bases, which also exhibit specific chelating properties (Salen *et al.,* 2023). Because of their wide range of pharmacological qualities, Schiff's base had identified as a noteworthy class of biologically active drug compounds that has attracted the interest of medicinal chemists. These substances had synthesized by numerous researchers to combat a variety of illnesses with the least amount of toxicity and greatest impact. These forecasts have given researchers the means to synthesized novel, physiologically active Schiff's base derivatives (Patil *et al.,* 2021). Since the "O" and "N" atoms in Schiff bases synthesized intermolecular hydrogen bonds, which are crucial for the formation of metal complexes and the proton transfer from hydroxyl "O" to imine "N" atoms, Schiff bases are frequently utilized as ligands in the field of coordination chemistry (Salama *et al.,* 2017).

Schiff base compounds are privileged ligands in medicinal chemistry and have proven therapeutic potential, due to –CH=N– functionality giving rise to strong activity and playing an essential role. The remarkable biological activities include antitumor, antibacterial, antifungal, antimalarial, antiviral, antioxidant, anti-inflammatory, analgesic, anticonvulsant, antiglycation, antihypertensive, antidepressant and lipid lowering properties (Mohamed, 2016). Biological reactions which are essential to life processes usually involve transition metals; these metals usually coordinate with O- or N-terminals from proteins in a variety of modes and play a vital crucial role in the conformation and function of biological macromolecules (Ajibade, 2015).

Schiff bases involving nitrogen and oxygen as donor atoms are of much interest and have many applications in pharmaceutical chemistry. Recent advances in spectroscopy and their outstanding antibacterial, antifungal, and anticancer capabilities have given Schiff base ligands and their complexes a well-deserved and important significance. The metal complexes of pyrazole-based Schiff bases have received considerable attraction in different fields due to their structural characteristics and certainly advantageous biologic applications. These ligands have always been relevant to a bonding occurrence with the transition metal ions (Kouser *et al.,* 2023).

Schiff base metal complexes have garnered increased attention due to the growth of the bioinorganic chemistry. It is well acknowledged that numerous Schiff base metal complexes have potential biological uses (Yadav *et al.,* 2019). There exist numerous studies indicating the potential biological activities of Schiff base metal complexes with donor oxygen, sulfur, and nitrogen atoms. Their applicability across numerous domains, stability, and ease of preparation are among the major factors that caught attention of researchers in the field of bioinorganic chemistry *(*Adil *et al.,*2019). Schiff bases have attracted considerable attention of organic chemists due to their significant biological activities. They used as substrates in the preparation of several industrial and biologically active compounds. Moreover, Schiff bases are also known to have biological activities such as antimicrobial, antifungal and anti-bacterial anti-virus agents, antioxidants, radical inhibitors, anti-tumor agents, antimalarial, anti-proliferative, anti-inflammatory, antiviral and antipyretic, anti-hypertensive, herbicidal (Siham, 2023).

2.1.1. Methods for the Synthesis of Schiff base Ligands

Schiff base ligands, a class of molecules having imine groups, have grown in popularity due to their physiological and pharmacological properties. Many studies have been conducted on the synthesis of Schiff bases. They have been synthesized using conventional and green synthetic methods (Scheme 2.3). Heat is required in many condensation processes, and conventional reaction conditions often involve heating the reactants in a metal, oil, or sand bath for hours or even days (Ramhari *et al.*, 2022).

Schiff bases are mostly synthesized by the condensation reaction of amines with aldehydes or ketones under conventional or microwave heating. Since the first reported procedure by Schiff in 1864, tremendous efforts have emerged regarding the successful synthesis of a diversity of molecules with this functional feature (Kareem, 2022).

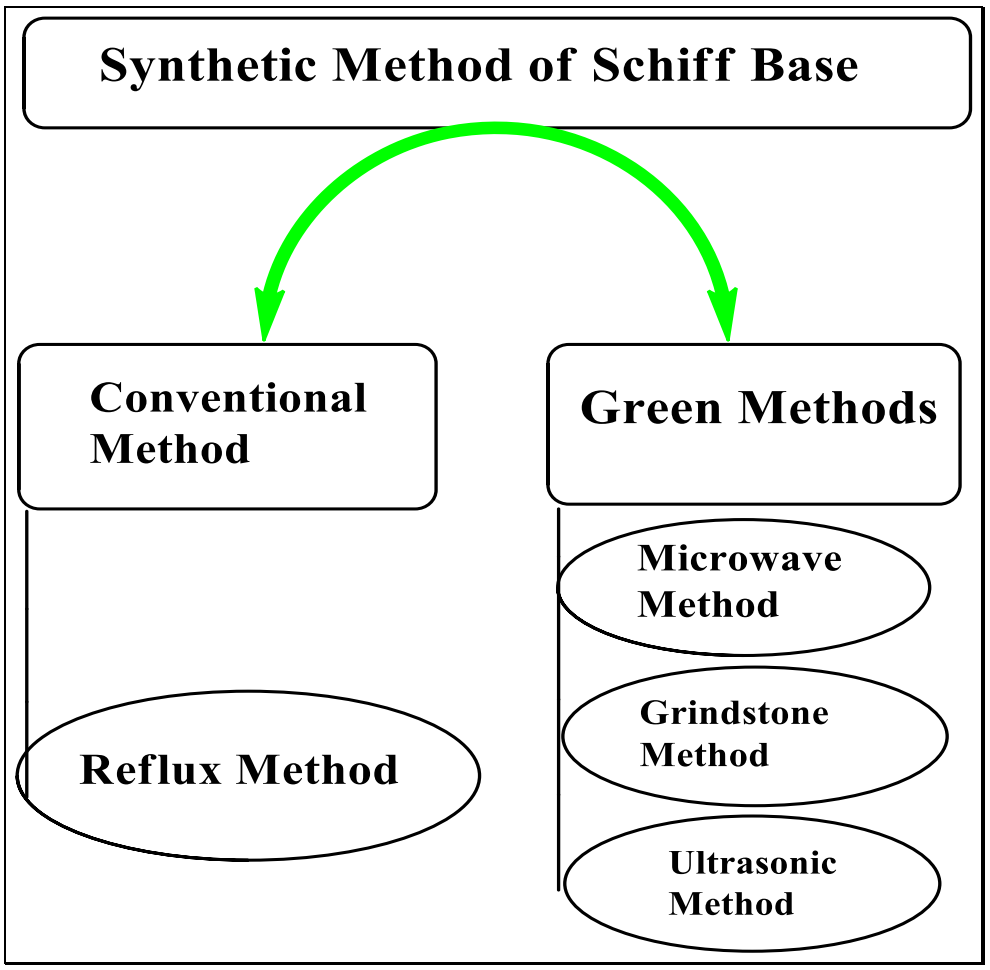

Figure 2.5: Synthetic methods for the Synthesis of Schiff base ligands (Ramhari *et al.*, 2022)

Microwave-assisted synthesis of Schiff bases could be carried out without solvent or low-solvent conditions and reduced reaction time to improve conversion and increases selectivity. Since its development, solvent less microwave synthesis of Schiff bases, has become the most well-known and simple technique for these reactions and is used in various applications. Many researchers reported the use of microwave-assisted synthesis of various types of Schiff bases and their derivatives (Ramhari *et al.*, 2022).

Using a mortar and pestle to ground the substrate crystals and reagent, the grindstone method reaction generates localized heat. Reactions initiated by grinding, which uses friction to transfer a very little amount of energy. Glassy substance can occasionally formed by a combination and reagents. Reactions regarded as more affordable and environmentally beneficial in chemistry since they are easy to manage, remove contaminants, and run at a relatively lower cost. Solid-state

reactions are more efficient and selective than solution reactions due to the tightly packed, regular arrangement of molecules in a crystal (Ramhari *et al.,* 2022).

Conventional Method

The conventional method of synthesis of the Schiff base involves refluxing or stirring different aldehydes or ketones with various types of primary amines. Recent reports confirm that green approaches that avoids the use of harmful organic solvents and improve selectivity, reduce reaction time, and simplify product isolation over conventional methods have become alternative approaches for the synthesis of variety of Schiff base ligands (Ramhari *et al.,* 2022). The Synthesis of Schiff bases involves the condensation of different aromatic amines (0.004 mol) and salicylaldehyde (0.004 mol) in 10 milliliters of water, followed by a stirring process at room temperature. TLC was used to track the reaction's advancement. The product was separate from the methanol once the reaction was complete, and it had a yellow color. It was then filtered, dried, and recrystallized (Chu *et al.,* 2019).

Microwave Method

The synthesis of amino acid Schiff bases in water using grindstone chemistry, microwave irradiation, and conventional heating in conjunction with alanine amino acid stirring at room temperature and variably substituted aromatic aldehydes/heterocyclic aldehydes. Research comparing the amount of time needed to synthesize four different Schiff bases under four different conditions discovered that although the grindstone approach produced a higher yield of product, it also took a lot longer than processes. After the reaction mixture was left overnight (8 h) and ground for 30 to 35 minutes, product yields varied between 72 and 78%. In 40–45 minutes, at room temperature (15–20°C), the reactants were agitated in water to produce product yields of 69–73% (Ramhari et al., 2022). In a microwave tube, salicylaldehyde (0.004 mol) and substituted aromatic amines (0.004 mol) in 1 mL of water were added. For around 30 to 2 minutes, the contents were exposed to 200W of microwave radiation. TLC tracked the reaction's advancement. Once the reaction was finished, a solid product was formed in the reaction mixture, which was then filtered and used methanol to recrystallize it. The title compounds are obtained as solid crystals through recrystallization (Chu *et al.,* 2019).

Compounds synthesized by standard heating methods and microwave radiation. Yields of 70–72% obtained under microwave irradiation in 5–6 minutes, which is significantly faster than the grinding process. The approach yielded the highest yield and the lowest reaction time.

Sonication is the process of exciting particles for a variety of reasons using high power. Ultrasonication is a procedure that typically uses ultrasonic at frequencies higher than 20 kHz. It is usually utilized in the lab in conjunction with an ultrasonic bath or probe, which is referred to as a sonicator (Ramhari *et al.*, 2022).

2.1.2. Quinolines Derivative Schiff Base Ligand

Quinolines are aromatic compounds that consist of a benzene ring fused with a pyridine heterocyclic system. Quinolines are known also as benzo[b]pyridine and 1-azanaphthalene with one nitrogen atom in one benzene ring and none in the other ring or at the ring junction. Heterocycles containing a nitrogen atom possess high and interesting medicinal and pharmaceutical properties (Wafaa *et al.,* 2018). The chemistry of quinoline-2,4-diones is unique due to their roles in natural and synthetic chemistry and their biologically and pharmacological activities (Ashraf *et al.,* 2020). Interesting pharmacological properties have been associated with 2-chloroquinoline-3-carbaldehydes and their derivatives, have shown antimicrobial, antimalarial, anti-inflammatory, antitumor and anti-parasitic activity (Bakr *et al.*,2012).

Quinoline is classified under the alkaloid class of natural products and is present in various plants, pharmaceuticals, agrochemicals, and dyes. It had used as a chelating agent due to its N-donor ligands in coordination chemistry to form complexes. Quinoline and its derivatives have numerous applications in the biological field such as to design of many synthetic compounds with diverse pharmacological properties. Interesting pharmacological properties have been associated with quinoline derivatives like 2-oxo-quinoline, 2-chloro-quinoline, and 2-chloroquinoline-3-carbaldehyde shows antimicrobial, antimalarial, anti-inflammatory, antitumor, anti-parasitic, antiproliferative, antineoplastic, antidiabetic, antifungal, cytotoxic activity, anticonvulsant, antiviral and anticancer activities (Bakr *et al.*, 2012; Damena *et al.,* 2022a; Damena *et al.*, 2022; Patil *et al.*, 2021; Rajewar *et al.*, 2015; Shah *et al.*, 2024).

In nature, quinoline and quinolone (Figure 2.1) are abundant and typically function as structural building blocks of more complex natural compounds. Quinoline and quinolone derivatives are significant classes of bioactive heterocyclic compounds in the pharmaceutical industry because of their varied pharmacological qualities, which include antibacterial, anti-inflammatory, anti-cancer, anti-HCV, anti-tubercular, anti-malarial, anti-HIV, and anti-alzheimer effects (Chu *et al.,* 2019).

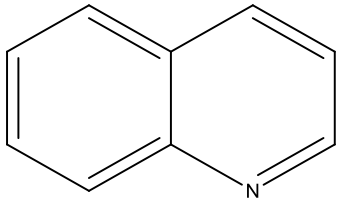

Figure 2.1: Quinoline structure

Quinolines are widely distributed, physiologically active natural and manmade chemicals that are pyridine derivatives. Their Schiff base derivatives linked to several different medicinal uses. Even though several free Schiff base ligands known to be bioactive, research has indicated that adding metal to these ligands increases their activity. This has recently fueled the study of medications based on metals. The transition metal ions ruthenium, copper, zinc, cobalt, and platinum thought to be possible biological agents. Nonetheless, there is growing interest in investigating the potential cytotoxicity action of silver (I) and its complexes as effective DNA and protein binders, antioxidants, and antimicrobials (Adeleke *et al.*, 2021).

The antibacterial, antiproliferative, antineoplastic, antimalarial, anticonvulsant, and anti-inflammatory properties of quinoline and its derivatives are encouraging. Moreover, a quinoline derivative with anticancer properties has been identified; its mechanism of action includes disruption of cell migration, death, cell cycle arrest, and suppression of angiogenesis (Patil *et al.*, 2021). Quinolines are a class of synthetic bactericidal drugs having a wide range of activity and high bioavailability. These qualities make them promising treatments for a variety of infectious disorders, including those of the skin, urinary tract, respiratory system, bones, and gastrointestinal tract (Măciucă, 2020).

Quinoline and 4-quinolone (Figure 2.6) moieties were used as a scaffold for drug development. The most successful drug based on quinoline scaffold is chloroquine (Figure 2.7), which was specifically developed as antimalarial agent. Until today, numerous quinoline-based compounds and drugs were developed as antimalarial agents, designed to target all stages of parasite life cycle. In fact quinolines still serve as inexhaustible models for design and development of new semisynthetic or synthetic quinoline/quinolone antimicrobial agents (Chu et al., 2019).

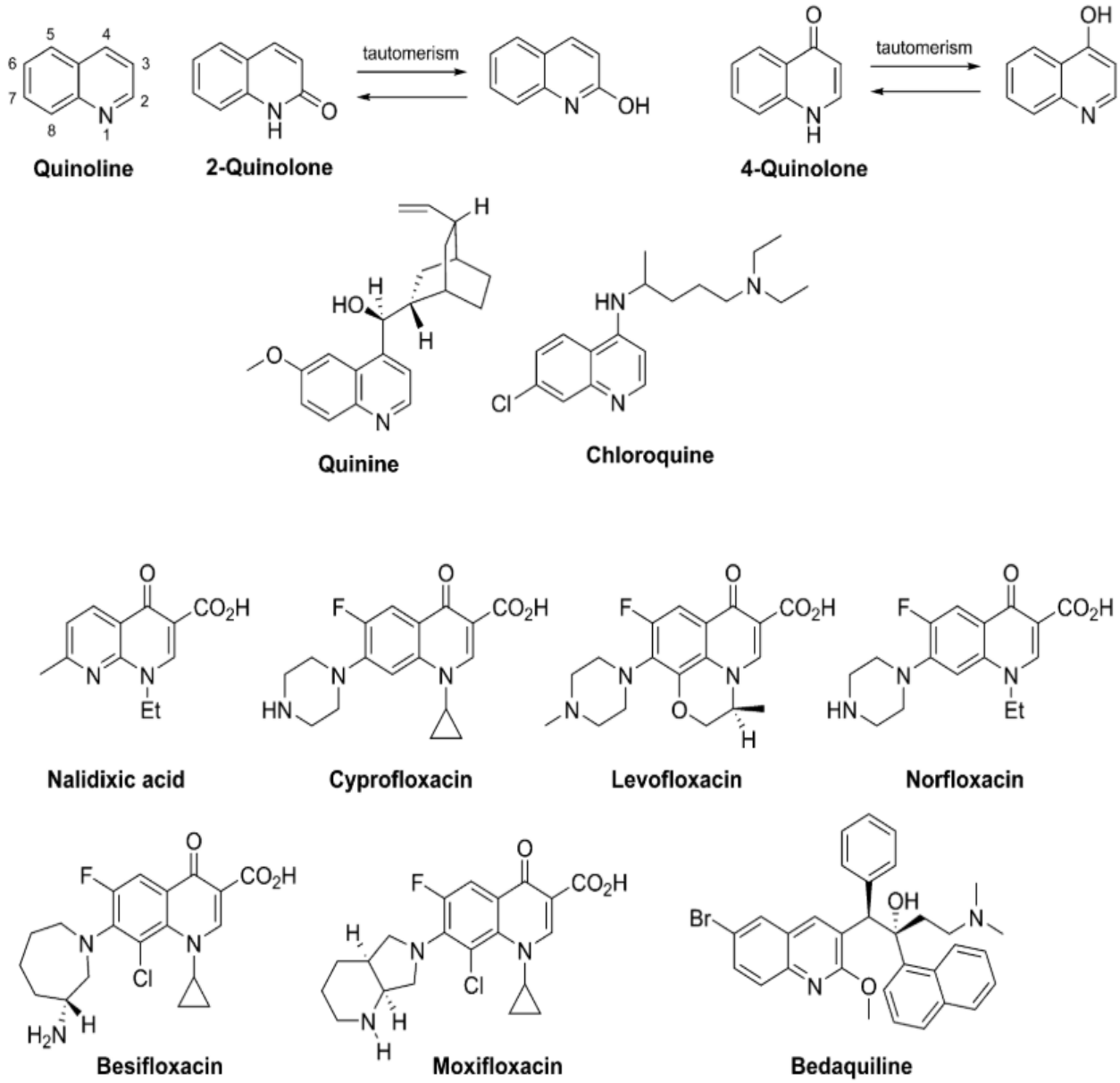

Figure 2.6: Quinoline and quinolone scaffolds and their best-known drugs (Spasi et al., 2020)

In this respect, complexes of metal ions with Schiff base derived from salicylaldehyde and amino acids have been synthesized and characterized by using different physical techniques and coordination geometry structures were proposed based on their results (Salama *et al.*, 2017).

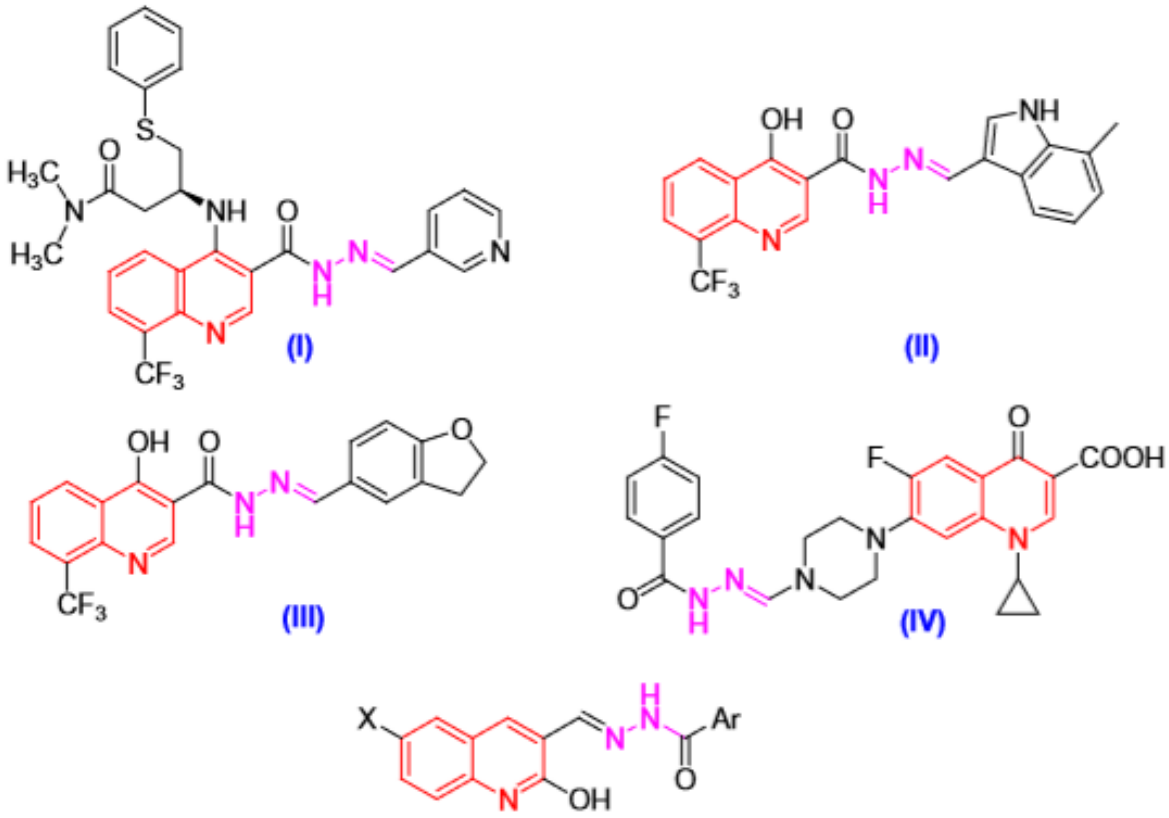

Figure 2.7: Some examples of Quinoline derivatives (Mandewale *et al.*, 2018)

2.1.3. Amino acids as primary amines for Schiff base synthesis

A molecule called an amino acid Schiff base is typically synthesized when an amino acid and several active carbonyl groups condense together (Ashraf *et al.,* 2020). Schiff bases are essential for the synthesis of many commercial and physiologically useful chemicals through replacement, cycloaddition, and closure reactions. They are also well known for having a variety of biological properties, including the ability to scavenge free radicals, inhibit allergies, reduce inflammation, and have analgesic and antioxidative effects, among others (Habila *et al.*,2020). Due to its numerous uses in a variety of industries, including sophisticated nanomaterials, chemotherapeutics, and the development of new drugs, Schiff bases have drawn a lot of attention (Ommenya *et al.,* 2020).

Amino acid Schiff base ligand typically, an amino acid and several active carbonyl groups condense to generate the Schiff base ligand. These are the condensation product of an active carbonyl group acting as an electrophile and an amino group as a nucleophile. Particularly

powerful chelating ligands with carboxylate, COO–, and azomethine –C = N– groups are amino acid Schiff bases ligands. These ligands easily bind to a variety of transition metal ions, generating chemically and thermally stable metal complexes (Ejidike *et al.,* 2015). Schiff bases still regarded as one of the potential groups of organic compounds for facile preparations of metallo-organic hybrid materials. In the past two decades, the properties of Schiff bases stimulated much interest for their noteworthy contributions to single molecule-based magnetism; material science, the interest in Schiff base compounds as analytical reagents is increasing since they enable simple and inexpensive determinations of different organic and inorganic substances (Siham, 2023).

In the field of metal-based pharmaceuticals, Schiff base chemicals and their metal complexes are exceptional. Schiff base complexes have been thoroughly investigated cognizant of their numerous medical applications (Ashraf *et al.,* 2020). Due to their structural varieties and unique characteristics, these are the most versatile studied ligands in coordination chemistry. The transition metal complexes with the various Schiff base ligands containing amino acids were of particular interest to the researchers because they are excellent biological organic chelates that readily react with aromatic carbonyl groups to form Schiff bases and, more intriguingly, with ortho-hydroxy aldehydes to form a tridentate Schiff base transition metal complex. These complexes are synthesized using amino acids, which also function as an efficient chelating agent (Sayed *et al.,* 2020).

Among the Schiff base derivatives, those having phenol moiety (Fig.2.8) have attracted considerable attention due to their wide range of biological activities. Metal complexes containing Zn, Cd, Co, Ni, Pd, Ag, and Hg have shown appreciable biological activities such as antimicrobial, antifungal, antioxidant and anticancer (Mohammed *et al.,* 2020). Sakıyan and co-authors have studied the *in-vitro* antibacterial and antifungal activities of five different amino acid Schiff bases derived from the reaction of 2-hydroxy-1-naphthaldehyde with glycine, L-alanine L-phenylalanine, L-histidine, L-tryptophan and the manganese (III) complexes of these bases against some Gram-positive (*Staphylococcus aureus and Bacillus polymyxa*) and Gram-negative (*Escherichia coli*) bacteria and the fungus *Candida albicans*. And their finding showed that the antimicrobial activities tended to decrease with the increasing size of the amino acid residues (Zoubi, 2013).

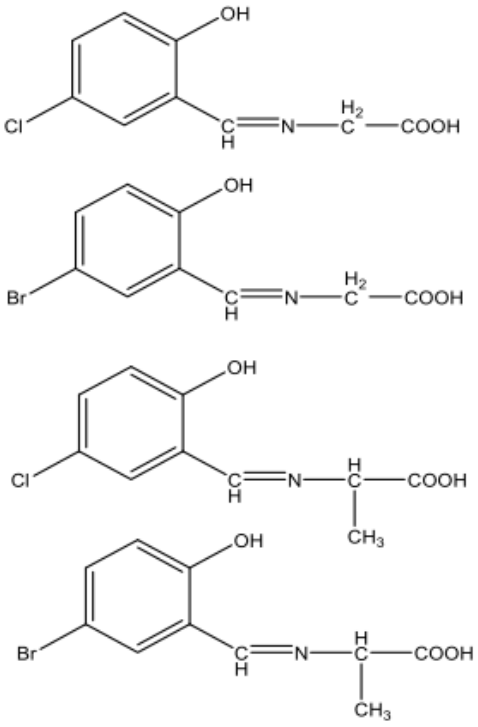

Figure 2.8: Some examples of Amino Acid Schiff Bases (Zoubi, 2013)

2.2. Schiff Base Metal Complexes

Metal complexes are prepared via the addition of the Schiff-base ligand to a metal precursor in an appropriate ratio together with suitable experimental conditions (Ejidike *et al.*, 2015). The transition metal complexes of ligands containing some heteroatoms, like oxygen, nitrogen and sulfur donors show the carcinostatic, antitumor, antiviral, antifungal and antibacterial activities (Aruna, 2017).

Like amines, amides, and phosphines, Schiff bases act as L-type ligands, in these complexes by donating two electrons without experiencing electron modifications on their valence shells. The electron donating ligand atom coordinates with the d-block metal ion to form the complex, which modifies the metal's steric and electrical environment. As a result, the metal ion's reactivity could stabilized and regulated, which is particularly helpful for less stable ions at higher oxidation states. Co(II) and Ni(II) ions, readily form complexes with bidentate and tridentate Schiff base ligands (Dhayalan, 2022).

Metal Schiff base complexes of Co(II),Cu(II) and Zn(II) have played a central role in the development of co-ordination chemistry. A characteristic of metals is that they easily lose electrons to form positively charged ions, which tend to be soluble in biological fluids. It is in this cationic form that metals play their role in biology. Metal ions are electron deficient, whereas most biological molecules such as proteins and DNA are electron rich. The attraction of these opposing charges leads to a general tendency for metal ions to bind and interact with biological molecules (Saddam *et al.*, 2018). Many biologically active compounds used as drugs possess modified pharmacological and toxicological potentials when administered in the form of metal-based compounds. Various metal ions potentially and commonly used are cobalt, copper, nickel and zinc because of forming low molecular weight complexes and therefore, prove to be more beneficial against several diseases (Pradeep *et al.*, 2023).

Schiff bases and their metallic complexes are the most important chemical compounds having common features in most of the essential compounds and active medicinal agents. These compounds have a broad range of applications. Schiff bases have important biological activities such as antioxidant, antibacterial, antifungal, anticancer, and antidiabetic. These compounds have considerable chelating capacity. The analysis of structure, activity, and mechanism of action of these compounds is required for the advances indicates that Cu(II) complexes of Schiff bases have good scavenging activity compared to others metal complexes of Schiff bases like Co, Zn, and Ni (Abdel-rahman *et al.*, 2022).

Schiff bases are widely studied ligands that coordinate to metal ions via azomethine nitrogen. In azomethine derivatives, the C = N linkage is essential for biological activity, and the presence of this group have made its complexes to be considered as important stereochemical models in the main group and transition metal coordination chemistry due to ease in preparation and variety in structure. The interaction of metal ions with N, O, and S atoms from Schiff base organic compounds has gained much attention in recent years and provided a passionate series of ligands possessing properties that can be modified by inserting different organic substituents, which bring about the variation in the fundamental donor properties. The use of Schiff bases in

biological or therapeutic applications as promising drug agents or biological probes and analytical tools has been reported by several researchers (Ejidike *et al.*, 2015).

2.3. Metal (II) complexes in biological process

Recently, metal ion(s) bearing pharmaceutical compounds used significantly in medicines. Various transition metals such as Co, Cu, Zn, Ni, Mn, Fe, V and Cr present in trace amount play a vital role in living organisms (Seema, 2020). Researchers are still interested in the chemistry of metal complexes with Schiff base ligands that have nitrogen and oxygen as donor atoms. Under various reaction circumstances, these ligands known to coordinate to the metal atom in different ways (Adeleke *et al.*, 2021).

Co(II), Ni(II), Cu(II), Zn(II), Cd(II), Hg(II), UO_2(II), and Th(IV) complexes, with X = Cl or NO_3 and Schiff base [L] derived from the condensation of benzofuran-2 carbohydrazide with 5-methylsalicylaldehyde or 5-chlororosalicylaldehyde, were synthesized, characterized, and subjected to antibacterial studies. The findings demonstrated that when the ligands assessed as metal complexes, their activity was increased. The antibacterial and antioxidant investigations of the unsymmetrical Schiff base complexes of Co(LL), Ni(LL), Cu(LL), and Zn(LL) have been reported by Ejidike and Ajibade 2015: From 2′,4′-dihydroxyacetophenone, ethylenediamine, and acetylacetone, (E)-4-[(2-{(E)-[1-(2,4-dihydroxyphenyl)ethylidene] amino}ethyl)imino]pentan-2-one.

Because of their extensive antibacterial and antifungal bioactivities, metal complexes, have find widespread application in the medical and pharmaceutical industries (Hanan *et al.*, 2020). Transition metal ions played a significant role in biological processes within the human body. They are present at the active sites of many enzymes or as structural elements of many of them (Patil *et al.*, 2021). They potential and affinity in DNA binding and cleavage under physiological circumstances have attracted attention (Demircioğlu, 2021). Essential metallic elements for life, manganese, cobalt, nickel, copper, and zinc show increased biological activity when they are part of specific metal protein complexes, involved in oxygen transport, electron transfer processes, or ion storage (Adeleke *et al.*, 2021). Nowadays, metal ions found in a number of inorganic pharmaceuticals that used as medications to treat a wide range of illnesses, from cancer to fungal and bacterial infections. Furthermore, the N-heterocycles, pyrazolones, and quinazolinone

derivatives serve as ligands and modify the complex's environment in a way that boosts their lipophilicity is an important aspect of drug design (Saddam , 2018).

Numerous medications have altered pharmacological and toxicological characteristics in the form of metal complexes, and it is likely that Schiff bases are adaptable C=N (Imine)-containing compounds with a wide range of biological activity. The addition of metals in the form of complexes has been shown to have some degree of antibacterial, antifungal, antitumor, and anti-inflammatory properties (Demircioğlu, 2021). Since the biological, chemical, and electrochemical activities of metal centers are governed and enhanced by the contact between the metal and the ligand, coordination compounds containing Schiff base ligand have been researched and produced extensively. Metal complexes with Schiff base ligands including halogen groups and both nitrogen and oxygen donor atoms are an interesting area of investigation because of their biological antibacterial properties (Julius *et al.*, 2023).

For chemists and researchers who have achieved pharmaco-therapeutic success in the field of treating severe diseases and improving a number of medications, coordination chemistry is an appealing field. Schiff bases are adaptable chemical compounds containing an imine group (azomethine, -C=N-), which are synthesized when primary amines condense with carbonyl compounds (Raman *et al.,* 2005).

Transition metal ions (Co, Ni, Cu, and Zn) are crucial for the diverse biological processes that drive the evolution of living things. The use of metal ions to biotic systems for the treatment of disease is the main area of study in the field of bioinorganic chemistry. A metal ion can easily get a positive charge by losing an electron, which enables it to dissolve in biological fluids. They operate in biological systems as positively charged ions. Proteins and DNA, which are rich in electrons, can easily bind and form associations with metal centers that lack electrons. Most of the research show that increased ligand bioactivity results from these metals' complexation with Schiff base ligand (Salama *et al.,* 2017). A class of chemicals known as copper complexes has been the focus of extensive investigation due to its potential medicinal implications, specifically as antibacterial and anticancer agents. It has been discovered that certain thiosemicarbazone copper complexes are active in both the suppression of DNA synthesis and the death of cells (Ajibade, 2015).

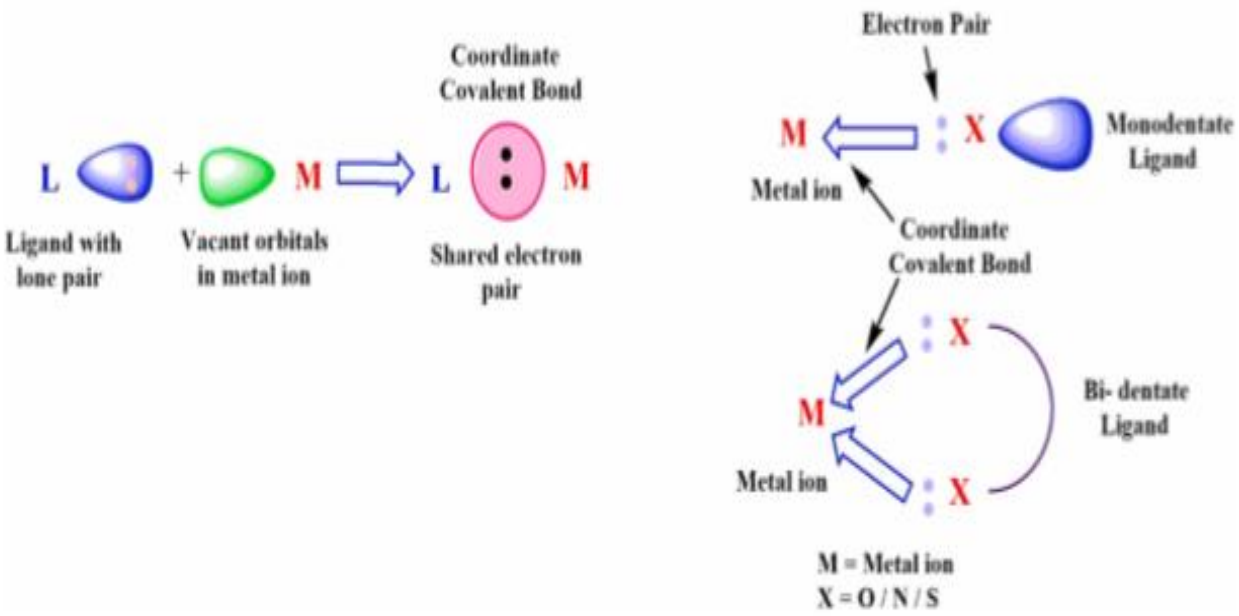

Scheme 2.9: General reaction mechanism of metal complex (Yusuf *et al.*, 2021b)

2.3.1. Nickel (II) complex

Nickel, as an essential trace element for human beings, animals, microorganisms, and plants, had known as a component in many enzymes, playing a crucial role in important metabolic reactions. In addition to this, various nickel (II) complexes have been synthesized and evaluated as metal-based drugs which demonstrated many bioactivities such as anticonvulsant, antibacterial, antifungal, antimicrobial, antioxidant, and anticancer (Li *et al.*, 2020).

Nickel (II) Schiff base complexes considered above other metals owing to their remarkable application in the biological and medicinal field. It had proved that nickel (II) and copper (II) ions could easily coordinate through oxygen and nitrogen donor atoms forming mono and polynuclear complexes having structural diversity and varying chemical activity. Schiff bases having N/O donor sites and their nickel/copper complexes (Aprajita, 2023).

The remarkable applications of nickel (II) Schiff base complexes in the biological and therapeutic fields have led to consideration of other metals among the group. It had demonstrated that oxygen and nitrogen donor atoms might readily coordinate nickel (II) ions to produce mono and polynuclear complexes with a variety of structural configurations and chemical activities. The

antiviral properties of Schiff bases with N/O donor sites and their nickel/copper complexes have been thoroughly investigated, with particular attention paid to their inhibitory effect on the major protease (Mpro) of SARS-CoV-2, applications for Schiff base-based metal complexes include antiviral capabilities (Aprajita, 2023).

A crucial component of the active centers of several enzymes in several microbial processes, including the carbon cycle involving CO dehydrogenase (CODH), acetyl-CoA synthase (ACS), and methyl-coenzyme M reductase (MCR), nickel is a potentially necessary trace mineral. A virulence-determining factor for Helicobacter pylori, a human stomach pathogen, is nickel. The pathogen possesses two kinds of nickel enzymes that are necessary for in vivo colonization: [NiFe] hydrogenase and urease. These enzymes that traffic in nickel contribute to virulence and are likely targets for treatment in the event of H. pylori infections. Since nickel is present in RNA, it thought that nickel affects how proteins function. It believed that nickel plays a role in both the synthesis of prolactin and the breakdown of glucose. The biological roles of nickel in plants and microbes are well understood, but its involvement in human biology are yet unknown (Aruna, 2017). All the prepared Schiff base ligands and their Ni(II) complexes were nonhygroscopic and stable at room temperature. The complexes were mostly insoluble in organic solvents except for DMF and DMSO (Aruna, 2017).

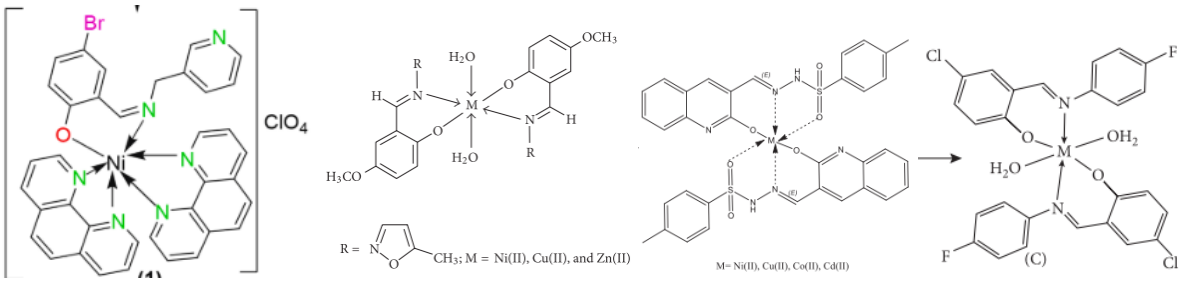

Figure 2.11: Some examples of Nickel Schiff base complexes (Aprajita, 2023; Ommenya *et al*., 2020;Kumar *et al.*, 2013; Patil *et al.*, 2021)

2.3.2. Copper (II) complex

Copper is found in all living organisms and is a crucial trace element in redox chemistry, growth, and development. It is important for the function of several enzymes and proteins involved in energy metabolism, respiration, and DNA synthesis. The major functions of copper in biological

compounds involve oxidation-reduction reactions in which copper containing biological molecules react directly with molecular oxygen to produce free radicals. Copper plays a pivotal role in cell physiology as a catalytic cofactor in the redox chemistry of mitochondrial respiration, iron absorption, free radical scavenging, and elastin cross-linking (Marzano *et al.*, 2009). Copper stands out among transition metals for its remarkable affinity for biological ligands and redox properties that make it an ideal metal to drive biochemical reactions involving redox and oxygen chemistry (Zabiulla *et al.*, 2023a).

Copper complexes characterized by great potential for biomedical applications, which is confirmed by numerous studies. Recently, much attention paid to the development and use of copper complexes with the superoxide dismutase (SOD) mimetic activity. To test free-radical-scavenging properties of drugs is a promising protocol for enlarging the applicability of the clinic drugs (Zabiulla *et al.*, 2023a).

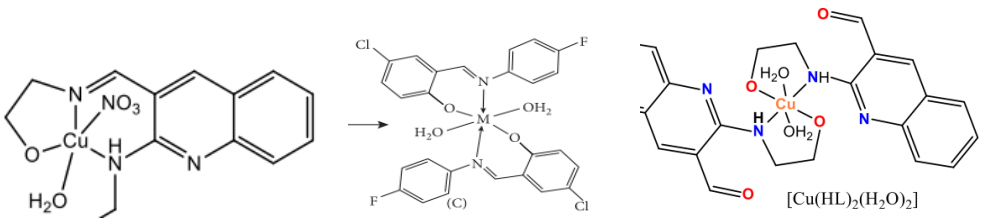

Figure 2.12: Some examples of Copper Schiff base complex (Damena *et al.,* 2022b, Ommenya *et al.,* 2020)

Cu(II) complexes tailored for various medical applications. An illustrative example is the application of Cu(II) indomethacin complexes as anti-inflammatory agents in veterinary medicine (Tufa *et al.*, 2018). On the other hand, Cu(II) based complexes recently come back into focus in inorganic synthesis investigations, where researchers have created Cu(II) complexes for a variety of medical reasons. For instance, Cu(II) indomethacin complexes used as anti-inflammatory drugs in veterinary medicine (Tufa *et al.*, 2018). Several investigations have shown copper complexes to have a high potential for biomedical uses. With its exceptional affinity for biological ligands and redox characteristics, copper stands out among transition metals as the best metal to drive biochemical reactions (Demircioğlu, 2021; Raczuk *et al.*, 2022).

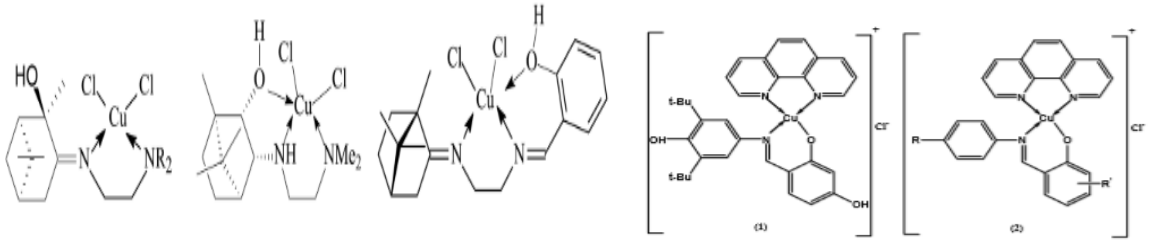

Figure 2.13: Copper Schiff base complexes (Gur'eva *et al.*, 2022; Zoubi, 2013)

2.3.2. Zinc (II) complex

Among the transition metals, Zinc is the second-most prevalent trace metal in the human body and has the ability to catalyze over 300 enzymes, including those involved in the production of DNA and RNA (Aljahdali *et al.*, 2020). The anti-inflammatory, antidiabetic, antioxidant, and antibacterial properties of Zn (II) complexes have also been shown in studies (Damena *et al.*, 2022a). An *in vitro* antibacterial activity study against four bacterial species, including *Escherichia coli*, *Pseudomonas aeruginosa* (Gram-negative), *Staphylococcus aureus*, and *Bacillus subtilis* (Gram-positive), was demonstrated in prior studies of Zn (II) complexes of quinoline derivative ligands (Abdel-rahman *et al.*, 2022; Damena *et al.*, 2022a). The results of *in vitro* test showed a moderate antibacterial activity compared with standard drug.

Zn(II) d^{10} electronic configuration permits a wide range of symmetries and coordination numbers. Since d^{10} configuration affords no crystal field stabilization, the stereochemistry of a particular compound depends on the size, polarizing power of the Zn(II) cation and the steric requirement of the ligands. The electronic spectra of complexes reveal a charge transfer bands π-π and n-π transitions in the vicinity of the Schiff base ligand and complexes, suggesting square planar geometry (Kouser *et al.*, 2023).

Zinc (II) metal complexes have shown significant antifungal activities compared to its Schiff base ligand and moderate antibacterial activity. Schiff base Zn(II) metal complexes can be used not only as an approach to enhance their activity but also to overcome the drug resistance (Yamgar *et al.*, 2014). Study of Zinc (II) complexes of Schiff bases and nitrogen donor ligands has become a focal point of interest for researchers in recent times, not only for their varied structural features, but also for their potential application in various fields (Spasić *et al.*, 2020).

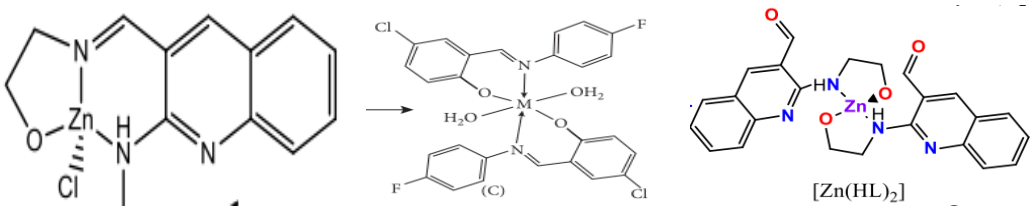

Figure 2.14: Zinc Schiff base complexes (Damena *et al.*, 2022b, 2022a; Ommenya *et al.*, 2020)

2.4. Synthesis of Schiff bases and their complexes

2.4.1. Synthesis of Schiff base ligands

In the synthesis of Schiff bases, electrophilic carbonyl compounds attacked by nucleophilic amines through a nucleophilic addition process, resulting in the formation of a hemi-aminal group. This hemi-aminal group subsequently dehydrated to produce imine compounds. The amine combines with the ketone or aldehyde in the initial step of the process to produce the unstable addition product carbinolamine. Carbinolamine dehydrates when it is catalyzed by an acid or a base (Ramhari *et al.*, 2022). Dhanaraj and Raj described the synthesis of SB ligand in two steps. First step included the refluxing of ethanolic solution of 4-aminoantipyrine and acetamide to yield 4-aminopyridine derivative. In the second step, ethanolic solutions of p-phenylenediamine were refluxed in order to get the SB ligand (Alka *et al.*, 2023).

The Schiff base ligand *E*)-2-(((7-chloro-2-hydroxyquinolin-3-yl) methylene) amino)-3-phenylpropanoic acid and (*E*)-2-(((7-chloro-2-hydroxyquinolin-3-yl) methylene) amino)-3-methylbutanoic acid was synthesized by refluxing an equimolar amount of 2,7-dichloroquinoline-3-carboaldehyde and Phenylanine/Valine in a 30 mL ethanol solution. A few drops of glacial acetic acid added into the organic phase reaction, which subjected to continuous string for a duration of 5hr. The yellowish precipitate that formed was filtered, washed and dried at room temperature for a day (Venkatesh *et al.*, 2024).

Primary amines react with aldehydes or ketones to form Schiff bases. The great stability and suitable solubility of Schiff bases in common solvents make them useful as ligands in many applications. An enormous amount of interest is generated by the properties of metal complexes, particularly Schiff base ligands, and their numerous uses. Because the ligand structures can change depending on which aldehyde and amine are utilized, the field of Schiff base complexes is expanding quickly (Leila *et al.*, 2019). An ethanolic solution (50 cm^3) of 3-

salicylideneacetylacetone (1.02 g, 0.05 mol) and 4- aminoantipyrine (2.03 g, 0.01 mol) was boiled under reflux for 3h. The resultant solution was cooled to room temperature. The yellow solid 3-salicylidene-2,4-di (imino-4′- antipyrinyl) pentane (3SDAP) formed was filtered and recrystallized in EtOH (Raman *et al.,* 2005).

.

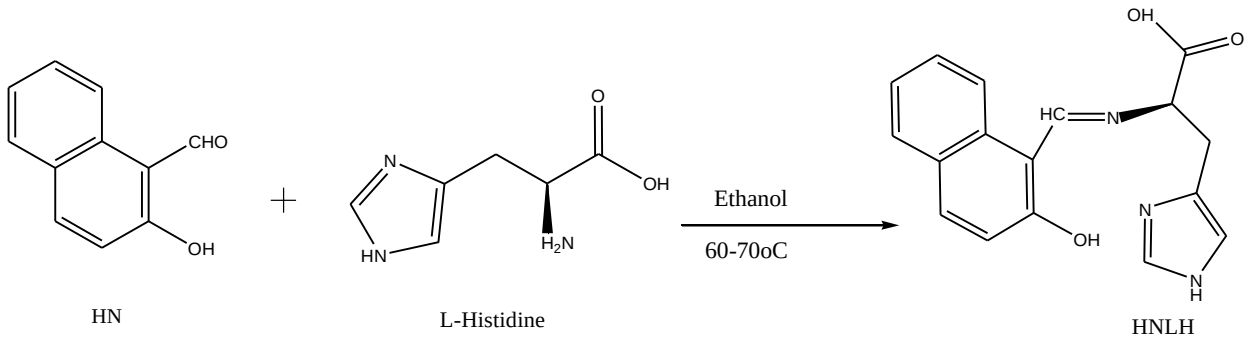

Where R= Cys,His and Try

Figure 2.15: Synthesis of Schiff base ligands using amino acids (Eunice *et al.,* 2020; Salama *et al.,* 2017; Sayed *et al.,* 2020)

The chemical compounds containing azomethine group called Schiff bases are an excellent class of ligands and are widely used in coordination chemistry. These chemicals have the ability to react with metal ions producing versatile coordination metal complexes, which have wide applications in different fields. It is well established in the literature that the presence of the main functional azomethine group (–CH=N–) in the structure of the Schiff bases is a characteristic feature of these compounds and responsible for their various biological potentials and medicinal actions (Hanan, 2020).

2.4.2. Synthesis of metal complexes

Metal complexes of Cu(II), Ni(II) and Zn(II) were prepared by refluxing 1:1 molar mixture of metal chlorides of selected metals with Schiff base ligand for an hours. The solid complex

obtained was filtered and dried for a day (Dhayalan, 2022). Novel metal complexes of the Schiff base ligand, (*E*)-2-(((7-chloro-2-hydroxyquinolin-3-yl) methylene) amino)-3-phenylpropanoic acid and (*E*)-2-(((7-chloro-2-hydroxyquinolin-3-yl) methylene) amino)-3-methylbutanoic acid have been synthesized in EtOH in a 1:1 (M:L) molar ratio in EtOH, Where, M = Ni(II), Cu(II) and Zn(II). By using, the experimental procedures that previously reported. The coloured solid complexes were obtained and were filtered off, ethanol-washed and finally allow to dried at room temperature for a days (El *et al.*, 2022).

Vinusha and co-workers 2019, described the synthesis of SB ligand by taking 5-amino-4H-1,2,4-triazole-3-thiol and 3-hydroxy-4- methoxy benzaldehyde. The metal Co(II), Ni(II) and Cu(II) chloride salts were taken in 2L:1M stoichiometric ratio for the synthesis of metal complexes. The structural analysis of Ligand and its metal chelate carried out by using proton/carbon NMR, mass, FT- IR and TGA spectroscopic techniques. The analysis results confirmed tridentate nature of Ligand and octahedral geometry of complexes (Alka *et al.*, 2023).

Metal complexes synthesized by the following general method. To a solution of the Ligand in hot ethanol (10 mL) in a round bottle flask was added appropriate metal salt dissolved in the minimal amount of ethanol: $NiCl_2 \cdot 6H_2O$, $CoCl_2 \cdot 6H_2O$ and $CuCl_2 \cdot 2H_2O$. The solutions mixtures refluxed with stirring for two hours. The resultant solution cooled at room temperature for overnight. Thus, the formed complex was filtrated, collected, and then washed several times with hot ethanol until the filtrate becomes colorless. The complex was dried in desiccator over silica gel (Hasan *et al.*, 2021).

Metal complex synthesized by dissolving dehydrated metal chloride salt into 20 mL of ethanol with continuous stirring at room temperature (Fig 4.3 and 4.4). The Schiff base ligand dissolved in 30 mL of ethanol in a separated beaker. The two solutions mixed in a 250 mL round bottom flask and the pH of the mixture adjusted to the 6–8 range using a 25% ammonia solution. The mixture was set to react for one hour at room temperature with constant stirring before refluxing. The mixture then refluxed for five hours at temperatures between 80-90^{o}C, while tracking the reaction progress using TLC. Following the reaction's completion, the mixture was cooled to room temperature, filtered, and washed using ethanol before being allowed to dry at

room temperature (Alhazmi *et al.*, 2022; Kapadnis *et al.*, 2016; Joshi *et al.*, 2022; Muleta *et al.*, 2022; Sumathi, 2022; Tufa *et al.*, 2018).

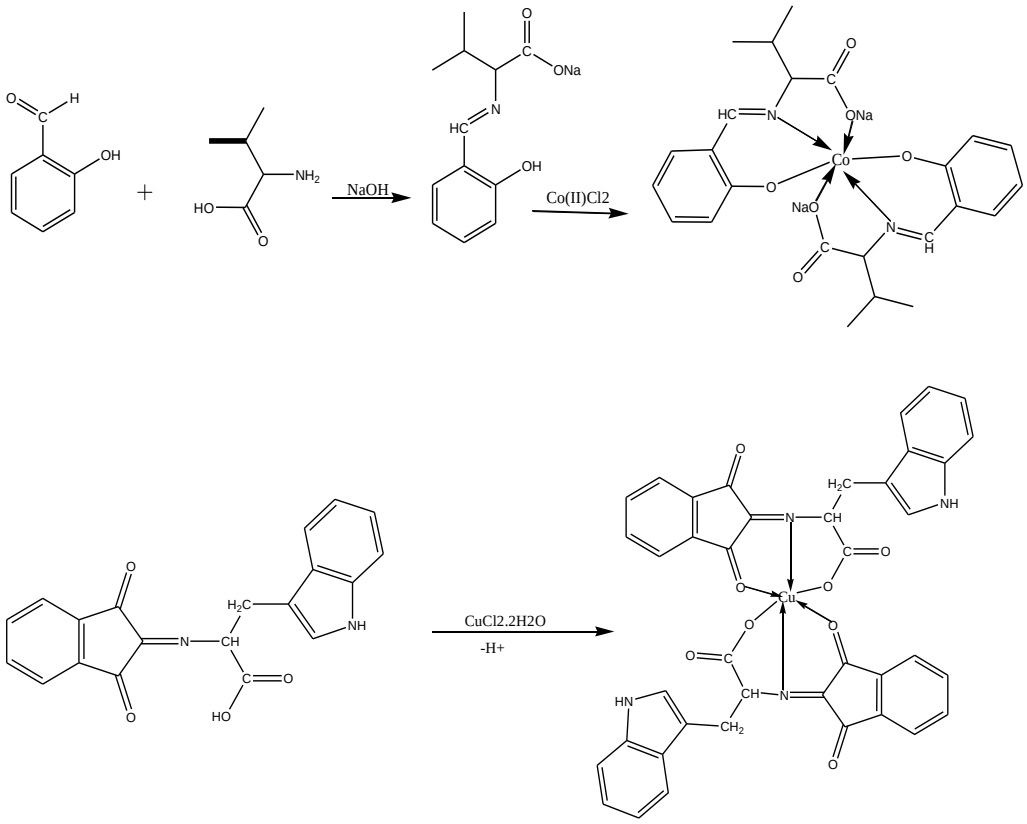

Figure 2.16: Synthesis of Amino acid Schiff base Metal complexes (Eunice *et al.*, 2020; Salama *et al.*, 2017; Sayed *et al.*, 2020)

Report indicates the targeted coordination; metal complexes were prepared successfully by reacting to the metal salts of the selected metals with the prepared Schiff base ligands in (1:2) stoichiometric ratio. The separated metal complexes were stable solids at room temperature and nonhygroscopic. They were solids insoluble in common organic solvents but soluble in DMF and DMSO. All prepared metal complexes had high melting points (above 300°C). The elemental analysis measurements suggested 1:2 metal to ligand stoichiometric ratio forming tetra-coordinate monomeric Cu(II) and Zn(II) metal complexes (Hanan, 2020).

Co(II), Ni(II), Cu(II), and Zn(II) complexes of Schiff base ligand have been prepared from the condensation of cuminaldehyde and L-histidine. The spectral data and magnetic measurements suggested that Co(II) and Ni(II) complexes are tetrahedral, whereas Cu(II) complex possesses a

distorted square-planar geometry. XRD revealed that Co(II), Cu(II), and Zn(II) complexes are crystalline in nature, whereas Ni(II) complex is amorphous (Ejidike *et al.*, 2015). The Schiff bases purified by recrystallization using hot ethanol and were in good yields (78–94%). They were mostly yellow colored and were soluble in hot ethanol, N,N-dimethylformamide and dimethyl sulfoxide (Hanan *et al.*, 2020).

The Schiff base ligand is soluble in hot ethanol and solvents such as DMF and DMSO. The imine and its metal (II) complexes are colored solids, which are stable in air. The complexes were insoluble in common organic solvents such as methanol, dichloromethane, ethanol, and acetone but soluble in DMSO and DMF. The melting points of the complexes were higher than that of the Schiff base ligand indicating that the complexes are more stable than the ligand (Ommenya *et al.*, 2020).

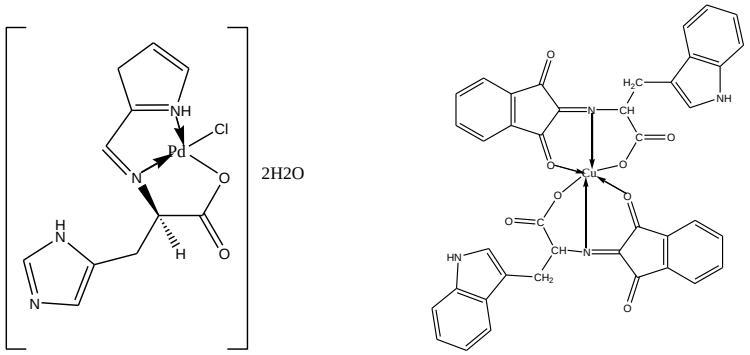

Figure 2.17: The structure of Amino acid Schiff base metal complexes (Eunice *et al.*, 2020; Sayed *et al.*, 2020)

2.5. Characterization of the Schiff base and its metal complex

Several methods, conventional and modern, are available for the characterization of ligands and their metal complex compounds. The synthesized Schiff base ligands (*E*)-2-(((7-chloro-2-hydroxyquinolin-3-yl) methylene) amino)-3-phenylpropanoic acid and (*E*)-2-(((7-chloro-2-hydroxyquinolin-3-yl) methylene) amino)-3-methylbutanoic acid and their corresponding metal complexes. Were distinctly colored and characterized by using physical and spectroscopic techniques using FT-IR, UV-Vis, ^{1}H NMR, ^{13}C NMR TGA/DTA, pXRD techniques and density functional theory (DFT) calculations (Al-Shboul *et al.*, 2022).

2.5.1. FT-IR spectroscopy

The IR spectra of the synthesized molecule reveal the presence of every specified functional group. The IR spectra of the complexes ML were compared to those of the free ligand L in order to validate the chelation of the ligand to metal ion M(II). In the case of complexes, the ν(C=N) vibration is assigned a weak band between 1611 and 1624 cm^{-1} in the IR spectra; for the free ligand L, this band appears at 1632 cm^{-1}. This negative shift, ν(C=N) = 8 to 23 cm^{-1}, can be ascribed to the coordinated metal's electron-withdrawing effect, which lowers the imine bond's ν(C=N) frequency by reducing the electron density. This implies that the imine group's nitrogen atom participates in complexation with metal ions. Further confirmation of the complexation between the ligand L and metal ions can be obtained by looking for new bands between 534–686 cm^{-1} and 449–626 cm^{-1}, which correspond to ν(M–N) and ν(M–O), respectively (Salen *et al.*, 2023). The ligand revealed that the phenolic OH group is responsible for a band at 3400 cm^{-1}. All of the complexes' absence of the νOH band points to the phenolic group's subsequent deprotonation and the coordination of its oxygen with the metal ion (Vairalakshmi , 2019). Strong bands in the 3140.3–3446.6 cm^{-1} area was also visible in the complexes FT-IR spectra, indicating the presence of coordinated/lattice water inside them. The appearance of a non-ligand band in the 692.6–699.7 cm^{-1} region served as additional confirmation (Ommenya *et al.,* 2020;Ajibade, 2015).

2.5.2. UV-Visible spectra

The UV-Vis spectra of ligand and metal complexes ML recorded in DMSO at 298 K in 200 – 800 nm. The ligand showed four absorption bands that appeared in the range of 257-414 nm. The first band assigned to π→π* transition related to molecular orbitals localized on phenolic chromophore. The second and the third bands are attributed to π→π* and n→π* transitions of imine chromophore. The lower energy of the observed fourth band may be related to charge transfer transitions from bonding orbital of donor atom of ligand to non- or anti-bonding orbital of metal (LMCT) or metal to ligand (MLCT) (Salen *et al.*, 2023;Vairalakshmi, 2019). The nature of the ligand field around the metal ion assumed from the electronic spectra. The bands at 329, 339 and 378 nm are attributable to intra-ligand π-π* and n-π* transitions. In the electronic spectra of the complexes, the intra-ligand transitions are slightly shifted as a result of coordination in the region at 374–380 nm (Ajibade, 2015).

2.5.3. NMR Spectral Analysis

The ^{1}H and ^{13}C NMR spectra of the Schiff base ligand and its diamagnetic Zn(II) complexes recorded in DMSO-d_6. The ^{1}H NMR spectrum of the Schiff base showed a singlet peak at $\delta = 8.92$ ppm corresponding to the azomethine proton (–N=CH–), an indication that the Schiff base was formed during the condensation reaction. Observation of a peak at $\delta = 162.82$ ppm in the ^{13}C NMR spectrum was further proof that the ligand was successfully synthesized (Ommenya, 2020).

2.5.4. TGA/DTA analysis

The thermal stability of the metal complexes investigated based on the TGA and DTA method within a temperature range from room temperature to 1000 °C. The curves indicated the absence of hydrated and coordinated water and revealed that all complexes are stable until 300 °C and show a stage of decomposition after this temperature (Salen *et al.,* 2023).

2.5.5. pXRD analysis

Shimadzu 6100 diffractometer (Cukα = 1.54060 Å) was used to examine the crystal proprieties of all compounds, X-ray working parameters, which are 40 kV/30 mA, with 0.02° step, with a start of 5° and stop 80° diffraction angle and continuing scanning mode, were used for the measurement taken (Salen *et al.*, 2023).

2.6. Biological Application of Schiff bases and their metal complexes

The advances in the field of bio-inorganic chemistry increases the interest in Schiff base complexes, keeping the idea in mind that many of these complexes may serve as models for biologically important species (Yusuf *et al.,* 2021a).

The bioactivity of Schiff base compounds as antibacterial, antiradical, anticancer, antifungal, and antiviral agents has been reported (Ejidike *et al.,* 2015). Yu-Ye Yu *et al*. synthesized Mn(II), Co(II), Ni(II), Cu(II) and Cd(II) complexes with Schiff base ligand 2-[(4-methylphenylimino) methyl]-6-methoxyphenol, obtained by condensation of o-vanillin (2-hydroxy-3-methoxybenzaldehyde) with p-toluidine have been tested *in vitro* to evaluate their antibacterial activity against bacteria, viz., *Escherichia coli*, *Staphylococcus aureus* and *Bacillus subtilis* (Saddam *et al.,* 2018). The *in vitro* biological activities of the synthesized compounds

against the bacterial strains *E. coli*, *B. subtilis*, *P. aeruginosa*, and *S. aureus* and fungal species *A. niger*, *A. flavus*, and *C. albicans* using the disc diffusion method indicated that the complexes exhibited more activity than the ligand (Ejidike *et al.*, 2015).

Valine, Leucine and Isoleucine Schiff base ligands free ligands are biologically active against gram positive bacteria (*Staphylococcus aureus and Bacillus subtilis*) and gram negative bacteria (*Escherichia coli and Pseudomonas aeruginosa*), their Co(II) complexes show more bacterial activity against most bacterial species. The ligands are inactive against fungi (*Candida albicans and Aspergillus flavus*) but their complexes better show activity against *Candida albicans*. These results may be explained on the bases that the metal complexes penetrate more easily through the bacterial cell wall, due to the protein denaturation of the sulphydrile group, destroying the bacterial cell wall (Salama *et al.*, 2017).

On the other hand, transition metal complexes resulting from the coordination between Schiff bases and metal salts have drawn considerable interest in several domains. They are widely reported to display good photochromic, catalytic, and optoelectronic properties. They display also potent biological actions such as antibacterial, antifungal, anti-inflammatory, antiviral, antioxidant, antiproliferative and anticancer, etc. View this diversity of applications that exhibit Schiff's bases and their corresponding metal complexes, particularly those obtained from diamines and salicylaldehyde. Importance was hence given to studying these systems in our laboratories (Salen *et al.*, 2023).

Metal complexes of Schiff base ligands possess a variety of applications in the biological, analytical, clinical, and industrial areas. In recent times, transition metal complexes of Schiff base ligands have gained considerable attention, not only due to their spectroscopic properties and applications but also due to their remarkable antifungal, antibacterial and antitumor activities (Siham, 2023). Schiff base compounds and their metal complexes are outstanding in the field of metal-based drugs. The Schiff base complexes have been extensively studied in this perspective due to their wide applications in medicine (Kareem, 2022).

Transition metal complexes have attracted curiosity due to DNA binding and cleavage properties under physiological conditions. Applications of metal complexes as chemical nucleases are the focus of current research. It has been demonstrated that inorganic complexes as chemical

nucleases are the focus of current research. It has been demonstrated that inorganic complexes can be used in foot printing studies as sequence specific DNA binding agents, as diagnostic agents in medicinal applications and for genomic research (Vinusha *et al.,* 2019).

2.6.1. Antibacterial activities of Schiff base ligand and its metal complexes

Infectious diseases that directly related to bacteria exhibiting multiple resistances to antibiotics have increased the world's mortality rate. Therefore, the need to develop novel antibacterial drugs with excellent mechanisms of action and structural-activity relationship has become an urgent biomedical necessity. Schiff base ligands and their biologically active complexes providing potential sites for biochemically active compounds had studied extensively over the past few decades for their antimicrobial and anticancer properties. Schiff base-transition and inner-transition metal complexes are one of such adaptable and thoroughly studied systems used as model molecules for biological oxygen carrier systems. Transition metals involved in various biological processes are essential to life processes; hence, they can coordinate with O- or N-terminals from proteins in a variety of models, play an important part in the conformation and utility of living macromolecule and act as an antimicrobial agent, this interesting biological activity could be enhanced upon the complexation with the metal ions (Ejidike *et al.*, 2015). Schiff bases are one of such compounds bearing core molecular scaffolds found in natural products (Chioma, 2019).

The antibacterial activity of Schiff base and its complexes was evaluated using disc diffusion concept of the Kirby–Bauer sensitivity test. Human pathogens such as *Bacillus subtilis, Staphylococcus aureus, Escherichia coli,* and *Proteus mirabilis* are reported (Vairalakshmi, 2019). The higher antibacterial activity of Schiff base metal complexes than the free Schiff base ligands can be explained by chelation of the Schiff base with metal ions as metal chelates display both polar and nonpolar properties; this makes them suitable for permeation into cells and tissues. The polarity of the metal ion be reduced largely due to the overlap of the ligand orbital upon chelation, and partial sharing of the positive charge of the metal ion with donor groups. Chelation increases the delocalization of π-electrons over the entire chelate ring and enhances the penetration of the complexes into lipid membranes. It also increases the hydrophilic and lipophilic nature of the central metal ions, probably leading to liposolubility and permeability through the lipid layer of

cell membranes. Further, lipophilicity, which controls the rate of entry of molecules into the cell, is modified by coordination, so the metal complex can become more active than the free Schiff base ligand (Ajibade, 2015).

The biological activities of the Schiff bases were less than that of the standard, *Ampicillin*. In addition, metal complexes were more effective than the ligands. Nevertheless, this phenomenon is probably because of the more lipophilic feature of the complexes. Additionally, the enhanced metal chelates activity can be clarified based on Overtone's concept and Tweedy's chelation theory. According to Overtone's concept of cell permeability, only the lipid soluble materials let to pass the lipid membrane surrounding the cell. In this respect, liposolubility is a substantial factor determining the anti-microbial activity. When chelation occurs, an overlap occurs between the orbital of the ligand and metal ion's positive charge partial sharing with donor groups, as a result, the polarity of the metal ion was reduced as a consequence (Leila, 2019).

The antibacterial activity of the new Mn(II), Co(II), Ni(II), Cu(II), and Zn(II) complexes of the Schiff base ligand, 4-chloro-2-{(E)-[(4-fluorophenyl)imino]methyl}phenol has been reported. The antibacterial evaluation results revealed that the metal complexes, with a proposed six coordinated octahedral geometry, exhibited higher antibacterial activity than the free Schiff base ligand against Gram-negative bacteria (*E. coli* and *P. aeruginosa*) and Gram-positive bacteria (*B. subtilis* and *S. typhi*) (Ommenya, 2020). The ligands exhibited moderate antibacterial activity against the Gram-positive bacterial types with zones of inhibitions in the range of 8–25 mm. The corresponding metal complexes, in general, showed some enhancement antibacterial activity against both Gram-positive *S. aureus and E. faecalis* bacterial strains with zones of inhibitions in the range of 18–32 mm (Hanan, 2020).

2.6.2. Antifungal activities

The antifungal activity was carried out by disc diffusion method. The ligand and its Cu(II), Zn(II), Ni(II), and Co(II) complexes have been tested for their antifungal activity at 100 µg/mL concentration. The results showed that copper complex exhibits enhanced activity against A. niger and A. flavus than the standard drug nystatin and it showed moderate effect on R. bataticola and C. albicans. In this regard, copper and zinc complexes exhibited good activity against A. niger, A.

flavus, R. bataticola, and C. albicans. Nickel and cobalt complexes exhibited moderate activity against niger, *A. flavus, R. bataticola*, and *C. albicans* (Vairalakshmi, 2019).

The antifungal activity of the free ligand and its complexes was shown to be higher than that of the control during antifungal investigations employing *Aspergillus fumigatus* (Ketoconazole). The free ligand and its complexes demonstrated substantial antifungal activity against *Candida albicans*, with the free ligand exhibiting the strongest activity compared to the standard drug (Abduh *et al.*, 2022).

2.6.3. Mechanisms of action of antibiotics and multi-drug resistance

Antibiotic agents' mechanisms of action can be categorized according to the functions they impact. These functions include the synthesis of cell walls, the synthesis of nucleic acids, the function of ribosomes, the function of cell membranes, and the metabolism of folate (A) Disruption of cell membrane integrity: (1) random insertion into the membrane, (2) alignment of hydrophobic sequences, and (3) removal of membrane sections and formation of pores. (B) Inhibition of DNA synthesis. (C) Blocking of RNA synthesis. (D) Inhibition of enzymes necessary for linking cell wall structural proteins. (E) Inhibition of ribosomal function and protein synthesis. (F) Blocking of chaperone proteins necessary for proper folding of proteins. (G) Targeting of mitochondria: - (1) inhibition of cellular respiration and induction of ROS formation and (2) disruption of mitochondrial cell membrane integrity and efflux of ATP and NADH (Muleta, 2023).

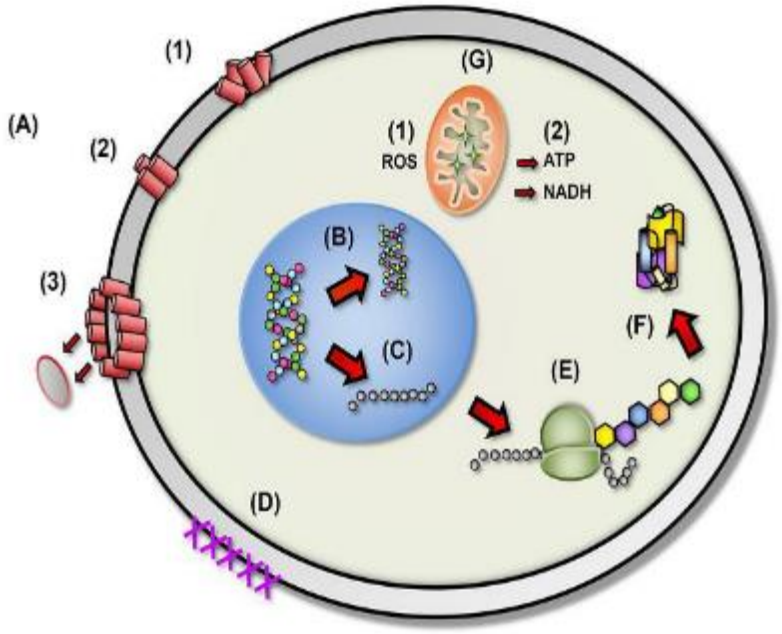

Figure 2.18. The proposed mechanistic modes of action of antimicrobial agents in microbial cells

3. MATERIAL AND METHODS

3.1. Chemical and Reagents

In this research work, all the chemicals and the reagents used for the investigation were analytical grade chemicals and solvents which includes; 3-chloroaline, acetic anhydride, zinc powder, acetic acid, phosphorus oxychloride, sodium hydroxide, hydrochloric acid, glacial acetic acid, dimethyl sulphoxide, copper chloride salt, zinc chloride salt, nickel chloride salt, ethanol, N,N-dimethylformamide, diethyl ether, Valine and Phenylanine. Were obtained from Alchem and Atomic Pvt. Ltd., Addis Ababa.

3.2. Instruments and Apparatus

The progress reaction were monitored by using analytical thin-layer chromatography. Analytical run by UV 254 (MACHEREY-NAGEL GmbH & Co.KG, Germany). Spots detected by a UV lamp. The absorbance of solutions were determined in UV/Vis range (Scan Wavelength: 200 – 800 nm, Test Mode: Abs Mode). The UV/Vis spectra of the ligand and its metal complexes were recorded at a wavelength range of 200−800 nm using a diluted sample solution in DMSO at room temperature. The molar absorption coefficients (ε) were determined at the given temperature according to the Beer Lambert's law ($A = \varepsilon bc$, where A for absorbance, ε for molar absorption coefficient, b base of cuvette standard (1.0 cm) and c for concentration of the solution) at maximum wavelength λ_{max}. FTIR spectra were generated within the range 400–4000 cm^{-1} (FTIR Model No. BX). ^{1}H-NMR and ^{13}C-NMR spectra were recorded using Bruker Advance 400 spectrometer at 400 MHz in deuterated dimethylsulphoxide (DMSO–d_6). Thermal analyzer DTG-60H simultaneous TGA and DTA apparatus SHIMADZU was used to measure the mass loss over ranges of temperature. The scanning done up to 1,500 K at a heating speed of 10.0 deg/min, under N_2 gas tolerable to pass at a speed of 20 cc/min. The crystallinity of the metal complexes was determined by powder X-ray diffraction (Panalytical's X'pert pro-X-ray diffractometer with Cu $K\alpha$ radiation; $K\alpha$ = 1.5418 Å), with the 2θ angle varying between 0° and 90°. The average crystallite size (D) was calculated from the pXRD pattern using the Debye-Scherer equation.

3.3. Synthesis of the Schiff base ligands

The synthesis of Schiff base ligands (*E*)-2-(((7-chloro-2-hydroxyquinolin-3-yl) methylene) amino)-3-phenylpropanoic acid) (SBL1) and (*E*)-2-(((7-chloro-2-hydroxyquinolin-3-yl)methylene)amino)-3-methylbutanoic acid (SBL2) derived from 2,7-dichloroquinoline-3-carboaldehyde and amino acids (Phenylaniline and Valine) were carried out based on previously established procedures with slight modifications (Tembei *et al.*, 2020).

3.3.1. Synthesis of Schiff Base ligand (SBL1)

Schiff base ligand (*E*)-2-(((7-chloro-2-hydroxyquinolin-3-yl)methylene) amino)-3-phenylpropanoic acid) (SBL1) derived from 2,7-dichloroquinoline-3-carboaldehyde and Phenylanine was synthesized based on previously reported procedures with slight modifications (Tembei *et al.*, 2020). Phenylanine (2.6430 g; 0.016 mol) and sodium hydroxide (0.6400 g; 0.016 mol) were dissolved in 30.0 mL ethanol in a beaker and stirred continuously by magnetic stirrer at room temperature. An equimolar amount of 2,7-dichloroquinoline-3-carbaldehyde (3.9360 g; 0.016 mol) and hydrochloric acid (1.33 mL, 0.016 mol; 37%) were dissolved in 40.0 mL of ethanol and added drop wise to the resulting mixture under constant stirring condition. The reaction was allowed to react for one hour and its progress was monitored using TLC to check completion of reaction. After evaporating the solvent, the solution filtered and washed with 10 mL of ethanol. A pale-yellow solid collected and allowed to dry further at room temperature. The solid product was stored in an airtight vial, until its further use.

3.3.2. Synthesis of Schiff Base ligand (SBL2)

The Schiff base ligand, (*E*)-2-(((7-chloro-2-hydroxyquinolin-3-yl)methylene)amino)-3-methylbutanoic acid SBL2 derived from 2, 7-dichloroquinoline-3-carboaldehyde and Valine (Fig 4.20) was synthesized following reported procedure with minor modification (Tembei *et al.*, 2020). Valine (1.87 g; 0.016 mol) and sodium hydroxide (0.64 g; 0.016 mol) were dissolved in 30.0 mL ethanol in a beaker and stirred continuously over magnetic stirrer at room temperature. An equimolar amount of 2, 7-dichloroquinoline-3-carbaldehyde (3.94 g; 0.016 mol) with hydrochloric acid (1.33 mL, 0.016 mol) (37%) were dissolved in 40.0 mL of ethanol. This was added drop wise to the resulting mixture while stirring continuously. The reaction was allowed to proceed for one hour and its progress followed by TLC to check for reaction completion. After

one hour, the solution was left to stand overnight by adding equimolar (0.922 mL; 0.016 mol) of acetic acid and the resulting solution was filtered and washed with 10 mL of ethanol. Finally, the yellowish solid collected allowed drying further at room temperature. The solid product was stored in an airtight vial, until its further use.

3.4. Synthesis of the metal complexes

In this research work, the chloride salts of Ni(II), Cu(II) and Zn(II) ions were dissolved in ethanol under the same condition using magnetic stirring beads and in the other separate beaker, the newly synthesized Schiff base ligands were dissolved in ethanol. Then the two solutions were mixed in 250 mL round bottom flask, the pH of the solution was adjusted between 6 and 8 using 25% ammonia solution and the solution was left to reacted for one-hour at room temperature under constant stirring before refluxing. The mixture was refluxed using oil bath in the temperature range of 80-90 ^{o}C for 5 hours. The reaction progress was followed using TLC. On cooling, the precipitates of metal complexes of different colour were obtained, filtered and dried at room temperature (Damena *et al.,* 2022a; Kapadnis *et al.,* 2016; Joshi *et al.,* 2022; Mohammed *et al.*, 2020; Vinusha *et al.,* 2019; Yamgar *et al.,* 2014).

3.4.1. Synthesis of ZnSBL1 Complex

An equimolar amount of zinc chloride (2.736 g, 0.016 mol) was dissolved in 20.0 mL of ethanol with constant stirring at room temperature. The Schiff base ligand (5.664 g, 0.016 mol) was dissolved in 30.0 mL of ethanol in a separate beaker. The two solutions were mixed in a 250 mL round bottom flask and the pH of the mixture adjusted to a range of 6–8 using a 25% ammonia solution. The mixture was reacted for one hour at room temperature with constant stirring before refluxing. The mixture was completely mixed before being refluxed for five hours at temperatures between 80-90 ^{o}C, while monitoring its progress using TLC. Following the completion of reaction, the mixture was cooled at room temperature, filtered, and washed using ethanol then allowed to dry at room temperature as reported else ware (Alhazmi *et al.,* 2022; Kapadnis *et al.*, 2016; Joshi *et al.,* 2022; Muleta *et al.*, 2022; Sumathi, 2022; Tufa *et al.*, 2018).

3.4.2. Synthesis of CuSBL1 Complex

An equimolar amount of dehydrated copper chloride (2.704 g, 0.016 mol) was dissolved in 20.0 mL of ethanol with constant stirring at room temperature. The Schiff base ligand (5.664 g,

0.016 mol) was dissolved in 30.0 mL of ethanol in a separate beaker. The two solutions was mixed in a 250 mL round bottom flask and the pH of the mixture adjusted to the 6–8 range using a 25% ammonia solution. The mixture was reacted for one hour at room temperature with constant stirring before refluxing. The mixture was refluxed for five hours at temperatures range 80 and 90 ^{o}C, while tracking the reaction progress using TLC. After the completion of reaction indicated by TLC, the mixture was cooled to room temperature, filtered, and washed by ethanol before being allowed to dry at room temperature as reported else ware (Alhazmi *et al.*, 2022;Kapadnis *et al.,* 2016; Joshi *et al.,* 2022; Muleta *et al.,* 2022; Sumathi, 2022; Tufa *et al.,* 2018).

3.4.3. Synthesis of NiSBL1 Complex

An equimolar amount of dehydrated nickel chloride (5.5152g, 0.016mol) was dissolved in 20.0 mL of ethanol with continuous stirring at room temperature. The Schiff base ligand (5.664 g, 0.016 mol) was dissolved in 30.0 mL of ethanol in a separate beaker. The two solutions were mixed in a 250 mL round bottom flask and the pH of the mixture was adjusted between 6 and 8 range using a 25% ammonia solution. The mixture was set to react for one hour at room temperature with constant stirring before refluxing. The mixture were refluxed for five hours at temperature range 80 and 90 ^{o}C, while tracking the reaction progress using TLC. Following the reaction's completion, the mixture was cooled at room temperature, filtered, and washed using ethanol and allowed to dry at room temperature as reported procedures (Alhazmi *et al.,* 2022; Kapadnis *et al.,* 2016; Joshi *et al.,* 2022; Muleta *et al.,* 2022; Sumathi, 2022; Tufa *et al.,* 2018).

3.4.4. Synthesis of $ZnSBL_2$ Complex

Zinc chloride (2.736 g, 0.016 mol) was dissolved in 20.0 mL of ethanol with constant stirring at room temperature. In a separate beaker, Schiff base ligand (5.664 g, 0.016 mol) was dissolved in 30.0 mL of ethanol. In a 250 mL round bottom flask, the two solutions were combined, and the pH of the resulting mixture was raised between 6 and 8 by adding a 25% ammonia solution to the mixture. Prior to refluxing, the mixture was stirred at room temperature for an hour. The mixture was thoroughly blended before being refluxed for five hours between 80 and 90 ^{o}C while monitoring the reaction using TLC. After the reaction was completed, the mixture was cooled at room temperature, filtered, and washed with ethanol and allowed to dry at room temperature as

reported else ware (Damena *et al.,* 2022a; Kapadnis *et al.*, 2016; Joshi *et al.*, 2022; Yamgar *et al.*, 2014).

3.4.5. Synthesis of $CuSBL_2$ Complex

Copper chloride (2.704 g, 0.016 mol) was dissolved in 20.0 mL of ethanol with constant stirring at room temperature. The Schiff base ligand (5.664 g, 0.016 mol) was dissolved in 30.0 mL of ethanol in a separate beaker. The two solutions were mixed in a 250 mL round bottom flask and the pH of the mixture adjusted between 6 and 8 using a 25% ammonia solution. The mixture reacted for one hour at room temperature with constant stirring before refluxing. The mixture completely mixed before refluxed for five hours at temperature range 80 and 90 ^{o}C while TLC tracked the reaction's progress. The mixture was cooled at room temperature, filtered, and washed by ethanol and allowed to dry at room temperature as reported else ware (Damena *et al.,* 2022a; Kapadnis *et al.,* 2016; Joshi *et al.*, 2022; Yamgar *et al.,* 2014).

3.4.6. Synthesis of $NiSBL_2$ Complex

Nickel chloride (5.5152 g, 0.016 mol) was dissolved in 20.0 mL of ethanol with constant stirring at room temperature. The Schiff base ligand (5.664 g, 0.016 mol) was dissolved in 30.0 mL of ethanol in a separate beaker. The two solutions were mixed in a 250 mL round bottom flask and the pH of the mixture adjusted between 6 and 8 using a 25% ammonia solution. The mixture reacted for one hour at room temperature with constant stirring before refluxing. The mixture were refluxed for five hours at temperatures between 80 and 90 ^{o}C while TLC tracked the reaction's progress. The mixture was cooled at room temperature, filtered, and washed by ethanol and allowed to dry at room temperature as reported else ware *(Damena et al., 2022a; Kapadnis et al.,*2016; Joshi *et al.*, 2022; Yamgar *et al.*, 2014).

3.5. Characterizations of the ligands and the metal complexes

The physical and spectral characterization of the synthesized compounds provides the important information that is essential for structure elucidation and stereochemistry. The characterization techniques employed for the present research are as follows.

3.5.1. Electronic spectral analysis of metal complexes

The measurement of absorption of near-UV and visible light a sample along with its intensity, is known as electronic spectroscopy. For organic compounds and inorganic ions or complexes, UV-Vis spectroscopy is typically used. Outer electron excitation is correlated with the absorption of UV or visible light. The UV-vis absorption spectral analysis serves to investigate charge transfer phenomena within the molecular structure (Venkatesh *et al.,* 2024).

3.5.2. Molar conductivity

The molar conductivity values of the synthesized complexes were measured in M/1000 solution of complexes in dimethyl sulfoxide solvent by direct reading using an electrical conductometer (AD8000). To know the oxidation number and stereochemistry of the central metal ion in coordination complexes, molar conductivity values are used in conjunction with electronic spectra (Muleta *et al.,* 2022).

3.5.3. Melting point determination

Thomas Hoover melting point device was used to determine the melting points of the synthesized compounds using the capillary tube method. The melting point of the synthesized organic ligands and their complexes were determined by introducing required amount of sample into a capillary tube, attached to the stem of a thermometer centered in a heating bath. The bath was heated slowly, and the temperatures at which melting begins and complete was recorded where the average melting point was calculated and recorded.

3.5.4. FT-IR spectra analysis

FT-IR studies were conducted to determine the functional group present in the ligands and the metal complexes. In this study, the Infrared spectra were recorded on the Perkin Elmer model FTIR type 1650 spectrophotometer in the wave-number region of 4000 - 400 cm^{-1} were used. The spectra of the 10 mg solid samples were recorded as KBr pellets. The position of bands provides significant bonding sites of the ligand molecules when forming complexes with metal (Muleta *et al.,* 2022).

3.5.5. NMR spectra analysis

NMR spectra of the ligands were recorded in dry DMSO-d_6. The proton NMR spectra enabled us to distinguish different chemical and magnetic environments corresponding to a proton in molecules. The NMR spectra obtained were able to provide detailed information about the chemical environment and structure of the ligands synthesized. The quantity and composition of C and H atoms in a compound can be identified by examining its nuclear magnetic resonance (NMR) spectrum and compound instant environment (Venkatesh *et al.*, 2024).

3.5.6. X-ray diffraction analysis

The particle nature of the complexes was studied using powder X-ray diffractometer (XRD), Philips X-pert pro diffractometer; PW 1830 with Cu Kα radiation was employed. The powder X-ray diffraction (pXRD) patterns of the synthesized metal complexes were recorded using 80 mg of dried powdered samples. The data was recorded at 2θ ranging from 10 to 80° at lambda (λ) value of 1.54 A°.

3.5.7. Thermogravimetric analyses

Thermogravimetric analysis (TGA) provides useful information about the thermal stability, thermal decomposition stages and fragmented parts of complexes. In addition, TGA analysis can verify the presence or absence of coordinated or lattice water molecules in complexes. Thermal analyses of the synthesized metal complexes were recorded under N_2-atmosphere (20 mL/min) using a 10 mg dried sample using the SHIMADZU's DTG-60H thermal analyzer. The weight losses were recorded with a heating rate of 10 ^{o}C/min.

3.6. Antimicrobial activity

The Schiff base ligands (SBL1) and their metal (II) complexes were assessed *in vitro* for their antimicrobial activity against different Gram-Positive (*S. aureus and B. cereus*) and Gram-negative (*E. coli and S. typhi*) bacterial and fungal (*C. albinas*) using disc diffusion method in DMSO at two different concentrations. Gentamicin for bacterial and Clotrimazole for fungal strain were used as control drugs (Abdel-rahman *et al.,* 2022; Hanan, 2020; Hasan *et al.,* 2021; Hassan *et al.,* 2023; Vairalakshmi, 2019).

The *in vitro* antibacterial activities of the Schiff base ligand (SBL2) and their metal (II) complexes were evaluated against the Gram-positive (+) bacterial (*E. coli and P. aeruginosa*) and gram-negative (-) bacterial (*S. aureus and S. pyogenes*) by using disk diffusion method. Ciprofloxacin were used as a positive control. Two different concentrations (100 and 200 μg/mL) of the test compounds and the positive control were prepared in DMSO. DMSO was used as a negative control and no activity was found (Abdel-Rahman *et al.,* 2022; Lemilemu *et al.,* 2021; Jeffrey, 1985; Rahman *et al.,* 2015; Spasić *et al.,* 2020). The zones of inhibition for each compound against the tested microorganisms measured in triplicate, and the average was taken.

3.7. Molecular Docking Studies

Molecular docking studies were conducted to predict the interaction of synthesized compounds with the proteins of *S. aureus* (PDB: 2w9h) and *E. coli* DNA Gyrase B (PDB: 6F86). Metal complex geometries were optimized using the B3LYP-GD3/6-311++G(d,p)/LanL2DZ method (Abdel-Rahman *et al.,* 2022; Damena *et al.,* 2022b; Kumar *et al.,* 2016; Tufa *et al.,* 2018) and the Gaussian 16 program package (Demircioğlu, 2021), and converted to PDB files using Gauss view. Auto Dock 4.2.6 software was employed for docking studies, following established protocols (Bitew *et al.,* 2021; Damena *et al.,* 2022b; Julius *et al.,* 2023; Lemilemu *et al.,* 2021). The proteins were downloaded from the protein database and cleaned to remove co-crystallized substrate and water molecules with MGL 1.5.6 software. Standard docking parameters were applied, and a grid box (120 × 120 × 120, spacing 0.375 Å) was constructed. Lamarckian genetic algorithm (LGA) with an adaptive whole method search (set at 100) was used, generating one hundred conformations for each molecule (Grolmusz, 2008). Discovery Studio software was used to visualize the interactions between active amino acids and molecules, focusing on conformers with the lowest binding free energies.

3.8. DFT Calculations

Density Functional Theory (DFT) employing B3LYP (Becke, 1993; Lee *et al.,* 1988; Burke, 1995; Sureshkumar *et al.,* 2021) hybrid functional together with 6–311++G(d, p) basis set for the light atoms and the Los Alamos National Laboratory 2-double-zeta (LanL2DZ) pseudopotential for the nickel, copper and zinc atoms (Krishnan *et al.,* 1980) were employed, respectively, using the Gaussian 16 program package (Krishnan *et al.,* 1980; Jeffrey, 1985).

Grimme's dispersion correction (Stefan et al., 2002) was employed to account for non-bonding interactions. Vibrational frequency calculations were used to ensure that the optimized geometries are real minima without imaginary frequencies. The time-dependent DFT (TD-DFT) was used to calculate absorption energies.

3.9. Statistical Analysis

All the antibacterial and antifungal data analyses generated by triplicate measurements were reported as mean plus standard deviation. The data were grouped and statistically evaluated with SPSS 16.0 software. The hypothesis testing method ANOVA followed by the 'least significant difference' test was used. A value of $P < 0.05$ was considered to indicate statistical significance. All results were expressed as mean ± Standard error mean (S.E.M) (Muleta, 2023).

4. RESULTS AND DISCUSSION

In this section, the results of the research work are presented along with the necessary discussion. The Ligands and all the metal complexes synthesized are stable at room temperature and are non-hygroscopic in nature. The complexes are insoluble in water but are soluble in DMSO. The analysis of the physicochemical properties, FT-IR, UV-Vis, ^{1}H-NMR and ^{13}C-NMR, pXRD and TGA-DTA analysis, antimicrobial activity and docking studies of the ligand and metal complexes summarized as follows.

4.1. Synthesis of ligands and their metal complexes

The synthesis of Schiff base ligand *E*)-2-(((7-chloro-2-hydroxyquinolin-3-yl) methylene) amino)-3-phenylpropanoic acid and (*E*)-2-(((7-chloro-2-hydroxyquinolin-3-yl)methylene)amino)-3-methylbutanoic acid derived from 2,7-dichloroquinoline-3-carboaldehyde and Phenylanine/Valine and its Cu(II), Zn(II) and Ni(II) complexes were successfully synthesized following the established procedure presented in sections 3.3 and 3.4 respectively with the necessary reaction conditions.

4.1.1. Synthesis of the Schiff base ligands

Schiff base ligands SBL1 and SBL2 derived from 2,7-dichloroquinoline-3-carboaldehyde and amino acids (Phenylaniline and Valine) were synthesized based on literature procedures with very slight modifications of amount and different chemicals (Tembei *et al.,* 2020). The 2,7-dichloroquinoline-3-carboaldehyde used as the starting materials for the synthesis of the Schiff base ligands, the general reaction mechanisms described in Scheme 4.1 and 4.2 below.

4.1.1.1. Schiff Base ligand (SBL1)

Schiff base ligand (*E*)-2-(((7-chloro-2-hydroxyquinolin-3-yl) methylene) amino)-3-phenylpropanoic acid) derived from 2,7-dichloroquinoline-3-carboaldehyde and Phenylanine synthetic reactions of SBL1 is depicted scheme 4.1 was synthesized based on the procedure given in method and material section.

Yield 89.75%; crystal; m.pt. > 170 ^{o}C; color pale yellow; UV/Vis $\lambda_{max}(\varepsilon)$ (DMSO): 239 nm, 253 nm, 311 nm and 324 nm; IR (υ cm^{-1}, KBr (pellet)): 1605ν (azomethine C=N), 3442ν (O-H attached to quinoline ring), 3147ν (O-H of carboxylic acid of amino), 1678 ν(C=O). ^{1}HNMR

(400 MHz, DMSO–d_6), δ_H (ppm): 7.50 (s,1H, C=NH), 2.49 (2H, CH_2, d,d, 7.63, 7.46), 7.69 (2H,d, 8.64), 7.72 (2H, d, 8.05), 7.22 (1H, d, 9.06) of phy-ring-H), 8.94 (1H, s), 9.04 (1H, d, 8.82), 8.39 (1H, d,d, 8.67, 2.26), 7.79 (1H, d, 2.17) of quinoline ring-H), 10.34 (2H, s, O-H); ^{13}C NMR (101 MHz, DMSO–d_6); δ_C (ppm): 38.83 (C, CH_2), 74.36 (C, CH), 189.19 (C, C-O), 160.53 (C, C=N), 127.7-137.9 (C, C, phy-ring) and 126.2-135.7 (C, C, quinoline ring).

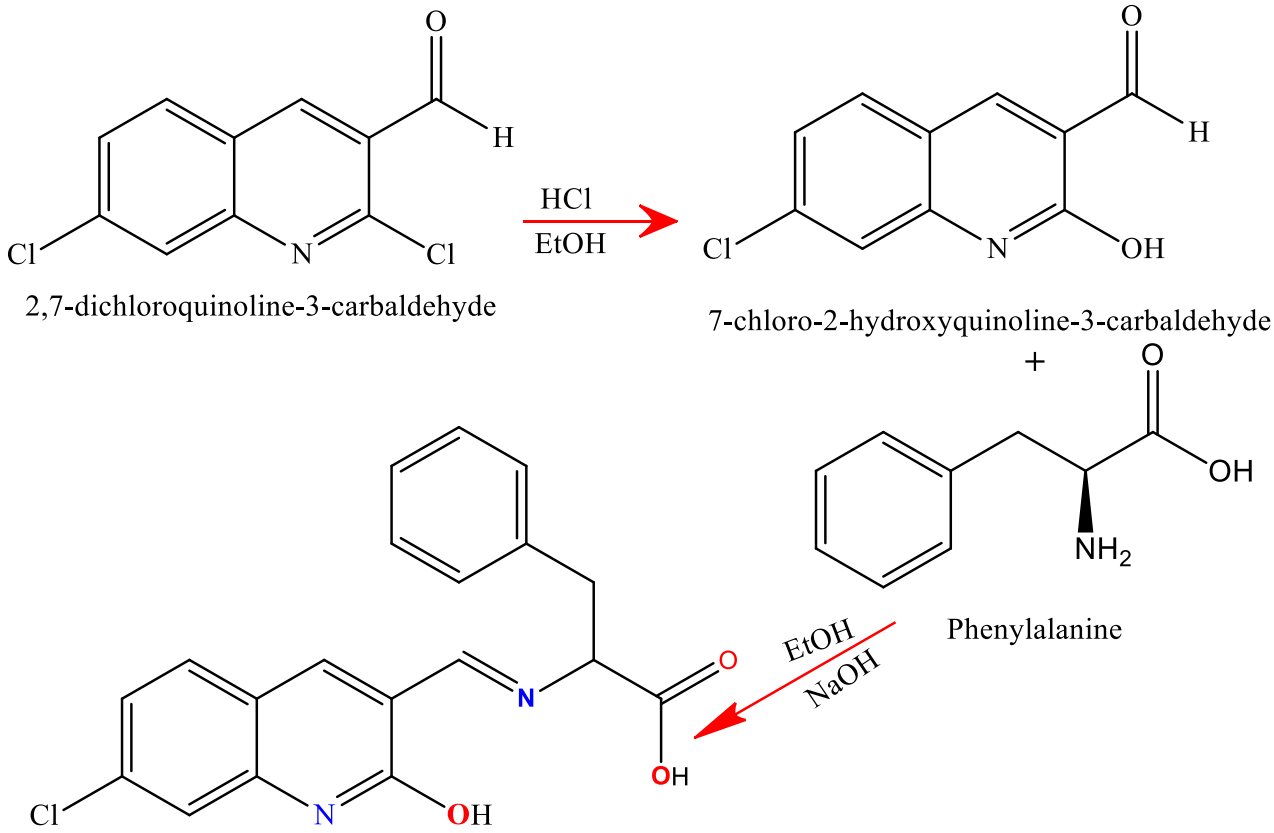

2,7-dichloroquinoline-3-carbaldehyde

7-chloro-2-hydroxyquinoline-3-carbaldehyde

Phenylalanine

(*E*)-2-(((7-chloro-2-hydroxyquinolin-3-yl)methylene)amino)-3-phenylpropanoic acid

Scheme 4.1: Synthesis reaction mechanism of Schiff base ligand (**SBL1)**

4.1.1.2. Schiff Base ligand (SBL2)

The Schiff base ligand, (*E*)-2-(((7-chloro-2-hydroxyquinolin-3-yl) methylene) amino)-3-methylbutanoic acid derived from 2, 7-dichloroquinoline-3-carboaldehyde and Valine synthetic reactions of SBL2 is depicted scheme 4.2 was synthesized following the procedure given in method and material section which yields yellowish solid collected.

Yield 82.67%; color: bright yellow, crystal; m.pt.>170 ºC; UV–Vis λ_{max} (DMSO): 276 nm, 311 nm, 326 nm and 348 nm; FT-IR (υ cm^{-1}, KBr (pellet)): 1556 cm^{-1} ν(azomethine C=N), 3456

cm^{-1} broad band at around (O-H attached to quinoline ring) and (O-H of carboxylic acid of amino), 1622 cm^{-1} ν(C=O).

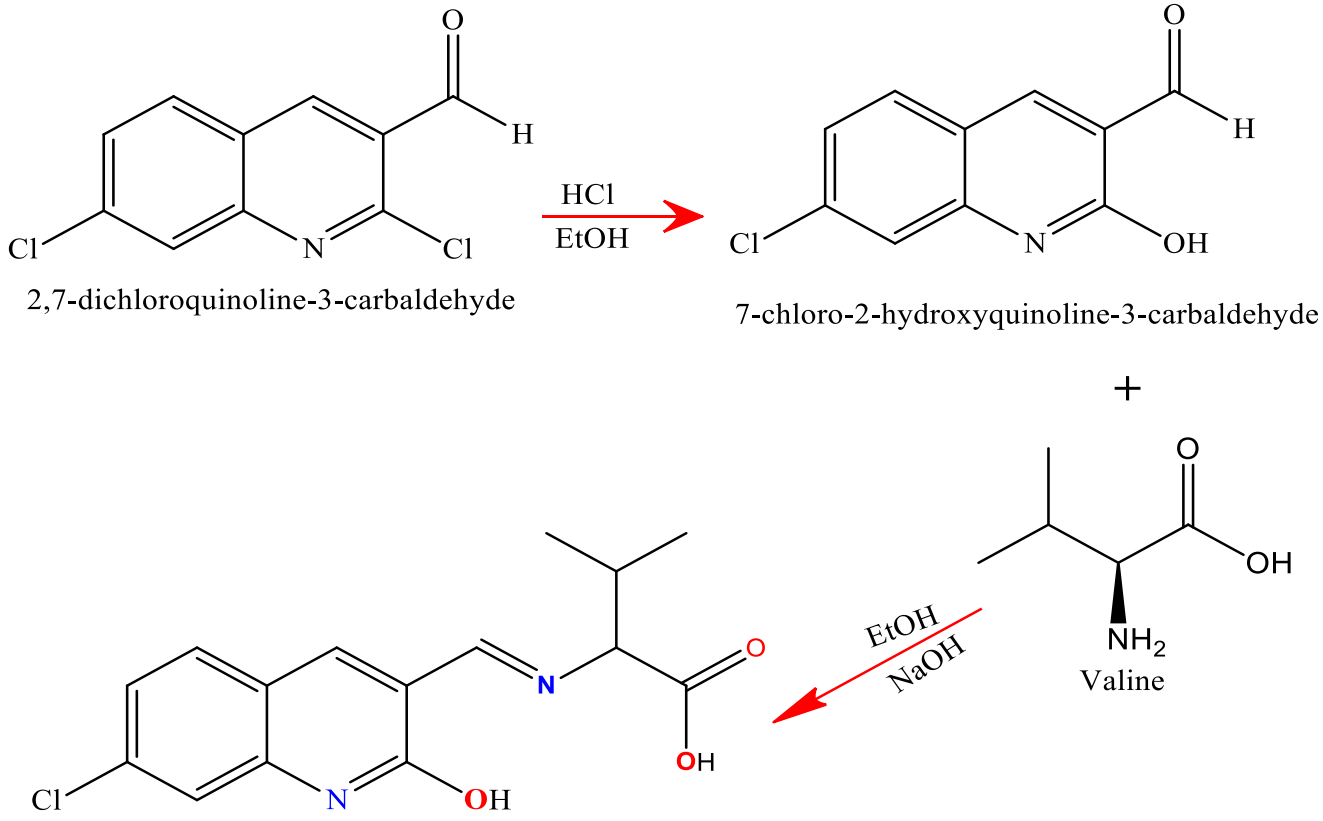

2,7-dichloroquinoline-3-carbaldehyde

7-chloro-2-hydroxyquinoline-3-carbaldehyde

(*E*)-2-(((7-chloro-2-hydroxyquinolin-3-yl)methylene)amino)-3-methylbutanoic acid

Scheme 4.2: Synthesis reaction mechanism of Schiff base ligand two (**SBL_2**)

4.1.2. Synthesis of metal complexes

Metal chloride of selected metals ($ZnCl_2$.$2H_2O$/$CuCl_2$.$2H_2O$/$NiCl_2$.$6H_2O$) dissolved in 20.0 mL of ethanol with continuous stirring at temperature range of 80-90 ^oC. Moreover, in the separate beaker, **SBL1** dissolved in to 30.0 mL of ethanol. Then the two solution were mixed in 250 mL round bottom flask, the pH of the solution was adjusted using 25% ammonia solution to 6-8 range and the solution tend to react for one-hour at room temperature under continuous stirring before refluxing. After the solution mixed completely then refluxed using oil bath at temperature range 80-90 ^oC for 5 hour and the reaction progress were monitored using TLC. After completion of the reaction, the mixture was cooled at room temperature and filtered, dried to room temperature

to get colored complexes at good yields (Damena *et al.*, 2022a; Kapadnis *et al.*, 2016; Mohammed *et al.*, 2020; Yamgar *et al.*, 2014).

4.1.2.1. Synthesis of ZnSBL1 Complex

Zinc chloride ($ZnCl_2.2H_2O$) salt and Schiff base ligand (*E*)-2-(((7-chloro-2-hydroxyquinolin-3-yl) methylene) amino)-3-phenylpropanoic acid) were dissolved in ethanol with constant stirring at temperature range 80-90 ^oC as stated in method and material section. Yield 78.16%; its colour was white; conductivity 149.2 $\mu S/cm^2$; m.pt. > 300 ^oC; FT-IR $\nu(cm^{-1})$: (O-H, 3333(w)), 2359(m), (C=N, 1613(s)), 1403(m), 1027(s), (Zn-O, 565(m)), (Zn-N, 466(m)). UV/vis (CH_2Cl_2) λ_{max} (ε): 239 nm, 253 nm, 311 nm and 324 nm.

4.1.2.2. Synthesis of CuSBL1 Complex

Copper chloride ($CuCl_2.2H_2O$) salt and Schiff base ligand (*E*)-2-(((7-chloro-2-hydroxyquinolin-3-yl) methylene) amino)-3-phenylpropanoic acid) was dissolved in ethanol with constant stirring at temperature range 80-90 ^oC as stated in method and material section. Yield 91.49%, with light blue colour, conductivity of 138.8 $\mu S/cm^2$, m.pt > 300 ^oC, FT-IR $\nu(cm^{-1})$: (O-H, 3404(w)), 2355(m), (C=N, 1622(s)), 1452(m), 1052(s), (Cu-O, 561(m)), (Cu-N, 470(m)). UV/Vis (CH_2Cl_2) λ_{max} (ε): 241 nm, 254 nm, 313 nm and 326 nm.

4.1.2.3. Synthesis of NiSBL1 Complex

Nickel chloride ($NiCl_2.6H_2O$) salt and Schiff base ligand (*E*)-2-(((7-chloro-2-hydroxyquinolin-3-yl) methylene) amino)-3-phenylpropanoic acid) was dissolved in ethanol with constant stirring at temperature range 80-90 ^oC as stated in method and material section. Yield 74.19%, light green colour, conductivity of 142.4 $\mu S/cm^2$, m.pt > 300 ^oC, FT-IR $\nu(cm^{-1})$: (O-H, 3436(w)), 2358(m), (C=N, 1630(s)), 1405(m), 1061(s), (Ni-O, 548(m)), (Ni-N, 439(m)). UV/Vis (CH_2Cl_2) λ_{max} (ε): 241 nm, 256 nm, 314 nm and 325 nm

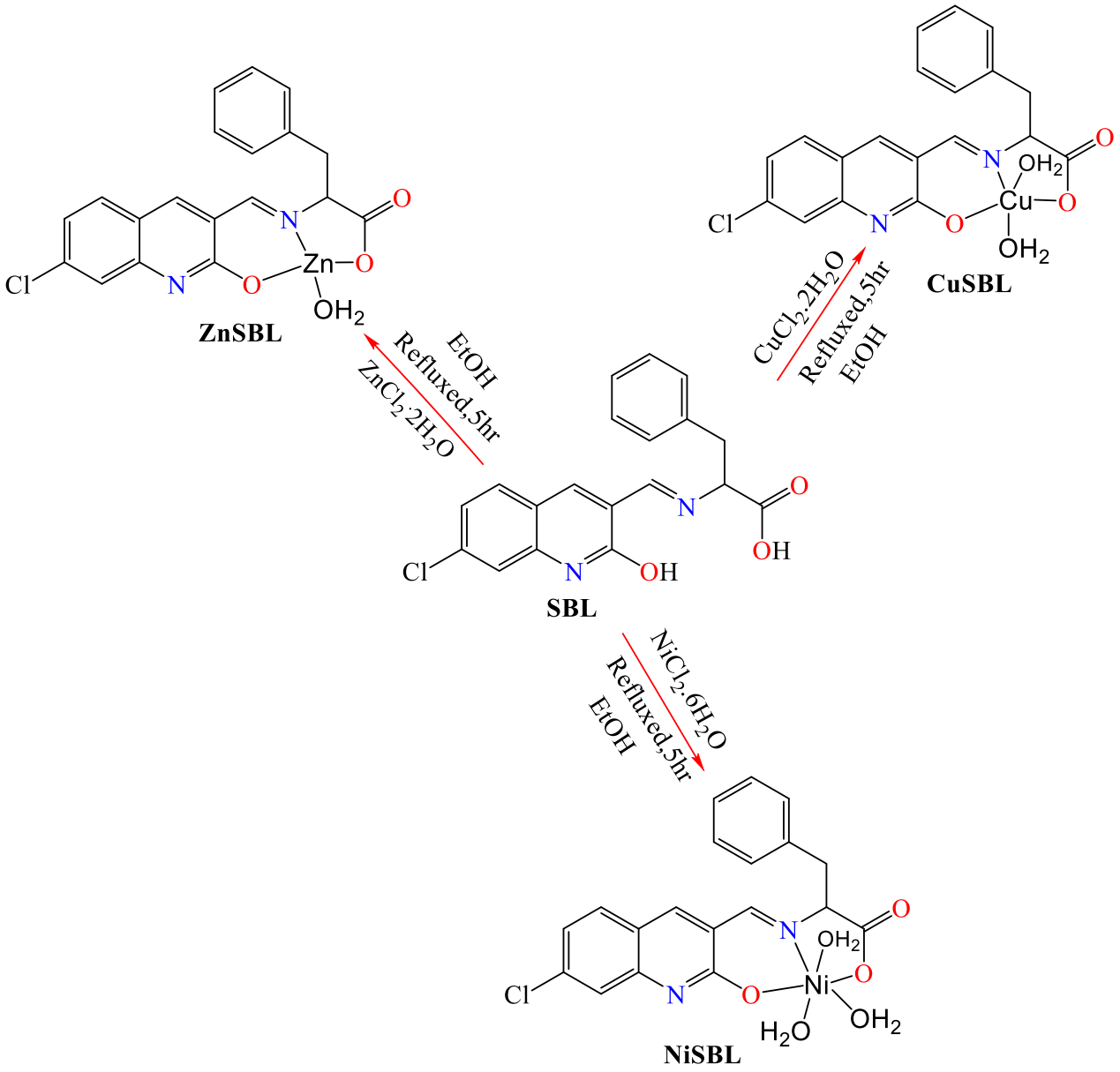

Scheme 4.3: Synthesis scheme of **ZnSBL1, CuSBL1 and NiSBL1** complexes

4.1.2.4. Synthesis of ZnSBL2 Complex

Zinc chloride ($ZnCl_2.2H_2O$) salt and Schiff base ligand (*E*)-2-(((7-chloro-2-hydroxyquinolin-3-yl) methylene) amino)-3-methylbutanoic acid was dissolved in ethanol with constant stirring at temperature range 80-90 ^oC as stated in method and material section. Yield = 74.12%; colour = white; conductivity = 136.2µS/cm^2 m.pt > 300^{0}C; FT-IR ν(cm^{-1}): (O-

H,3316(s)), 2330(m), (C=N,1606(s)), 1470(m), 1037(s), (Zn-O,538(m)), (Zn-N,466(m)). UV−vis (CH_2Cl_2) λmax (ε): 262, 312, 325 and 470 nm.

4.1.2.5. $CuSBL_2$ Complex

Copper chloride ($CuCl_2.2H_2O$) salt and Schiff base ligand (*E*)-2-(((7-chloro-2-hydroxyquinolin-3-yl) methylene) amino)-3-methylbutanoic acid was dissolved in ethanol with constant stirring at temperature range 80-90 ^oC as stated in method and material section. Yield = 88.24%; colour = blue; conductivity = 144.6μS/cm^2; m.pt > 300 ^oC; FT-IR ν(cm^{-1}): (O-H,3313(w)); 2343(m); (C=O,1606(s)) ;(C=N,1572(s)), 1452(m), 1043(s); (Cu-O,525(m)), (Cu-N,476(m)). UV−Vis (CH_2Cl_2) λmax (ε): 260, 312, 325 and 473 nm.

4.1.2.6. $NiSBL_2$ Complex

Nickel chloride ($NiCl_2.6H_2O$) salt and Schiff base ligand (*E*)-2-(((7-chloro-2-hydroxyquinolin-3-yl) methylene) amino)-3-methylbutanoic acid was dissolved in ethanol with continuous stirring at temperature range as stated in method and material section. Yield = 78.29%; colour = green; conductivity = 134.8 μS/cm^2; m.pt > 300 ^oC; FT-IRν(cm^{-1}):(OH,3331(w)),2337(m),(C=N,1581(s)),1411(m),1017(s),(Ni-O,535(m)),(Ni-N,416(m)). UV−vis (CH_2Cl_2) λmax (ε): 262, 312, 325 and 460 nm.

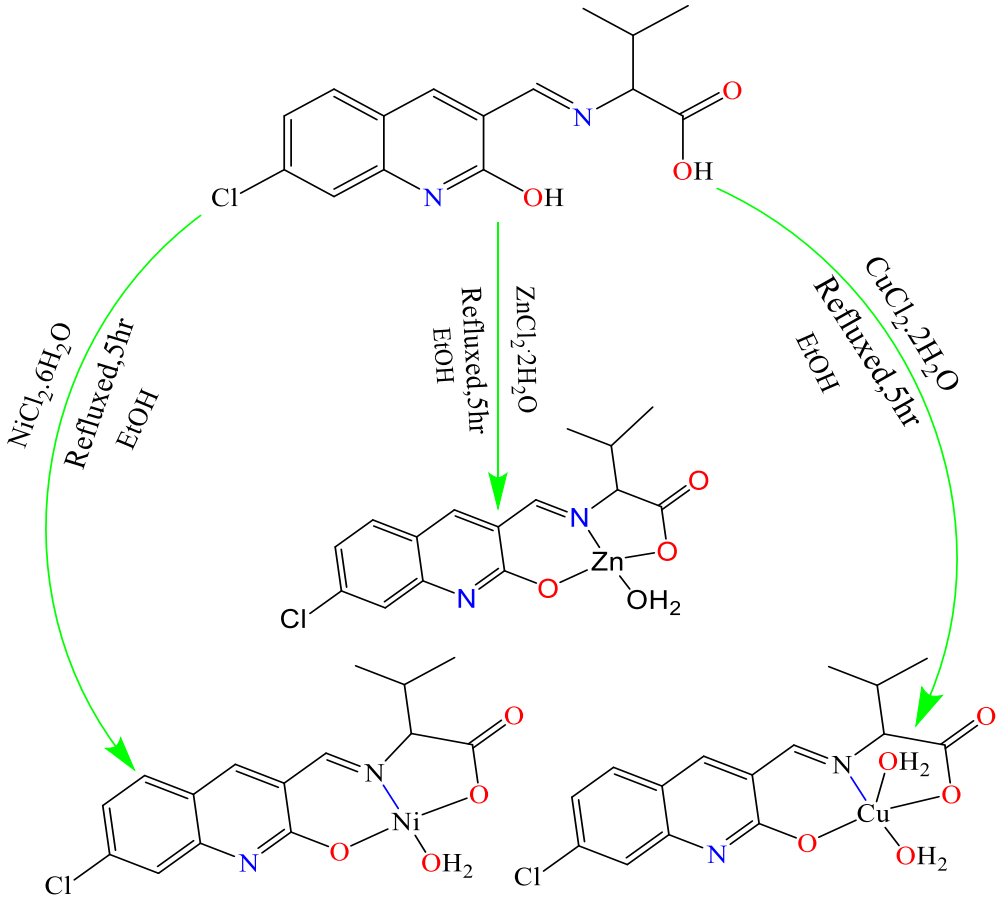

Scheme 4.4: Synthesis scheme of **$ZnSBL_2$, $CuSBL_2$ and $NiSBL_2$** complex

4.2. Physicochemical properties of the Schiff base ligand and metal complexes

Study of the physical properties, which includes colour, solubility, melting point and conductivity, provide important understanding of the behavior of SBLs and their metal complexes. These are very important to gain supportive information, regarding the ligand and complex formation during the chemical processes. The different compounds have their unique physical properties and their detailed study furnishes support in designing the mechanism of the reaction and helps in predicting the nature of the compounds.

The Schiff bases and their Cu(II) , Ni(II) and Zn (II) Complexes were obtained in good yields, the physical properties of the synthesized Schiff bases and their metal complexes were analyzed and presented in Table 4.1.

Table 4.1: Physicochemical Properties of the Schiff base Ligand and their Zn(II), Cu(II) and Ni(II) Complexes

Compounds	Color	Chloride test	Yield (%)	Conductivity $\mu S/cm^2$	Melting point
SBL1	Pale-yellow	----------	89.75	-------	>170
SBL2	Light-yellow	----------	82.67	--------	
ZnSBL1	White	White precipitate	78.05	149.2	>300
CuSBL1	Light-blue		91.80	138.8	
NiSBL1	Light-green		74.05	142.4	
ZnSBL2	White		74.12	136.2	
CuSBL2	Blue		88.24	144.6	
NiSBL2	Green		78.29	134.8	

The interaction of electron cloud of the ligand and metal ions split d-orbitals of metal ions into different energy levels, corresponding to the geometry of the complexes. The complex that absorbs electromagnetic radiation in the visible region of the spectrum emits energy complementary to absorbed radiation and produces color of the chemicals. Change in the color of the complexes is due to the different range of electronic absorption, either by π bonding or nonbonding or by free electrons. Electronic absorption in UV-visible region provides the characteristic color of the substances. Conjugation further enhances the intensity of color. The free electrons of metals in their complexes exhibit electronic absorption and produce various colors of the metal complexes. The different colors of the SBL1, SBL2 and synthesized complexes have been given in the Figure 4.1.

(a) (b) (c) (d)

(e) (f) (g) (h)

Figure 4.1: Color of (a) SBL1 ligand (b) ZnSBL1, (c) CuSBL1 and (d) NiSBL1 (e) SBL_2 ligand and (f) $ZnSBL_2$, (g) $CuSBL_2$ and (h) $NiSBL_2$ complexes.

It was found that the melting point of the Schiff bases is above 170 ^oC and the melting temperature of the complexes is above 300 ^oC, this is an indication of thermal stability of the ligand and its metal complexes. The molar conductance of the complexes presented in Table 4.1 indicate that the six metal complexes showed conductivities in the range of 134.8 to 149.2 S/cm^2 , suggesting electrolytic nature of the complexes (Hadjer et al., 2018; Veljovic et al., 2012; Al Zoubi et al., 2019; Muleta et al., 2022; Pandya, 2014). This suggested that there are anions present outside the coordination sphere of the complexes. This is mainly because the metal cations do not receive electrons from the ligand indicating a net charge of coordination sphere is different from zero. The chloride test also proves the existence of chloride ions in the outer of the coordination sphere. The molar conductance and chloride test results can also provide information about the proposed structures of the complexes.

4.2. 1. Solubility test of the ligands and metal complexes

The synthesized Schiff base and its metal complexes were subjected to solubility studies showing that all compounds were soluble in DMSO and DMF but slightly soluble ethanol and methanol at room temperature. Water and some common organic solvents were used to determine the solubility of the Schiff bases and their metal complexes. From the result of solubility test presented in Table 4.2, it can be seen that, the Schiff bases and their metal complexes were soluble in dimethylsulphoxide (DMSO) and dimethylformamide (DMF), slightly soluble in ethanol and methanol, and insoluble in water, acetone, chloroform, benzene and n-hexane (Srivastava, 2021; Mohammed et al., 2020; Zabiulla et al., 2023b).

Table 4.2 Solubility test of the Schiff bases and their metal complexes

Compound	Solvent								
	DMSO	DMF	Ethanol	Methanol	Water	Acetone	Chloroform	Benzene	Hexane
SBL1	Sol.	Sol.	Slightly sol	Slightly sol	Insol.	Insol.	Insol.	Insol.	Insol.
SBL2	Sol.	Sol.	Slightly sol	Slightly sol	Insol.	Insol.	Insol.	Insol.	Insol.
ZnSBL1	Sol.	Sol.	Slightly sol	Slightly sol	Insol.	Insol.	Insol.	Insol.	Insol.
CuSBL1	Sol.	Sol.	Slightly sol	Slightly sol	Insol.	Insol.	Insol.	Insol.	Insol.
NiSBL1	Sol.	Sol.	Slightly sol	Slightly sol	Insol.	Insol.	Insol.	Insol.	Insol.
ZnSBL2	Sol.	Sol.	Slightly sol	Slightly sol	Insol.	Insol.	Insol.	Insol.	Insol.
CuSBL2	Sol.	Sol.	Slightly sol	Slightly sol	Insol.	Insol.	Insol.	Insol.	Insol.
NiSBL2	Sol.	Sol.	Slightly sol	Slightly sol	Insol.	Insol.	Insol.	Insol.	Insol.

4.3. Characterization of ligands and metal complexes

4.3.1. FT-IR Spectra analysis of ligands and its metal complexes

The FT-IR spectral information is another tool used to allocate the vibrational frequencies that confirm the important functional groups that exist in the newly synthesized Schiff base ligands and metal complexes. The important FT-IR bands and assignments of the main functional groups of the synthesized ligands: (*E*)-2-(((7-chloro-2-hydroxyquinolin-3-yl) methylene) amino)-3-phenylpropanoic acid), (*E*)-2-(((7-chloro-2-hydroxyquinolin-3-yl) methylene) amino)-3-methylbutanoic acid and their copper(II), nickel(II) and zinc(II) complexes data were presented in Table 4.3 and 4.4 and Figures 4.2 and 4.3. The spectra of the ligands were compared to the spectra of their complexes to analyze changes that occurred during coordination to confirm complex formation.

4.3.1.1. FT-IR spectra analysis of SBL1

In FT-IR spectra, the Schiff base showed peaks at (C=N) 1605 cm^{-1} (Hassan et al., 2023; Kareem, 2022) , 3442 cm^{-1} and 3147cm^{-1} are due to (C-OH)(attached to the Quinoline ring) and (C-OH)(carboxylic group) stretching frequency, respectively which confirms the formation of the newly expected ligand (Abdel-rahman *et al*., 2022; Adil *et al.*, 2019; Kavitha *et al.*, 2016; Patil *et al.*, 2021). There are three possible locations for the ligand to bind to the metal ion. These three sites are the hydroxyl group oxygen attached to quinoline ring, the hydroxyl group oxygen attached to carboxylic group and the azomethine (-C=N-) compound's nitrogen atom (Aroua *et al.*, 2023).

Table 4.3: Important characteristic FT-IR bands (cm^{-1}) of SBL1 and its metal complexes

Cpd	ν(C=N)	ν(C=O)	ν(C-O)	ν(O-H)	$\nu(O\text{-}H)_{(acidic)}$	ν(M-O)	ν(M-N)
SBL1	1605	1678	1035	3442	3147	------	-----
ZnSBL1	1613		1027	3333		565	466
CuSBL1	1622		1052	3404		561	470
NiSBL1	1630		1061	3436		548	439

4.3.1.2. FT-IR Spectra Analysis of metal complexes of SBL1 ligand

The FT-IR spectra of the ligand and its metal complex recorded in KBr disc between 4000 cm^{-1} to 400 cm^{-1} (Fig. 4.2 for **SBL1** and Fig. 4.3 for its metal complex). The FTIR spectra were recorded (υ, cm^{-1}, KBr (pellet)), revealed absorptions peaks at 1613, 1622 and 1630 cm^{-1} corresponding to ν(azomethine C=N) for **ZnSBL1, CuSBL1** and **NiSBL1** metal complexes, respectively. The peak observed at 3333, 3404 and 3436 cm^{-1} confirms ν(O-H) of water molecules in **ZnSBL1, CuSBL1** and **NiSBL1** metal complexes, respectively. The new peaks at 565 ν(Zn-O), 561 ν(Cu-O) and 548 ν(Ni-O); 466 ν(Zn-N), 470 ν(Cu-N) and 439 ν(Ni-N) which confirm the ONO binding to Zinc(II),Copper(II) and Nickel(II) during complex formation of metal with the SBL1. The FT-IR spectrum of the free Schiff base ligand has showed a strong υ(C=N) azomethine band at 1605 cm^{-1}, however, for metal complexes shifted to higher values at 1613 cm^{-1}, 1622 cm^{-1} and 1630 cm^{-1} for complexes of **ZnSBL1, CuSBL1** and **NiSBL1** respectively (Hasan *et al.*, 2021; Muleta *et al.,* 2022).

In FT-IR spectra, Schiff base showed peaks at 1605 cm^{-1}, 3442 cm^{-1} and 3147 cm^{-1}, which were due to (C=N) and O-H (attached to the Quinoline ring) and O-H (carboxylic from amino acids) stretching frequency, respectively (Kareem, 2022). However, in case of M(II) complexes, C=N stretching frequency peaks were observed at 1613 cm^{-1},1622 cm^{-1} and 1630 cm^{-1} respectively. Peak at 3442 cm^{-1} and 3147 cm^{-1} disappears which confirms that the two hydroxyl groups were undergo complexation and more over new peaks observed at 565 ν(Zn-O), 561 ν(Cu-O) and 548 ν(Ni-O) and 466 ν(Zn-N), 470 ν(Cu-N) and 439 ν(Ni-N) appears which confirms the metal to oxygen and nitrogen bond formation (Abdel-rahman *et al.*, 2022; Adil *et al*., 2019; Kavitha *et al.,* 2016; Patil *et al.,* 2021).

Hence, the weak and broad band stretching frequencies that are observed (3200 −3500 cm^{-1}) could be assigned as the stretching vibrations of the O−H of the water molecules present in the coordination sphere (Damena *et al.,* 2022; Fonkui *et al.,* 2019). The disappearance of the weak and broad band of the hydroxyl group gave important evidence of the complexation of the phenolic groups. Moreover, two new bands, in the ranges of 400–470 cm^{-1} and 500–570 cm^{-1} due to M-N and M-O stretching, appeared in the metal complexes' spectra and represent the ONO coordination to metals (Al-Shboul *et al.,* 2022). These facts suggest that the shifts are due to coordination of ligand to the metal atom by the azomethine nitrogen and phenolic oxygen. The presence of

coordinated water molecules in all the complexes could be confirmed by a broad band in the 3273–3361 cm^{-1} range and weaker bands around 773–794 cm^{-1} range, which could be assigned to OH stretching, rocking, and wagging vibrations, respectively (Kumar *et al.*, 2013).

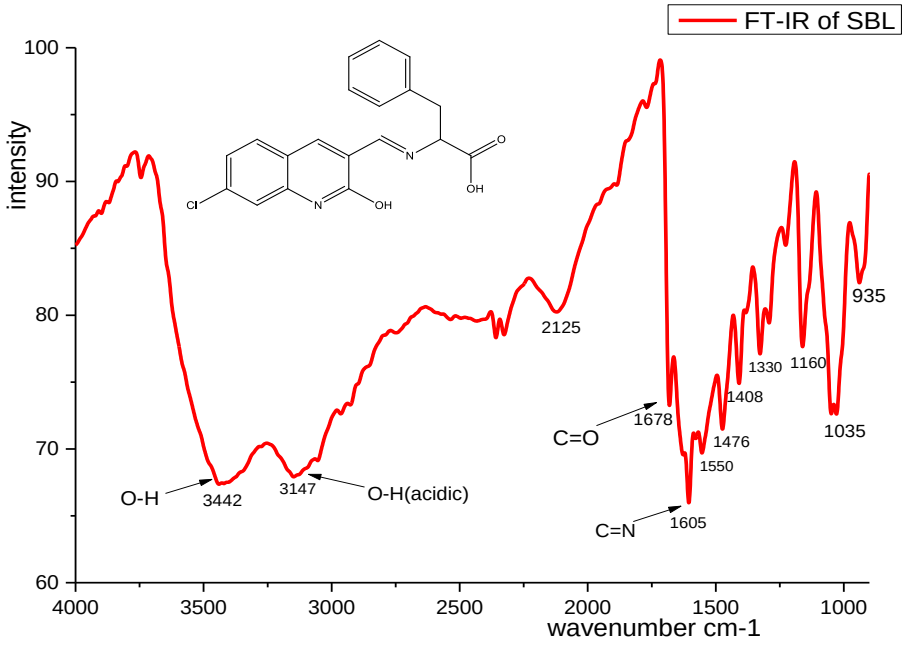

Figure 4.2: FT-IR spectra of Schiff base ligand **SBL1**

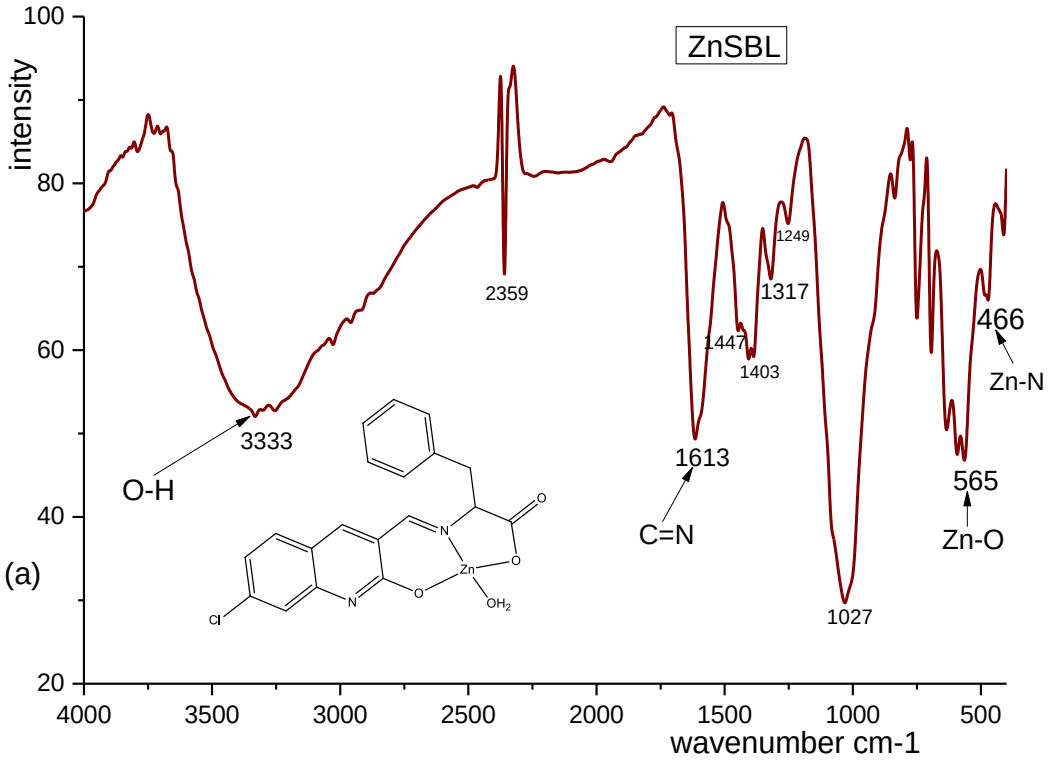
ZnSBL
intensity
100
80
60
40
20
4000
3500
3000
2500
2000
1500
1000
500
wavenumber cm-1
(a)
O-H
3333
2359
1613
C=N
1447
1403
1317
1249
1027
565
Zn-N
Zn-O
466
Cl
N
O
Zn
OH2

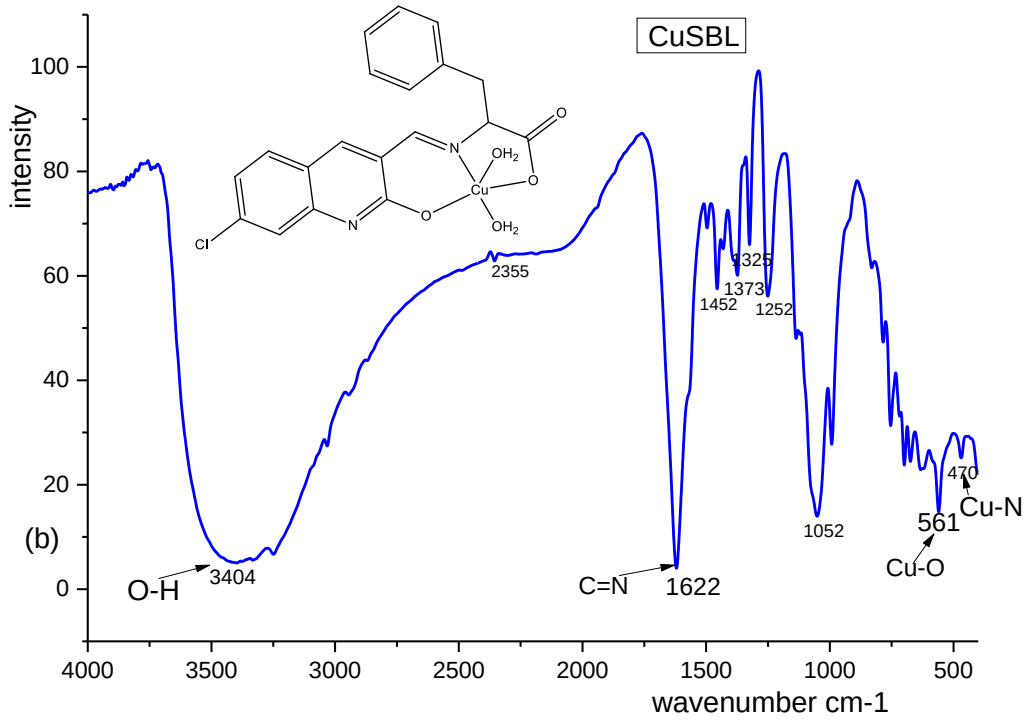
CuSBL
intensity
100
80
60
40
20
0
4000
3500
3000
2500
2000
1500
1000
500
wavenumber cm-1
(b)
O-H
3404
2355
C=N
1622
1452
1373
1325
1252
1052
561
Cu-O
470
Cu-N
Cl
N
O
Cu
OH2

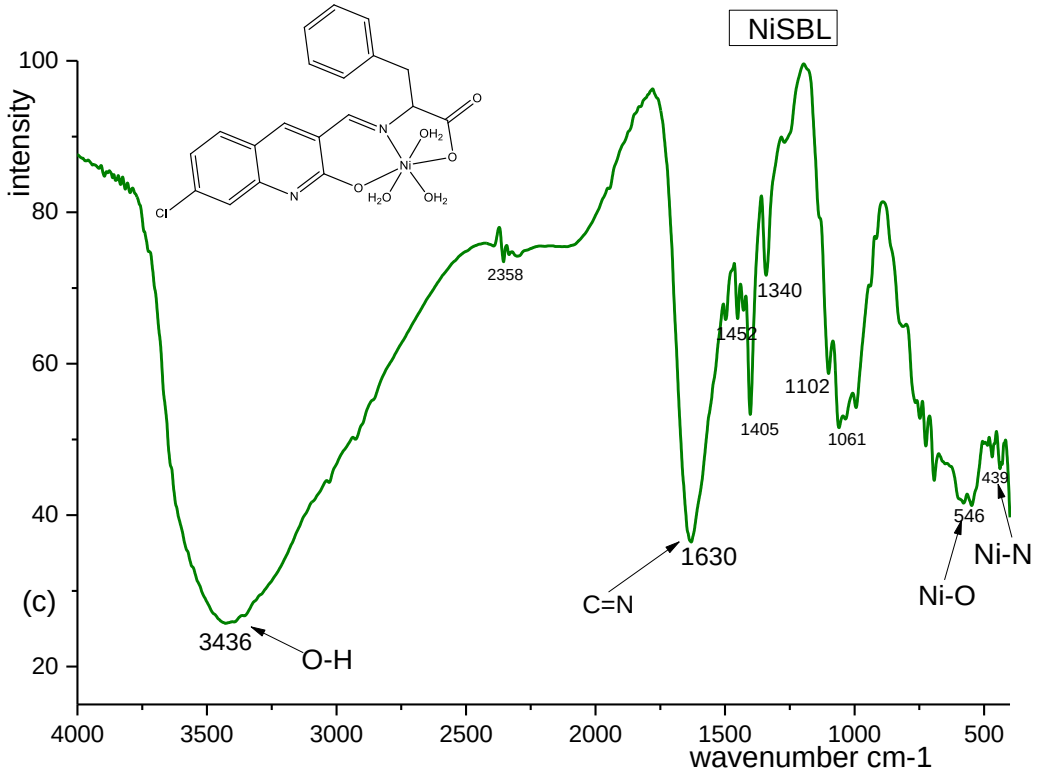

Figure 4.3: FT-IR spectra of (a) ZnSBL1, (b) CuSBL1 and (c) NiSBL1 complex of SBL1 ligand respectively

4.3.1.3. FT-IR spectra analysis of SBL2

The FT-IR spectra analyses of the Schiff base ligand indicate the presence of three distinct binding sites for the synthesized ligand to interact with metal ions. These three sites are the hydroxyl group oxygen attached to quinoline ring, the hydroxyl group oxygen attached to carboxylic group and the azomethine (-C=N-) compound nitrogen atom (Aroua *et al.*, 2023). The FT-IR spectra (υ cm^{-1}, KBr (pellet)) of the ligand found were at 1556 ν (azomethine C=N), 3456 ν(O-H attached to quinoline ring), 3020 ν(O-H of carboxylic acid of amino acid part of the ligand), 1622 ν(C=O) (Fig. 4.3). The FT-IR spectra found (υ cm^{-1}, KBr (pellet)) 1556 cm^{-1} ν(azomethine C=N), 3456 ν(O-H attached to quinoline ring), 3020ν(O-H of carboxylic acid of amino acid part of the ligand), 1622 ν(C=O) (Fig 4.3). FT-IR spectra of Schiff base show peaks at (C=N) 1556 cm^{-1} which agree with literature (Kareem, 2022), 3456cm^{-1} and 3020cm^{-1} are due to (C-OH) (attached to the Quinoline ring) and (C-OH) (carboxylic group) stretching frequency, respectively which confirms the formation of the new expected ligand (Abdel-rahman *et al.*, 2022; Adil *et al.*, 2019; Kavitha *et al.*, 2016; Patil *et al.*, 2021). The Schiff base showed IR peaks at 1556 cm^{-1} (C=N)

(Kareem, 2022; Yusuf *et al.*, 2021b), 3456 cm^{-1} and 3020 cm^{-1} are due to (C-OH) (attached to the Quinoline ring) and (C-OH) (carboxylic group) stretching frequency, respectively which confirms the formation of the ligand, (*E*)-2-(((7-chloro-2-hydroxyquinolin-3-yl)methylene)amino)-3-methylbutanoic acid (Abdel-rahman *et al.*, 2022; Adil *et al.*, 2019; Kavitha *et al.*, 2016; Patil *et al*., 2021).

Table 4.4: Important characteristic FT-IR bands (cm^{-1}) of SBL2 and its metal complexes

Cpd	ν(C=N)	ν(C=O)	ν(C-O)	ν(O-H)	$\nu(O\text{-}H)_{(acidic)}$	ν(M-O)	ν(M-N)
SBL2	1556	1622	1023	3456	3020	------	-----
ZnSBL2	1590		1037	3316		538	466
CuSBL2	1572		1043	3313		525	476
NiSBL2	1581		1017	3331		535	416

4.3.1.4. FT-IR spectra analysis of metal complexes of SBL2

The FT-IR spectra of the ligand and its metal complex were recorded in KBr disc between 4000 cm^{-1} to 400 cm^{-1}. The FTIR- spectra had signals at 1590 cm^{-1}, 1572 cm^{-1} and 1581 cm^{-1} ν(azomethine C=N) (υ, cm^{-1}), respectively for **$ZnSBL_2$, $CuSBL_2$** and **$NiSBL_2$** metal complexes(Fig 4.4). The peak at 3316 cm^{-1}, 3313 cm^{-1} and 3331 cm^{-1}corresponds to ν(O-H) of water molecules respectively in **$ZnSBL_2$, $CuSBL_2$** and **$NiSBL_2$** complexes (Ara, 2014). The new peaks at 538 *ν*(Zn-O), 525 *ν*(Cu-O) and 535 *ν*(Ni-O); 466 *ν*(Zn-N), 476 *ν*(Cu-N) and 416 *ν*(Ni-N) which confirms the ONO complexation to Zinc(II), Copper(II) and Nickel(II) during complex formation of metal with the **SBL_2** ligand (Heba *et al.*, 2023; Kouser *et al.*, 2023).

FT-IR spectrum of the free Schiff base ligand has showed a strong υ(C=N) azomethine band at 1556 cm^{-1} however for metal complexes shifted to higher values at 1590 cm^{-1}, 1572 cm^{-1} and 1581 cm^{-1} for complexes of **$ZnSBL_2$, $CuSBL_2$** and **$NiSBL_2$** respectively (Hasan *et al.*, 2021; Muleta *et al.*, 2022). The Schiff base showed peaks at 1556 cm^{-1}, 3456 cm^{-1} and 3020 cm^{-1}, which were due to (C=N) and O-H (attached to the quinoline ring) and O-H (carboxylic from amino acids) stretching frequency, respectively (Ara, 2014; Kareem, 2022; Nagesh, 2014). The peak at around 749 cm^{-1} which indicate the C-Cl stretching vibration bond existence in the structure of the

SBL$_2$ confirmation (Erturk, 2019). However, in case of **ZnSBL$_2$, CuSBL$_2$** and **NiSBL$_2$** complexes, C=N stretching frequency peaks were observed at 1590 cm^{-1}, 1572 cm^{-1} and 1581 cm^{-1}, respectively.

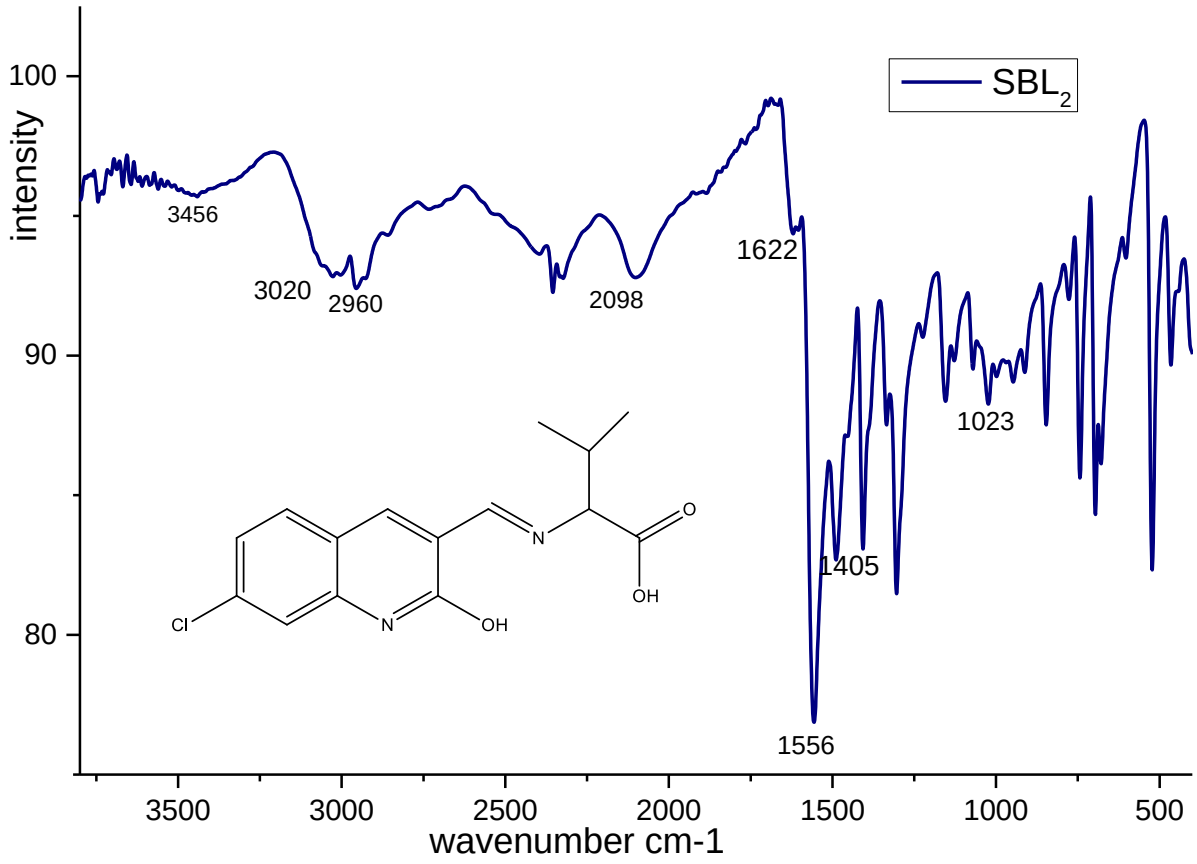

Figure 4.4: The FT-IR spectra of Schiff base ligand two (**SBL$_2$**)

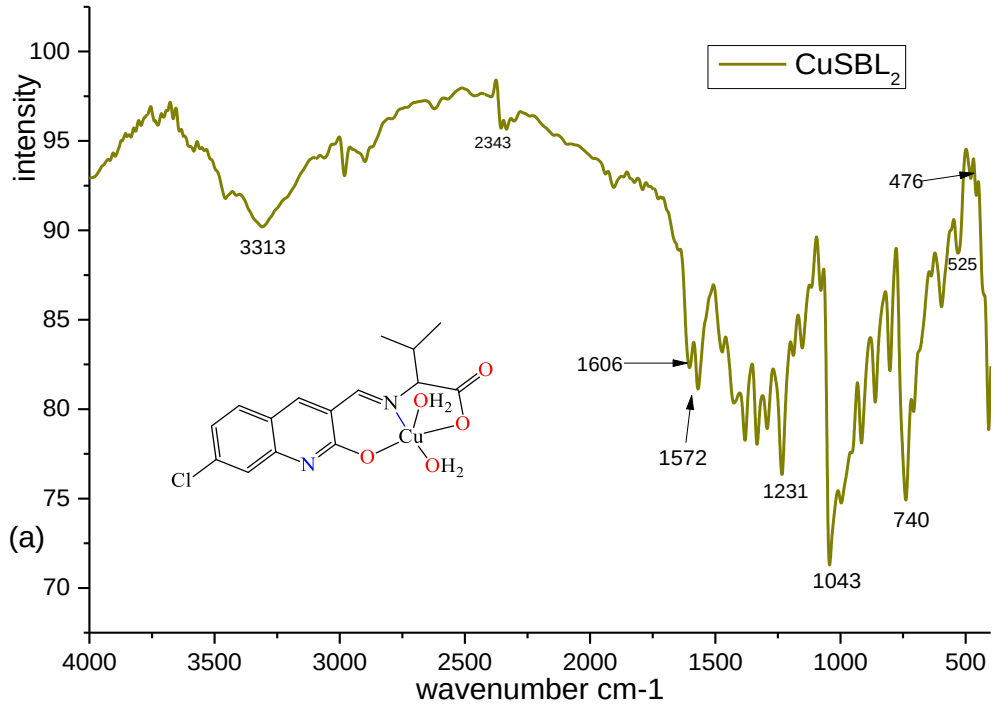
CuSBL2
intensity
100
95
90
85
80
75
70
3313
2343
476
525
1606
1572
1231
1043
740
(a)
4000
3500
3000
2500
2000
1500
1000
500
wavenumber cm-1
Cl
N
O
OH2
Cu

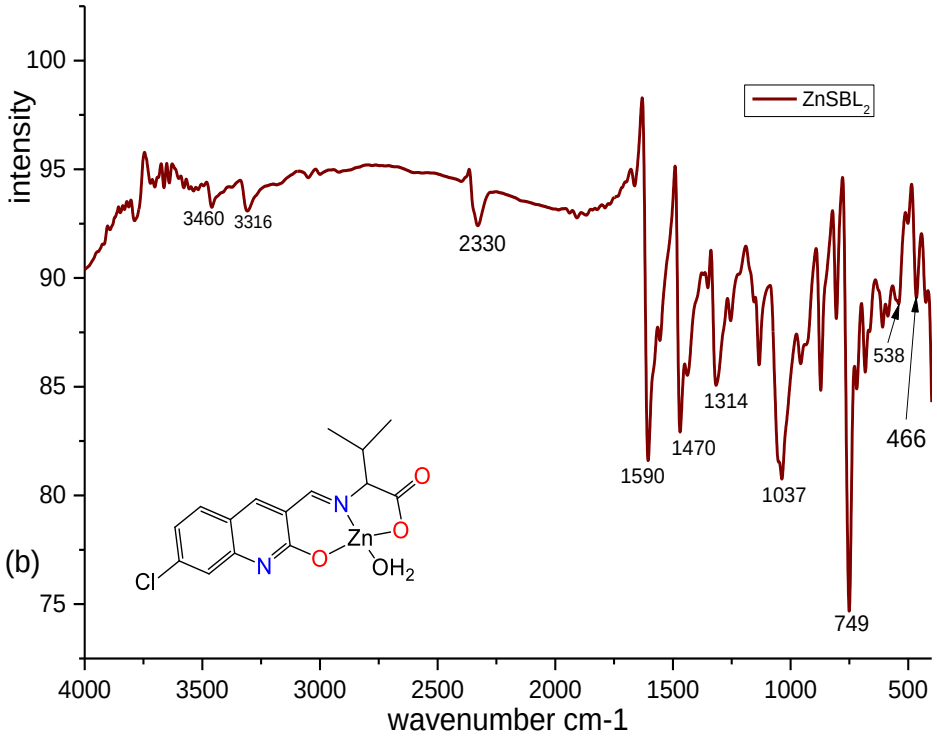
ZnSBL2
intensity
100
95
90
85
80
75
3460
3316
2330
1590
1470
1314
1037
538
466
749
(b)
4000
3500
3000
2500
2000
1500
1000
500
wavenumber cm-1
Cl
N
O
Zn
OH2

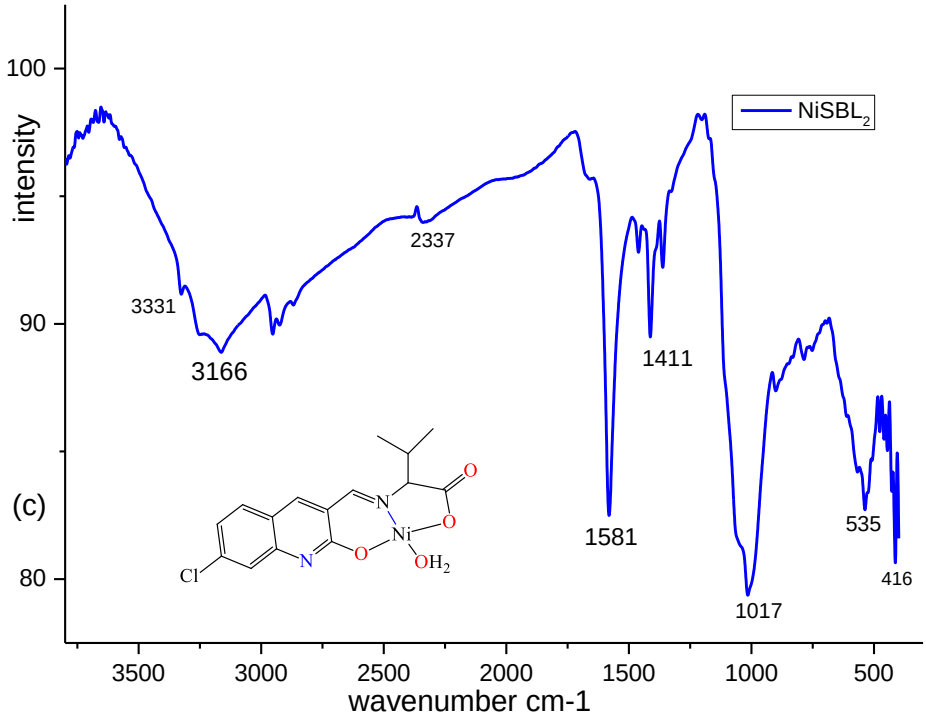

Figure 4.5: FT-IR spectra of (a) $CuSBL_2$, (b) $ZnSBL_2$ and (c) $NiSBL_2$ respectively

4.3.2. Electronic spectral analysis of ligands and metal complexes

UV-Vis spectra are associated with electronic transitions of the molecules that absorb energy in the form of ultraviolet or visible light going from the ground electronic state into excited states. The UV-Vis spectra of the ligands and their metal complexes were record in the wavelength range 200 - 800 nm using 1×10^{-5} M DMSO solution as a solvent of the samples at room temperature and the spectra graphs were shown in Appendix number 1.

4.3.2.1. UV−Vis Spectra analysis of SBL1

In the UV-Vis spectral data (DMSO, nm): The absorption bands of the Schiff base ligand are commonly due to π−π* and n−π* electronic transitions, which undergo a red shift during metal complexation. The free ligand exhibited absorption bands at 239 nm, and 253 nm which could be attributed to π→π* while 311 nm and 324 nm could be attributed to n→π* electronic transitions. The calculated absorption spectra using TD-B3LYP functional to provide further insight into the spectra of the ligand and its complexes. The calculated absorption spectra are in good agreement with the corresponding experimental results (Fig.4.6).

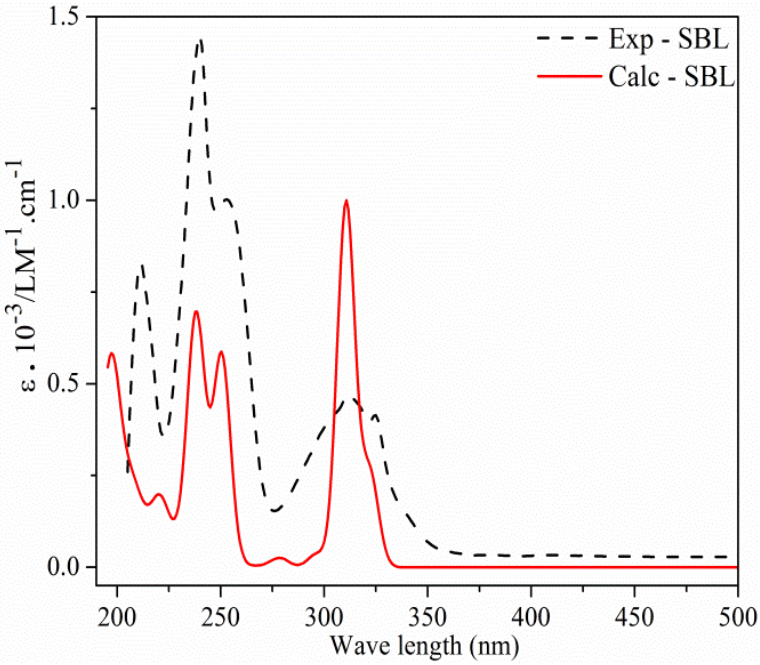

Figure 4.6: Experimental and TD-B3LYP-GD3/ 6-31++G**/PCM/ methanol calculated UV-Vis absorption spectra of the ligand **SBL** the calculated spectrum was blue-shifted by 30 nm for better comparison

4.3.2.2. UV−vis spectra analysis of metal complexes of SBL1 ligand

The UV-Vis spectra also revealed that the **ZnSBL1**, **CuSBL1** and **NiSBL1** complexes have bands in the spectral range of 241-257 nm and 313-327 nm, which indicate π→π* and n→π* electronic transitions respectively.

For **ZnSBL1** complex, the bands at 242 nm and 257 nm correspond to π→π*, those at 313 nm and 327 nm correspond to n→π* electronic transitions. In case of **CuSBL1**, the spectra observed at 241 nm and 254 nm correspond to π→π*, whereas those at 313 nm and 326 nm correspond to n→π* electronic transitions. Likewise, the absorption bands at 241 nm and 256 nm for **NiSBL1** correspond to π→π*, while 314 nm and 325 nm correspond to n→π* electronic transitions. In all the complexes, the absorption bands were red shifted (bathochromic shift) compared to the free ligand which confirms the formation of the complexes (Damena et al., 2023). This shift may be caused due to the contribution of lone pair of electrons of nitrogen of azomethine of the ligand to a metal ion (Damena *et al.*, 2022b; Patil *et al.*, 2021; Vinusha *et al.*, 2019). The

calculated absorption spectra are in good agreement with the corresponding experimental results, which further confirms the successful syntheses of the three complexes (Damena *et al.*, 2022).

Table 4.5: Absorption bands of the SBL1, ZnSBL1, CuSBL1 and NiSBL1 complexes

Compounds	Absorption (nm)	Electronic transitions	Assignment	Geometry
SBL1	239 and 253	π-π*	ILCT	----------
	311 and 324	n-π*	ILCT	
ZnSBL1	242 and 257	π-π*	LMCT	Tetrahedral arrangement
	313 and 327	n-π*	LMCT	
CuSBL1	241 and 254	π-π*	LMCT	Trigonal bipyramid arrangement
	313 and 326	n-π*	LMCT	
NiSBL1	241 and 256	π-π*	LMCT	Octahedral arrangement
	314 and 325	n-π*	LMCT	

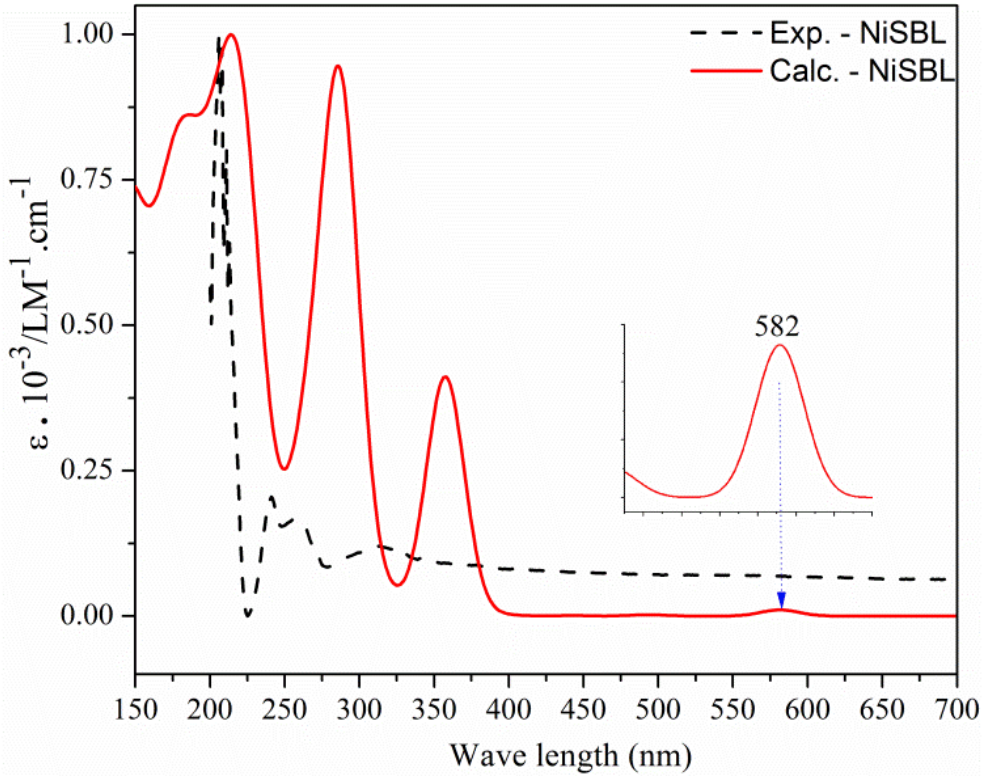

(a)

(b)

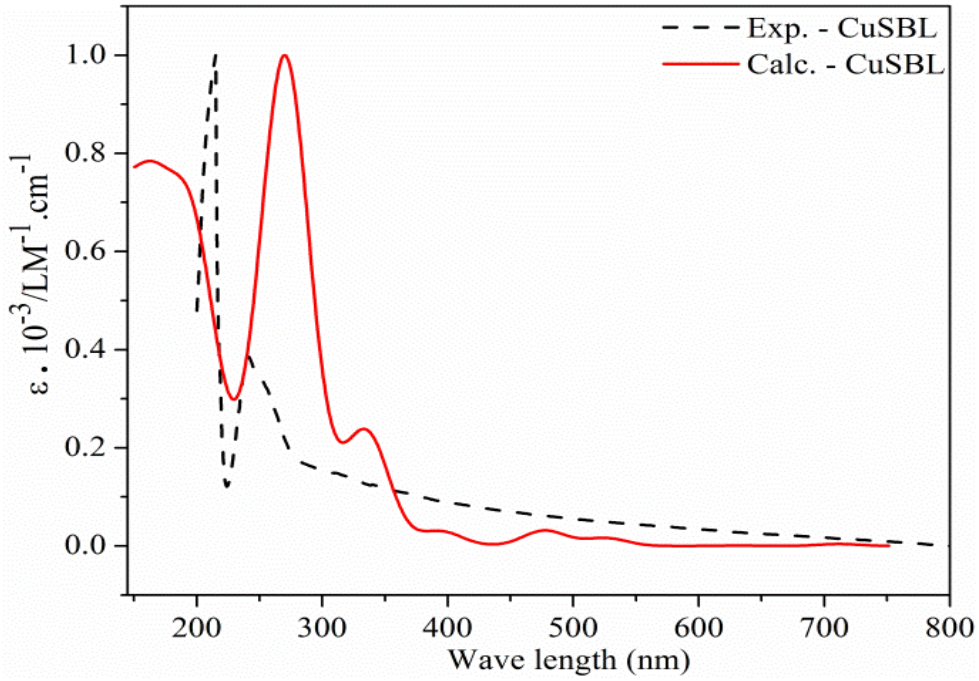

(c)

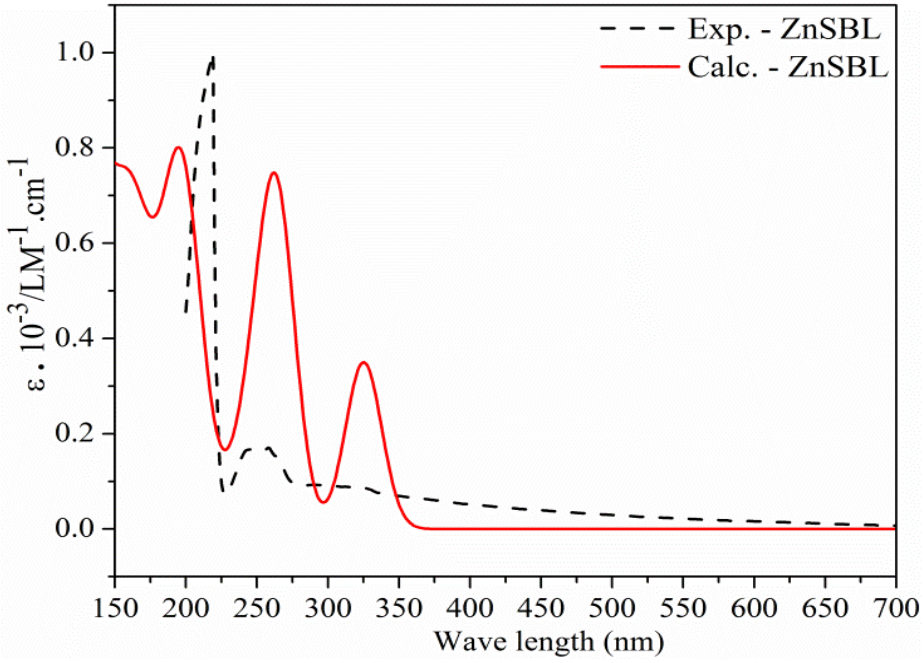

Figure 4.7: Experimental and TD-B3LYP-GD3/ 6-31++G**/PCM/ methanol calculated UV-Vis absorption spectra of the (a) NiSBL1 (b) CuSBL1 and (c) ZnSBL1 the calculated spectrum was blue-shifted by 30 nm for better comparison

4.3.2.3. UV-Vis spectra analysis of SBL_2 Ligand

The absorption bands of the Schiff base ligand primarily arise from π–π* and n–π* electronic transitions, which experience a red shift upon forming a metal complex. Initially, the free ligand displays absorption bands at 276 nm and 311 nm due to π→π* while 326 nm and 348 nm associated with n→π* electronic transition. The absorption spectra has been also calculated using TD-B3LYP functional to provide further insight into the spectra of the ligand. The calculated absorption spectra resulted in good agreement with the experimental results (Fig.4.8), which further confirms the successful syntheses of the ligand (Damena *et al.*, 2022; (Damena *et al.*, 2023; Patil *et al.*, 2021; Vinusha *et al.*, 2019).

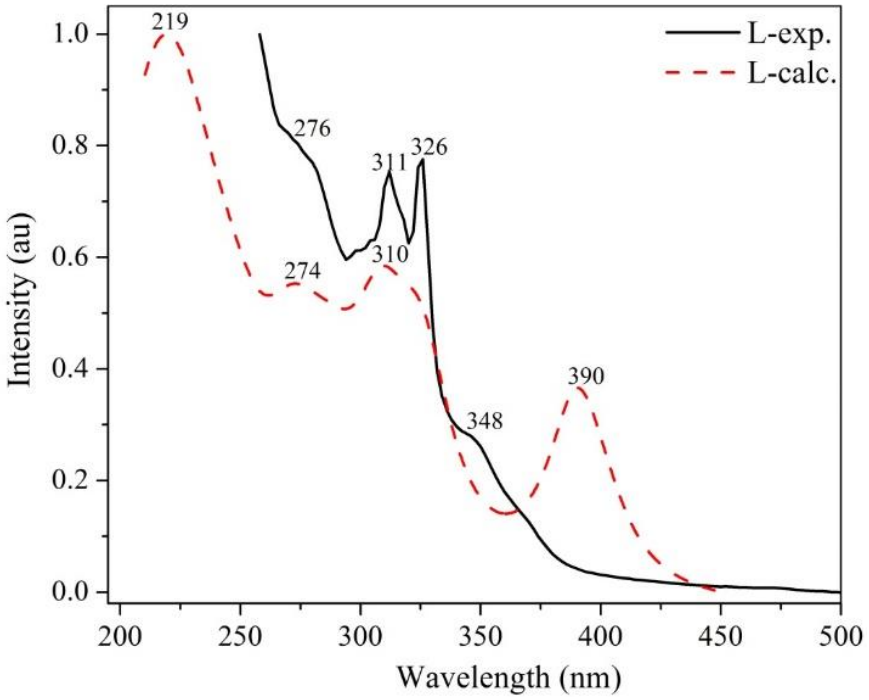

Figure 4.8: Experimental and TD-B3LYP-GD3/ 6-31++G**/PCM/ methanol calculated UV-Vis absorption spectra of the ligand SBL_2 the calculated spectrum was blue-shifted by 30 nm for better comparison.

4.3.2.4. UV−vis Spectra Analysis of metal complexes of ligand SBL2

The UV−Vis spectra of the ligand (SBL_2) and its metal complexes was recorded at a wavelength range (200−800 nm) using a diluted sample solution in DMSO at room temperature. The free ligand exhibited absorption bands at 276 nm and 311 nm which could be attributed to

π→π* while 326 nm and 348 nm could be attributed to n→π* electron transition. The Uv-Vis spectra of the **$ZnSBL_2$**, **$CuSBL_2$** and **$NiSBL_2$** complexes showed bands in the spectral range around 260 nm and 325 nm, which corresponding to π→π* and n→π* electron transitions and absorbance around 470 nm could be due to LMCT. For $ZnSBL_2$ complex, the UV-Vis spectra value of 260 nm and 312 nm corresponding to π→π*, whereas the spectra at 325 nm and 470 nm refer to n→π* electron transition. The shift confirms the successful formation of $ZnSBL_2$ complex (Damena *et al.*, 2023; Vinusha *et al.*, 2019)

Moreover, the broad bands observed at around 470 nm, 473 nm and 460 nm for $ZnSBL_2$, $CuSBL_2$ and $NiSBL_2$ complexes could be assigned to the ligand to metal charge transfer (LMCT). This could serve as an additional confirmation for the participation of the ligand donor atoms in complex formation (Damena *et al*., 2022). The shifting of absorption band at higher wavelengths/red shift in metal complexes was due to coordination of Schiff base ligand (Patil *et al.*, 2021; Vinusha *et al.*, 2019). Additionally the calculated absorption spectra using TD-B3LYP to provide insight into the spectra of the ligand and metal complexes. The experimental results are in good agreement with the predicted results, as shown in Figure 4.9, after comparison of the experimental electronic spectra with the DFT computed results for the absorption spectra, this further confirms the successful syntheses of the expected complexes (Damena *et al.*, 2022).

Table 4.6: Electronic Spectra of the **SBL_2** and **$ZnSBL_2$**, **$CuSBL_2$** and **$NiSBL_2$** Complexes

Compound	Absorption (nm)	Transition	Assignment	Geometry
SBL_2	276 and 311	π-π*	ILCT	----------
	326 and 348	n-π*	ILCT	
$ZnSBL_2$	262 and 312	π-π*	LMCT	Tetrahedral arrangement
	325 and 470	n-π* and LMCT	LMCT	
$CuSBL_2$	260 and 312	π-π*	LMCT	Trigonal bipyramid arrangement
	325 and 473	n-π* and LMCT	LMCT	
$NiSBL_2$	262 and 312	π-π*	LMCT	Square planar arrangement
	325 and 460	n-π* and LMCT	LMCT	

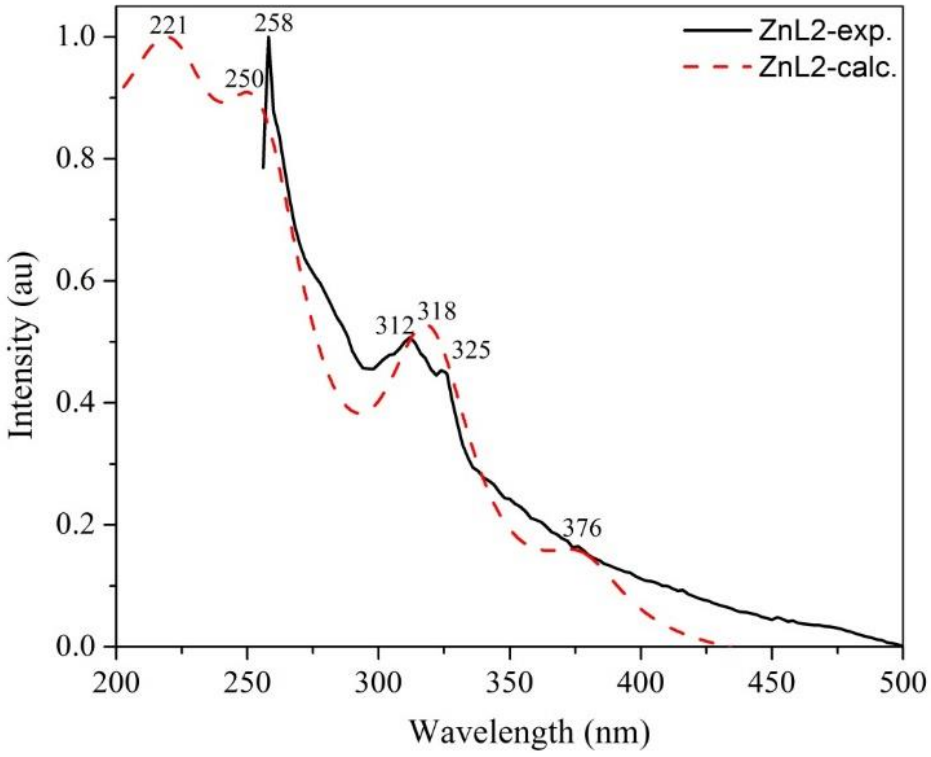
ZnL2-exp.
ZnL2-calc.
221
258
250
312
318
325
376
Intensity (au)
Wavelength (nm)
1.0
0.8
0.6
0.4
0.2
0.0
200
250
300
350
400
450
500

(a)

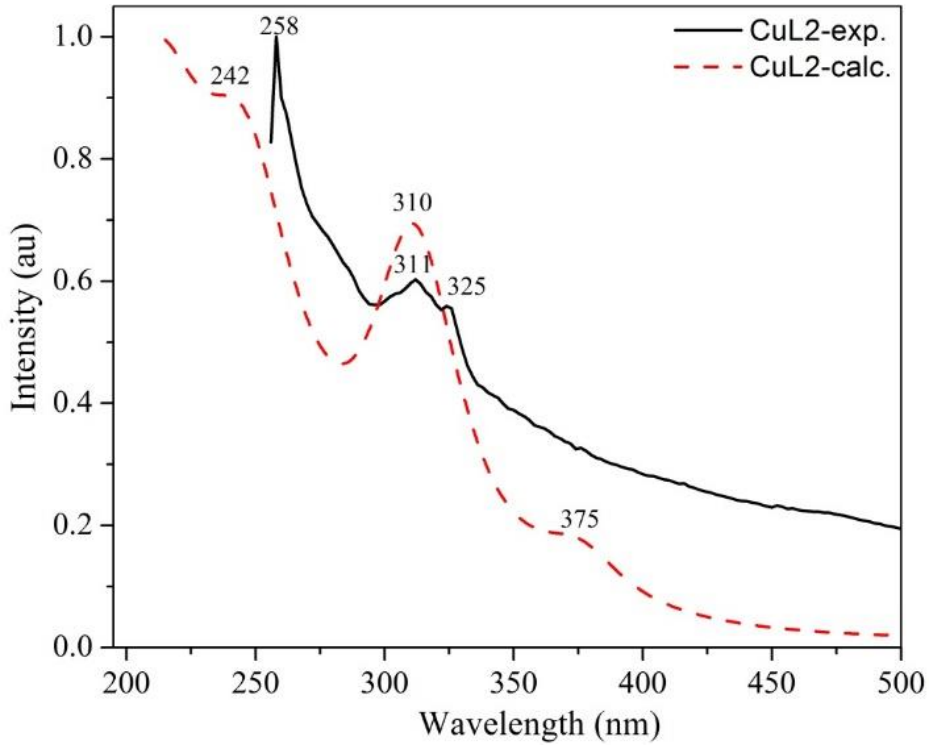
CuL2-exp.
CuL2-calc.
258
242
310
311
325
375
Intensity (au)
Wavelength (nm)
1.0
0.8
0.6
0.4
0.2
0.0
200
250
300
350
400
450
500

(b)

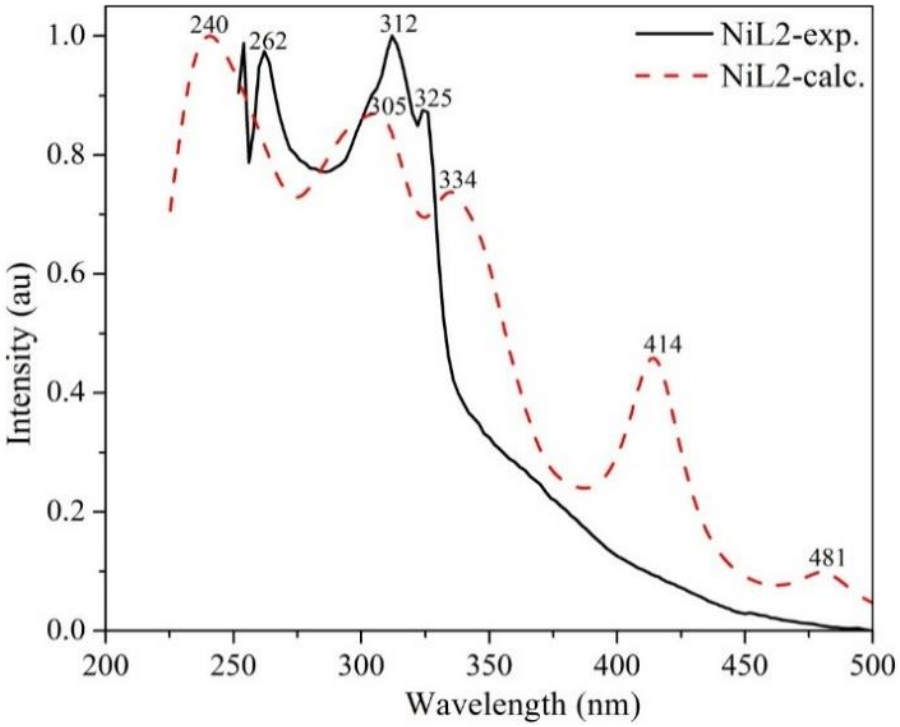

(c)

Figure 4.9: Experimental and DFT calculated UV-Vis spectra of the synthesized (a) $ZnSBL_2$, (b) $CuSBL_2$ and (c) $NiSBL_2$ complexes

4.3.3. NMR Spectra analysis of the synthesized ligands

The ^{1}H NMR and ^{13}C-NMR spectrum data, which provides precise information regarding the positional elucidation and number of proton and carbon atoms, were used to confirm the structures of the synthesized compounds. The quantity and composition of atoms in a compound can be identified by examining its nuclear magnetic resonance spectrum and calculating their proportions throughout the compound's immediate environment (Venkatesh *et al.*, 2024).

4.3.3.1. ^{1}H NMR Spectral analysis of SBL1

In the ^{1}H NMR Spectra of the Schiff base ligand (**SBL1**), the protons of azomethine are observed in the range 7.00-7.50 ppm. Moreover, the peaks in the range around 10.00-11.00 ppm, can be attributed to aromatic -OH proton in the newly synthesized Schiff base ligand (Hanan, 2020). The signals that appeared in the range of 7.15-7.25 ppm could be assigned to (HC=N) proton which best agrees with literature report (Srivastava, 2021).

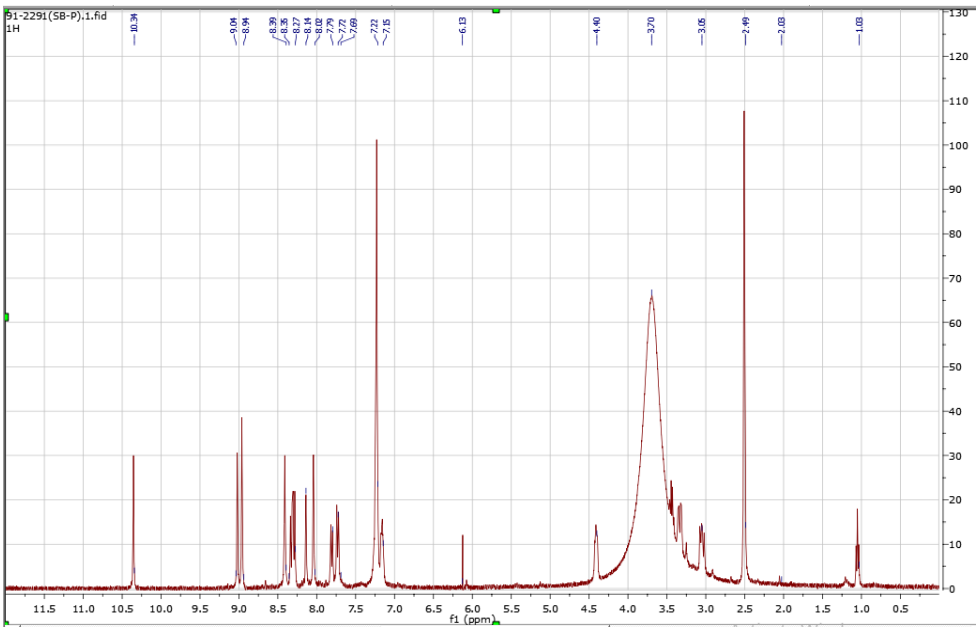

Figure 4.10: ^{1}H-NMR spectra of SBL1

4.3.3.2. ^{13}C NMR Spectra analysis of SBL1 ligand

In ^{13}C NMR, the signal at δ_C 38.83 ppm was due to the presence of the aromatic $-CH_2$ group. The C-O carbon are observed at δ_C178.13 and 177.3 ppm. The signals at δ_C 160.53 ppm might refer to carbon atoms in the azomethine C=N carbon atom that is also in good agreement with reported literature. The signals appeared at δ_C 150.36, 137.91, 135.37, 128.76, 126.82 and 125.44 ppm were due to the quinoline and Phenylanine ring carbon atoms (Hanan, 2020; Patil *et al.*, 2021; Srivastava, 2021).

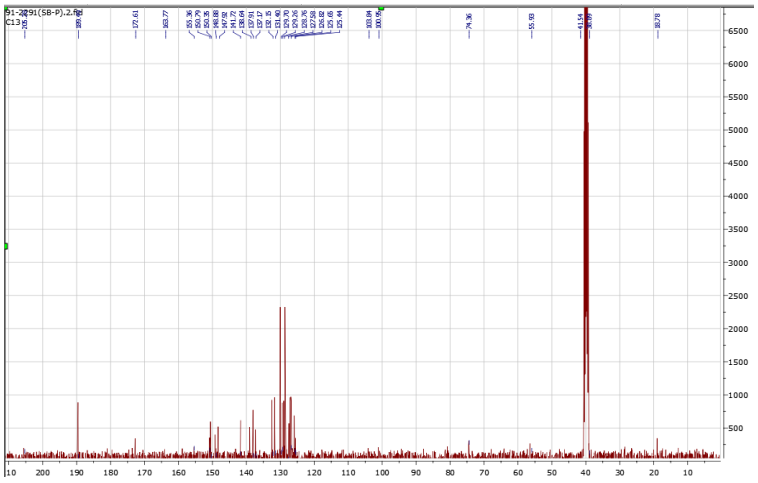

Figure 4.11: ^{13}C-NMR spectra of SBL1

4.3.3.3. ^{1}H NMR spectra analysis of SBL2 ligand

^{1}H NMR Spectra of the Schiff base ligand (Fig 4.12), the protons of azomethine observed in the range 7.00-7.50 ppm. Peaks observed in the range 10.00-11.00 ppm attributed to aromatic -OH proton in the newly synthesized Schiff base ligand. The signal observed in the range of 7.00 - 7.50 ppm confirmed that the formation of HC=N is estimated from the chemical formula using chemdraw software and best agrees with reported literature (Hanan, 2020; Dinku *et al.*, 2024; Srivastava, 2021; Vinusha *et al.*, 2019).

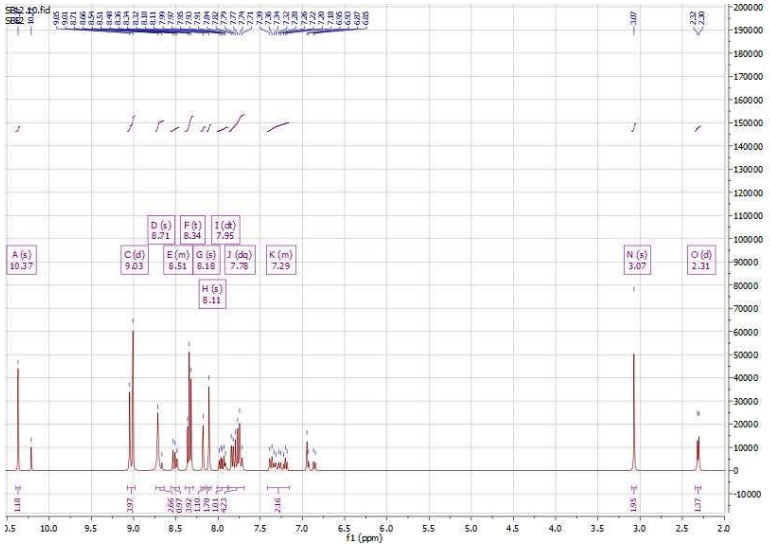

Figure 4.12. ^{1}H NMR spectra of Schiff base Ligand (SBL2)

4.3.4. Thermogravimetric Analysis of the metal complexes

The newly synthesized Zn(II), Cu(II) and Ni(II) complexes under ambient conditions were subjected to thermal analysis and stability studies using a thermogravimetric analyzer (TGA) and differential thermogravimetric analysis (DTA).

4.3.4.1. Thermogravimetric Analysis of the metal complexes of SBL1 ligand

The degradation pattern of the complexes evaluated using TGA were presented in (Fig.4.13 and Table 4.7). Accordingly, the thermogravimetric examination indicated that ZnSBL1, CuSBL1 and NiSBL1 complexes had a weight loss of 4.13%, 7.96% and 11.61%, respectively, which are equivalent to the weight of a water molecule. This weight loss occurred at temperatures around 245 ^{o}C for ZnSBL1, 250 ^{o}C for CuSBL1, and 170 ^{o}C for NiSBL1 complex that confirms the water molecules are coordinated to the central metal atoms (Damena *et al.*, 2023). These water molecules

are more strongly bonded to the metal ions thus eliminated at higher temperatures (Gaikwad *et al.*, 2022). Further heating, the weight loss of the residue continued until 650 ^{o}C for ZnSBL1, 750 ^{o}C for CuSBL1 and 600 ^{o}C for NiSBL1, in which the complexes became stable. The DTA data confirms that the complexes are best described as endothermic (Ara, 2014).

Table 4.7 Thermal analyses data (TGA/DTA) for metal complexes of SBL1 ligand

Compound	Empirical formula	Tem.range (^{o}C)	% Weight loss	Lost fragment	Probable residue	DTA	
						max (° C)	endo/exo
ZnSBL1	[Zn($C_{19}H_{15}O_3N_2Cl$)]	245	4.13%	loss of one H_2O	ZnO	650	Exo
		245- 450	33.94%	loss of $C_9H_8O_2$			
		450-650	43.23%	loss of $C_{10}H_5N_2Cl$			
CuSBL1	[Cu($C_{19}H_{17}O_4N_2Cl$)]	250	7.96%	loss of two H_2O	CuO	750	Exo
		400-600	32.74%	loss of $C_9H_8O_2$			
		600-750	40.82%	loss of $C_{10}H_5N_2Cl$			
NiSBL1	[Ni($C_{19}H_{19}O_5N_2Cl$)]	170	11.61%	loss of three H_2O	NiO	600	Exo
		150- 350	31.83%	loss of $C_9H_8O_2$			
		350- 600	40.54%	loss of $C_{10}H_5N_2Cl$			

TGA/DTA curves of CuSBL1 complex (Figure 4.11) showed that the complex is stable up to 250 °C and no weight loss was observed before this temperature. The first stage of degradation occurred at 250 °C, with the loss of the two H_2O molecules. The resultant complex on further degradation gave a break at around 400-600 °C by the Phenylanine branch of the Schiff base ligand, which has expected formula of $C_9H_8O_2$. The resultant complex underwent third stage of decomposition in range of 600-750 °C due to loss of molecule $C_{10}H_5N_2Cl$ of quinoline moiety and further, the complex showed corresponds to copper oxide residue (Damena *et al.*, 2022a).

The thermogram of the ZnSBL1 complex (Figure 4.13) revealed that it was first breaking down at around 245 ^{o}C due to the loss of a single H_2O, and then gradually breaking down at around 250-450 ^{o}C with the organic part of the Phenylanine branch of the Schiff base ligand, which has the formula C_9H_8O. Finally, the complex gradually lost the organic moiety of the quinoline part, which has the formula $C_{10}H_5N_2Cl$, and after that, it showed a gradual breakdown up to 450-650 °C due to the loss of the remaining organic moiety. Zinc oxide (ZnO) is the ultimate residue that matches the metal (Yernale *et al.*, 2014).

TGA and DTA curves of NiSBL1 complex (Figure 4.11) show that the complex is stable up to 170 °C and no weight loss was observed before this temperature. The first stage of degradation occurred at 170 °C, with the loss of the three H_2O molecules. The resultant complex on further degradation gave a break at around 150-250 °C by the Phenylanine branch of the Schiff base ligand, which has the formula $C_9H_8O_2$. The resultant complex underwent third stage of decomposition at 350-600 °C due to loss of molecule $C_{10}H_5N_2Cl$ of quinoline moiety and further, the complex showed corresponds to nickel oxide as residue (Chioma, 2019; Khalaf-Alla, 2020).

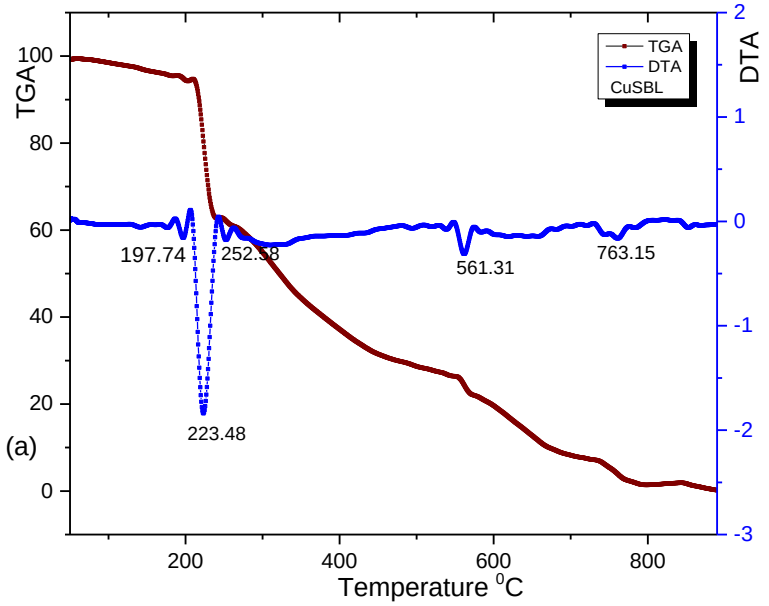
TGA
DTA
CuSBL
TGA
DTA
100
80
60
40
20
0
2
1
0
-1
-2
-3
197.74
252.58
223.48
561.31
763.15
(a)
200
400
600
800
Temperature ^{0}C

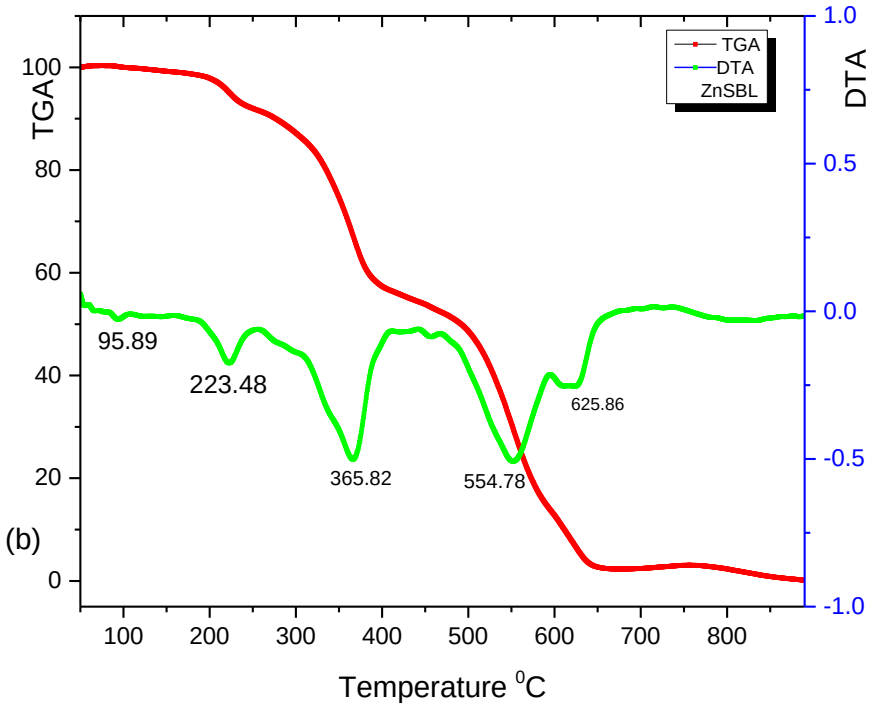
TGA
DTA
ZnSBL
TGA
DTA
100
80
60
40
20
0
1.0
0.5
0.0
-0.5
-1.0
95.89
223.48
365.82
554.78
625.86
(b)
100
200
300
400
500
600
700
800
Temperature ^{0}C

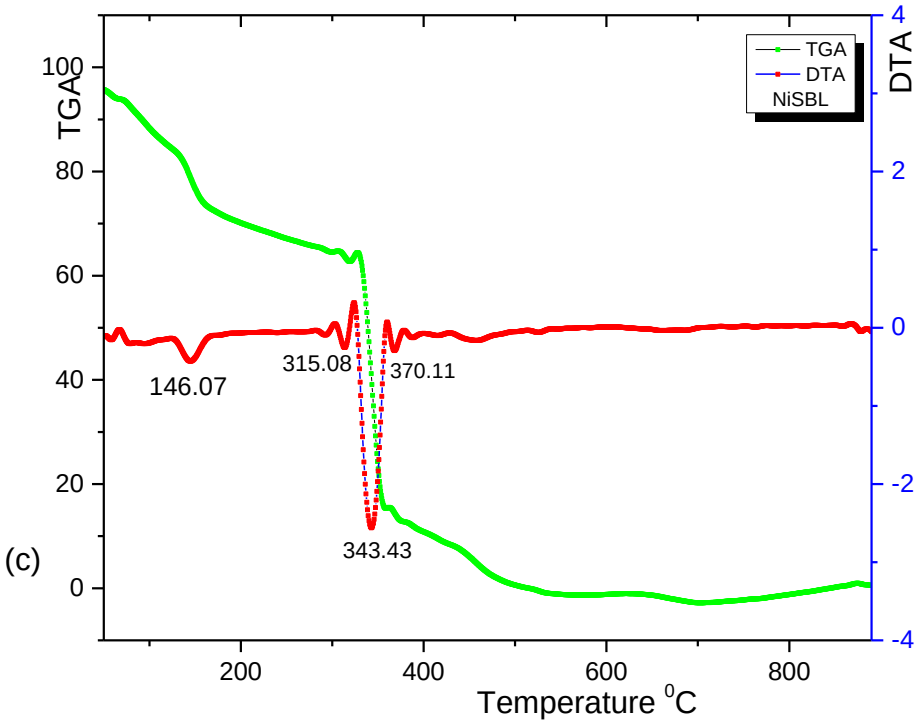

Figure 4.13: TGA/DTA graph of (a) CuSBL1, (b) ZnSBL1 & (c) NiSBL1 complex

4.3.4.2. Thermogravimetric Analysis of metal complexes of SBL2 ligand

In order to examine the thermal stability of the complexes, thermo gravimetric (TG) and differential thermal analyses (DTA) were carried out (Yernale *et al*., 2014). The degradation pattern of the complexes were presented below (Fig. 4.14 and Table 4.8). The thermogravimetric analysis of complexes showed a decomposition pattern between 124 ^{o}C and 732 ^{o}C may be due to the removal of the coordinated molecules, ions or organic part of the compounds. Since the decomposition started above 124 ^{o}C, the presence of any solvent/water molecules may not be expected out sphere of the complexes (Kouser *et al*., 2023). Accordingly, the Thermogravimetric data indicated $ZnSBL_2$, $CuSBL_2$ and $NiSBL_2$ complexes, had a weight loss of 4.64%, 8.91%, and 4.72% respectively which confirms the loss of a water molecule. This weight loss occurred at temperatures around 181 ^{o}C for $ZnSBL_2$ 204 ^{o}C for $CuSBL_2$ 124 ^{o}C for $NiSBL_2$ complex confirming the water molecules are coordinated to the central metal atom (Damena *et al*., 2023; Vinusha *et al*., 2019).

This further tells us that the coordinated water molecules occupy some position in the coordination sphere of the central metal ion. These water molecules are more strongly bonded to the metal ions thus eliminated at the higher temperatures (Gaikwad *et al.*, 2022). Subsequent heating caused a steady weight loss with temperature increase, showing that the samples had been decomposed at high temperatures and that metal oxide was the final byproduct (Vinusha *et al.*, 2019).

Presence of water molecules further confirmed by the endothermic bands observed in the respective DTA curve. In addition to the endothermic bands, the DTA curves of complexes also show exothermic bands. This band appeared at higher temperatures which represent phase transition, oxidation, and/or decomposition of the compound (Kumar *et al.*, 2013). On extra heating, the weight of the residue continued until 647 ^{o}C for $ZnSBL_2$ 732 ^{o}C for $CuSBL_2$ and 647 ^{o}C for $NiSBL_2$ respectively, after which the complex became stable and the DTA data confirms the complexes are best described as endothermic (Ara, 2014).

Table 4.8 Thermal analyses data (TGA/DTA) for metal complexes of SBL2 ligand

Compound	Empirical formula	Tem.range (^{o}C)	% Weight loss	Lost fragment	Probable residue	DTA	
						max (° C)	endo/ exo
ZnSBL2	$[Zn(C_{15}H_{15}O_4N_2Cl)]$	181	4.64%	loss of H_2O	ZnO	650-- Exo	
		250- 450	25.00%	loss of $C_5H_5O_2$			
		450-650	48.58%	loss of $C_{10}H_5N_2Cl$			
CuSBL2	$[Cu(C_{15}H_{17}O_5N_2Cl)]$	204	8.91%	loss of two H_2O	CuO	750-- Exo	
		250- 550	24.01%	loss of $C_5H_5O_2$			
		550-750	46.65%	loss of $C_{10}H_5N_2Cl$			
NiSBL2	$[Ni(C_{15}H_{15}O_4N_2Cl)]$	124	4.72%	loss of H_2O	NiO	650-- Endo	
		150- 300	25.46%	loss of $C_5H_5O_2$			
		350-650	49.34%	loss of $C_{10}H_5N_2Cl$			

The thermogram of the ZnSBL2 complex (Figure 4.14) revealed that it was first degrade down at around 150-250 ^{o}C due to the loss of a single H_2O, and then gradually breaking down at around 250-450 ^{o}C with the organic part of the Valine branch of the Schiff base ligand, which has the formula $C_5H_8O_2$. Finally, the complex gradually lost the organic moiety of the quinoline part, which has expected formula of $C_{10}H_5N_2Cl$ at temperature range of 450-650 $^{\circ}$C. Zinc oxide (ZnO) is the ultimate residue that matches the metal (Yernale *et al.*, 2014).

TGA/DTA curves of CuSBL2 complex (Figure 4.14) showed that the first stage of degradation occurred at 204 °C, with the loss of H_2O molecules. The resultant complex on further degradation gave a break at around 250-550 °C by the Valine branch of the Schiff base ligand, which has the expected formula of $C_5H_8O_2$. The resultant complex underwent third stage of decomposition at temperature range of 550-750 °C due to loss of molecule $C_{10}H_5N_2Cl$ of quinoline moiety. And further, the complex residue were copper oxide (Damena *et al.*, 2022a).

TGA/DTA curves of NiSBL2 complex (Figure 4.14) showed that the complex was stable up to 124 °C and no weight loss was observed before this temperature. The first stage of degradation occurred at around 124 °C, with the loss of the H_2O molecule. The resultant complex on further degradation gave a break at around 150-300 °C by the Valine branch of the Schiff base ligand, which has the expected formula of $C_5H_8O_2$. The resultant complex underwent third stage decomposition at temperature range of 350-650 °C due to loss of molecule $C_{10}H_5N_2Cl$ of quinoline moiety. And further, the complex showed corresponds to nickel oxide residue (Chioma, 2019; Khalaf-Alla, 2020).

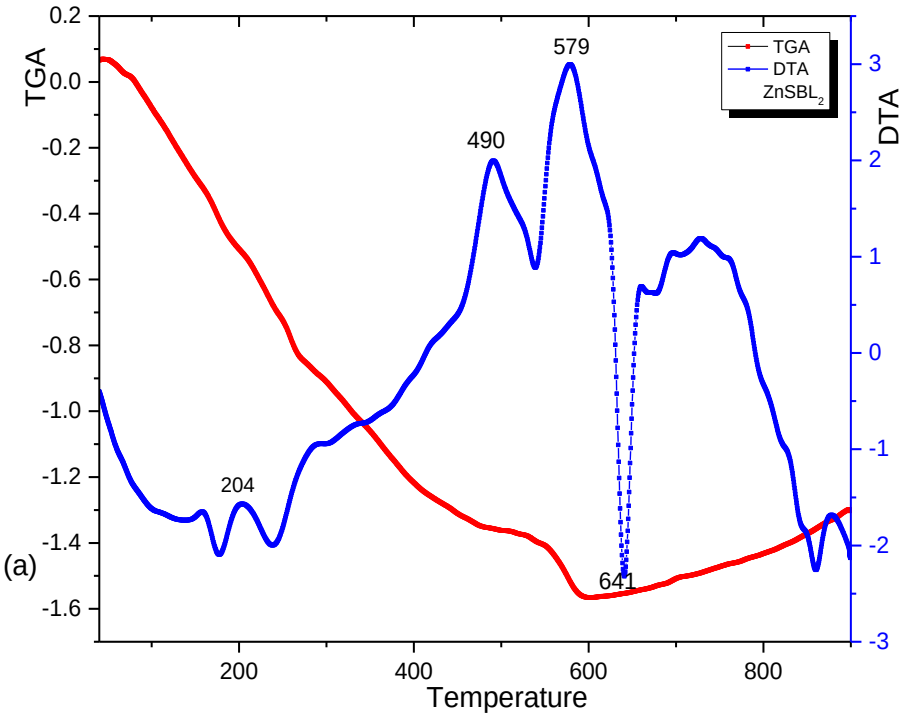
TGA
DTA
ZnSBL2
579
490
204
641
(a)
Temperature
TGA
DTA

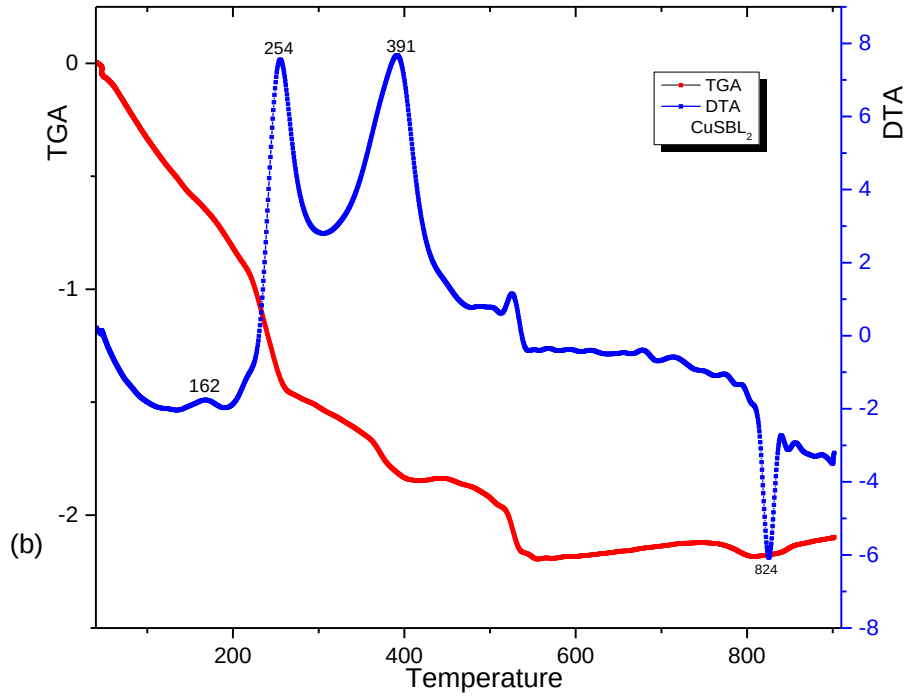
TGA
DTA
CuSBL2
254
391
162
824
(b)
Temperature
TGA
DTA

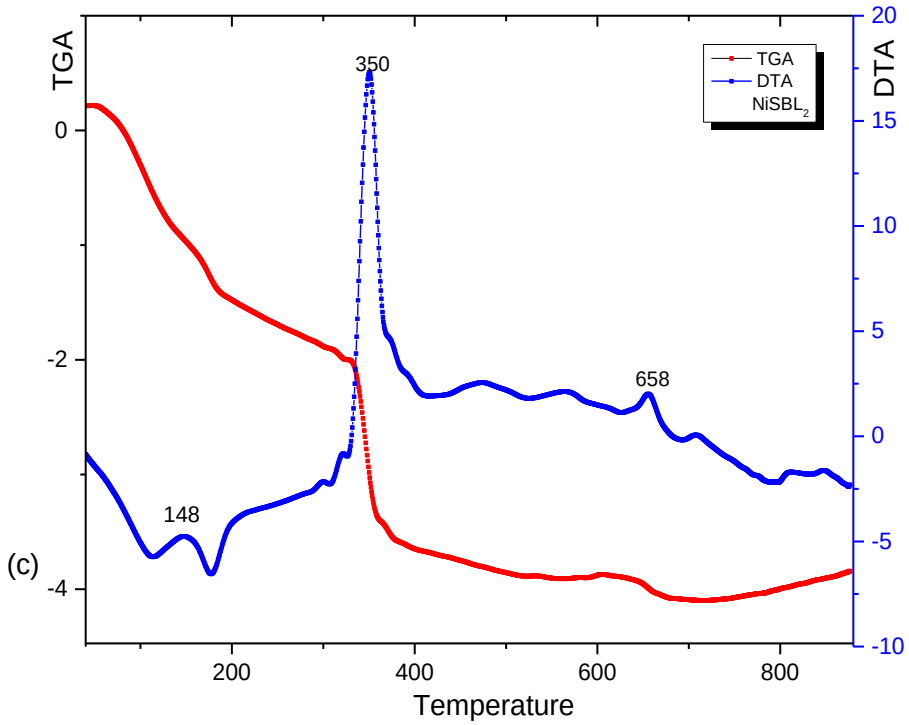

Figure 4.14: TGA/DTA graph of (a) $ZnSBL_2$, (b) $CuSBL_2$ and (c) $NiSBL_2$ complexes

4.3.5. Powder XRD analysis of the metal complexes

X-ray diffraction is a method used to verify the crystallinity and structure of a sample by identifying the underlying crystal structure of a substance. Using Cu Kα radiation, the compounds' crystalline nature of the compound were examined using a powder X-ray diffractometer (PXRD). The data, with a lambda (λ) value of 1.54 Å, was recorded at 2θ and ranged from 10 to 80°.

4.3.5.1. Powder XRD analysis of the metal complexes of SBL1 ligand

The powder X-ray diffraction (XRD) patterns of the synthesized ZnSBL1, CuSBL1 and NiSBL1 complexes were studied (Figure 4.15). The diffraction patterns of metal complexes indicated that the metal complexes revealed a polycrystalline structures. Figure 4.15 displays the ZnSBL1, CuSBL1, and NiSBL1 complexes powder X-ray diffraction (XRD) patterns as well as the crystalline nature of the metal complexes studied.

The diffraction patterns exhibit several peaks, indicative of their polycrystalline structures. The reference peak width at angle is used in the equation, where is the X-ray wavelength (1.5406

Å), *K* is the Scherer constant (0.94), and is the width of the reference diffraction peak at half maximum, measured in radians. The average crystalline size of the complexes were calculated using the Debye-Scherer equation. As a result, ZnSBL1, CuSBL1, and NiSBL1 complexes had typical crystal sizes of 45.7 nm, 29.7 nm, and 31.6 nm, respectively (Ara, 2014).

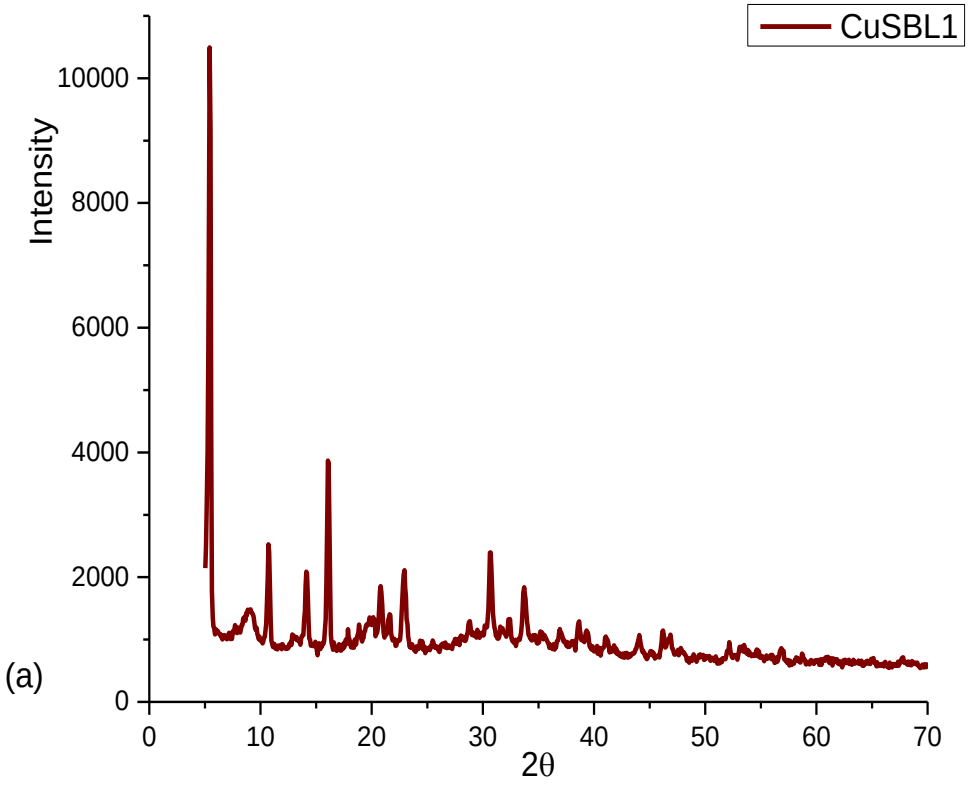

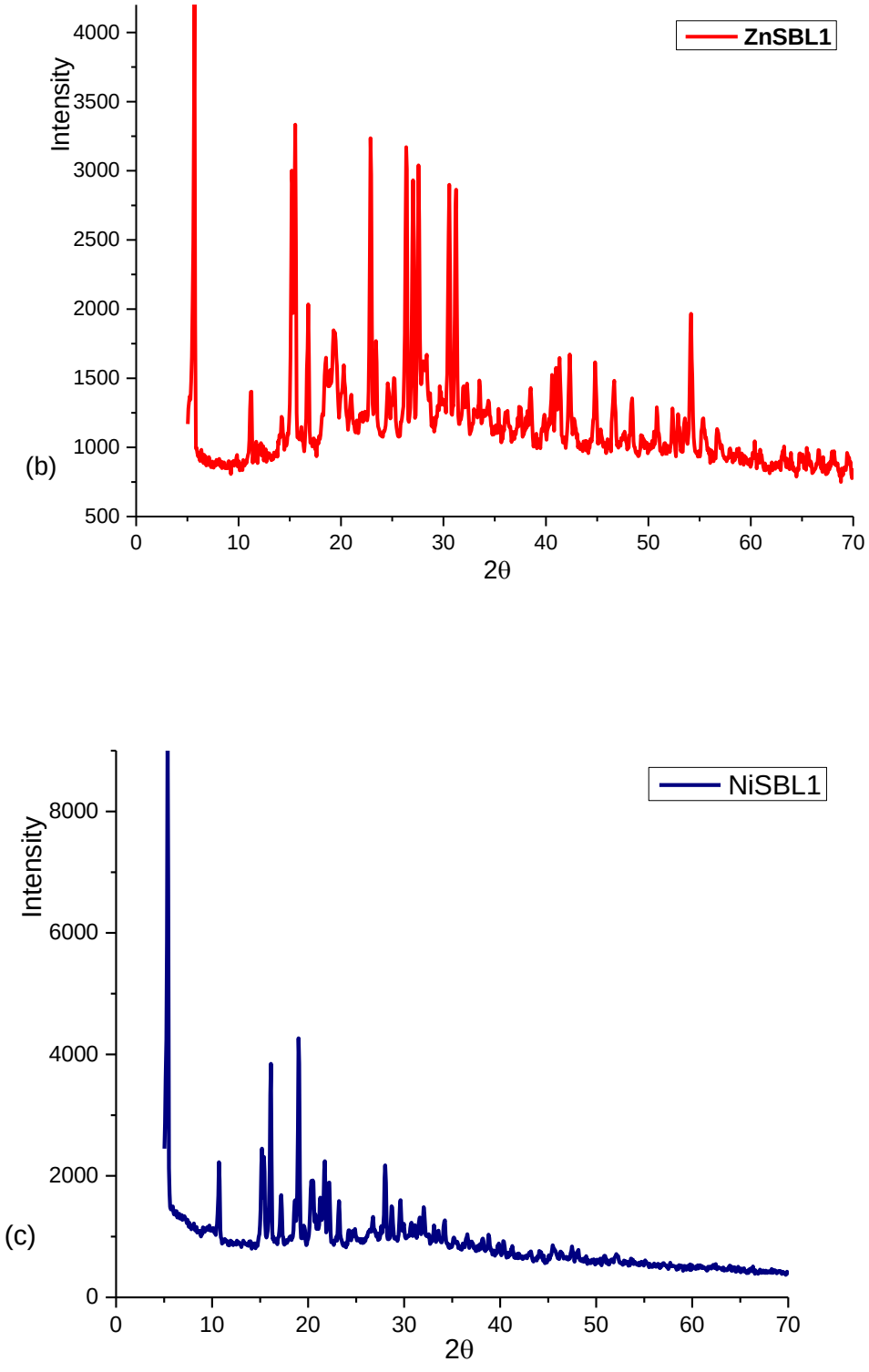

Figure 4.15: pXRD of (a) CuSBL1, (b) ZnSBL1 and (c) NiSBL1 complexes

4.3.5.2. Powder XRD analysis of the metal complexes of SBL2 ligand

The diffraction patterns profile of $CuSBL_2$ complex indicates predominantly amorphous nature. The presence of weak peaks at $2\theta = 5-80°$ indicated presence of small crystalline domains in the amorphous matrix. On the other hand, the NiSBL2 and ZnSBL2 counterpart complexes exhibited as well crystalline structure (Fig. 4.16). Using the Debye-Scherer equation, the average crystallite size (D) was determined from the XRD pattern.

The reference peak width at angle is used in the equation, where is the X-ray wavelength (1.5406 A^0), K is the Scherer constant (0.94), and is the width of the reference diffraction peak at half maximum, measured in radians. The Debye Scherer equation used to determine the complexes' average crystalline size. Accordingly, the average crystal size of $ZnSBL_2$ and $NiSBL_2$ complexes is 15.27 nm and 29.46 nm respectively (Ara, 2014).

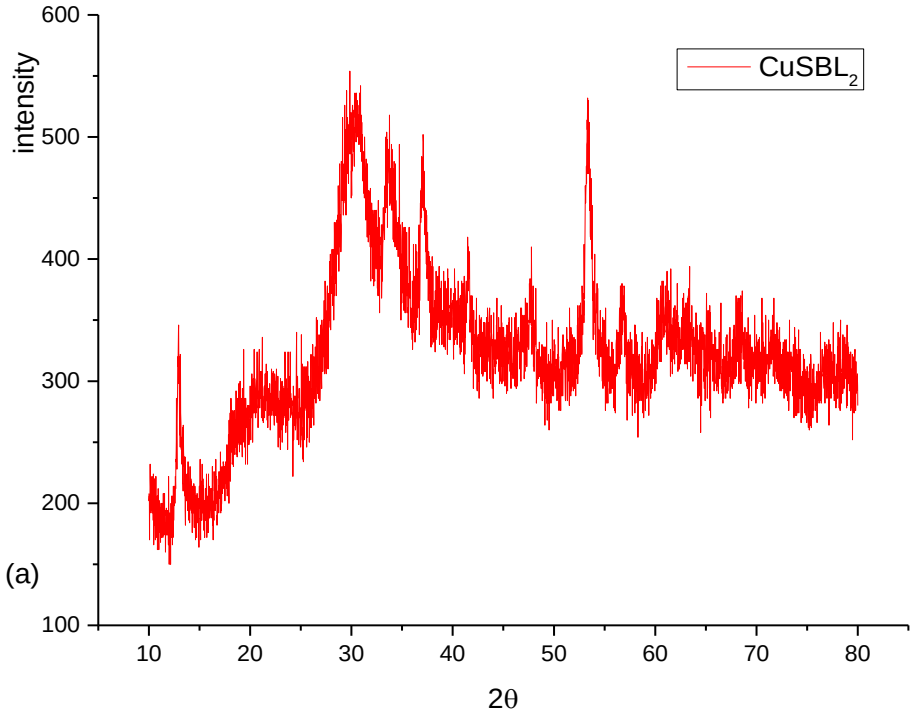

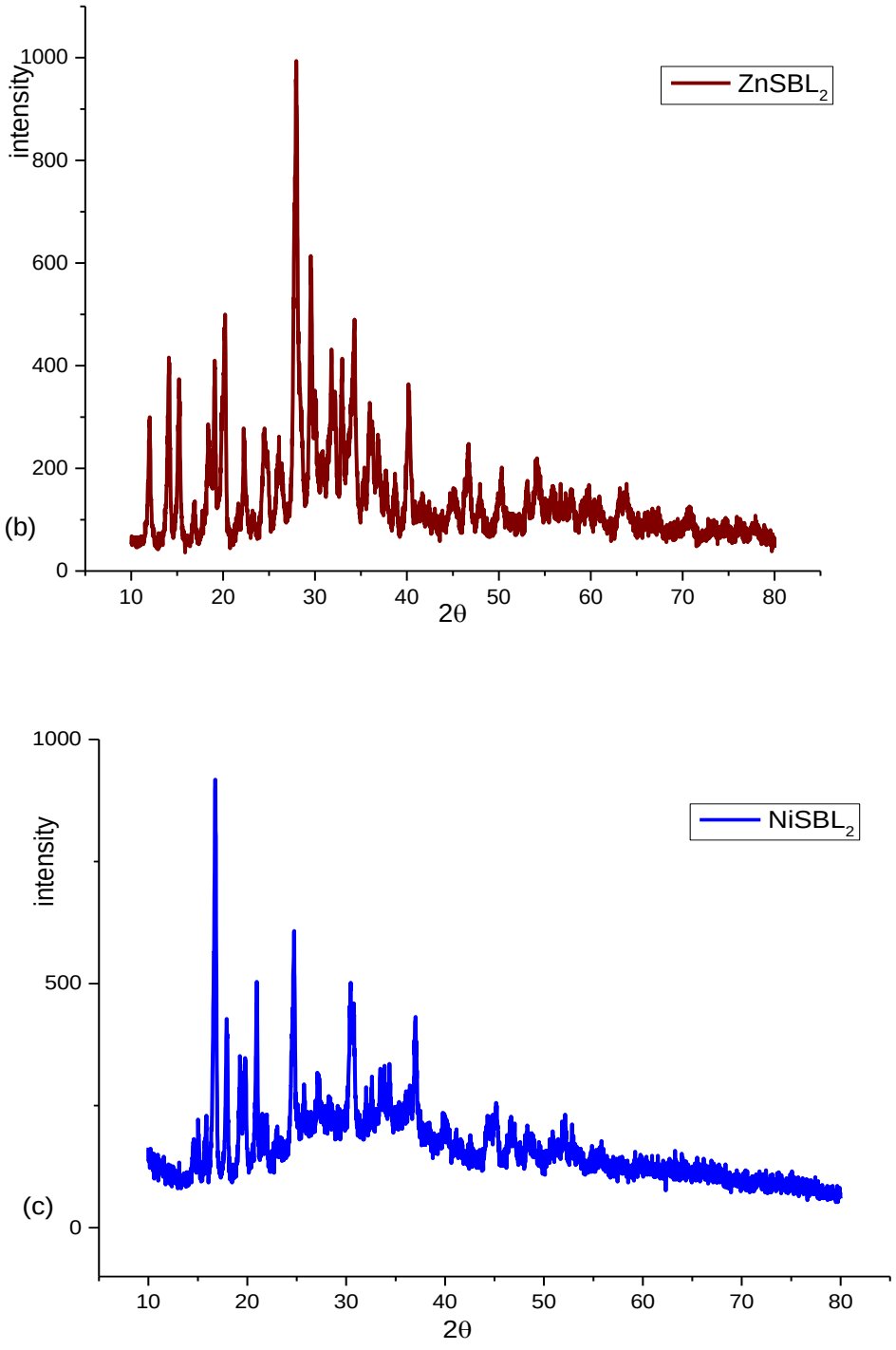

Figure 4.16: pXRD of (a) $CuSBL_2$, (b) $ZnSBL_2$ and (c) $NiSBL_2$ Complexes

4.4. Biological application of Schiff base ligand and its metal complexes

One of the current problems to public health is the rise of multi-drug resistance (MDR) bacterial strains to current antibiotics in the market. The idea of forming metal complexes with different kinds of bioactive organic ligands is useful strategy to increase the efficacy of the bioactive ligands against MDR microbial. Thus, in this study Schiff base ligands and their Zn(II), Cu(II), and Ni(II) complexes have been synthesized and their biological activities have been evaluated against one fungal strain, two Gram-positive and two Gram-negative bacterial pathogens.

4.4.1. Antimicrobial activities of SBL1 and its metal complexes

The antimicrobial activities of the **SBL1** and its **ZnSBL1**, **CuSBL1** and **NiSBL1** complexes were assessed against different Gram-Positive (*S. aureus, B. cereus*) and Gram-negative (*E. coli, S. typhi*) bacterial strains using disc diffusion and fungal (*C. albinas*) strain using disc diffusion method in DMSO as a solvent at two different concentrations. Gentamicin for bacterial strain and Clotrimazole for fungal strain were used as control drugs (Al-Shboul *et al.*, 2022; Erturk, 2019; Tembei *et al.*, 2020). The zones of inhibition for each compound against the tested microorganisms measured in triplicate, and the average were considered. The results are summarized in (Table 4.9). The zone of inhibition for each of the compound against the tested organisms was measured in triplicate, and the average is presented as mean ± SD (Abdel-rahman *et al.*, 2022).

Table 4.9**:** Bacterial and fungal strains' inhibition zones (in mm) of **SBL1** and the **ZnSBL1**, **CuSBL1** and **NiSBL1** complexes

Compound	Conc. (µg/mL)	**Gram Positive**		**Gram Negative**		**Fungi**
		B. cereus	***S. aureus***	***E. coli***	***S. typhi***	***C. albinas***
SBL1	100	10.00±0.41	6.05±0.21	8.00±0.408	7.17±0.236	11.25±0.204
	200	11.00±0.40	7.08±0.31	9.00±0.40	9.00±0.408	12.25±0.204
ZnSBL1	100	7.17±0.23	9.00±0.40	7.08±0.31	6.50±0.204	10.33±0.236
	200	9.33±0.62	12.08±0.42	9.50±0.40	6.75±0.204	12.08±0.312
	100	18.67±0.41	25.05±0.41	21.08±0.31	22.05±0.071	24.08±0.425

CuSBL1	200	21.08±0.312	26.00±0.40	28.08±0.31	23.17±0.623	25.00±0.816
NiSBL1	100	6.05±0.216	6.58±0.11	6.08±0.11	6.50±0.204	7.50±0.250
	200	7.50±0.408	8.08±0.236	7.58±0.118	8.00±0.357	8.50±0.204
Gentamycin	200	25.08±0.312	27.08±0.425	29.00±0.353	28.00±0.408	-
Clotrimazole	200	-	-	-	-	21.03±0.379

The data revealed that the CuSBL1 complexes have higher antimicrobial activities than the free ligand SBL1. Whereas and ZnSBL1 and NiSBL1 complex has lower or equal antimicrobial activities than the free ligand SBL1. The increased biological activity or efficacy is due to more cell permeability in the presence of Zn^{2+} metal ions. Observed increase in activity is based on the over tone concept and chelation theory (Sharma, 2013). As per overtone theory, of cell permeability, the lipid membrane surrounding the cell allows the passage of only lipid molecules; hence, lipophilicity is the major factor for exhibiting antimicrobial property. Upon formation of coordination complexes, the polarity of metal ion is reduced due to partial sharing of cationic charge with the donor groups of the ligand. In addition to this, chelation also increases the delocalization of pi-electrons over the chelate ring and ensuing in increase of lipophilic nature of the central ion. The increased lipophilic feature of the drug enhances the easy penetration into the cell through the lipid membranes (Takacs *et al.*, 1990).

However, there also evidences and studies proving that these metal complexes reduce the anti-microbial property of the quinolines. One such example is Ciprofloxacin in combination with metal ions has low permeability into the cell wall and forms inactive chelate resulting in decrease of the antibiotic action (Benjamin, 2015). Thus, Ni^{2+} metal ion in combination with SBL1 has low permeability into the cell wall and forms inactive chelate resulting in decrease of the antibiotic action.

Among the test, copper complex exhibited the greatest microbial inhibition activity than both complexes and the ligand SBL1. This is due to the least band gap energy of HOMO and LUMO of copper complex than both complexes and the ligand SBL1. The decrease in band gap energy increases the delocalization of pi-electrons over the chelate ring and ensuing in increase of lipophilic nature of the Cu^{2+} ion. The increased lipophilic feature of the drug enhances the easy

penetration into the cell through the lipid membranes. The sensitivity of compounds in inhibiting four bacterial strains decreases in the order of: gentamycin > CuSBL1 > ZnSBL1 > NiSBL1. The sensitivity of compounds in inhibiting fungal strain decreases in the order of: CuSBL1 > Clotrimazole > ZnSBL1 > NiSBL1.

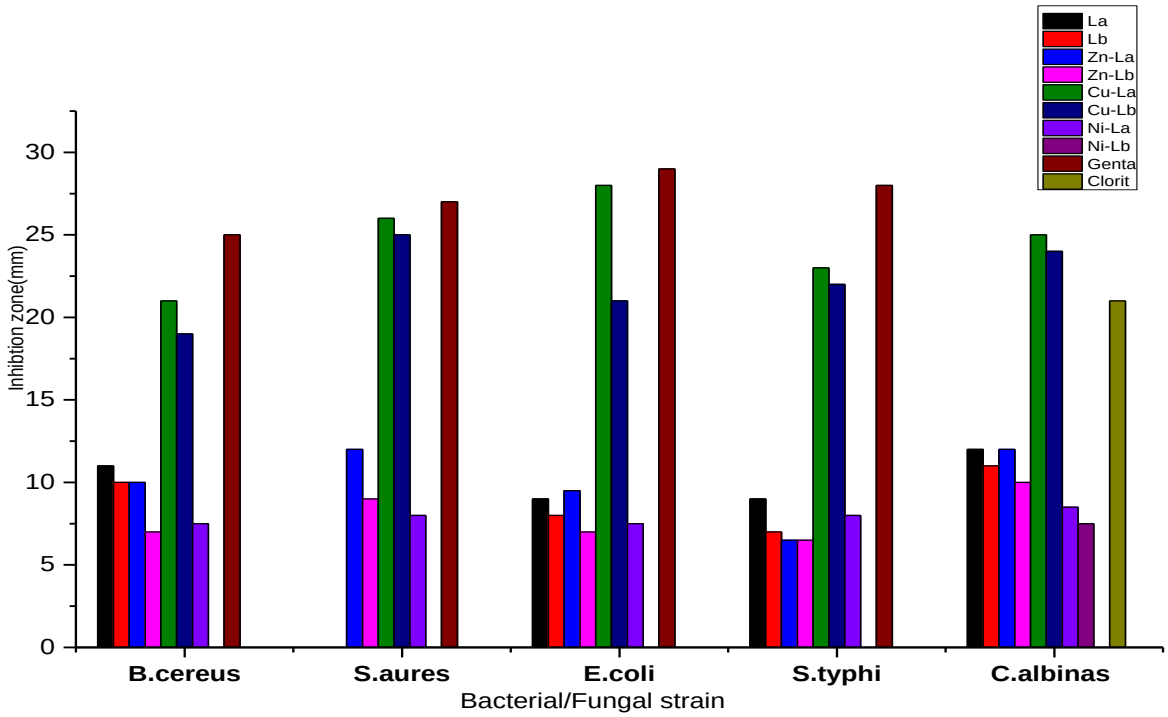

Chart 4.1: Bacteria growth inhibition chart **SBL1 and ZnSBL1, CuSBL1 and NiSBL1** complexes

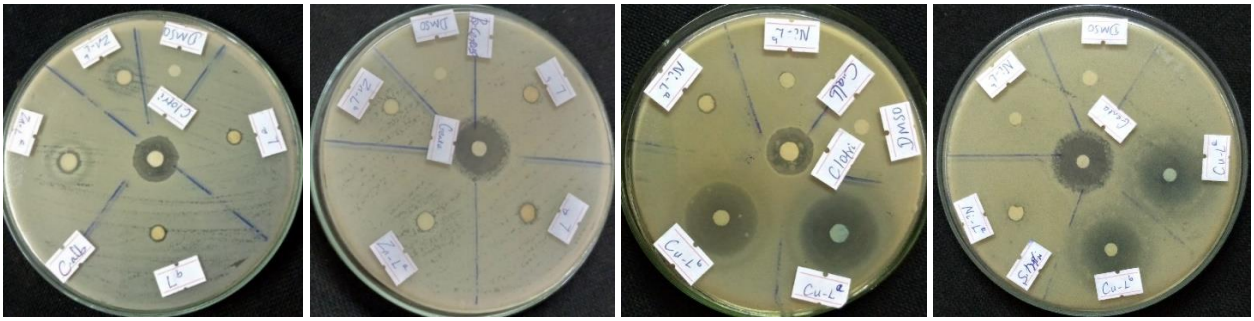

Figure 4.17: Selected pictures of inhibition zone of **SBL1** and **ZnSBL1**, **CuSBL1** and **NiSBL1** complexes

4.4.2. Drug-likeness of SBL1 ligand and its metal complex

Analysis of a compound is a crucial metric in the research of bioactive pharmacological agents. Bioactive substances are considered drug candidates if they satisfy "Lipinski's rule of five". The drug-likeness (pharmacokinetics) studies of the ligands evaluated based on the rule. Lipinski's rule states that potential compounds considered for a drug must satisfy the following criteria; (1) lower than 10 hydrogen-bond acceptors (HBAs), (2) lower than 5H-bond donors (HBDs), (3) logP not more than 5, (4) a molecular weight less than 500 Da and (5) total polarity nature must be < 140 A˚. The Swiss ADME workout findings show that the entire compound tested to fit the standards with no violations, concluding that the sample compounds possess a drug–like molecular property. Tables 4.10 summarize the ADME features of the samples, thus all the compounds have shown high absorption by GI but all have shown no blood-brain barrier absorptivity (Muleta et al., 2022).

Table 4.10: ADME predictions, done by Swiss ADME

Cpds	SPV (Log Kp) cm/s	GIA	BBBp	Inhibitor Interaction					
				Pgps	CYP1A2 inhibitor	CYP2C19 inhibitor	CYP2C9 inhibitor	CYP2D6 inhibitor	CYP3A4 inhibitor
SBL1	-5.54	High	No	No	No	No	Yes	No	No
ZnSBL1	-6.06	High	No	Yes	Yes	Yes	No	Yes	No
CuSBL1	-6.50	High	No	Yes	Yes	Yes	No	Yes	Yes
NiSBL1	-6.91	High	No	Yes	Yes	No	No	No	No
Gentamicin	-12.12	Low	No	Yes	No	No	No	No	No
SPV (skin permeability value), GIA (gastrointestinal absorptivity), BBB(blood-brain barrier permeability), CYP (cytochrome-P), and P-gp (P-glycoprotein substrate)									

4.4.3. Antibacterial activity of SBL2 and its metal complexes

The antibacterial activity of the SBL_2 and its $ZnSBL_2$, $CuSBL_2$ and $NiSBL_2$ complexes were assessed against Gram-Positive (*S.aureus and S.pyogene)* and Gram-negative (*E.coli and P.aurega*) bacterial strains using disc diffusion method in DMSO as a solvent at two different concentration. The drug Ciprofloxacin were used as control drug for antibacterial study. The zones of inhibition for each compound against the tested bacteria were measured in triplicate, and the

average value was taken (Table 4.11). The inhibition zones of the ligands and complexes were compared with a standard antibiotic drug *viz.* Ciprofloxacin (Abdel-rahman *et al.,* 2022; Hanan, 2020; Hasan *et al*., 2021; Vairalakshmi, 2019).

Table 4.11: Inhibition zone (in mm) of SBL_2 and its $ZnSBL_2$, $CuSBL_2$ and $NiSBL_2$ complexes

Compound	Conc.(µg/mL)	**Gram Positive**		**Gram Negative**	
		S.pyogene	***S.aures***	***E.coli***	***P.aurega***
SBL2	100	8.67 ± 0.471	8.33 ± 0.471	12.00 ± 0.816	6.67 ± 0.471
	200	9.83 ± 0.235	9.33 ± 0.471	14.83 ± 0.235	8.50 ± 0.408
CuSBL2	100	9.67 ± 0.471	11.50 ± 0.408	11.67 ± 0.312	10.67 ± 0.471
	200	10.67 ± 0.235	12.67 ± 0.471	12.67 ± 0.235	11.67 ± 0.471
NiSBL2	100	7.67 ± 0.471	6.67 ± 0.471	7.33 ± 0.312	8.67 ± 0.471
	200	8.33 ± 0.471	7.75 ± 0.353	8.67 ± 0.471	10.33 ± 0.235
ZnSBL2	100	6.75 ± 0.353	7.67 ± 0.471	7.25 ± 0.540	6.67 ± 0.471
	200	7.75 ± 0.353	8.33 ± 0.471	8.42 ± 0.425	7.67 ± 0.471
Ciprofloxacin	200	27.50 ± 0.408	28.02 ± 0.816	29.83 ± 0.624	29.10 ± 0.816

The results of the antibacterial activity test showed that the free Schiff base ligands are more active than the corresponding complexes NiSBL2 and ZnSBL2 metal complexes against Gram-Positive bacteria (*S.aureus & S.*pyogene). However, the free ligand had less activity as compared to corresponding CuSBL2 complex. For Gram-negative (*E.coli &* P.aurega) the Schiff base ligand shows 14.83 ± 0.235 more active than all metal complexes against *E.coli* but less in activity than the corresponding metal complexes against *P.aurega* (Vinusha *et al*., 2019).

As presented in Table 4.11, CuSBL2 complex had a greater antibacterial activity against all the selected bacteria strains. However, for *E.coli,* the activity for Schiff base ligand with a mean inhibition zone of 14.83 ± 0.235 mm at 200 µg/mL and 12.00 ± 0.816 mm at 100 µg/mL (Table 4.11, chart 4.2 and Fig.4.18). The inhibition zones of copper complex lie from medium to high that

ranges from 9.67 ± 0.471 mm to 12.67 ± 0.471 mm at concentrations 100 and 200 µg/mL for the bacterial strains (*E. coli, S.pyogene,*P. *aurega,* and *S. aureus*) (Damena *et al.*, 2022).

Accordingly, the CuSBL2 complexes exhibited that it has the potential antibacterial activity against the bacterial species used in these studies. Hence, it is possible to conclude that the CuSBL2 complex have enhanced antibacterial activity than Schiff base ligand (Gur'eva *et al.*, 2022; Tufa *et al.*, 2018).

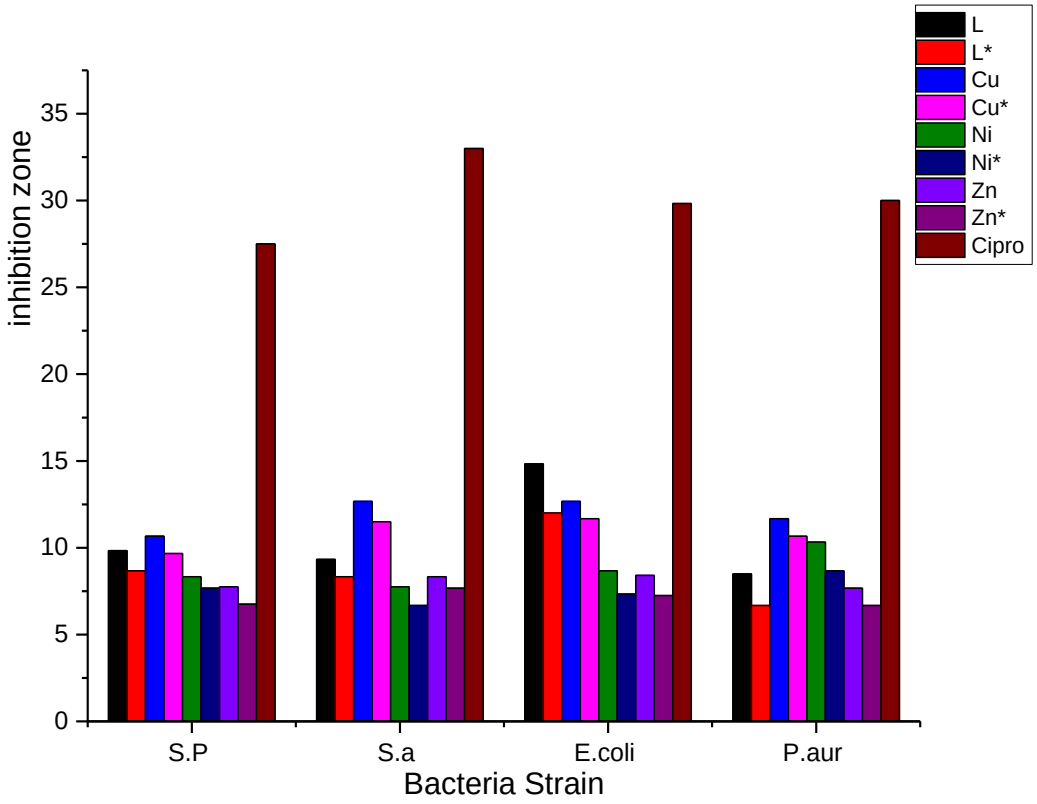

Chart 4.2: Bacteria growth inhibition chart SBL2, ZnSBL2, CuSBL2 and NiSBL2 complex

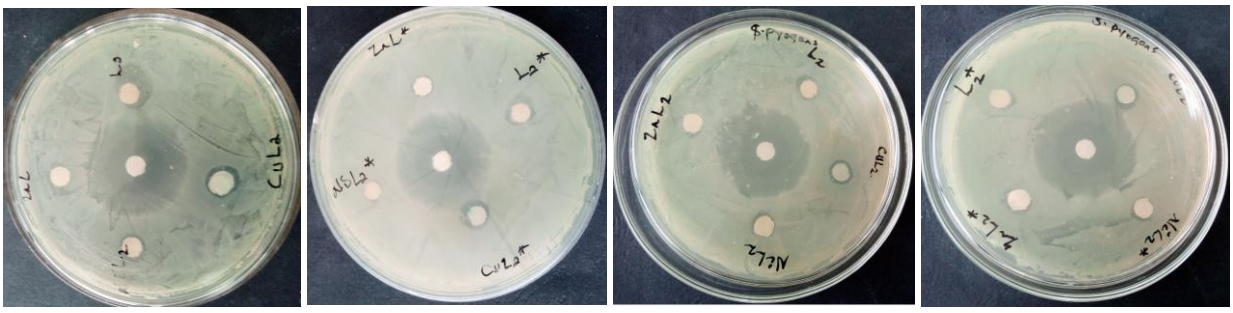

Figure 4.18: Selected pictures of inhibition zone of SBL2, ZnSBL2, CuSBL2 and NiSBL2

Many biologically active compounds used as drugs possess modified pharmacological and toxicological potentials when administered in the form of metal-based compounds. Various metal ions potentially and commonly used are cobalt, copper, nickel and zinc because of forming low molecular weight complexes and therefore, prove to be more beneficial against several diseases (Rizzotto, 2012). The higher activity of the metal complexes may be due to the effect of metal ions on the normal cell membrane. Metal chelates stand polar and nonpolar properties together; this makes them appropriate for penetration to the cells and tissues. The antibacterial activity of metal complexes were better than the supporting ligand, which can be explained based on the oxidation state of the metal ion, Overton's and Tweedy's concepts as well as chelation theory. The polarity of the metal ion reduced largely on chelation because of ligand orbital overlap and positive charge partial sharing of the metal ion with donor groups (Hasan *et al.,* 2021).

The antimicrobial activity results suggested that there is enhancement in activity of the free ligands upon coordination with the metal ions, which can be explained, based on chelation theory. Liposolubility is an important factor that controls the antimicrobial activity. On chelation, the polarity of the metal ion reduced due to overlap of ligand orbital and partial sharing of the positive charge of the metal ion with donor groups. The increasing of delocalization of π-electrons over the completely chelate ring, resulting in an increase in the lipophilicity of the metal complexes. This improved lipophilicity enhances the concentration of complexes in the lipid membrane and limits the multiplicity of microorganisms. It is suggested that the antimicrobial activity of the complexes is due to either by killing the microbes or inhibiting their multiplication by blocking their active sites (El *et al.,* 2022).

4.4.4. Drug-likeness of SBL2 ligand and its metal complex

Analysis of a compound is a crucial metric in the research of bioactive pharmacological agents. Bioactive substances are considered drug candidates if they satisfy "Lipinski's rule of five". The drug-likeness (pharmacokinetics) studies of the ligands evaluated based on the rule. Lipinski's rule states that potential compounds considered for a drug must satisfy the following criteria; (1) lower than 10 hydrogen-bond acceptors (HBAs), (2) lower than 5 H-bond donors (HBDs), (3) logP not more than 5, (4) a molecular weight less than 500 Da and (5) total polarity nature must be < 140 A˚. The Swiss ADME workout findings show that the entire compound tested to fit the standards with no violations, concluding that the sample compounds possess a drug–like

molecular property. Tables 4.12 summarize the ADME features of the samples, thus all the compounds have shown high absorption by GI but all have shown no blood-brain barrier absorptivity (Muleta *et al.*, 2022).

Table 4.12: ADME predictions, done by Swiss ADME

Cpds	SPV (Log Kp) cm/s	GIA	BBBp	Inhibitor Interaction					
				Pgps	CYP1A2 inhibitor	CYP2C19 inhibitor	CYP2C9 inhibitor	CYP2D6 inhibitor	CYP3A4 inhibitor
SBL2	-5.69	High	No	No	Yes	No	Yes	No	No
ZnSBL2	-6.22	High	No	Yes	No	Yes	No	Yes	No
CuSBL2	-6.65	High	No	Yes	No	No	No	No	No
NiSBL2	-6.18	High	No	Yes	No	Yes	No	Yes	No
Cipro	-7.87	High	No	Yes	No	No	No	No	No
SPV (skin permeability value), GIA (gastrointestinal absorptivity), BBB(blood-brain barrier permeability), CYP (cytochrome-P), and P-gps (P-glycoprotein substrate)									

4.5. Molecular docking analysis of Schiff base and metal complexes

Molecular docking is a computational approach that routinely used for understanding ligand-protein interactions with various molecules. The docking process was studied by simulating the interactions of the Schiff base ligands and their metal complexes with the receptor proteins (Aprajita *et al.*, 2023). It provides different information used for drug design and discovery (Khobragade *et al.*, 2021). The docking results revealed that the complexes have a higher docking score than the ligand, which supports the notion that they are promising antibacterial drug candidates.

To find out the possible mode of action of the synthesized Schiff bases and M(II) complexes, molecular docking calculations used (Gaikwad *et al.*, 2022). Molecular docking was used to examine the inhibitory activity on ERK2 (PDB code: 5buj) and to display the modes of binding between our chosen compounds and the active site (Aroua *et al.*, 2023). Molecular docking studies were conducted to predict the interaction of synthesized compounds with the proteins of *S. aureus* (PDB: 2w9h) and *E. coli* DNA Gyrase B (PDB: 6F86). Metal complex geometries were optimized using the B3LYP-GD3/6-311++G(d,p)/LanL2DZ method (Damena *et al.*, 2022b; Ghanghas *et al.*, 2021; Krishnan *et al.*, 1980; Burke, 1995; Sureshkumar *et al.*, 2021) and the

Gaussian 16 program package (Demircioğlu, 2021) and converted to PDB files using Gauss view. Auto Dock 4.2.6 software was employed for docking studies, following established protocols (Bitew *et al.*, 2021; Damena *et al.*, 2023; Damen *et al.*, 2022b; Lemilemu *et al.*, 2021). The proteins were downloaded from the protein database and cleaned, removing co-crystallized substrate and water molecules with MGL 1.5.6 software. Standard docking parameters were applied, and a grid box (120 × 120 × 120, spacing 0.375 Å) was constructed. Lamarckian genetic algorithm (LGA) with an adaptive whole method search (set at 100) was used, generating one hundred conformations for each molecule (Ördög, 2008). Discovery Studio software was used to visualize the interactions between active amino acids and molecules, focusing on conformers with the lowest binding free energies.

4.5.1. Molecular docking against E. coli DNA Gyrase B (PDB: 6F86)

The ligand SBL1 shows a total of 20 interactions (Fig. 4.19): two hydrogen bonding, Asp73 and Asn46; five π-alkyl/π-Sigma, Val167, Val71, Val43, Ala53, Ala47;thirteen van der Walls, Ile59, Gln72, Val44, Met166, Ile94, Arg76, Thr165, val120, Met95, Leu132, Asp49, Glu50, Ile78 with a binding affinity of −5.72 kcal/mol and an inhibition constant of 64.24 μM.

The NiSBL1 shows fifteen interactions: three hydrogen bonding with Gly77, Glu50, Asn46; six π-alkyl/π-Sigma with Ile78, Thr165, Ile94, Val43, Val71, Ala47 and six van der Walls interactions with Asp49, Arg76, Pro79, Asp73, Val120, Val167, and with a binding affinity of −7.78 kcal/mol and an inhibition constant of 1.97 μM.

Whereas the CuSBL1 complex (Fig.4.20) shows a total of thirteen interactions: three hydrogen bonding with Glu50, Asp73, Arg76; six π-alkyl/π-Sigma with Ile78, Asn46, Thr165, Ala47, Val47, Val43, Val167 and four van der Walls interaction with Gly77, Pro79, Ile94, Val120, Val71, and a binding affinity of −7.89 kcal/mol and an inhibition constant of 2.75 μM.

On the other hand, the ZnSBL1 complex shows a total of twelve interactions: three hydrogen bonding with Glu50, Asn46, Arg76; five π-alkyl/π-Sigma with Ile78, Ile94, Thr165, Val167, Ala47 and four van der Walls interactions with Asp73, Gln72, Val43, Val120, Val71, and a binding affinity of −7.45 kcal/mol and an inhibition constant of 3.47 μM (Fig. 4.19). The docking result reveals that the complexes have a higher docking score than the ligand, which supports the notion that they are promising antibacterial medication candidates.

Table 4.13: Molecular docking scores and the corresponding prominent residual amino acid interactions of the ligand and its metal complexes against *E. coli DNA Gyrase B* (6F86)

Cpd	**Binding energy (kcal/mol)**	**Inhibition constant (K_i)**	**H-bonding with**	**π-Sigma/π-Alkyl**	**van der Waals**
SBL1	-5.72	64.24 μM	Asp73, Asn46	Val167,Val71,Val43,Ala53,Ala47	Ile59,Gln72,Val44,Met166,Ile94,Arg76,Thr165,val120,Met95,Leu132,Asp49,Glu50,Ile78
NiSBL1	-7.78	1.97 μM	Gly77,Glu50, Asn46	Ile78,Thr165,Ile94,Val43,Val71,Ala47	Asp49,Arg76,Pro79,Asp73,Val120,Val167
CuSBL1	-7.89	2.75 μM	Glu50,Asp73, Arg76	Ile78,Asn46,Thr165,Ala47,Val47, Val43,Val167	Gly77,Pro79,Ile94,Val120,Val71
ZnSBL1	-7.45	3.47 μM	Glu50,Asn46, Arg76	Ile78,Ile94,Thr165,Val167,Ala47	Asp73,Gln72,Val43,Val120,Val71
Gentamycin	-10.32	27.22 μM	Glu50,Asn46, Arg76,Asn73, Val43	Ile78,Ile94,Val71,Val167	Asp49,Ala47,Val44,Met166,Val120,Thr165,Gly75,Gly77,Gly164

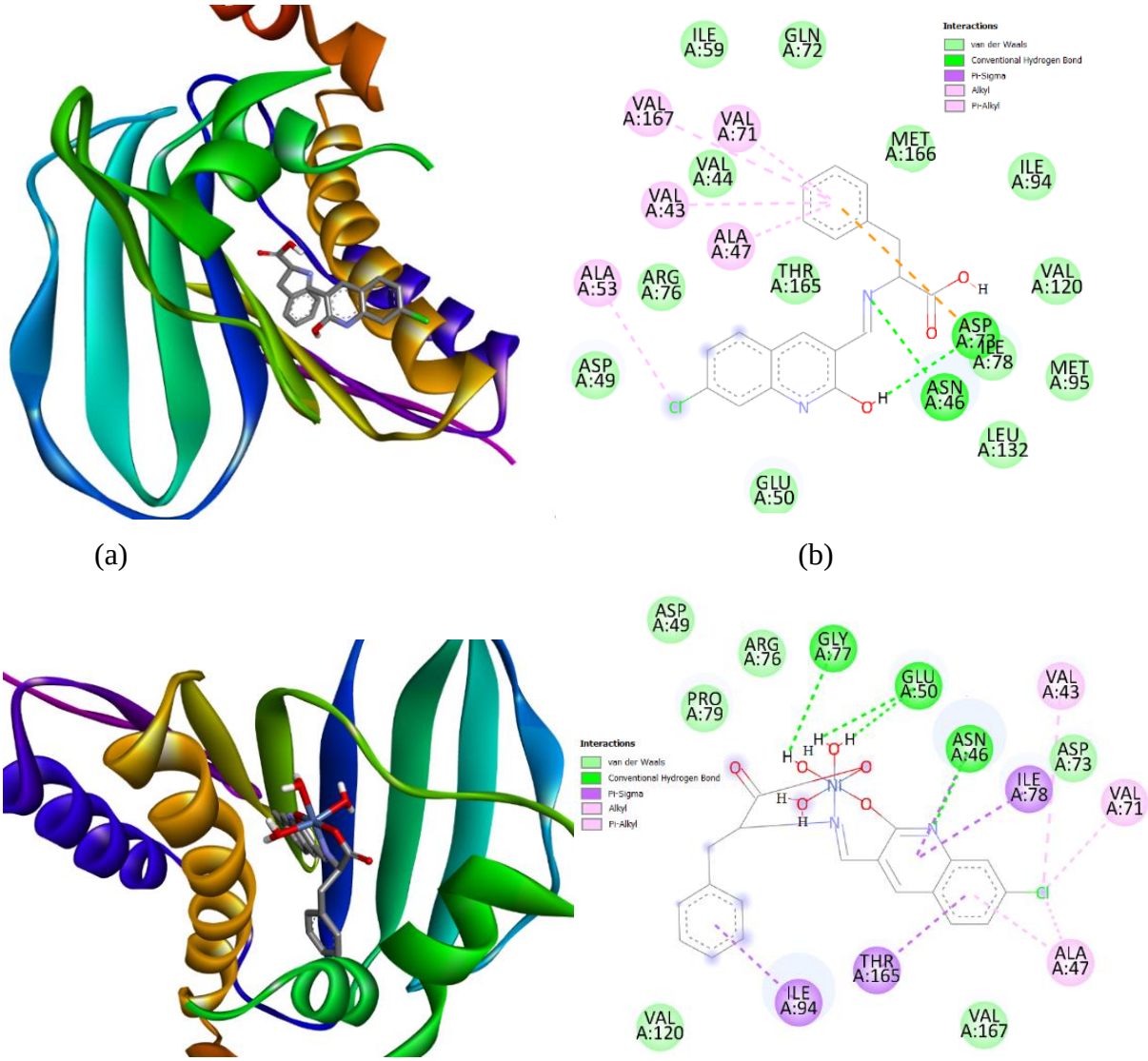

Figure 4.19: (a**)** 3D and (b) 2D representations of the binding interactions of SBL1 (top panel) and NiSBL1 (bottom panel) against *E. coli DNA Gyrase B* (6F86)

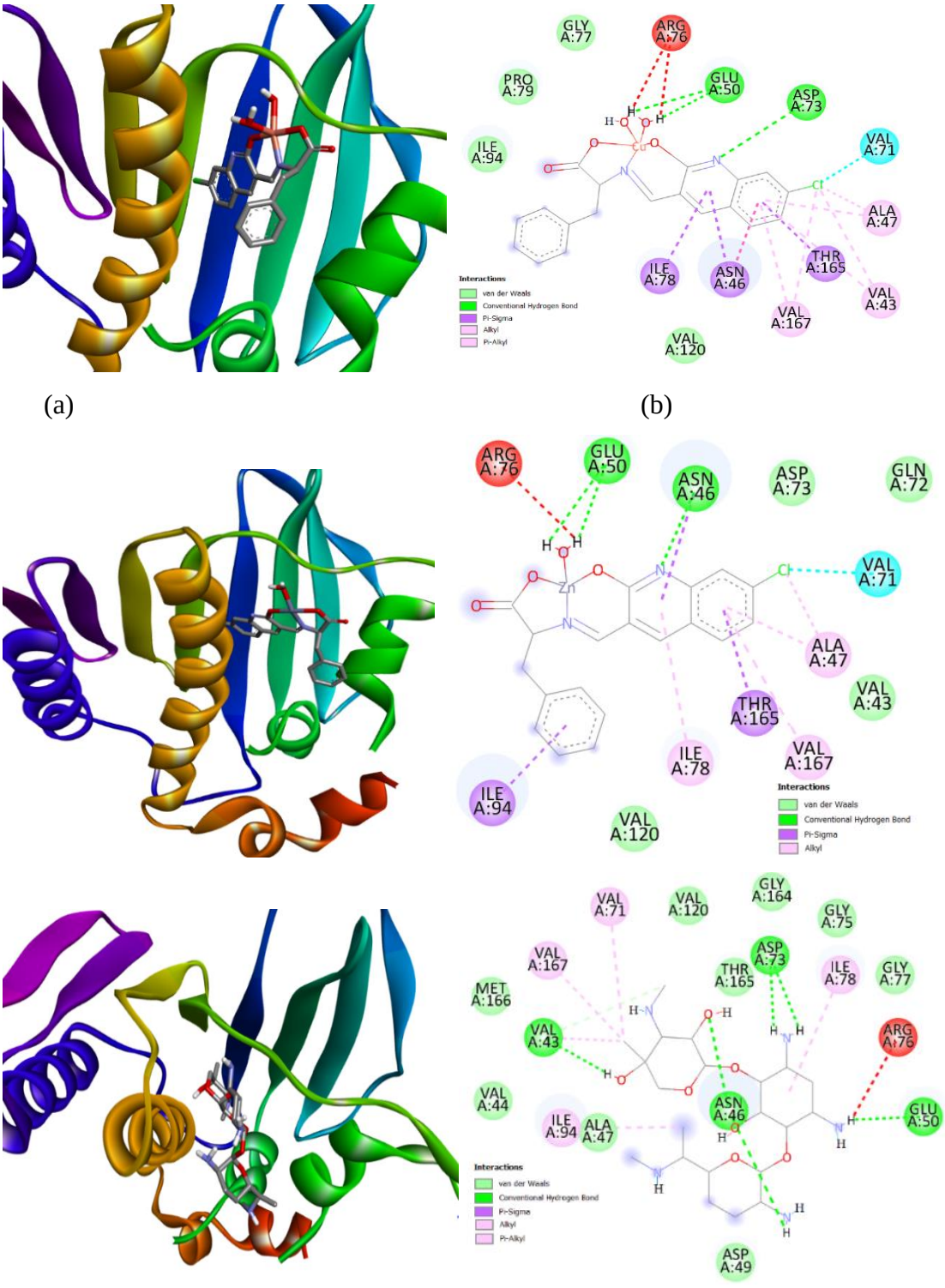

Figure 4.20**:** (a) 3D and (b) 2D representations of the binding interactions of CuSBL1 (top panel), ZnSBL1 (middle panel) and the control gentamycin (bottom panel) against *E. coli DNA Gyrase B* (6F86)

4.5.2. Molecular docking against S. aureus (PDB: 2w9h)

The ligand SBL1 shows a total of 18 interactions (Fig. 4.21): one hydrogen bonding with Ile14; three π-alkyl/π-sigma interaction with Val6, Ala7, Leu20; fourteen van der Waals interactions with Asp27, Val31, Leu5, Ile50, Ser49, Gln19, Asn18, Gly15, Gly95, Thr46, Phe98, Gly93, Gly94, Phe92 with a binding affinity −8.57 kcal/mol and an inhibition constant of 0.52 μM.

The NiSBL1 complex shows a total of 18 interactions (Fig. 4.21): three hydrogen bonding, Ile14, Asn18, Lys45; four-π-alkyl/π-Sigma with Val6, Leu5, Val31, Phe92 and eleven van der Waals with Ala7, Phe98, Gly93, Thr96, Gly94, Thr121, Thr46, Gln19, Ser49, Gly15, Leu20, and a binding affinity of −11.99 kcal/mol and an inhibition constant of 0.003 μM.

The CuSBL1 complex on the hand shows a total of 24 interactions (Fig. 4.22): two hydrogen bonding, Ile14, Asn18; four π-alkyl/π-sigma interactions with Lys45, Leu20, Val6, Val31 and eighteen van der Waals with Thr96, Thr121, Gln19, Gly15, Phe16, Pro21, Asp27, Leu5, Ala7, Phe92, Phe98, Gly93, Thr46, Ser49, Gly94, Gln95, Gly43, Leu97, and a binding affinity of −12.99 kcal/mol and an inhibition constant of 0.002 μM.

The ZnSBL1 complex shows a total of 20 interactions (Fig. 4.22): two hydrogen bonding with Ser49, Asn18; five π-alkyl/π-sigma interactions with Val31, Ala7, Phe92, Leu20, Lys45 and thirteen van der Waals with Gln19, Ile50, Leu54, Leu28, Asp27, Leu5, Val6, Phe98, Gly94, Thr46, Ile14, Thr121, Gly15, and a binding affinity of −11.31 kcal/mol and an inhibition constant of 0.005 μM. The docking score results indicated that the metal complexes have better binding affinity that the control drug gentamycin with a binding affinity of -10.51 and inhibition constant of 0.002 μM.

Table 4.14: Molecular docking scores and the corresponding prominent residual amino acid interactions of the ligand and its metal complexes against *S. aureus* (PDB: 2w9h)

Cpd	**Binding energy (kcal/mol)**	**Inhibition constant (K_i)**	**H-bonding with**	**π-Sigma/π-Alkyl**	**van der Waals**
SBL1	-8.57	0.52 μM	Ile14	Val6,Ala7, Leu20	Asp27,Val31,Leu5,Ile50,Ser49, Gln19,Asn18,Gly15,Gly95,Thr 46,Phe98,Gly93,Gly94,Phe92
NiSBL1	-11.99	0.003 μM	Ile14,Asn 18,Lys45	Val6,Leu5, Val31,Phe9 2	Ala7,Phe98,Gly93,Thr96,Gly9 4,Thr121,Thr46,Gln19,Ser49,G ly15,Leu20
CuSBL1	-12.99	0.002 μM	Ile14,Asn 18	Lys45,Leu2 0,Val6,Val3 1	Thr96,Thr121,Gln19,Gly15,Ph e16,Pro21,Asp27,Leu5,Ala7,Ph e92,Phe98,Gly93,Thr46,Ser49, Gly94,Gln95,Gly43,Leu97
ZnSBL1	-11.31	0.005 μM	Ser49,Asn 18	Val31,Ala7, Phe92,Leu2 0,Lys45	Gln19,Ile50,Leu54,Leu28,Asp2 7,Leu5,Val6,Phe98,Gly94,Thr4 6,Ile14,Thr121
Gentamycin	-10.51	0.02 μM	Ile14,Ile5 0,Asn27	Val31,Leu2 0,Val6,Phe n98	Gly94,Thr46,Leu28,Leu5,Leu5 4,Ala7,Phe92,Gly93,Ser49, Asn18,Phe16,Gly15,Thr121,Ly s45,Gln95

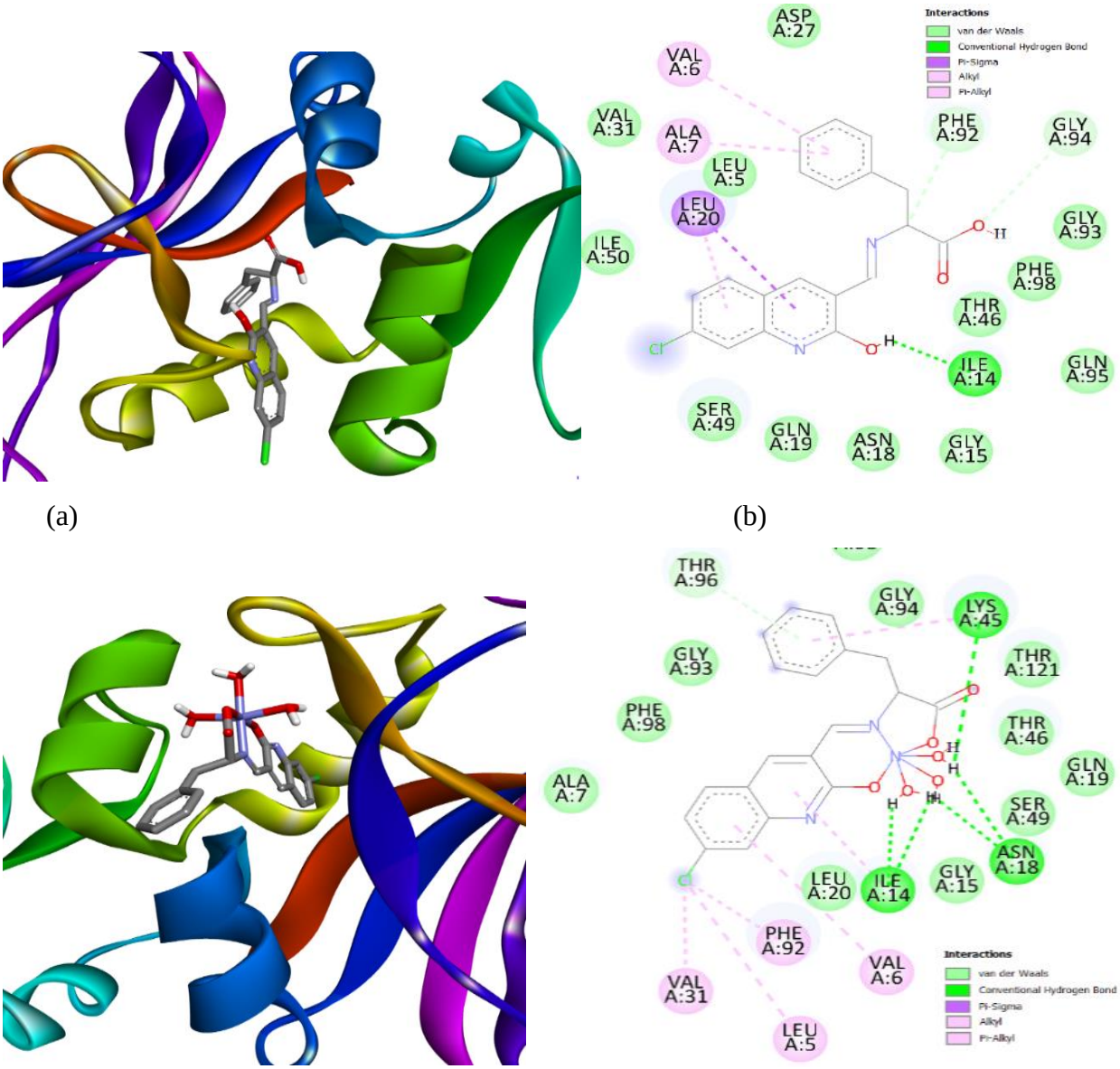

Figure 4.21: **(a)** 3D and (b) 2D representations of the binding interactions of SBL1 (top panel) and NiSBL1 (bottom panel) against *S. aureus* (PDB: 2w9h)

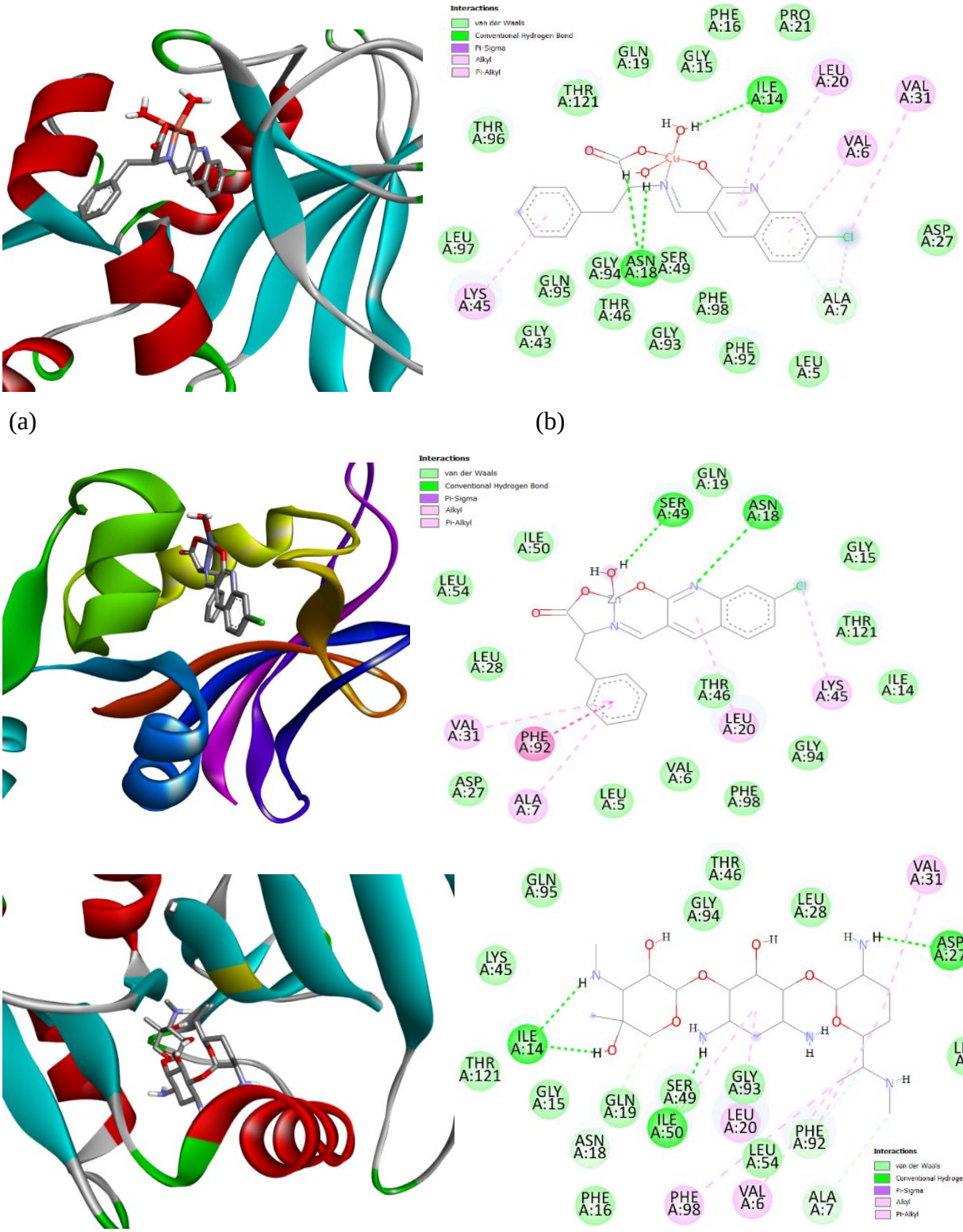

Figure 4.22: (a) 3D and (b) 2D representations of the binding interactions of **CuSBL1 (top panel), ZnSBL1** (middle panel) and the control **gentamycin** (bottom panel) against ***S. aureus*** **(PDB: 2w9h)**

4.5.3. Molecular docking against S. aureus (PDB: 2w9h)

The ligand SBL_2 shows a total of 16 interactions (Fig.4.23): three hydrogen bonding, Lys45,Arg44,Thr96; two π-alkyl/π-Sigma, Leu97 and Gly94; eleven van der Walls, Thr46,Ser49,Asn18,Gly15,Ile14,Thr121,Phe16,Gln95,Gly93,Gly43,Leu62 with a binding affinity of −7.89 kcal/mol and an inhibition constant of 1.63μM.

The $NiSBL_2$ shows 13 interactions: two hydrogen bonding with Asn18 and Ser49; four π-alkyl/π-Sigma with Leu54,Leu28,Ile50,Val31and seven van der Walls interactions with Gln19,Gly15,Thr46,Ile14,Leu20,Phe92,Lys32 and with a binding affinity of −11.27 kcal/mol and an inhibition constant of 0.06 μM.

Whereas the $CuSBL_2$ complex (Fig.4.23) shows a total of 15 interactions: two hydrogen bonding with Asn18 and Lys45; four π-alkyl/π-Sigma with Val6,Val31,Ile14,Phe92 and nine van der Walls interaction with Thr121,Thr96,Gln95,Gly94,Gly93,Phe98,Leu5,Thr46,Leu20 and a binding affinity of −10.18 kcal/mol and an inhibition constant of 0.36 μM.

On the other hand, the $ZnSBL_2$ complex shows a total of twelve interactions: three hydrogen bonding with Ser49 and Phe92; five π-alkyl/π-Sigma with Leu20,Leu54,Val31,Leu28,Ile50 and eight van der Walls interactions with Ile14,Gly15,Thr121,Asn18,Lys54,Phe98,Gly93,Gly94 and a binding affinity of −9.58 kcal/mol and an inhibition constant of 0.95 μM (Fig.4.23). The docking result reveals that the complexes have a higher docking score than the ligand, which supports the notion that they are promising antibacterial medication candidates.

Table 4.15: Molecular docking scores and the corresponding prominent residual amino acid interactions of the ligand and its metal complexes against *S. aureus* (PDB: 2w9h)

Cpd	**Binding energy (kcal/mol)**	**Inhibition constant (K_i)**	**H-bonding**	**van der Waals**	**π-alkyl/sigma**
SBL2	-7.89	1.63 µM	Lys45,Arg44,Thr96	Thr46,Ser49,Asn18,Gly15,Ile14,Thr121,Phe16,Gln95,Gly93,Gly43,Leu62	Leu97,Gly94,
NiSBL2	-11.27	0.06 µM	Asn18,Ser49	Gln19,Gly15,Thr46,Ile14,Leu20,Phe92,Lys32	Leu54,Leu28,Ile50,Val31
CuSBL2	-10.18	0.36 µM	Asn18,Lys45	Thr121,Thr96,Gln95,Gly94,Gly93,Phe98,Leu5,Thr46,Leu20	Val6,Val31,Ile14,Phe92
ZnSBL2	-9.58	0.95 µM	Ser49,Phe92	Ile14,Gly15,Thr121,Asn18,Lys54,Phe98,Gly93,Gly94	Leu20,Leu54,Val31,Leu28,Ile50
Cipro.	-8.66	0.45 µM	Asn18,Asp27	Thr46,Ser49,Lys45,Gly93,Ile14,Gly94,Phe98,Val6,Leu5,Thr111,Val31,Leu28	Leu20,Ala7

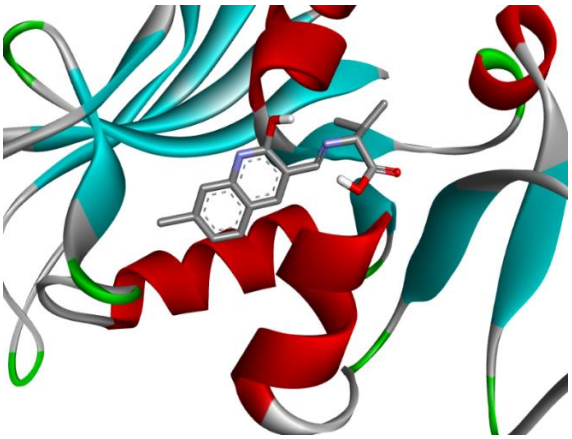

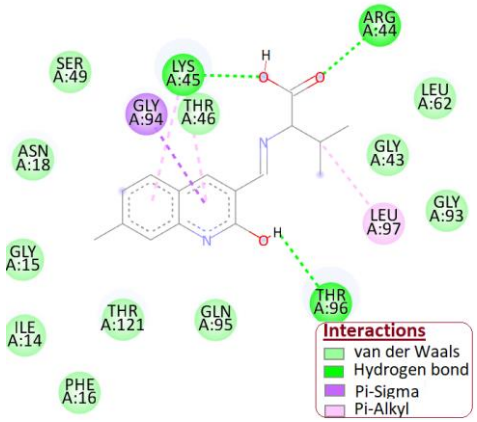
ARG A:44
SER A:49
LYS A:45
LEU A:62
GLY A:94
THR A:46
ASN A:18
GLY A:43
LEU A:97
GLY A:93
GLY A:15
THR A:96
THR A:121
GLN A:95
ILE A:14
PHE A:16
Interactions
van der Waals
Hydrogen bond
Pi-Sigma
Pi-Alkyl

(a) (b)

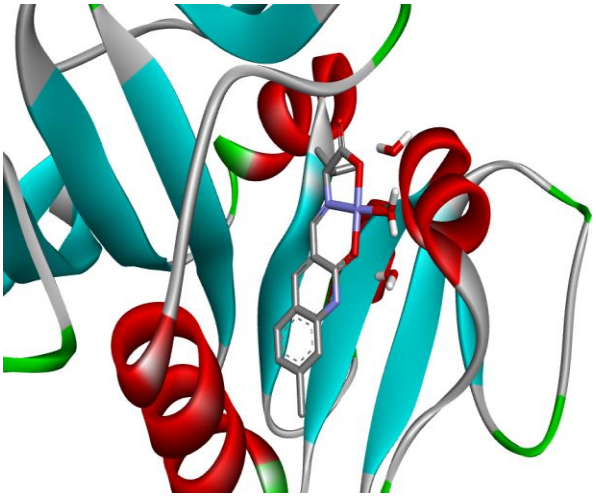

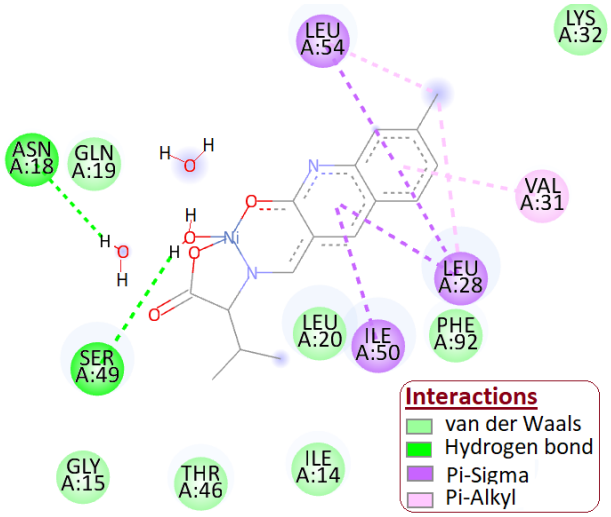
LEU A:54
LYS A:32
ASN A:18
GLN A:19
VAL A:31
LEU A:28
LEU A:20
ILE A:50
PHE A:92
SER A:49
Interactions
van der Waals
Hydrogen bond
Pi-Sigma
Pi-Alkyl
GLY A:15
THR A:46
ILE A:14

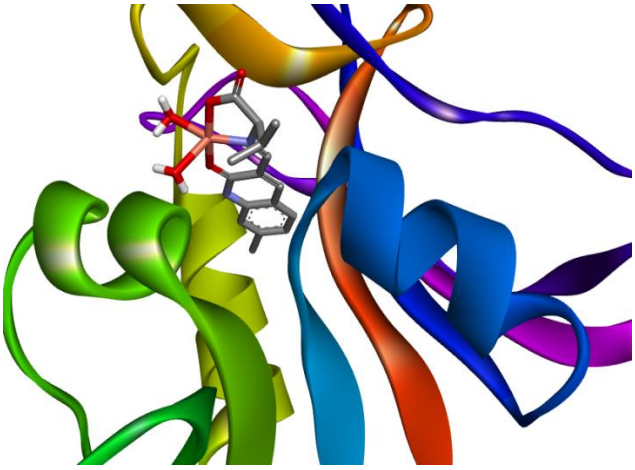

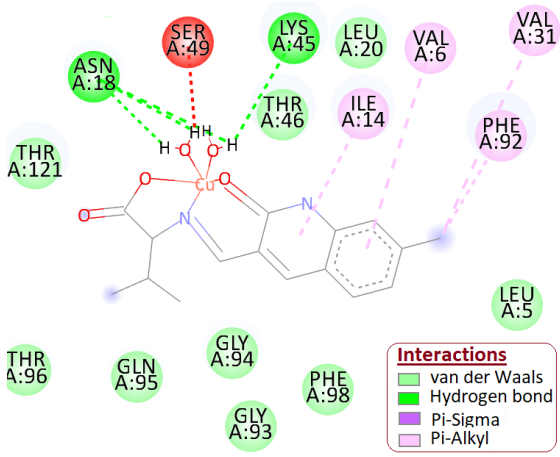
SER A:49
LYS A:45
LEU A:20
VAL A:6
VAL A:31
ASN A:18
THR A:46
ILE A:14
PHE A:92
THR A:121
LEU A:5
THR A:96
GLN A:95
GLY A:94
PHE A:98
GLY A:93
Interactions
van der Waals
Hydrogen bond
Pi-Sigma
Pi-Alkyl

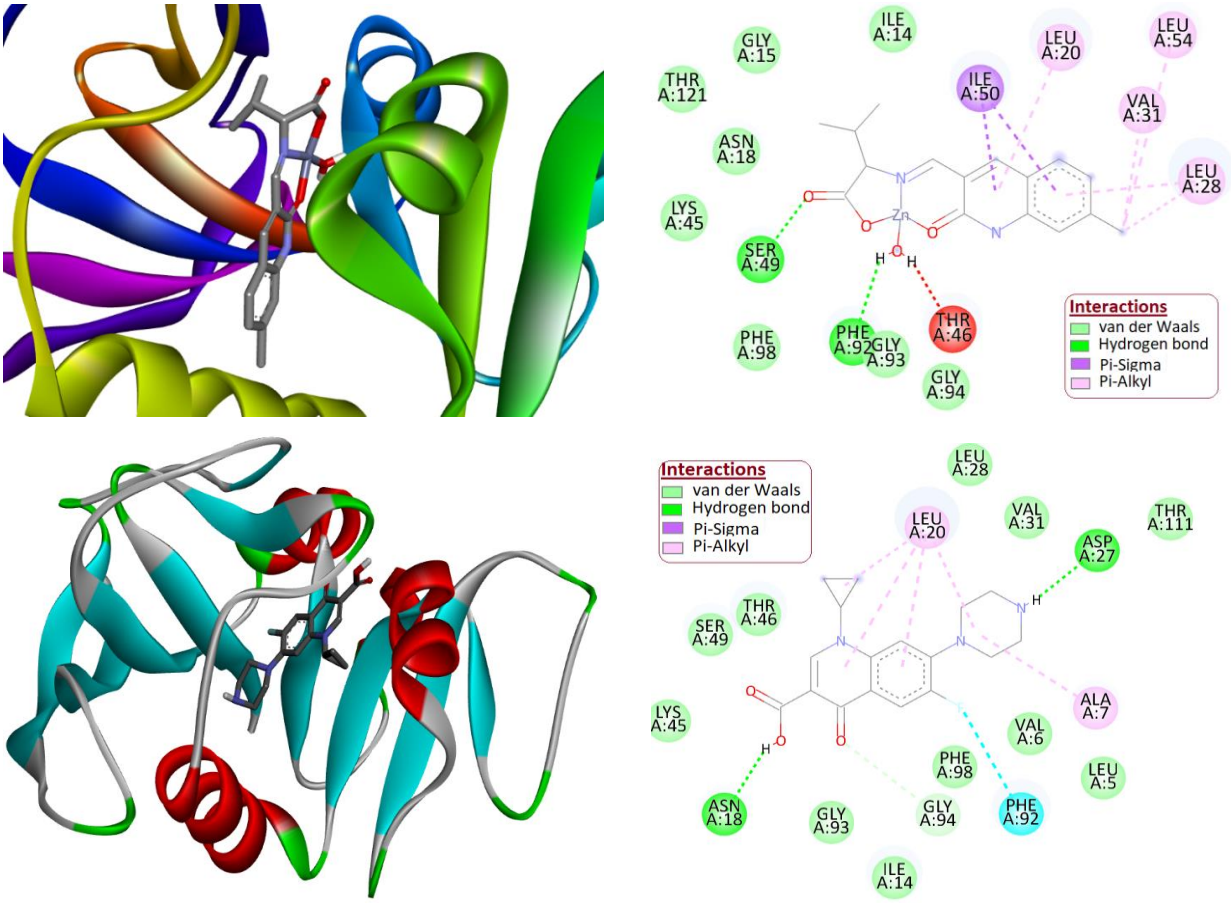

Figure 4.23: (a) 3D and (b) 2D representations of the binding interactions of SBL2, NiSBL2, CuSBL2, ZnSBL2 complexes and Ciprofloxacin against *S. aureus* (PDB: 2w9h)

4.5.4. Molecular docking against E. coli (PDB: 6F86)

The ligand shows a total of 14 interactions (Fig. 4.24): four π-alkyl/π-sigma interaction with Ala53,Ile78,Val167,Val43,Asp49 ; ten van der Waals interactions with Arg76,Glu50,Gly77,Asp73,Thr165,Met166,Val71,Ala47,Asn46 with a binding affinity −5.66 kcal/mol and an inhibition constant of 71.04 μM.

The $NiSBL_2$ complex shows a total of 13 interactions (Fig. 4.24): two hydrogen bonding, Glu50,Asp73; four-π-alkyl/π-Sigma with Ile78,Ile94,Val167,Pro79 and seven van der Waals with Gly77,Cys56,Ala47,Thr165,Val43,Val120,Asn46 and a binding affinity of −7.15 kcal/mol and an inhibition constant of 5.77 μM.

The $CuSBL_2$ complex on the hand shows a total of 17 interactions (Fig. 4.24): three hydrogen bonding, Val43,Asn46,Val167; three π-alkyl/π-sigma interactions with Val71,Ala47,Ile78 and eleven van der Waals with Met95,Leu132,Val120,Met166,Thr165,Gln72,Ile59,Val44,Asn50,Glu50,Arg76 and a binding affinity of −7.43 kcal/mol and an inhibition constant of 3.57 μM.

The $ZnSBL_2$ complex shows a total of 17 interactions (Fig. 4.24): two hydrogen bonding with Val167,Asn46; five π-alkyl/π-sigma interactions with Ala47,Val71,Ile78,Gly77,Pro79 and ten van der Waals withGlu50,Asp73,Ile59,Thr165,Gln72,Val44,Met166,Val43,Val120,Ile94 and a binding affinity of −7.45 kcal/mol and an inhibition constant of 3.48μM. The docking score results indicated that the metal complexes have better binding affinity that the control drug Cipro with a binding affinity of -6.19 and inhibition constant of 28.85 μM.

Table 4.16: Molecular docking scores and the corresponding prominent residual amino acid interactions of the ligand and its metal complexes against *E. coli* (PDB: 6F86)

Cpd	**Binding energy (kcal/mol)**	**Inhibition constant (K_i)**	**H-bonding**	**van der Waals**	**π-alkyl/sigma**
SBL2	-5.66	71.04 μM		Arg76,Glu50,Gly77,Asp73,Thr165,Met166,Val71,Ala47,Asn46	Ala53,Ile78,Val167,Val43,Asp49
NiSBL2	-7.15	5.77 μM	Glu50,Asp73	Gly77,Cys56,Ala47,Thr165,Val43,Val120,Asn46	Ile78,Ile94,Val167,Pro79
CuSBL2	-7.43	3.57 μM	Val43,Asn46, Val167	Met95,Leu132,Val120,Met166,Thr165,Gln72,Ile59, Val44,Asn50,Glu50,Arg76	Val71,Ala47,Ile78

ZnSBL2	-7.45	3.48 µM	Val167,Asn46	Glu50,Asp73,Ile59,Thr165,Gln72,Val44,Met166,Val43,Val120,Ile94	Ala47,Val71,Ile78,Gly77,Pro79
Cipro.	-6.19	28.85 µM	Arg136,Gly77,Asp49	Thr165,Asn46	Pro79,Ile78

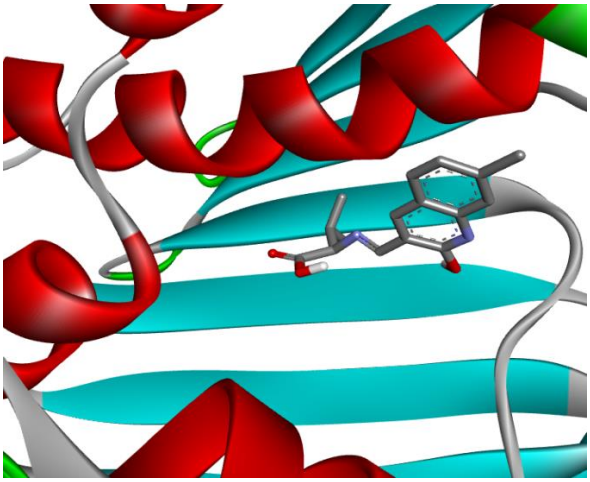

(a)

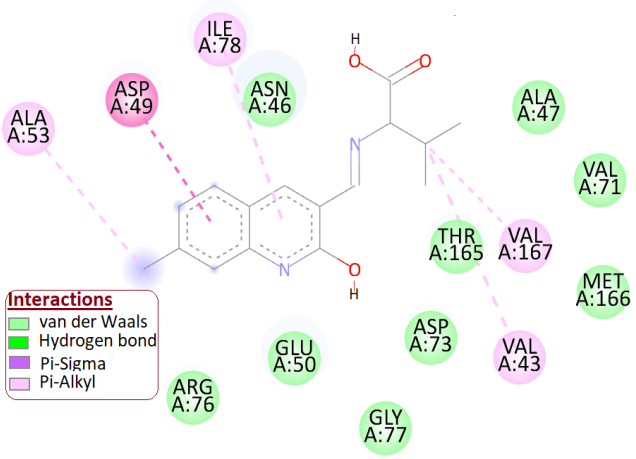

(b)

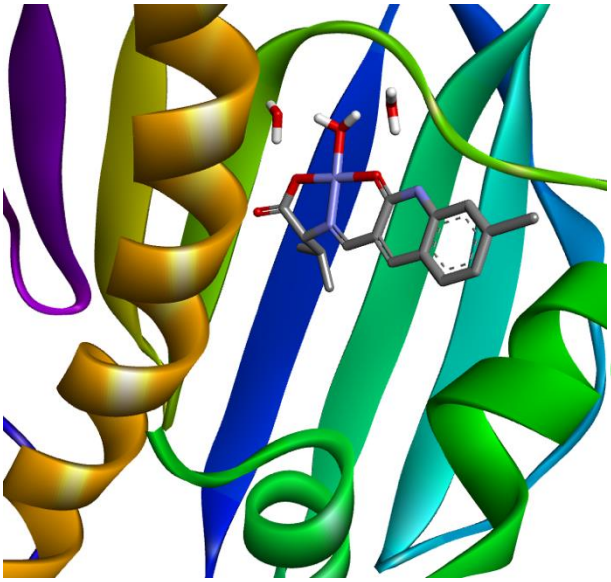

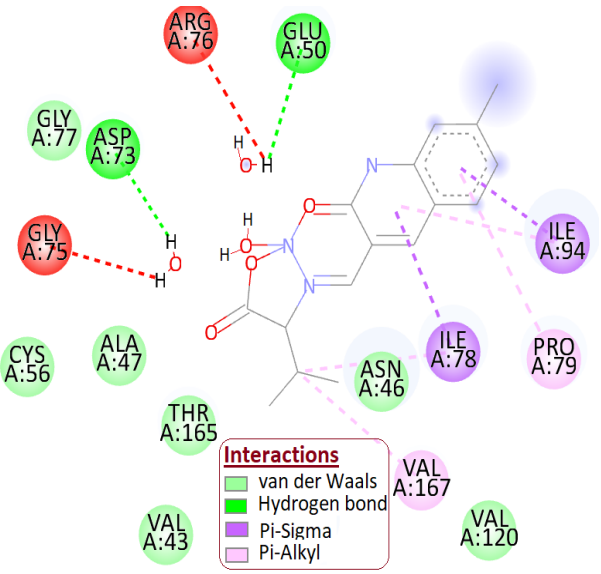

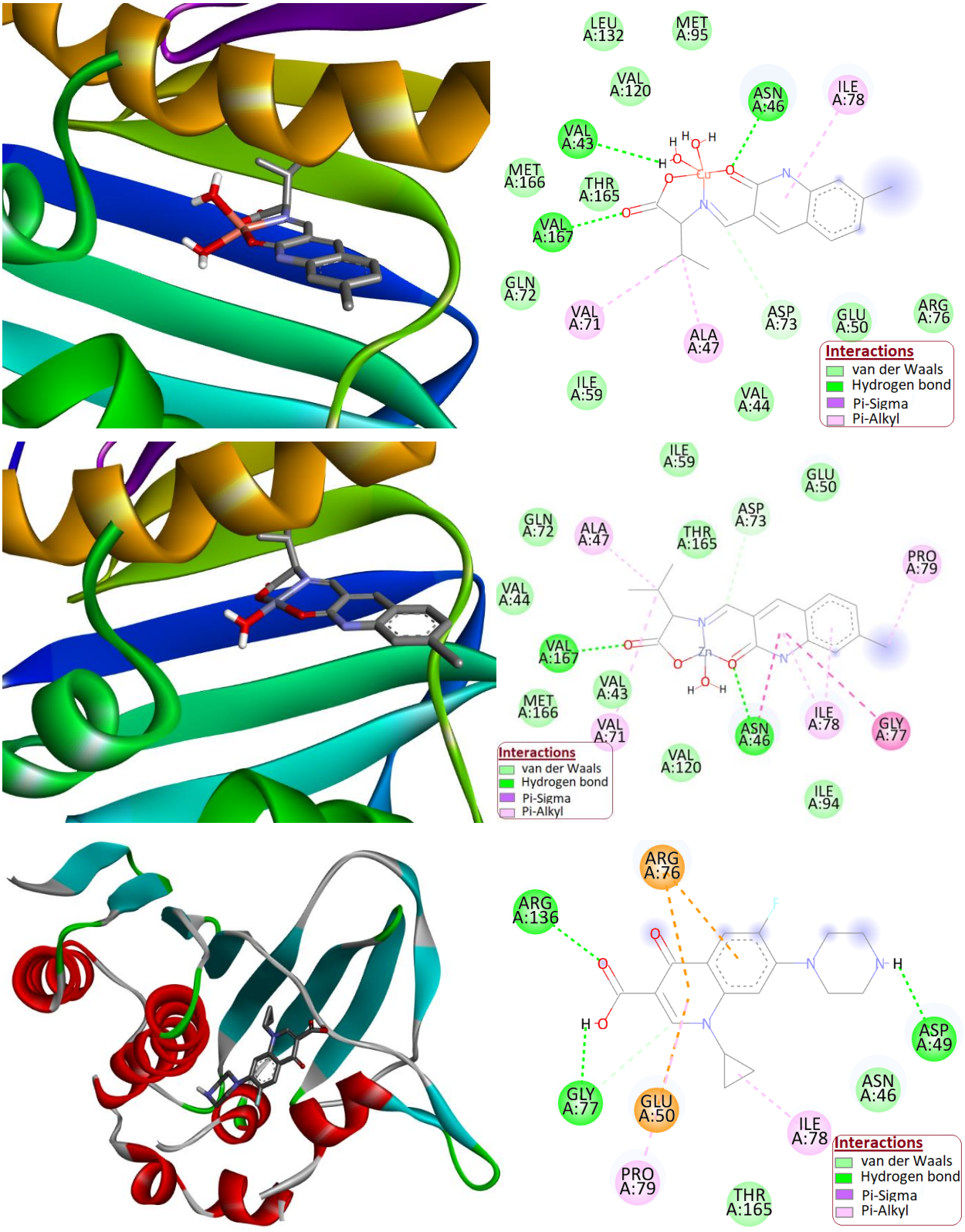

Figure 4.24: (a) 3D and (b) 2D representations of the binding interactions of SBL2, NiSBL2, CuSBL2, ZnSBL2 complexes and Ciprofloxacin against *E. coli* (PDB: 6F86)

5. CONCLUSION

Schiff base ligand (*E*)-2-(((7-chloro-2-hydroxyquinolin-3-yl)methylene)amino)-3-phenylpropanoic acid (SBL1) and (E)-2-(((7-chloro-2-hydroxyquinolin-3-yl)methylene)amino)-3-methylbutanoic acid (SBL2) and their Zn(II), Cu(II) and Ni(II) complexes were synthesized and characterized using ^{1}H NMR, ^{13}C NMR, FT-IR, pXRD, UV−Vis and TGA/DTA. The *in vitro* antibacterial activities of the free ligands and its metal complexes were tested using the disk diffusion method against two Gram-positive and Gram-negative bacterial strain.

The synthesized Schiff bases act as a tri-dentate ligand coordinated with the M(II) ion through phenolic oxygen, imine nitrogen and carboxylic oxygen atoms in ONO fashion. The *in vitro* antibacterial activities of the free ligand and its metal complexes were analyzed using the disk diffusion method against two Gram-positive (S. aureus and B. cereus) and Gram-negative (E. coli and S. typhi) and fungi (C. albinas) strains. Antimicrobial activity of the ligand and its metal complexes against the bacterial and fungal strains exhibited that Schiff base ligand is biologically less active than its metal complexes. Overall, the nickel complex exhibited the lowest antibacterial activity whereas the copper complexes displayed the highest antibacterial and antifungal activities. Notably, the copper complex, with values such as 18.67±0.41 against B. cereus and 24.08±0.43 against C. albinas, demonstrated superior overall antimicrobial potential, which may be due to its small crystalline size, which increases the lipophilic character of the complexes than the other two metal complexes. The results of the molecular docking study also indicated that the metal complexes exhibited greater binding affinity compared to the Schiff base ligand.

Schiff base ligand SBL_2, (*E*)-2-(((7-chloro-2-hydroxyquinolin-3-yl)methylene)amino)-3-methylbutanoic acid was synthesized from 2, 7-dichloroquinoline-3-carboaldehyde and valine in ethanol and its $ZnSBL_2$,$CuSBL_2$ and $NiSBL_2$ complexes were synthesized. The SBL2 ligand exhibited two oxygen and one nitrogen atoms (ONO) donor in a tridentate fashion active sites for complexation. The *in-vitro* antibacterial activities of the free ligand and its metal complexes were identified by disk diffusion method against two Gram-positive (*S. pyogenes* and *S. aureus*) and Gram-negative (*E. coli* and *P. aeruginosa*). Among the metal complexes, the $CuSBL_2$ complex showed better activities against the bacterial strains considered in this study than the free ligand and the $NiSBL_2$ and $ZnSBL_2$ complexes. The molecular docking results indicated prominent interactions between the synthesized molecules and the target proteins. The docking results revealed that the complexes have a higher docking score than the ligand, which supports the notion

that they are promising antibacterial drug candidates. The higher binding affinity (-7.43 kcal/mol) of $CuSBL_2$ complex would be due to its greater number of interactions with binding site amino acids residues of the bacterial strain *E. coli* (PDB: 6F86) which best agree with the experimental activity.

6. RECOMMENDATIONS

In current study, a novel concept of bioinorganic chemistry was implement as an important strategy to synthesize Schiff base ligand and metal complexes from quinoline derivative and amino acids as primary amines. The synthesized Schiff base ligands and metal complexes, characterization techniques, and their antibacterial and antifungal activities reported here. The results showed that the Schiff base ligand and their metal complexes were effective antibacterial and antifungal activities.

However, the researcher recommend further for the *in-vivo* studies of these newly synthesized Schiff base ligand and its metal complexes. Based on our findings, we recommend conducting *in-vivo* studies specifically focused on the antimicrobial activity of the copper complex to substantiate and validate its promising therapeutic potential. Further Schiff base ligands may be the promising method for improving metal-based drug development. Therefore, it is also recommended that future studies will give more attention to Schiff base Ligand synthesized using amino acid as primary amines based Schiff base ligands and their metal complexes.

.

7. REFERENCES

A.Ajibade, I. P. E. and P. (2015). Synthesis, Characterization and Biological Studies of Metal(II) Complexes of (3E)-3-[(2-{(E)-[1-(2,4-Dihydroxyphenyl)ethylidene]amino}ethyl)imino]-1-phenylbutan-1-one Schiff Base. *Molecules*, *20*, 9788–9802. https://doi.org/10.3390/molecules20069788

Abdel-Rahman, L. H., Adam, M. S. S., Al-Zaqri, N., Shehata, M. R., El-Sayed Ahmed, H., & Mohamed, S. K. (2022). Synthesis, characterization, biological and docking studies of ZrO(II), VO(II) and Zn(II) complexes of a halogenated tetra-dentate Schiff base. *Arabian Journal of Chemistry*, *15*(5), 103737. https://doi.org/10.1016/j.arabjc.2022.103737

Abdel-rahman, L. H., Shaker, M., Adam, S., Al-zaqri, N., Shehata, M. R., Ahmed, H. E., & Mohamed, S. K. (2022). Synthesis , characterization , biological and docking studies of ZrO (II), VO (II) and Zn (II) complexes of a halogenated tetra-dentate Schiff base. *Arabian Journal of Chemistry*, *15*(5), 103737. https://doi.org/10.1016/j.arabjc.2022.103737

Abduh, M. S., Ayesh, S., Saghir, M., & Al-gabri, N. (2022). *Synthesis , Characterization and Biological Activities of New Schiff Base Compound and Its Lanthanide Complexes*. 1–15.

Adeleke, A. A., Zamisa, S. J., Islam, S., Olofinsan, K., Salau, V. F., Mocktar, C., & Omondi, B. (2021). Quinoline Functionalized Schiff Base Silver (I) Complexes: Interactions with Biomolecules and In Vitro Cytotoxicity, Antioxidant and Antimicrobial Activities. *Molecules,MDPI*, *26*, 1205. https://doi.org/https://doi.org/ 10.3390/molecules26051205

Adil A Awad, Mohammed Mujbel Hasson , Alaa abbas fadhe, B. faron A. (2019). Synthesis and characterization of a New Schiff base ligand type N2O2 and their Cobalt (II), Nickel (II), Copper (II), and Zinc (II) complexes Synthesis and characterization of a New Schiff base ligand type N2O2 and their Cobalt (II), Nickel (II. *J. Phys.*, *I*. https://doi.org/10.1088/1742-6596/1294/5/052040

Al-redha, H. M. A., Ali, S. H., & Mohammed, S. S. (2022). Syntheses , Structures and Biological Activity of Some Schiff Base Metal Complexes Abstract : Introduction : Material and Methods : *Baghdad Science Journal*, *19*(3), 704–715. https://doi.org/http://dx.doi.org/10.21123/bsj.2022.19.3.0704

Al-Shboul, T. M. A., El-khateeb, M., Obeidat, Z. H., Ababneh, T. S., Al-Tarawneh, S. S., Al Zoubi, M. S., Alshaer, W., Abu Seni, A., Qasem, T., Moriyama, H., Yoshida, Y., Kitagawa, H., & Jazzazi, T. M. A. (2022). Synthesis, Characterization, Computational and Biological

Activity of Some Schiff Bases and Their Fe, Cu and Zn Complexes. *Inorganics*, *10*(8). https://doi.org/10.3390/inorganics10080112

Alhazmi, F. S., Morad, M., Abou-Melha, K., & El-Metwaly, N. M. (2022). Synthesis and Characterization of New Mixed-Ligand Complexes; Density Functional Theory, Hirshfeld, and In Silico Assays Strengthen the Bioactivity Performed In Vitro. *ACS Omega*. https://doi.org/10.1021/acsomega.2c07407

Aljahdali, M. S., & El-sherif, A. A. (2020). Synthesis and Biological Evaluation of Novel Zn (II) and Cd (II) Schiff Base Complexes as Antimicrobial , Antifungal , and Antioxidant Agents. *Bioinorganic Chemistry and Applications*, *2020*, 17. https://doi.org/https://doi.org/10.1155/2020/8866382

Alka, Gautam, S., Kumar, R., Singh, P., Gandhi, N., & Jain, P. (2023). Pharmacological aspects of Co(II), Ni(II) and Cu(II) schiff base complexes: An insight. *Results in Chemistry*, *5*(January), 100849. https://doi.org/10.1016/j.rechem.2023.100849

Ana-Mădălina Măciucă, A.-C. M. and V. U. (2020). Quinolone Complexes with Lanthanide Ions : An Insight into their Analytical Applications and Biological Activity. *Molecules,MDPI*, *6*.

Aprajita, & Choudhary, M. (2023). New Ni(II) and Cu(II) Schiff base coordination complexes derived from 5-Bromo-salicylaldehyde and 3-picoyl amine/ethylenediamine: Synthesis, structure, Hirshfeld surface and molecular docking study with SARS-CoV-2 7EFP-main protease. *Polyhedron*, *232*(January), 116296. https://doi.org/10.1016/j.poly.2023.116296

Ara, S. (2014). Bioorganic & Medicinal Chemistry Letters Synthesis , characterization , biological and catalytic applications of transition metal complexes derived from Schiff base. *BIOORGANIC & MEDICINAL CHEMISTRY LETTERS*. https://doi.org/10.1016/j.bmcl.2014.05.046

Aroua, L. M., Alhag, S. K., Al-shuraym, L. A., Messaoudi, S., Mahyoub, J. A., Alfaifi, M. Y., & Al-otaibi, W. M. (2023). Synthesis and characterization of different complexes derived from Schiff base and evaluation as a potential anticancer , antimicrobial , and insecticide agent. *Saudi Journal of Biological Sciences*, *30*(3), 103598. https://doi.org/10.1016/j.sjbs.2023.103598

Aruna, K. (2017). *SYNTHESIS , SPECTROSCOPIC , AND BIOLOGICAL ACTIVITY STUDIES OF THE NI (II) COMPLEXES OF TRIDENTATE SCHIFF BASES*. *10*(4), 1511–1520.

https://doi.org/10.7324/RJC.2017.1041951

Ashraf A. Aly, Essmat M. El-Sheref, Aboul-Fetouh E. Mourad, Momtaz E. M. Bakheet, S. B. (2020). 4-Hydroxy-2-quinolones: syntheses, reactions and fused heterocycles. *Molecular Diversity*, *24*(2), 477–524. https://doi.org/10.1007/s11030-019-09952-5

Awolope, R. O., Ejidike, I. P., & Clayton, H. S. (2023). Schiff base metal complexes as a dual antioxidant and antimicrobial agents. *Journal of Applied Pharmaceutical Science*, *13*(03), 132–140. https://doi.org/10.7324/JAPS.2023.91056

Bakr F. Abdel-Waha, Rizk E. Khidre, Abdelbasset A. Farahat, and A.-A. S. E.-A. (2012). 2-Chloroquinoline-3-carbaldehydes : synthesis , reactions and applications. *ARKIVOC*, *2012*(i), 211–276.

Becke, A. D. (1993). *Density - functional thermochemistry . III . The role of exact exchange Density-functional thermochemistry . III . The role of exact exchange*. *98*, 5648–5652. https://doi.org/10.1063/1.464913

Belay, Y., Muller, A., Mokoena, F. S., Adeyinka, A. S., Motadi, L. R., & Oyebamiji, A. K. (2024). 1,2,3-triazole and chiral Schiff base hybrids as potential anticancer agents: DFT, molecular docking and ADME studies. *Scientific Reports*, 1–17. https://doi.org/10.1038/s41598-024-57689-5

Bitew, M., Desalegn, T., Demissie, T. B., Belayneh, A., Endale, M., & Eswaramoorthy, R. (2021). Pharmacokinetics and drug-likeness of antidiabetic flavonoids: Molecular docking and DFT study. *PLoS ONE*, *16*(12 December). https://doi.org/10.1371/journal.pone.0260853

Chioma Festus, S. N. O. and A. C. E. (2019). Heteroleptic Metal Complexes of a Pyrimidinyl Based Schiff Base Ligand Synthesis , Characterization , and Biological Studies. *Frointiers in Chemistry*, *7*, 1–12. https://doi.org/10.3389/fchem.2019.00862

Cholan, S. S., Nadu, T., Nadu, T., Subramaniam, K., Nadu, T., Ramasamy, S., Nadu, T., Karuppaiah, S., & Arabia, S. (2024). Unveiling the Promising Pharmaceutical benefits of Newly Synthesized Schiff Base : DFT , Molecular docking , In silico ADME / T and PASS analysis. *Research Square*, 1–26. https://doi.org/10.21203/rs.3.rs-3911323/v1

Chu, X. M., Wang, C., Liu, W., Liang, L. L., Gong, K. K., Zhao, C. Y., & Sun, K. L. (2019). Quinoline and quinolone dimers and their biological activities: An overview. *European Journal of Medicinal Chemistry*, *161*, 101–117.

https://doi.org/10.1016/j.ejmech.2018.10.035

Damena, T., Alem, M. B., Zeleke, D., Desalegn, T., Eswaramoorthy, R., & Demissie, T. B. (2022a). Novel Zinc (II) and Copper (II) Complexes of 2 - ((2- Hydroxyethyl) amino) quinoline-3-carbaldehyde for Antibacterial and Antioxidant Activities : A Combined Experimental , DFT , and Docking Studies. *ACS Omega*, *Ii*. https://doi.org/10.1021/acsomega.2c02205

Damena, T., Alem, M. B., Zeleke, D., Desalegn, T., Eswaramoorthy, R., & Demissie, T. B. (2022b). Synthesis, characterization, and biological activities of zinc(II), copper(II) and nickel(II) complexes of an aminoquinoline derivative. *Frontiers in Chemistry*, *10*(November), 1–21. https://doi.org/10.3389/fchem.2022.1053532

Damena, T., Bitew, M., Zeleke, D., Demissie, T. B., & Desalegn, T. (2023). Synthesis and computational studies of novel cobalt (II) and oxovanadium (IV) complexes of quinoline carbaldehyde derivative ligand for antibacterial and antioxidant applications. *Journal of Molecular Structure*, *1280*, 134994. https://doi.org/10.1016/j.molstruc.2023.134994

Damena, T., Zeleke, D., Desalegn, T., Demissie, T. B., & Eswaramoorthy, R. (2022). Synthesis, Characterization, and Biological Activities of Novel Vanadium(IV) and Cobalt(II) Complexes. *ACS Omega*, *7*(5), 4389–4404. https://doi.org/10.1021/acsomega.1c06205

Deepika, P., Vinusha, H. M., Begum, M., Ramu, R., Shirahatti, P. S., & Prasad, M. N. N. (2022). 2-methoxy-4-(((5-nitropyridin-2-yl)imino)methyl)phenol Schiff base ligand and its Cu (II) and Zn (II) complexes : synthesis , characterization and biological investigations. *Heliyon*, *8*(May), 09648. https://doi.org/10.1016/j.heliyon.2022.e09648

Demircioğlu, Z. (2021). Synthesis, crystal structure, spectroscopic characterization, chemical activity and molecular docking studies of (E)-2-(((3-chloro-4-methylphenyl)imino)methyl)-6-ethoxyphenol. *Journal of Molecular Structure*, *1246*, 131114. https://doi.org/10.1016/j.molstruc.2021.131114

Dhayalan, V., & Dhayalan, V. (2022). Synthesis and Applications of Asymmetric Catalysis Using Chiral Ligands Containing Quinoline Motifs. *SynOPen*, *6*, 31–57. https://doi.org/10.1055/a-1743-4534

Dinku, D., Demissie, T. B., Beas, I. N., Eswaramoorthy, R., Abdi, B., & Desalegn, T. (2024). Antimicrobial activities and docking studies of new Schiff base ligand and its Cu (II), Zn (II) and Ni (II) Complexes : Synthesis and Characterization. *Inorganic Chemistry*

Communications, *160*. https://doi.org/10.1016/j.inoche.2023.111903

Kapadnis Kailas H., Jadhav Sheetal P., Dr. Patil Anita P., D. H. A. P. (2016). FOUR SYNTHESIS METHODS OF SCHIFF BASE LIGANDS AND PREPARATION OF THEIR METAL COMPLEX WITH IR AND ANTIMICROBIAL INVESTIGATION. *WORLD JOURNAL OF PHARMACY AND PHARMACEUTICAL SCIENCES*, *5*(2), 1055–1063.

Ejidike, I. P., & Ajibade, P. A. (2015). Transition metal complexes of symmetrical and asymmetrical Schiff bases as antibacterial , antifungal , antioxidant , and anticancer agents : progress and prospects. *Inorganic Chemistry*, *35*(4), 191–224. https://doi.org/10.1515/revic-2015-0007

El-mossalamy, E. H., Al-harby, N. F., Aal, S. A., Ali, N. M., El-desawy, M., Elewa, M. M., & El, M. (2024). Tenability on schiff base Hydrazone derivatives and Frontier molecular orbital. *Heliyon*, *10*(January), e24472 Contents. https://doi.org/10.1016/j.heliyon.2024.e24472

El, M. A., Elzawawi, F. M., Aziz, A. A. A., Nassir, K. M., Abu, S. M., & Wafa, E. (2022). New Schiff base ligand and its novel Cr (III), Mn (II), Co (II), Ni (II), Cu (II), Zn (II) complexes : spectral investigation , biological applications , and semiconducting properties. *Scientific Reports*, *Iii*, 1–21. https://doi.org/10.1038/s41598-022-22713-z

Erturk, A. G. (2019). Synthesis, structural identifications of bioactive two novel Schiff bases. *Journal of Molecular Structure*, 127299. https://doi.org/10.1016/j.molstruc.2019.127299

Eunice A. Nyawade, Martin O. Onani, Samantha Meyer, P. D. (2020). Synthesis , characterization and antibacterial activity studies of new 2 - pyrral - L - amino acid Schiff base palladium (II) complexes. *Chemical Papers*, *74*(11), 3705–3715. https://doi.org/10.1007/s11696-019-00986-5

F. K. Ommenya , E. A. Nyawade, D. M. A. J. K. (2020). Synthesis , Characterization and Antibacterial Activity of Schiff Base , 4-Chloro-2- {(E) - [(4-Fluorophenyl) imino] methyl } phenol Metal (II) Complexes. *Journal of Chemistry*, *2020*, 8. https://doi.org/10.1155/2020/1745236

Fonkui, T. Y., Ikhile, M. I., Njobeh, P. B., & Ndinteh, D. T. (2019). Benzimidazole Schiff base derivatives : synthesis , characterization and antimicrobial activity. *BMC Chemistry*, *13*, 1–11. https://doi.org/10.1186/s13065-019-0642-3

Gaikwad, K. D., Ubale, P., Khobragade, R., Deodware, S., Dhale, P., Asabe, M. R., Ovhal, R. M., Singh, P., Vishwanath, P., Shivamallu, C., Achar, R. R., Silina, E., & Stupin, V. (2022). Preparation, Characterization and In Vitro Biological Activities of New Diphenylsulphone Derived Schiff Base Ligands and Their Co(II) Complexes. *Molecules*, *27*, 8576. https://doi.org/https://doi.org/10.3390/molecules27238576

Gautam, S., Kumar, R., Singh, P., Gandhi, N., & Jain, P. (2023). Results in Chemistry Pharmacological aspects of Co (II), Ni (II) and Cu (II) schiff base complexes : An insight. *Results in Chemistry*, *5*(February), 100849. https://doi.org/10.1016/j.rechem.2023.100849

Ghanghas, P., Choudhary, A., Kumar, D., & Poonia, K. (2021). Coordination metal complexes with Schiff bases : Useful pharmacophores with comprehensive biological applications. *Inorganic Chemistry Communications*, *130*(March), 108710. https://doi.org/10.1016/j.inoche.2021.108710

Gur'eva, Y. A., Zalevskaya, O. A., Shevchenko, O. G., Slepukhin, P. A., Makarov, V. A., & Kuchin, A. V. (2022). Copper(ii) complexes with terpene derivatives of ethylenediamine: synthesis, and antibacterial, antifungal and antioxidant activity. *RSC Advances*, *12*(15), 8841–8851. https://doi.org/10.1039/d2ra00223j

Habila A.N. Putaya, Naomi P. NDAHI, Hauwa S. BELLO, G. Malaa. A. O. and H. G. (2020). Synthesis , characterization and antimicrobial analysis of Schiff bases of o-phenylenediamine and 2-aminopyridine-3-carboxylic acid with ofloxacin and their metal (II) complexes. *Int. J. Biol. Chem. Sci.*, *14*(1), 263–278.

Hadjer, F., Tahar, B., Eddine, A. D., & Sofiane, D. (2018). Antioxidant and Antimicrobial Activity of Some Transition Metal Complexes with Non - natural Amino Acids Used As Ligand. *Journal of Materials and Environmental Sciences*, *9*(7), 2153–2157.

Hanan A. Althobiti, S. A. Z. (2020). New Schi ff bases of 2 - (quinolin - 8 - yloxy) acetohydrazide and their Cu (II) , and Zn (II) metal complexes : their in vitro antimicrobial potentials and in silico physicochemical and pharmacokinetics properties 1 Introduction. *Open Chemistry*, 591–607. https://doi.org/https://doi.org/10.1515/chem-2020-0085

Hasan, M., Ahsan, H., Saha, P., Naime, J., Kumar, A., Asraf, A., & Islam, A. B. M. N. (2021). Antioxidant , antibacterial and electrochemical activity of and its transition metal

complexes. *Results in Chemistry*, *3*, 100115. https://doi.org/10.1016/j.rechem.2021.100115

Hassan, A. S., Morsy, N. M., Aboulthana, W. M., & Ragab, A. (2023). Exploring novel derivatives of isatin-based Schiff bases as multi-target agents: design, synthesis, in vitro biological evaluation, and in silico ADMET analysis with molecular modeling simulations. *RSC Advances*, *13*(14), 9281–9303. https://doi.org/10.1039/d3ra00297g

Heba, & Al-sulHeba Alshater , Ahlam I. Al-Sulami, Samar A. Aly, E. M. A. and S. S. H. (2023). Antitumor and Antibacterial Activity of Ni(II), Cu(II), Ag(I), and Hg(II) Complexes with Ligand Derived from Thiosemicarbazones: Characterization and Theoretical Studies. *Molecules,MDPI*, *28*(Ii), 2590. https://doi.org/https://doi.org/10.3390/molecules28062590

James Tembei Titah, Coulibaly Wacothon Karime, Kevin Chambers, Anita Balogh, K. J. (2020). Synthesis , Characterization and Bacterial Growth Inhibitory Properties of Schiff-Base Ligands Derived from Amino Acids. *Science Journal of Chemistry*, *8*(1), 1–6. https://doi.org/10.11648/j.sjc.20200801.11

Joshi, N. R., Mule, S. G., Gore, V. A., Suryawanshi, R. D., Pawar, G. T., Bembalkar, S. R., & Pawar, R. P. (2022). Original Article Synthesis and Biological Study of Novel Schiff Base hydrazine) Ligand and Metal Complexes. *Journal of Exploratory Research in Pharmacology*, *7*(4), 202–207. https://doi.org/10.14218/JERP.2022.00021

Julius, L. G., Mapolelo, D. T., Koobotse, M. O., Nkwe, D. O., & Matshwele, J. T. P. (2023). Synthesis , characterization , molecular docking , and cytotoxicity study of ruthenium (II / III) polypyridyl complexes. *Applied Organometalic Chemistry*, *September*, 1–22. https://doi.org/10.1002/aoc.7341

Kareem, S. A.-A. J. and I. K. (2022). Synthesis , characterization and biological study of open multi dentate new Azo-Schiff ligand and it ’ s divalent metal ion complexes with copper , zinc and mercury V ’ LYDOHQW. *AIP Publishing*, *030014*. https://doi.org/https://doi.org/10.1063/5.0066818

Kavitha, P., Chary, M. R., Singavarapu, B. V. V. A., & Reddy, K. L. (2016). Synthesis , characterization , biological activity and DNA cleavage studies of tridentate Schiff bases and their Co (II) complexes. *Journal of Saudi Chemical Society*, *20*(1), 69–80. https://doi.org/10.1016/j.jscs.2013.03.005

Khalaf-Alla, P. A. (2020). Antioxidant , Antimicrobial and Antitumor Studies of Transition Metal Complexes Derived from Calculations and Molecular Docking Investigation. *Applied*

Organometalic Chemistry, *December 2019*, 1–16. https://doi.org/10.1002/aoc.5628

Khobragade, D., Wankhede, S., & Armarkar, A. (2021). Molecular Docking in Drug Discovery. *Journal of Pharmaceutical Research International*, *September*, 48–58. https://doi.org/10.9734/jpri/2021/v33i30B31639

Kouser, S., Joythi, M., Begum, A. B., Asha, M. S., Al-ostoot, F. H., Lakshmeesha, D. P., Ramu, R., & Ara, S. (2023). Molecular docking , synthesis and antimicrobial evaluation of metal complexes with Schiff base. *Results in Chemistry*, *5*(November 2022), 100650. https://doi.org/10.1016/j.rechem.2022.100650

Krishnan, R; Binkley, J S; Seeger, R; Pople, J. A. (1980). Self-consistent molecular orbital methods. XX. A basis set for correlated wave functions. *J. Chem. Phys*, *72*(1). https://doi.org/10.1063/1.438955

Krishnan, R., Binkley, J. S., Seeger, R., & Pople, J. A. (1980). Self-consistent molecular orbital methods. XX. A basis set for correlated wave functions. *The Journal of Chemical Physics*, *72*(1), 650–654. https://doi.org/10.1063/1.438955

Kumar, K. S., Chityala, V. K., Subhashini, N. J. P., & Prashanthi, Y. (2013). Synthesis , Characterization , and Biological and Cytotoxic Studies of Copper (II), Nickel (II), and Zinc (II) Binary Complexes of 3-Amino-5-methyl Isoxazole Schiff Base. *Inorganic Chemistry*, 7. https://doi.org/10.1155/2013/562082

Kumar, S., & Trivedi, A. V. (2016). A Review on Role of Nickel in the Biological System. *International Journal of Current Microbiology and Applied Sciences*, *5*(3), 719–727. https://doi.org/10.20546/ijcmas.2016.503.084

Kun Hu, *a Chensi Liu, a Jingui Lia and Fupei Liang*a, B. (2018). Copper(II) complexes based on quinoline derived Schiff-base ligands: synthesis,characterization, HSA/DNA binding ability, and anticancer activity. *ROYAL SOCIETY OF CHEMISTRY*. https://doi.org/10.1039/C8MD00223A

Lee, C.; Yang, W.; Parr, R. G. (1988). Development of the Colle-Salvetti correlation-energy formula into a functional of the electron density. *Phys. Rev. B*, 85–789.

Leila Kafi-Ahmadi and Ahmad Poursattar Marjanib. (2019). Mononuclear Schiff Base Complexes Derived from 5-Azophenylsalicylaldehyde with Co (II), Ni (II) Ions : Synthesis , Characterization , Electrochemical Study and Antibacterial Properties. *South African Chemical Institute*, *72*, 101–107.

Lemilemu, F., Bitew, M., Demissie, T. B., Eswaramoorthy, R., & Endale, M. (2021). Synthesis, antibacterial and antioxidant activities of Thiazole-based Schiff base derivatives: a combined experimental and computational study. *BMC Chemistry*, *15*(1), 1–18. https://doi.org/10.1186/s13065-021-00791-w

Li, L., & Burke, K. (1995). Recent developments in density functional theory. *Recent Advances in Density Functional Methods, Part 1*, *1*, 155–192. http://www.worldscientific.com/worldscibooks/10.1142/2914

Li, Y., Dong, J., Zhao, P., Hu, P., Yang, D., Gao, L., & Li, L. (2020). Synthesis of Amino Acid Schiff Base Nickel (II) Complexes as Potential Anticancer Drugs In Vitro. *Bioinorganic Chemistry and Applications*, *2020*, 15. https://doi.org/https://doi.org/10.1155/2020/8834859

Mandewale, M. C., Thorat, B., Nivid, Y., Jadhav, R., Nagarsekar, A., & Yamgar, R. (2018). Synthesis , structural studies and antituberculosis evaluation of new hydrazone derivatives of quinoline and their Zn (II) complexes. *Journal of Saudi Chemical Society*, *22*(2), 218–228. https://doi.org/10.1016/j.jscs.2016.04.003

Marzano, C., Pellei, M., Tisato, F., & Santini, C. (2009). Copper Complexes as Anticancer Agents. *Anti-Cancer Agents in Medicinal Chemistry*, *9*(March), 185–211. https://doi.org/10.2174/187152009787313837

Md. Saddam Hossain, C. M. Zakaria, M. K.-E.-Z. (2018). Metal Complexes as Potential Antimicrobial Agent. *American Journal of Heterocyclic Chemistry*, *4*(1), 1–21. https://doi.org/10.11648/j.ajhc.20180401.11

Mohamed F. AlAjmi, Afzal Hussain, A. A. and R. A. K. (2016). In vivo assessment of newly synthesized achiral copper(II) and zinc(II) complexes of a benzimidazole derived scaffold as a potential analgesic, antipyretic and anti-inflammator. *ROYAL SOCIETY OF CHEMISTRY*, *6*, 19475–19481. https://doi.org/10.1039/c5ra25071d

Mohammed, S., Obaid, H., Sultan, J. S., & Al-hamdani, A. A. S. (2020). *1311 Synthesis , Characterization and Biological Efficacies from Some New Dinuclear Metal Complexes for Base 3- (3 , 4-Dihydroxy-phenyl) -2- [(2-hydroxy-3-methylperoxy- benzylidene) -amino] -2-methyl Propionic Acid*. *20*(6), 1311–1322. https://doi.org/10.22146/ijc.49842

Muleta, F. (2023). *Synthesis , Characterization , and Molecular Docking Studies of Homoleptic and Heteroleptic Zinc (II), Copper (II), Nickel (II) Complexes of Semicarbazone and Thiosemicarbazone Derivative Ligands for Biological Applications Fekadu Muleta Gudeta*

A Ph. Ii.

Muleta, F., Desalegn, T., Demissie, T. B., Eswaramoorthy, R., Murthy, H. C. A., Chan, K. Y., Davids, B. L., & Ngwira, K. J. (2023). Synthesis, molecular docking, and biological studies of novel heteroleptic Cu(II) and Zn(II) complexes of natural product-based semicarbazone derivatives. *Journal of Molecular Structure*, *1274*. https://doi.org/10.1016/j.molstruc.2022.134405

Muleta, F., Desalegn, T., Eswaramoorthy, R., & Garg, A. (2022). Cu (II), Zn (II) complexes of semicarbazone , thiosemicarbazone derivatives of dehydrozingerone. *Journal of Molecular Structure*, *1268*, 133632. https://doi.org/10.1016/j.molstruc.2022.133632

Nagesh, G. Y., & Mruthyunjayaswamy, B. H. M. (2014). Synthesis, Characterization and Biological Relevance of Some Metal (II) Complexes with Oxygen, Nitrogen and Oxygen (ONO) donor Schiff base Ligand derived from Thiazole and 2-hydroxy-1-naphthaldehyde. *JOURNAL OF MOLECULAR STRUCTURE*, *12*(58). https://doi.org/10.1016/j.molstruc.2014.12.058

Ördög, R., & Grolmusz, V. (2008). Evaluating genetic algorithms in protein-ligand docking. *Lecture Notes in Computer Science (Including Subseries Lecture Notes in Artificial Intelligence and Lecture Notes in Bioinformatics)*, *4983 LNBI*, 402–413. https://doi.org/10.1007/978-3-540-79450-9_37

P.Jeffrey Hat, W. R. W. (1985). Ab initio effective core potentials for molecular calculations. Potentials for the transition metal atoms Sc to Hg. *J. Chem. Phys.*, *82*, 270–283. https://doi.org/10.1063/1.448799

Patil, S. K., & Vibhute, B. T. (2021). Synthesis , characterization , anticancer and DNA photocleavage study of novel quinoline Schiff base and its metal complexes. *Arabian Journal of Chemistry*, *14*(8), 103285. https://doi.org/10.1016/j.arabjc.2021.103285

Pradeep Kumar, M., Ayodhya, D., & Shivaraj. (2023). Novel copper (II) binary complexes with N,O-donor isoxazole Schiff base ligands: Synthesis, characterization, DPPH scavenging, antimicrobial, and DNA binding and cleavage studies. *Results in Chemistry*, *5*(February), 100845. https://doi.org/10.1016/j.rechem.2023.100845

Raczuk, E., Dmochowska, B., Samaszko-fiertek, J., & Madaj, J. (2022). Different Schiff Bases—Structure, Importance and Classification. *Molecules*, *27*, 787. https://doi.org/10.3390/molecules27030787

Rahman, L. H. A., Abu-dief, A. M., Hamdan, S. K., & Seleem, A. A. (2015). Nano Structure Iron(II) and Copper(II) Schiff Base Complexes of a NNO-Tridentate Ligand as New Antibiotic Agents : Spectral , Thermal Behaviors and DNA Binding Ability 2 Experimental 2 . 1 Materials and methods. *Internation Journal of Nanomaterials and Chemistry*, *77*(2), 65–77. http://dx.doi.org/10.12785/ijnc/010204

Rajewar, V. R., Dharmale, M. K., & Pingalkar, S. R. (2015). Synthesis and Spectral Characterization of Lanthanide Complexes Containing Bidentate Schiff Base Derived From Pyridine-2-Carbaldehyde and 2-Hydrazinylquinoline. *J.Pure App. Chem.Res.*, *4*(May), 42–52. https://doi.org/10.21776/ub.jpacr.2015.004.02.191

Raman, N., Thangaraja, C., & Johnsonraja, S. (2005). Synthesis, spectral characterization, redox and antimicrobial activity of Schiff base transition metal(II) complexes derived from 4-aminoantipyrine and 3-salicylideneacetylacetone. *Central European Journal of Chemistry*, *3*(3), 537–555. https://doi.org/10.2478/bf02479281

Ramhari Meena, Pooja Meena, Anita Kumari, N. S. and N. F. (2022). Schiff Bases and Their Metal Complexes: Synthesis, Structural Characteristics and Applications. *IntechOpen*. https://doi.org/http://dx.doi.org/10.5772/intechopen.108396

Rizzotto, M. (2012). Metal Complexes as Antimicrobial Agents. In *A search for Antibacterial Agents* (pp. 73–89).

Salama, M. M., Ahmed, S. G., & Hassan, S. S. (2017). Synthesis , Characterizations , Biological , and Molecular Docking Studies of Some Amino Acid Schiff Bases with Their Cobalt (II) Complexes. *Advances in Biological Chemistry*, *7*, 182–194. https://doi.org/10.4236/abc.2017.75013

Salen, T., Base, T. B., Es-sounni, B., Nakkabi, A., Bouymajane, A., & Elaaraj, I. (2023). Synthesis , Characterization , Antioxidant and Antibacterial Activities of Six Metal Complexes Based. *Biointerface Research in Applied Chemistry*, *13*(4), 1–14. https://doi.org/https://doi.org/10.33263/BRIAC134.333

Sayed Suliman Shah , Dawood Shah , Ibrahim Khan, Sajjad Ahmad , Umar Ali, A. ur R. (2020). An Synthesis and Antioxidant Activities of Schiff Bases and Their Complexes : An Updated Review. *Biointerface Research in Applied Chemistry*, *10*(6), 6939–6963.

Seema, S. and M. (2020). Mixed Ligand Complex of Ni (II) with Schiff Base Ligands derived from Isatin and its Bromo Derivative : Synthesis , Characterization and Biological

Screening. *International Journal of Chemical Sciences*, *18*(3), 1–10.

Senerovic, L., Opsenica, D., Moric, I., Aleksic, I., Spasi, M., & Vasiljevic, B. (2020). *Quinolines and Quinolones as Antibacterial , Antifungal , Anti- virulence , Antiviral and Anti-parasitic Agents*. *September 2019*, 37–69. https://doi.org/10.1007/5584

Senerovic, L., Opsenica, D., Moric, I., Aleksic, I., Spasić, M., & Vasiljevic, B. (2020). Quinolines and quinolones as antibacterial, antifungal, anti-virulence, antiviral and anti-parasitic agents. *Advances in Experimental Medicine and Biology*, *1282*, 37–69. https://doi.org/10.1007/5584_2019_428

Shah, A. A., Ali, M., Halim, S. A., Khan, A., Latif, A., Al-harrasi, A., & Ahmad, M. (2024). Novel hydrazone schiff ' s base derivatives of polyhydroquinoline : synthesis , in vitro prolyl oligopeptidase inhibitory activity and their Molecular docking study. *Journal of Biomolecular Structure and Dynamics*, *0*(0), 1–15. https://doi.org/10.1080/07391102.2024.2319677

Siham, L. (2023). *The synthesis and evaluation of antioxidant activity of Schiff bases ligands : investigation of their ion extraction capability from aqueous media*.

Siwach, P., Singh, K., & Sindhu, M. (2023). Synthesis, spectroscopic characterization and photophysical properties of transition metal complexes of 4-((3-fluoro-2-methylbenzylidene)amino)-5-methyl-4H-1,2,4-triazole-3-thiol. *Results in Chemistry*, *5*(June), 100990. https://doi.org/10.1016/j.rechem.2023.100990

Sridhar.G, Mohammed Bilal.I, Easwaramoorthy.D, Kutti Rani.S, S. K. B. and C. S. M. (2017). Synthesis, Characterization and Antimicrobial Activities of Copper, Nickel, Cobalt, Chromium Complexes Derived from (Z)-4-Fluoro-N-(2,7-dimethylhept-6-enylidene) benzenamine. *J. Braz. Chem. Soc*, *28*(5), 756–767.

Srivastava, V. K. (2021). Synthesis , characterization , and biological studies of some biometal complexes. *Future Journal of Pharmaceutical Sciences*, *7*, 15. https://doi.org/10.1186/s43094-021-00191-w

Stefan Grimme, Filipp Furche, R. A. (2002). An improved method for density functional calculations of the frequency-dependent optical rotation. *Chemical Physics Letters*, *361*(3–4), 321–328. https://doi.org/10.1016/S0009-2614(02)00975-2

Sumathi, S. (2022). Synthesis , characterization and biological activities of Co (II), Cu (II), Zn (II), and Cd (II) metal complexes of 1 , 10 phenanthroline based Schiff base. *Research*

Square. https://doi.org/https://doi.org/10.21203/rs.3.rs-1348908/v1

Sureshkumar, B., Mary, Y. S., Mary, Y. S., & Suma, S. (2021). Spectroscopic and DFT investigations of 8-hydroxy quinoline-5-sulfonic acid-5-chloro-8-hydroxyquinoline cocrystal. *Chemical Papers*, *75*(7), 3387–3399. https://doi.org/10.1007/s11696-021-01579-x

Teran, R., Guevara, R., Mora, J., Dobronski, L., Barreiro-costa, O., Beske, T., Araya-maturana, R., Rojas-silva, P., Poveda, A., & Heredia-moya, J. (2019). Characterization of Antimicrobial, Antioxidant, and Leishmanicidal Activities of Schi ff Base Derivatives of 4-Aminoantipyrine. *Molecules*, *24*, 2696.

Tufa, A., Endale, M., & Desalegn, T. (2018). Synthesis , Characterization and Antibacterial Activity of Copper (II) and Cobalt (II) Vanillin-Aniline Schiff Base Complexes. *Chemistry and Materials Research*, *10*(2), 38–45.

Vairalakshmi M, Princess R, J. R. S. (2019). Metal Complexes Of Novel Schiff Base Containing Isatin : Characterization , Antimicrobial , Antioxidant And Catalytic Activity Study. *Asian Journal of Pharmaceutical and Clinical Research*, *12*(8). https://doi.org/http://dx.doi.org/10.22159/ajpcr.2019.v12i8.34189

Veljovic, D., & Jokic, B. (2012). Biocompatibility and Antimicrobial Activity of Zinc (II) Doped Hydroxyapatite , Synthesized by Hydrothermal Method hydroxyapatite , synthesized by a hydrothermal method. *Journal of the Serbian Chemical Society*, *77*(12), 1787–1798. https://doi.org/10.2298/JSC121019131R

Venkatesh, G., Vennila, P., Kaya, S., Ahmed, S. Ben, Sumathi, P., Siva, V., Rajendran, P., & Kamal, C. (2024). Synthesis and Spectroscopic Characterization of Schiff Base Metal Complexes , Biological Activity , and Molecular Docking Studies. *ACS Omega*, *9*, 8123–8138. https://doi.org/10.1021/acsomega.3c08526

Vinusha, H. M., Prasad, S., Revanasiddappa, H. D., Ramu, R., Shirahatti, P. S., Prasad, M. N. N., Chandrashekar, S., & Begum, M. (2019). Results in Chemistry Preparation , spectral characterization and biological applications of Schiff base ligand and its transition metal complexes. *Results in Chemistry*, *1*, 100012. https://doi.org/10.1016/j.rechem.2019.100012

Wafaa S. Hamama, Mona E. Ibrahim, A. A. G. and H. H. Z. (2018). Recent advances in the chemistry of 2- chloroquinoline-3-carbaldehyde and related analogs. *Royal Society Of Chemistry*, *8*, 8484–8515. https://doi.org/10.1039/c7ra11537g

Yadav, P., Sarkar, A., & Kumar, A. (2019). SYNTHESIS AND BIOLOGICAL ACTIVITIES OF SCHIFF BASES AND THEIR SYNTHESIS AND BIOLOGICAL ACTIVITIES OF SCHIFF BASES AND THEIR DERIVATIVES : *Basic and Applied Engineering Research, February 2020*.

Yamgar, R. S., Nivid, Y., Nalawade, S., Mandewale, M., Atram, R. G., & Sawant, S. S. (2014). Novel Zinc (II) Complexes of Heterocyclic Ligands as Antimicrobial Agents : Synthesis , Characterisation , and Antimicrobial Studies. *Bioinorganic Chemistry and Applications*, 10. https://doi.org/10.1155/2014/276598

Yernale, N. G., Bennikallu, M., & Mathada, H. (2014). *In Vitro Cytotoxic Studies of Some Metal Complexes of Schiff Base Ligand Derived from Thiazole and Quinoline Moiety*. *2014*(L).

Yusuf, T. L., Oladipo, S. D., Zamisa, S., Kumalo, H. M., Lawal, I. A., Lawal, M. M., & Mabuba, N. (2021a). Design of New Schi ff -Base Copper (II) Complexes : Synthesis , Crystal Structures , DFT Study , and Binding Potency toward Cytochrome. *ACS*, *6*, 13704–13718. https://doi.org/10.1021/acsomega.1c00906

Yusuf, T. L., Oladipo, S. D., Zamisa, S., Kumalo, H. M., Lawal, I. A., Lawal, M. M., & Mabuba, N. (2021b). Design of New Schiff-Base Copper(II) Complexes: Synthesis, Crystal Structures, DFT Study, and Binding Potency toward Cytochrome P450 3A4. *ACS Omega*, *6*(21), 13704–13718. https://doi.org/10.1021/acsomega.1c00906

Zabiulla, Kouser, S., Joythi, M., Bushra Begum, A., Asha, M. S., Hezam Al-Ostoot, F., Lakshmeesha, D. P., Ramu, R., & Ara Khanum, S. (2023a). Molecular docking, synthesis and antimicrobial evaluation of metal complexes with Schiff base. *Results in Chemistry*, *5*(November 2022), 100650. https://doi.org/10.1016/j.rechem.2022.100650

Zabiulla, Kouser, S., Joythi, M., Bushra Begum, A., Asha, M. S., Hezam Al-Ostoot, F., Lakshmeesha, D. P., Ramu, R., & Ara Khanum, S. (2023b). Molecular docking, synthesis and antimicrobial evaluation of metal complexes with Schiff base. *Results in Chemistry*, *5*(September 2022), 100650. https://doi.org/10.1016/j.rechem.2022.100650

Zoubi, W. Al. (2013). Biological Activities of Schiff Bases and Their Complexes : A Review of Recent Works. *International Journal of Organic Chemistry*, *3*(November), 73–95. https://doi.org/10.4236/ijoc.2013.33A008

APPENDIX

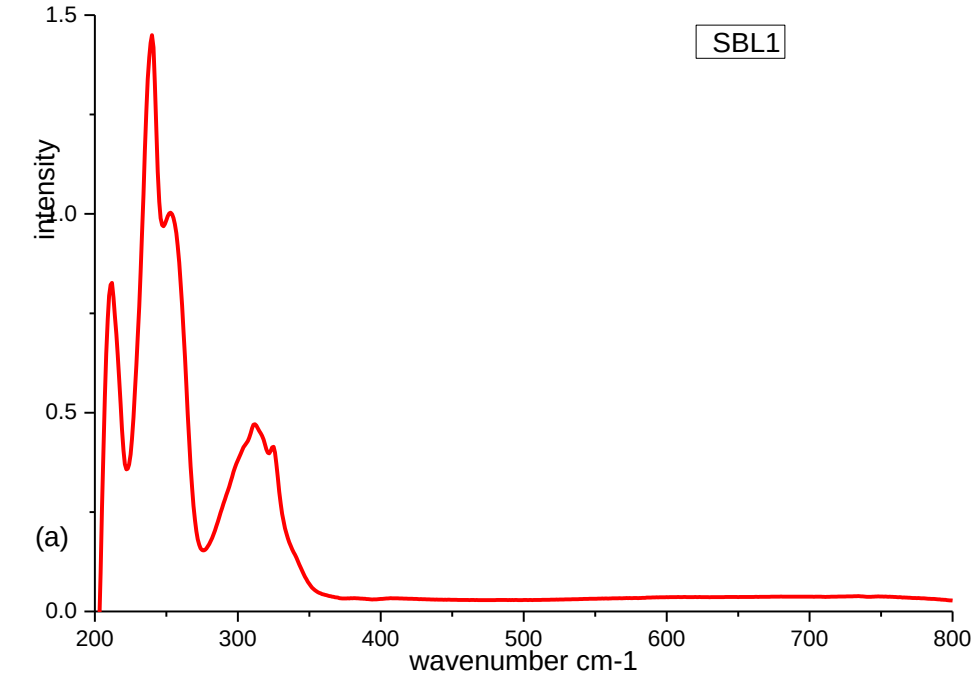
SBL1
intensity
1.5
1.0
0.5
0.0
(a)
200
300
400
500
600
700
800
wavenumber cm-1

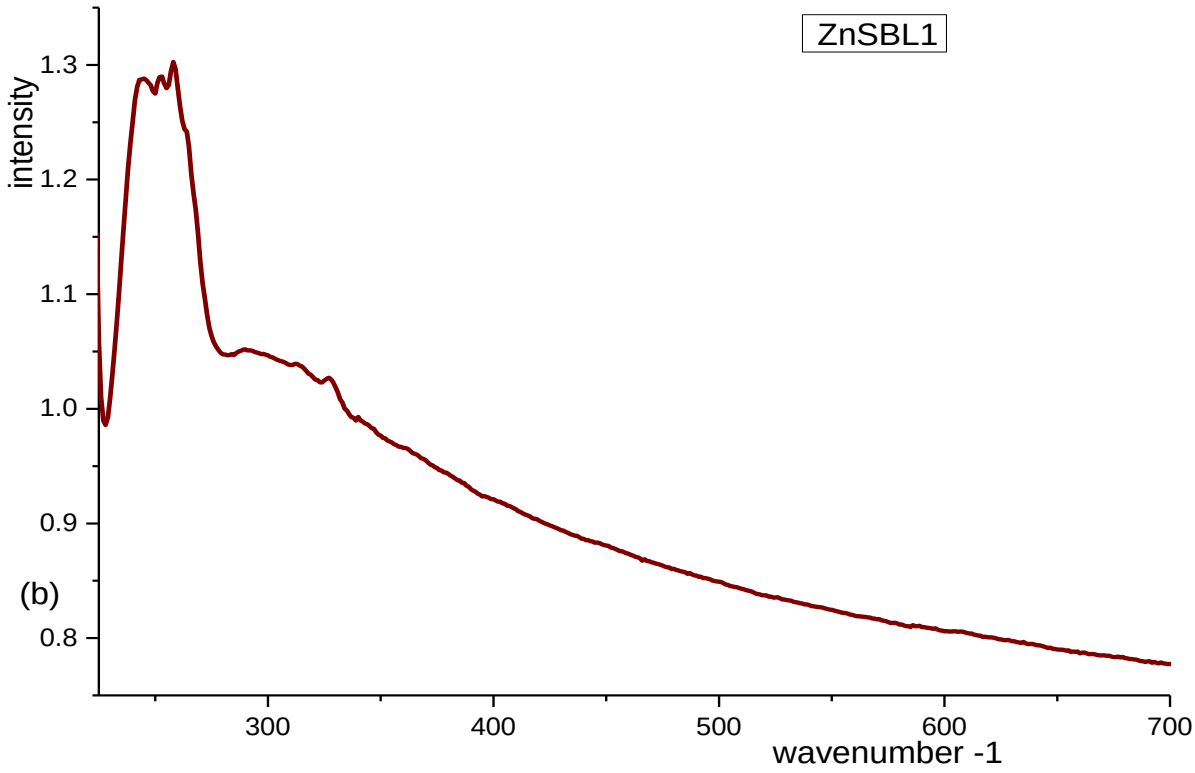
ZnSBL1
intensity
1.3
1.2
1.1
1.0
0.9
0.8
(b)
300
400
500
600
700
wavenumber -1

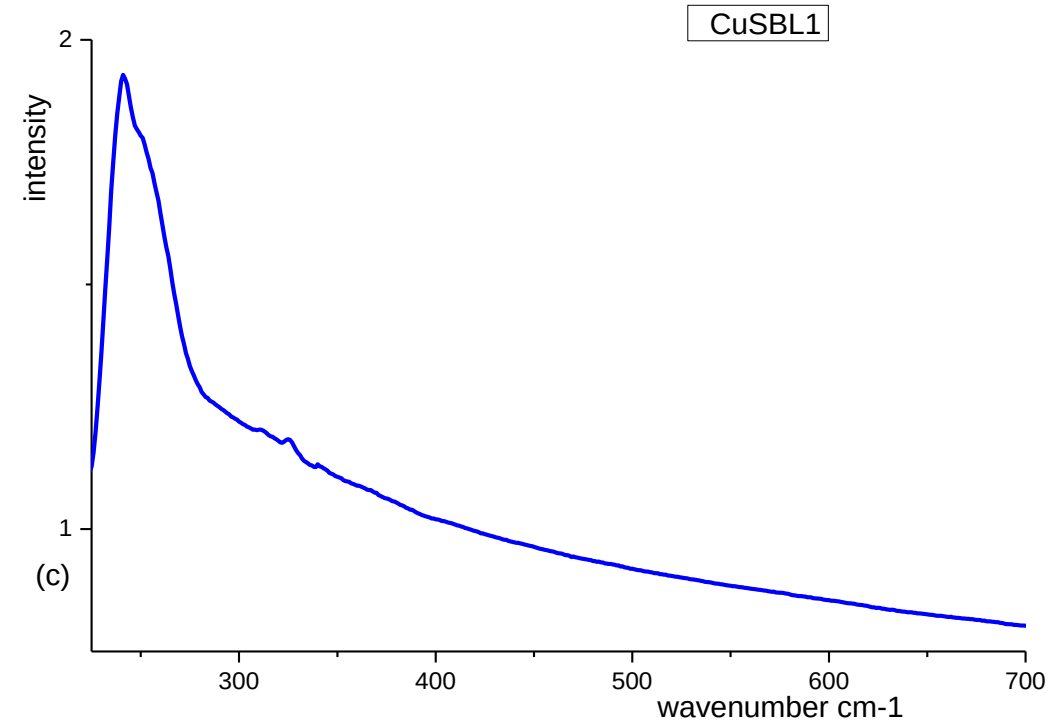

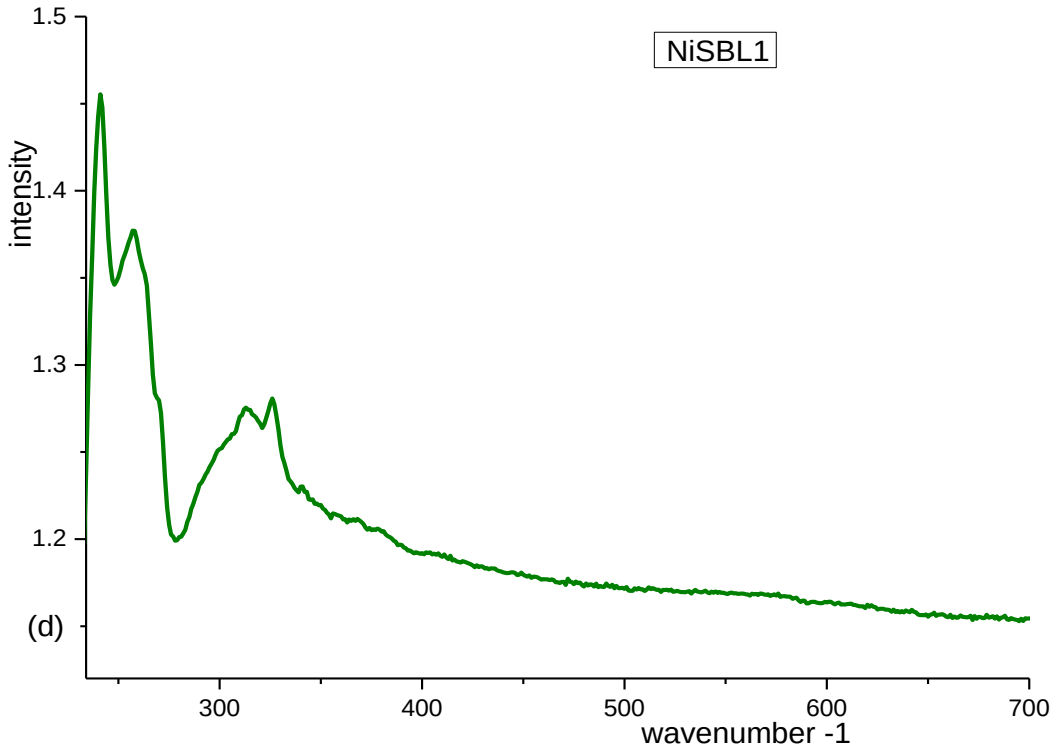

Appendix 1: UV-Vis of (a) SBL1, (b) ZnSBL1, (c) CuSBL1 and (d) NiSBL1 complexes

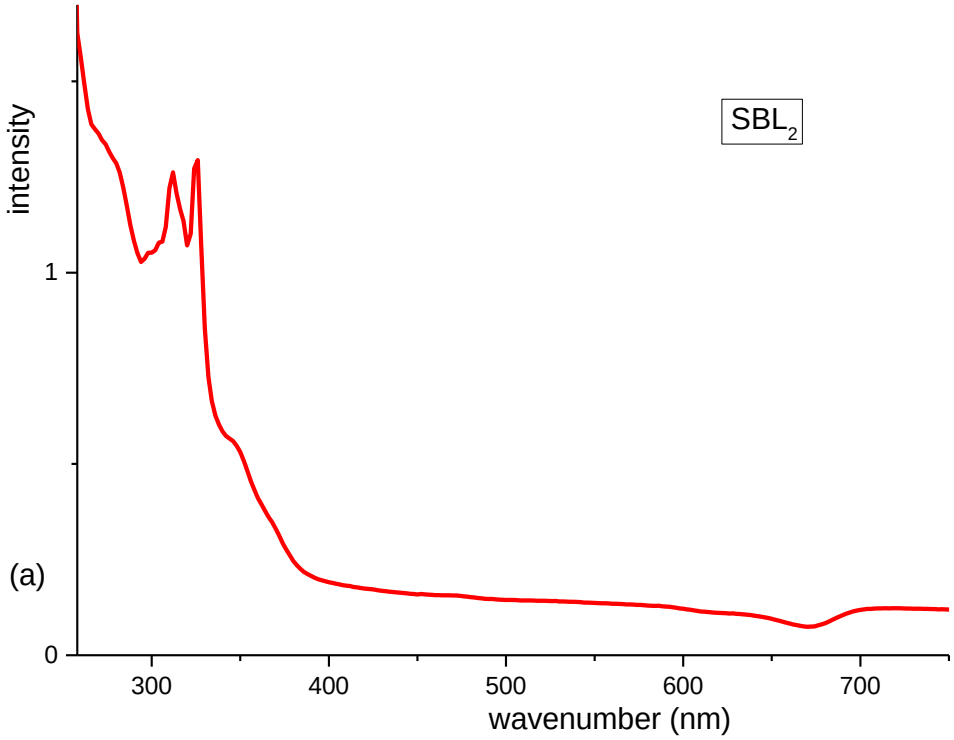
intensity
1
0
(a)
SBL2
300
400
500
600
700
wavenumber (nm)

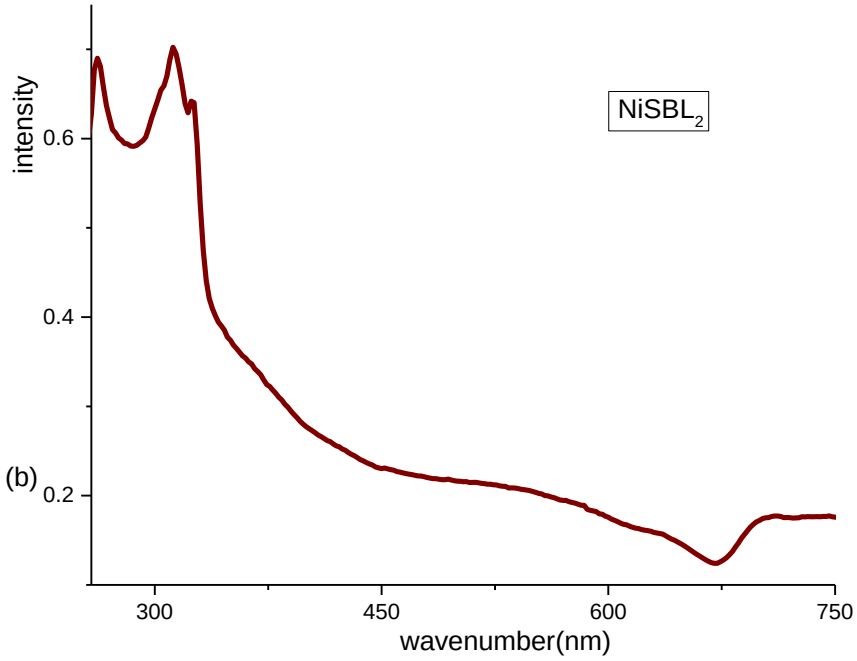
intensity
0.6
0.4
0.2
(b)
NiSBL2
300
450
600
750
wavenumber(nm)

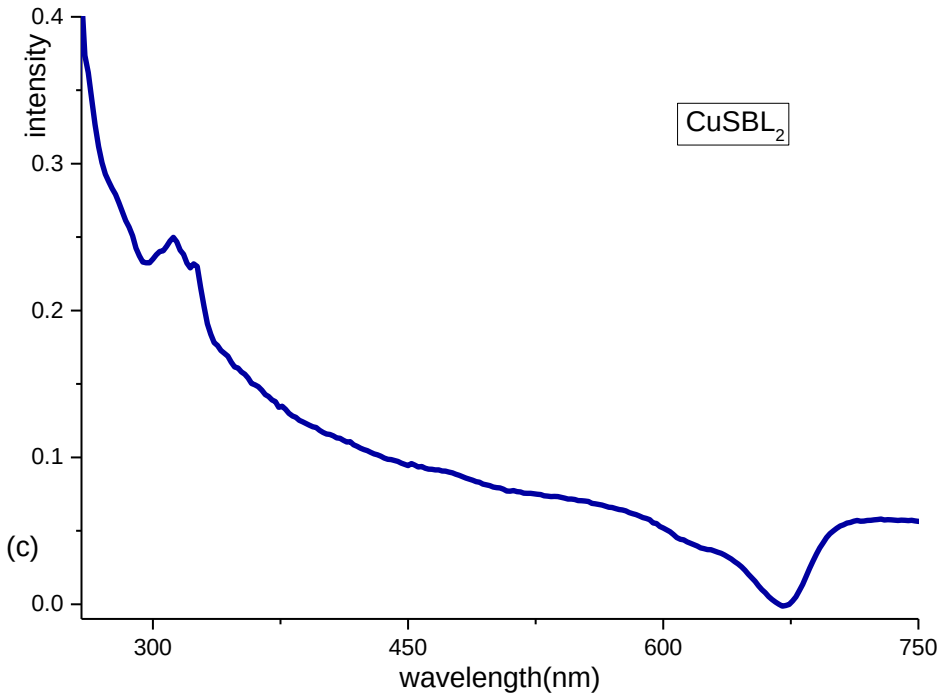

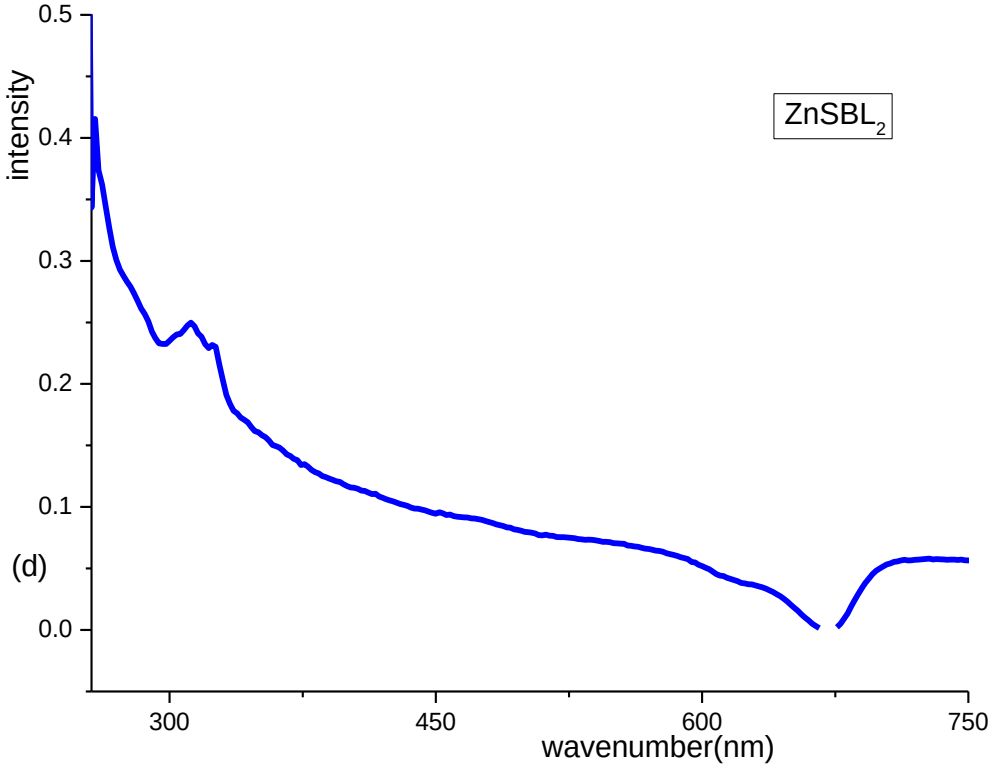

Appendix 2: UV-Vis of (a) SBL_2, (b) $NiSBL_2$, (c) $CuSBL_2$ and (d) $ZnSBL_2$ complexes

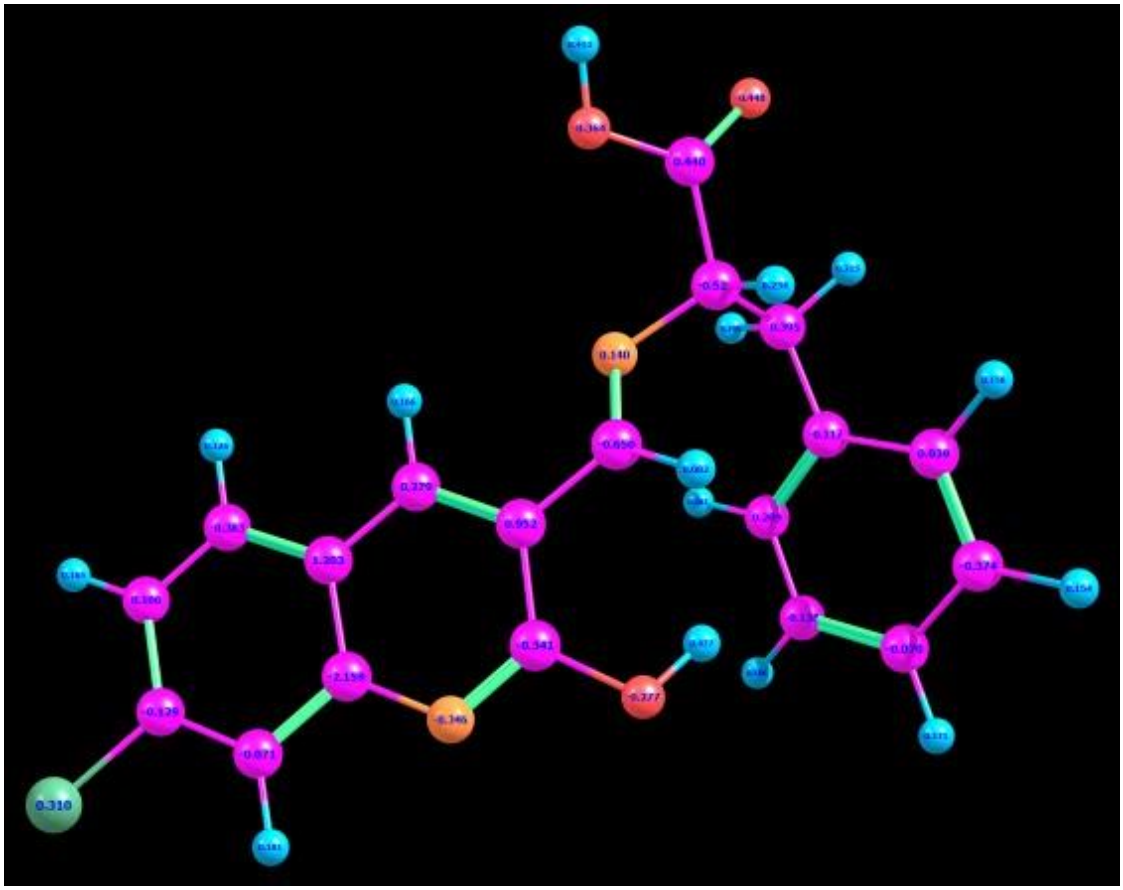

(a)

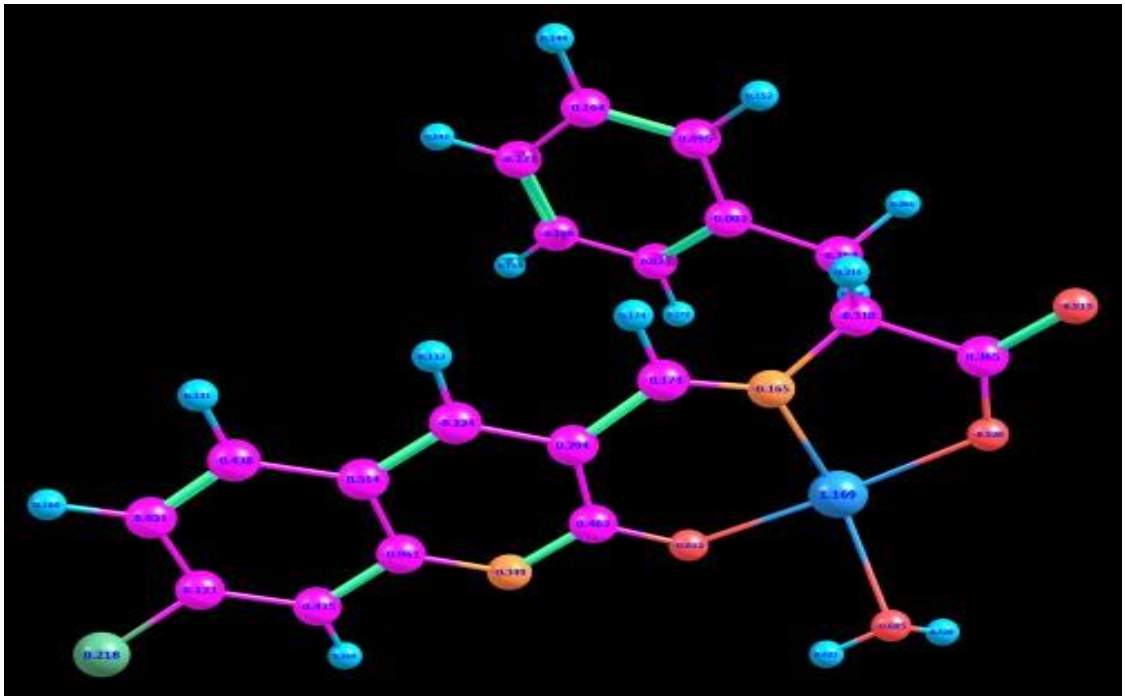

(b)

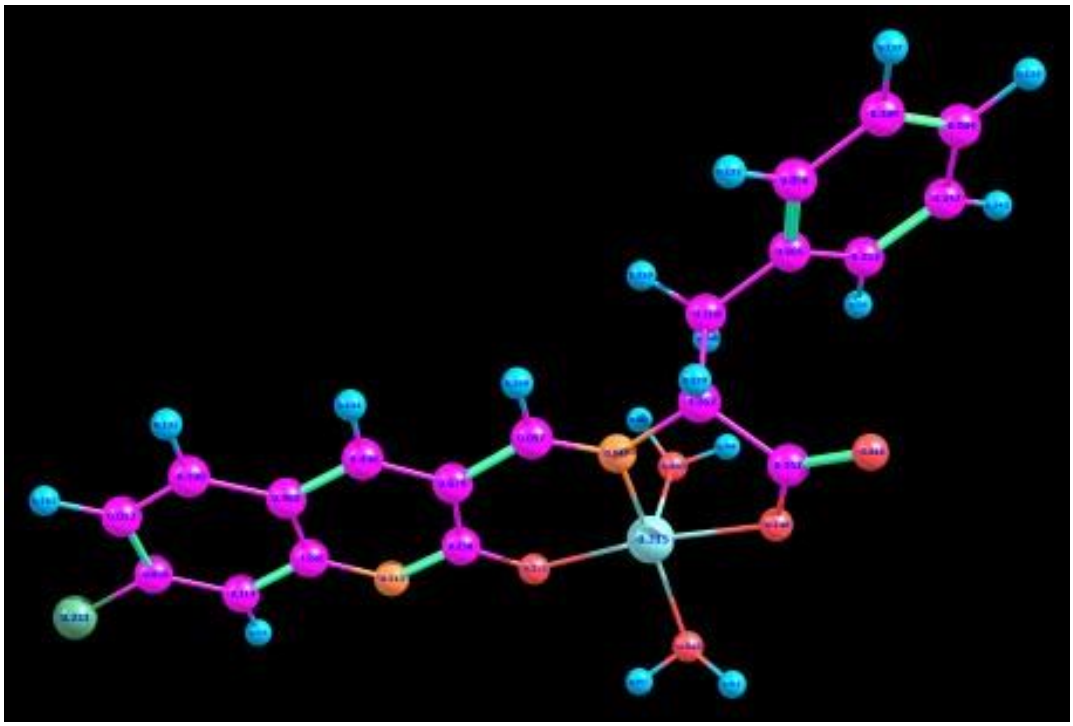

(c)

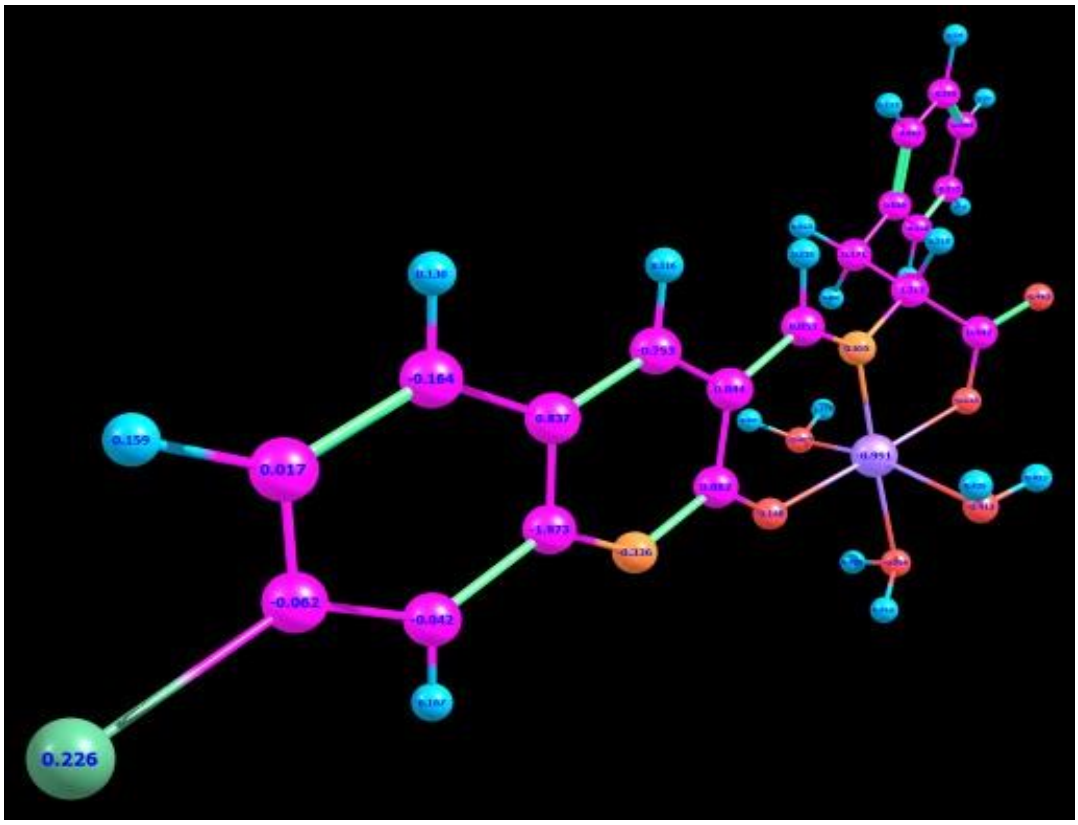

(d)

Appendix 3: Optimized geometry of (a) SBL1, (b) ZnSBL1, (c) CuSBL1 and (d) NiSBL1

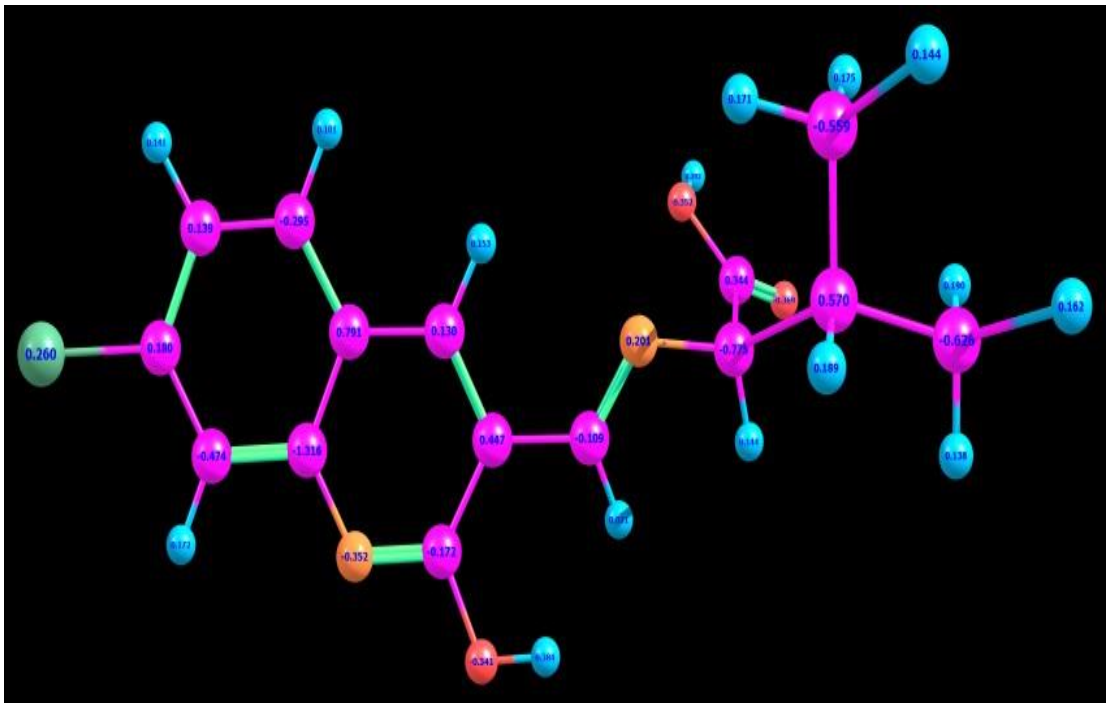
0.144
0.175
0.171
-0.559
0.139
-0.295
0.570
0.162
0.260
0.180
0.791
0.130
0.201
-0.775
-0.626
0.189
-0.474
-1.316
0.487
-0.109
0.138
-0.352
0.172
-0.341

(a)

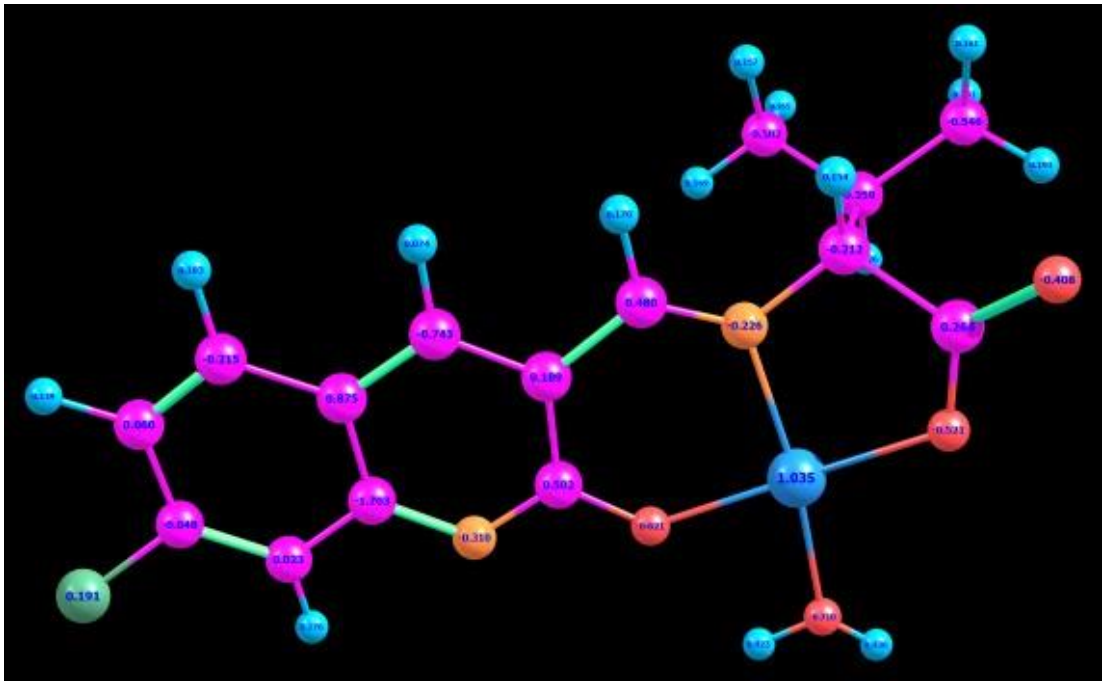
-0.546
-0.408
0.480
-0.226
-0.215
-0.743
0.875
0.080
1.035
0.502
0.310
0.023
0.191

(b)

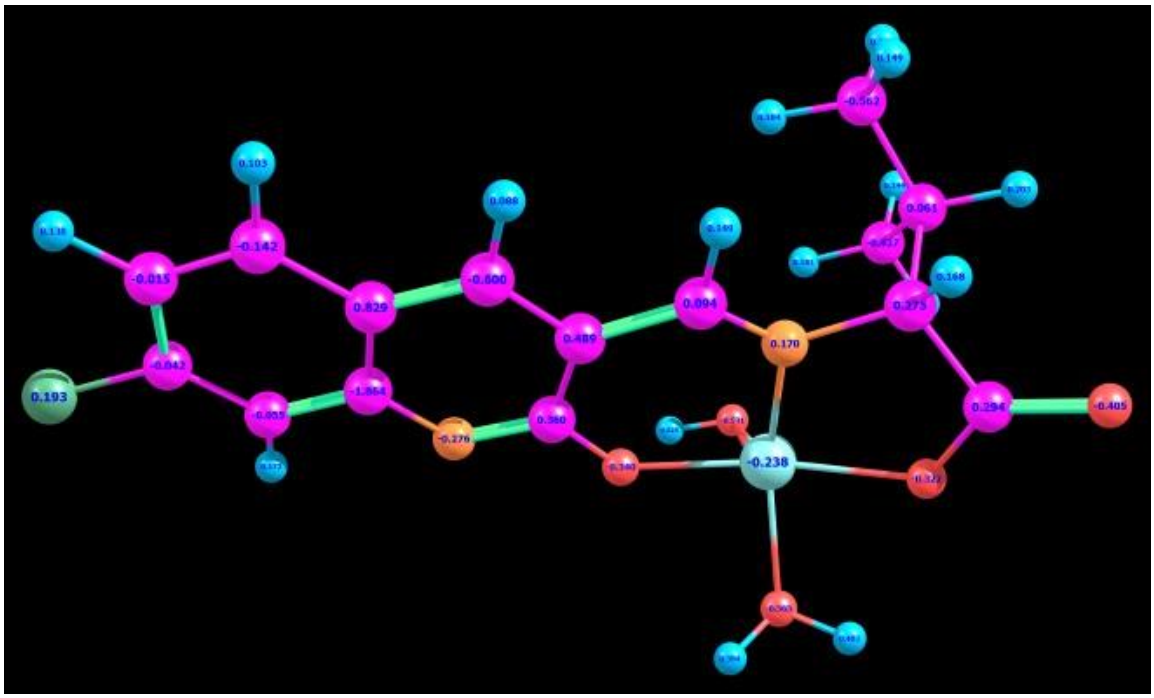

(c)

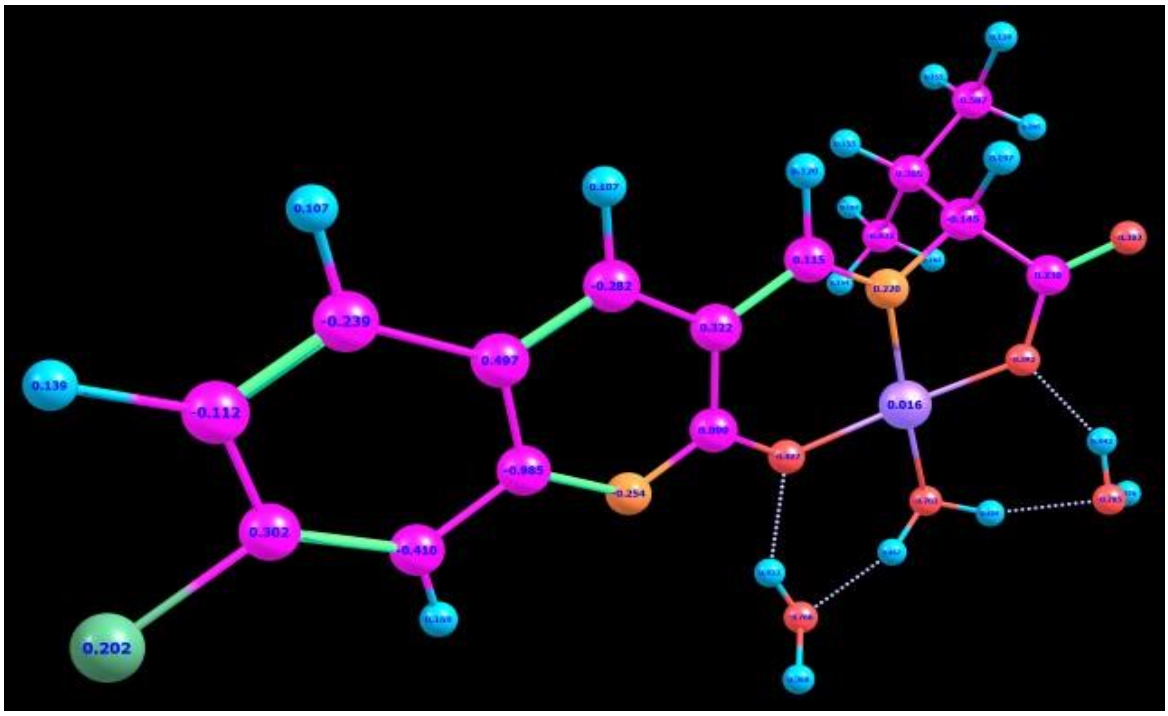

(d)

Appendix 4: Optimized geometry of (a) SBL2, (b) ZnSBL2, (c) CuSBL2 and NiSBL2

SBL1

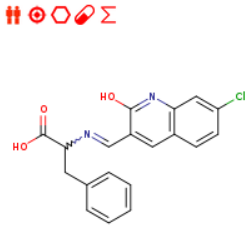

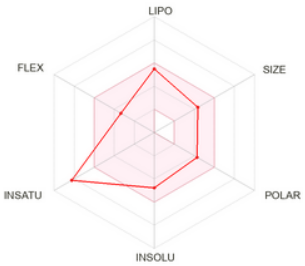

SMILES OC(=O)C(Cc1ccccc1)/N=C/c1cc2ccc(cc2nc1O)Cl

Physicochemical Properties	
Formula	C19H15ClN2O3
Molecular weight	354.79 g/mol
Num. heavy atoms	25
Num. arom. heavy atoms	16
Fraction Csp3	0.11
Num. rotatable bonds	5
Num. H-bond acceptors	5
Num. H-bond donors	2
Molar Refractivity	98.11
TPSA	82.78 Å²
Lipophilicity	
Log $P_{o/w}$ (iLOGP)	2.84
Log $P_{o/w}$ (XLOGP3)	4.12
Log $P_{o/w}$ (WLOGP)	3.71
Log $P_{o/w}$ (MLOGP)	2.59
Log $P_{o/w}$ (SILICOS-IT)	4.37
Consensus Log $P_{o/w}$	3.53

Water Solubility	
Log *S* (ESOL)	-4.78
Solubility	5.90e-03 mg/ml ; 1.66e-05 mol/l
Class	Moderately soluble
Log *S* (Ali)	-5.56
Solubility	9.66e-04 mg/ml ; 2.72e-06 mol/l
Class	Moderately soluble
Log *S* (SILICOS-IT)	-6.14
Solubility	2.59e-04 mg/ml ; 7.31e-07 mol/l
Class	Poorly soluble
Pharmacokinetics	
GI absorption	High
BBB permeant	No
P-gp substrate	No
CYP1A2 inhibitor	No
CYP2C19 inhibitor	No
CYP2C9 inhibitor	Yes
CYP2D6 inhibitor	No
CYP3A4 inhibitor	No
Log K_p (skin permeation)	-5.54 cm/s

Druglikeness	
Lipinski	Yes; 0 violation
Ghose	Yes
Veber	Yes
Egan	Yes
Muegge	Yes
Bioavailability Score	0.56
Medicinal Chemistry	
PAINS	0 alert
Brenk	1 alert: imine_1
Leadlikeness	No; 2 violations: MW>350, XLOGP3>3.5
Synthetic accessibility	3.16

ZnSBL1

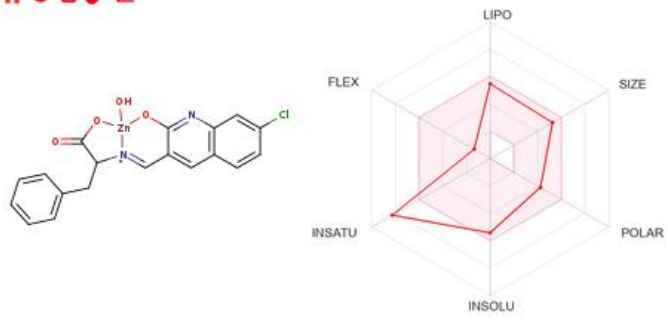

SMILES O=C1O[Zn]2([N]=Cc3c(O2)nc2c(c3)ccc(c2)Cl)C1Cc1ccccc1)O

Physicochemical Properties	
Formula	C19H14ClN2O4Zn
Molecular weight	435.16 g/mol
Num. heavy atoms	27
Num. arom. heavy atoms	16
Fraction Csp3	0.11
Num. rotatable bonds	2
Num. H-bond acceptors	5
Num. H-bond donors	1
Molar Refractivity	100.43
TPSA	81.01 Å²
Lipophilicity	
Log $P_{o/w}$ (iLOGP)	0.00
Log $P_{o/w}$ (XLOGP3)	4.07
Log $P_{o/w}$ (WLOGP)	3.21
Log $P_{o/w}$ (MLOGP)	1.77
Log $P_{o/w}$ (SILICOS-IT)	1.32
Consensus Log $P_{o/w}$	2.07

Water Solubility	
Log *S* (ESOL)	-5.41
Solubility	1.70e-03 mg/ml ; 3.90e-06 mol/l
Class	Moderately soluble
Log *S* (Ali)	-5.48
Solubility	1.45e-03 mg/ml ; 3.34e-06 mol/l
Class	Moderately soluble
Log *S* (SILICOS-IT)	-6.57
Solubility	1.18e-04 mg/ml ; 2.72e-07 mol/l
Class	Poorly soluble
Pharmacokinetics	
GI absorption	High
BBB permeant	No
P-gp substrate	Yes
CYP1A2 inhibitor	Yes
CYP2C19 inhibitor	Yes
CYP2C9 inhibitor	No
CYP2D6 inhibitor	Yes
CYP3A4 inhibitor	No
Log K_p (skin permeation)	-6.06 cm/s

Druglikeness	
Lipinski	Yes; 0 violation
Ghose	Yes
Veber	Yes
Egan	Yes
Muegge	Yes
Bioavailability Score	0.55
Medicinal Chemistry	
PAINS	0 alert
Brenk	1 alert: heavy_metal
Leadlikeness	No; 2 violations: MW>350, XLOGP3>3.5
Synthetic accessibility	4.61

CuSBL1

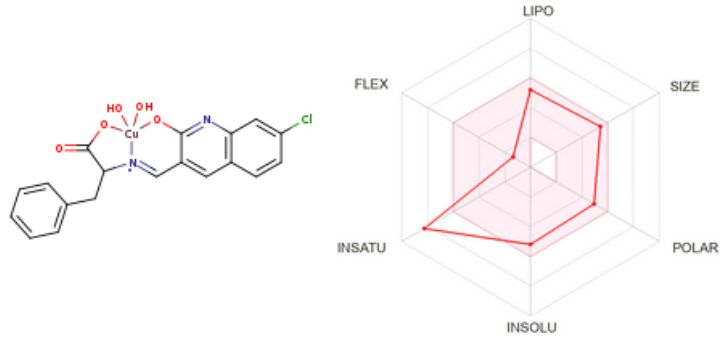

SMILES O=C1O[Cu]2([N](=Cc3c(O2)nc2c(c3)ccc(c2)Cl)C1Cc1ccccc1)(O)O

Physicochemical Properties	
Formula	C19H15ClCuN2O5
Molecular weight	450.33 g/mol
Num. heavy atoms	28
Num. arom. heavy atoms	16
Fraction Csp3	0.11
Num. rotatable bonds	2
Num. H-bond acceptors	6
Num. H-bond donors	2
Molar Refractivity	102.37
TPSA	101.24 Å²

Lipophilicity	
Log $P_{o/w}$ (iLOGP)	0.00
Log $P_{o/w}$ (XLOGP3)	3.59
Log $P_{o/w}$ (WLOGP)	3.03
Log $P_{o/w}$ (MLOGP)	0.97
Log $P_{o/w}$ (SILICOS-IT)	0.61
Consensus Log $P_{o/w}$	1.64

Water Solubility	
Log *S* (ESOL)	-5.18
Solubility	2.94e-03 mg/ml ; 6.54e-06 mol/l
Class	Moderately soluble
Log *S* (Ali)	-5.40
Solubility	1.78e-03 mg/ml ; 3.96e-06 mol/l
Class	Moderately soluble
Log *S* (SILICOS-IT)	-5.97
Solubility	4.79e-04 mg/ml ; 1.06e-06 mol/l
Class	Moderately soluble

Pharmacokinetics	
GI absorption	High
BBB permeant	No
P-gp substrate	Yes
CYP1A2 inhibitor	Yes
CYP2C19 inhibitor	Yes
CYP2C9 inhibitor	No
CYP2D6 inhibitor	Yes
CYP3A4 inhibitor	Yes
Log K_p (skin permeation)	-6.50 cm/s

Druglikeness	
Lipinski	Yes; 0 violation
Ghose	Yes
Veber	Yes
Egan	Yes
Muegge	Yes
Bioavailability Score	0.55

Medicinal Chemistry	
PAINS	0 alert
Brenk	0 alert
Leadlikeness	No; 2 violations: MW>350, XLOGP3>3.5
Synthetic accessibility	4.30

NiSBL1

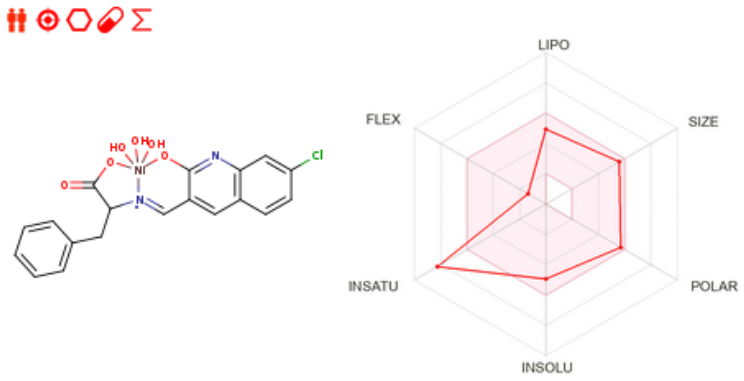

SMILES O=C1O[Ni]2([N](=Cc3c(O2)nc2c(c3)ccc(c2)Cl)C1Cc1ccccc1)(O)(O)O

Physicochemical Properties	
Formula	C19H16ClN2NiO6
Molecular weight	462.49 g/mol
Num. heavy atoms	29
Num. arom. heavy atoms	16
Fraction Csp3	0.11
Num. rotatable bonds	2
Num. H-bond acceptors	7
Num. H-bond donors	3
Molar Refractivity	104.30
TPSA	121.47 Å²

Water Solubility	
Log *S* (ESOL)	-4.95
Solubility	5.20e-03 mg/ml ; 1.12e-05 mol/l
Class	Moderately soluble
Log *S* (Ali)	-5.34
Solubility	2.12e-03 mg/ml ; 4.57e-06 mol/l
Class	Moderately soluble
Log *S* (SILICOS-IT)	-5.37
Solubility	1.96e-03 mg/ml ; 4.24e-06 mol/l
Class	Moderately soluble

Lipophilicity	
Log $P_{o/w}$ (iLOGP)	0.00
Log $P_{o/w}$ (XLOGP3)	3.12
Log $P_{o/w}$ (WLOGP)	2.86
Log $P_{o/w}$ (MLOGP)	0.18
Log $P_{o/w}$ (SILICOS-IT)	-0.11
Consensus Log $P_{o/w}$	1.21

Pharmacokinetics	
GI absorption	High
BBB permeant	No
P-gp substrate	Yes
CYP1A2 inhibitor	Yes
CYP2C19 inhibitor	No
CYP2C9 inhibitor	No
CYP2D6 inhibitor	No
CYP3A4 inhibitor	No
Log K_p (skin permeation)	-6.91 cm/s

Druglikeness	
Lipinski	Yes; 0 violation
Ghose	Yes
Veber	Yes
Egan	Yes
Muegge	Yes
Bioavailability Score	0.55

Medicinal Chemistry	
PAINS	0 alert
Brenk	0 alert
Leadlikeness	No; 1 violation: MW>350
Synthetic accessibility	4.12

Appendix 5: Swiss ADME predicted data of SBL1 ligand, and ZnSBL1, CuSBL1, NiSBL1 complex

SBL2

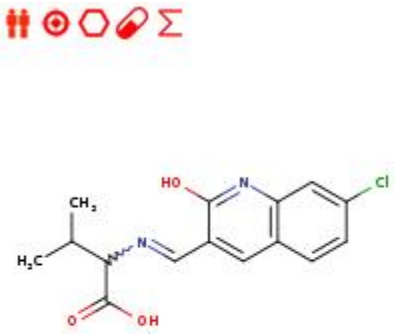

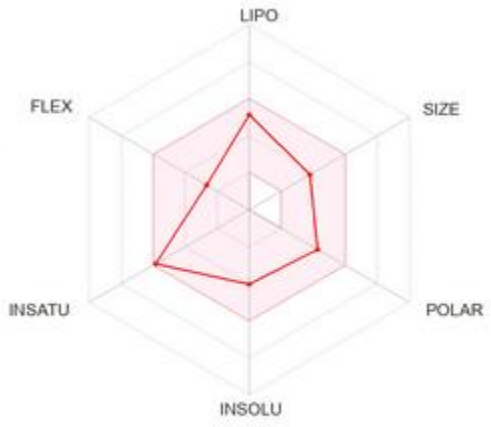

SMILES CC(C(C(=O)O)/N=C/c1cc2ccc(cc2nc1O)Cl)C

Physicochemical Properties	
Formula	C15H15ClN2O3
Molecular weight	306.74 g/mol
Num. heavy atoms	21
Num. arom. heavy atoms	10
Fraction Csp3	0.27
Num. rotatable bonds	4
Num. H-bond acceptors	5
Num. H-bond donors	2
Molar Refractivity	83.23
TPSA	82.78 Å²
Lipophilicity	
Log $P_{o/w}$ (iLOGP)	2.60
Log $P_{o/w}$ (XLOGP3)	3.50
Log $P_{o/w}$ (WLOGP)	3.12
Log $P_{o/w}$ (MLOGP)	1.87
Log $P_{o/w}$ (SILICOS-IT)	3.46
Consensus Log $P_{o/w}$	2.91

Water Solubility	
Log *S* (ESOL)	-4.04
Solubility	2.83e-02 mg/ml ; 9.22e-05 mol/l
Class	Moderately soluble
Log *S* (Ali)	-4.92
Solubility	3.67e-03 mg/ml ; 1.20e-05 mol/l
Class	Moderately soluble
Log *S* (SILICOS-IT)	-4.07
Solubility	2.63e-02 mg/ml ; 8.59e-05 mol/l
Class	Moderately soluble
Pharmacokinetics	
GI absorption	High
BBB permeant	No
P-gp substrate	No
CYP1A2 inhibitor	Yes
CYP2C19 inhibitor	No
CYP2C9 inhibitor	Yes
CYP2D6 inhibitor	No
CYP3A4 inhibitor	No
Log K_p (skin permeation)	-5.69 cm/s

Druglikeness	
Lipinski	Yes; 0 violation
Ghose	Yes
Veber	Yes
Egan	Yes
Muegge	Yes
Bioavailability Score	0.56
Medicinal Chemistry	
PAINS	0 alert
Brenk	1 alert: imine_1
Leadlikeness	Yes
Synthetic accessibility	2.99

ZnSBL2

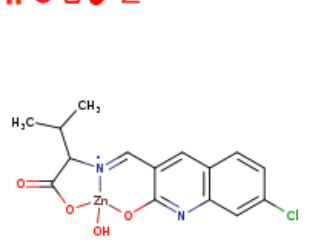

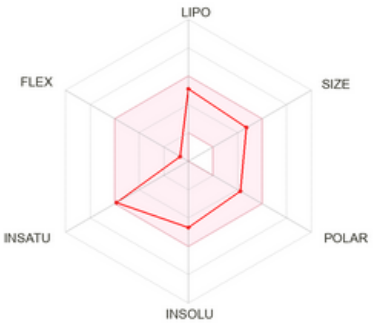

SMILES CC(C1C(=O)O[Zn]2([N]1=Cc1cc3ccc(cc3nc1O2)Cl)O)C

Physicochemical Properties	
Formula	C15H14ClN2O4Zn
Molecular weight	387.12 g/mol
Num. heavy atoms	23
Num. arom. heavy atoms	10
Fraction Csp3	0.27
Num. rotatable bonds	1
Num. H-bond acceptors	5
Num. H-bond donors	1
Molar Refractivity	85.56
TPSA	81.01 Å²
Lipophilicity	
Log $P_{o/w}$ (iLOGP)	0.00
Log $P_{o/w}$ (XLOGP3)	3.44
Log $P_{o/w}$ (WLOGP)	2.62
Log $P_{o/w}$ (MLOGP)	1.06
Log $P_{o/w}$ (SILICOS-IT)	0.51
Consensus Log $P_{o/w}$	1.53

Water Solubility	
Log *S* (ESOL)	-4.66
Solubility	8.41e-03 mg/ml ; 2.17e-05 mol/l
Class	Moderately soluble
Log *S* (Ali)	-4.82
Solubility	5.83e-03 mg/ml ; 1.51e-05 mol/l
Class	Moderately soluble
Log *S* (SILICOS-IT)	-4.51
Solubility	1.20e-02 mg/ml ; 3.09e-05 mol/l
Class	Moderately soluble
Pharmacokinetics	
GI absorption	High
BBB permeant	No
P-gp substrate	Yes
CYP1A2 inhibitor	No
CYP2C19 inhibitor	Yes
CYP2C9 inhibitor	No
CYP2D6 inhibitor	Yes
CYP3A4 inhibitor	No
Log K_p (skin permeation)	-6.22 cm/s

Druglikeness	
Lipinski	Yes; 0 violation
Ghose	Yes
Veber	Yes
Egan	Yes
Muegge	Yes
Bioavailability Score	0.55
Medicinal Chemistry	
PAINS	0 alert
Brenk	1 alert: heavy_metal
Leadlikeness	No; 1 violation: MW>350
Synthetic accessibility	4.50

CuSBL2

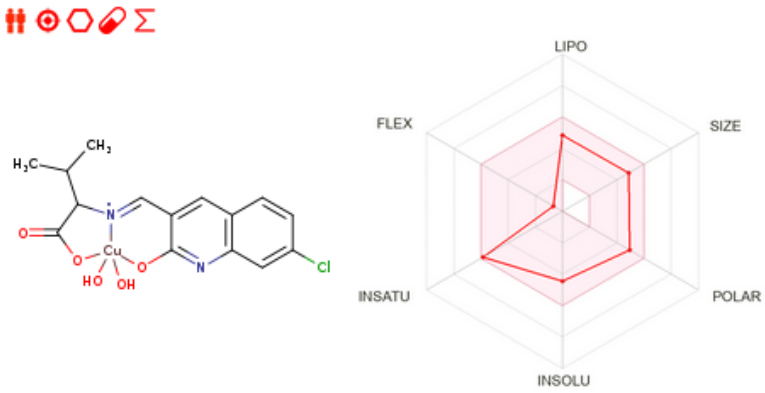

SMILES CC(C1C(=O)O[Cu]2([N]1=Cc1cc3ccc(cc3nc1O2)Cl)(O)O)C

Physicochemical Properties	
Formula	C15H15ClCuN2O5
Molecular weight	402.29 g/mol
Num. heavy atoms	24
Num. arom. heavy atoms	10
Fraction Csp3	0.27
Num. rotatable bonds	1
Num. H-bond acceptors	6
Num. H-bond donors	2
Molar Refractivity	87.49
TPSA	101.24 Å²
Lipophilicity	
Log $P_{o/w}$ (iLOGP)	0.00
Log $P_{o/w}$ (XLOGP3)	2.97
Log $P_{o/w}$ (WLOGP)	2.45
Log $P_{o/w}$ (MLOGP)	0.26
Log $P_{o/w}$ (SILICOS-IT)	-0.19
Consensus Log $P_{o/w}$	1.10

Water Solubility	
Log *S* (ESOL)	-4.45
Solubility	1.44e-02 mg/ml ; 3.57e-05 mol/l
Class	Moderately soluble
Log *S* (Ali)	-4.76
Solubility	7.00e-03 mg/ml ; 1.74e-05 mol/l
Class	Moderately soluble
Log *S* (SILICOS-IT)	-3.92
Solubility	4.84e-02 mg/ml ; 1.20e-04 mol/l
Class	Soluble
Pharmacokinetics	
GI absorption	High
BBB permeant	No
P-gp substrate	Yes
CYP1A2 inhibitor	No
CYP2C19 inhibitor	No
CYP2C9 inhibitor	No
CYP2D6 inhibitor	No
CYP3A4 inhibitor	No
Log K_p (skin permeation)	-6.65 cm/s

Druglikeness	
Lipinski	Yes; 0 violation
Ghose	Yes
Veber	Yes
Egan	Yes
Muegge	Yes
Bioavailability Score	0.55
Medicinal Chemistry	
PAINS	0 alert
Brenk	0 alert
Leadlikeness	No; 1 violation: MW>350
Synthetic accessibility	4.19

NiSBL2

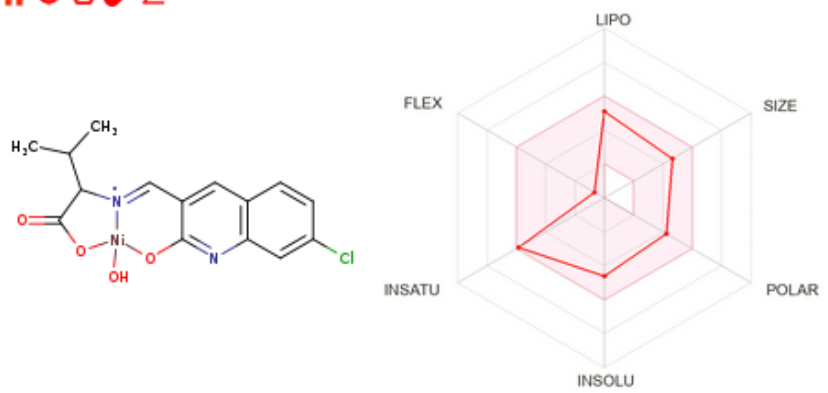

SMILES CC(C1C(=O)O[Ni]2([N]1=Cc1cc3ccc(cc3nc1O2)Cl)O)C

Physicochemical Properties	
Formula	C15H14ClN2NiO4
Molecular weight	380.43 g/mol
Num. heavy atoms	23
Num. arom. heavy atoms	10
Fraction Csp3	0.27
Num. rotatable bonds	1
Num. H-bond acceptors	5
Num. H-bond donors	1
Molar Refractivity	85.56
TPSA	81.01 Å²
Lipophilicity	
Log $P_{o/w}$ (iLOGP)	0.00
Log $P_{o/w}$ (XLOGP3)	3.44
Log $P_{o/w}$ (WLOGP)	2.62
Log $P_{o/w}$ (MLOGP)	1.06
Log $P_{o/w}$ (SILICOS-IT)	0.47
Consensus Log $P_{o/w}$	1.52

Water Solubility	
Log *S* (ESOL)	-4.62
Solubility	9.09e-03 mg/ml ; 2.39e-05 mol/l
Class	Moderately soluble
Log *S* (Ali)	-4.82
Solubility	5.73e-03 mg/ml ; 1.51e-05 mol/l
Class	Moderately soluble
Log *S* (SILICOS-IT)	-4.49
Solubility	1.23e-02 mg/ml ; 3.22e-05 mol/l
Class	Moderately soluble
Pharmacokinetics	
GI absorption	High
BBB permeant	No
P-gp substrate	Yes
CYP1A2 inhibitor	No
CYP2C19 inhibitor	Yes
CYP2C9 inhibitor	No
CYP2D6 inhibitor	Yes
CYP3A4 inhibitor	No
Log K_p (skin permeation)	-6.18 cm/s

Druglikeness	
Lipinski	Yes; 0 violation
Ghose	Yes
Veber	Yes
Egan	Yes
Muegge	Yes
Bioavailability Score	0.55
Medicinal Chemistry	
PAINS	0 alert
Brenk	0 alert
Leadlikeness	No; 1 violation: MW>350
Synthetic accessibility	4.12

Appendix 6: Swiss ADME predicted data of SBL2 ligand, and ZnSBL2, CuSBL2, NiSBL2 complex

LIST OF PUBLICATIONS

1. **Dadi Dinku**, Taye B. Demissie Isaac N. Beas Rajalakshmanan Eswaramoorthy, Bayan Abdi, Tegene Desalegn; Antimicrobial activities and docking studies of new Schiff base ligand and its Cu(II), Zn(II) and Ni (II) Complexes: Synthesis and Characterization; Journal of Inorganic Chemistry Communications160(2024)111903, https://doi.org/10.1016/j.inoche.2023.111903
2. **Dadi Dinku**, Taye B. Demissie, Isaac N. Beas, Tegene Desalegn; Synthesis, Molecular Docking, and antibacterial evaluation of Quinoline-Derived Ni(II), Cu(II) and Zn(II) complexes, Journal of Result in Chemistry 8(2024)101562, https://doi.org/10.1016/j.rechem.2024.101562